ACOUSTICAL SIGNATURE ANALYSIS OF HIGH PRESSURE FLUID PUMPING PHENOMENA

By

GEORGE EARL MARONEY

Bachelor of Science
Oklahoma State University
Stillwater, Oklahoma
1967

Master of Science
Oklahoma State University
Stillwater, Oklahoma
1969

Submitted to the Faculty of the
Graduate College of the
Oklahoma State University
in partial fulfillment of
the requirements for
the Degree of
DOCTOR OF PHILOSOPHY
May, 1976

ACOUSTICAL SIGNATURE ANALYSIS OF HIGH PRESSURE FLUID PUMPING PHENOMENA

Thesis Approved:

Thesis Adviser

Dean of the Graduate College

PREFACE

This dissertation is part of a continuing study of the exciting area of acoustical signature analysis. Presently, the principal objective of the study is to examine the potential of acoustical signature analysis as a non-intrusive diagnostic technique for high pressure fluid power systems. The reported study concentrated on high pressure hydraulic gear pumps. It is apparent, after completing the study, that acoustical signature analysis offers great potential as a diagnostic technique which can assist with our efforts to solve some of the engineering mysteries still plaguing the fluid power industry.

Consistent with the thoughts of Ernest O. Doebelin (52, pp. 4-5), an attempt was made during this study to maintain the proper balance of theory and experiment:

> In solving engineering problems, two general methods are available: theoretical and experimental. Many problems require the application of both methods. The relative amount of each employed depends on the nature of the problem. Problems on the frontiers of knowledge often require very extensive experimental studies since adequate theories are not yet available. Theory and experiment should thus be thought of as complementing each other, and the engineer who takes this attitude will, in general, be a more effective problem solver than one who neglects one or the other of these two approaches.

The author had to conduct "extensive experimental studies" because there is very little published information regarding

acoustical signature analysis of high pressure pump noise.

The conduct of an extensive experimental program was possibly "a last resort", but the implementation was enjoyable because the author has the same enthusiasm for this area of study that Davis (34, p. 48) exhibits for nomography:

> Each excursion into . . . unexplored territory . . . constitutes high adventure, fraught with . . . dangers and . . . romance, ... Few chemists and engineers will ever hunt lions in Liberia, uranium on Uranus, or even romance on the Rivieria, but no one need lack for a modest measure of these thrills while he can beg, borrow, or steal, or even determine (a last resort!) data to correlate.

The experimental program examined the sensitivity of pump noise levels to variations of hydraulic system operational parameters. This program has been in process for three years and the study has only begun. The results to date indicate that acoustical signature analysis will provide the fluid power industry with a viable non-intrusive diagnostic technique which can be used in-situ.

Theophrastus noted that "Time is the most valuable thing a man can spend." Certainly this study could not have progressed to its present level of success if numerous people had not contributed their very valuable time, either directly or indirectly as financial and material support. I thank all of them in general and, in the following paragraphs, a few in particular.

I am extremely grateful to Dr. E. C. Fitch, my major adviser, whose personal efforts made this study and indeed my formal education feasible. His contagious enthusiasm for engineering endeavors, guidance--based on a breadth of

engineering experience, and support throughout my formal studies is greatly appreciated.

To the other members of my committee, Professors: J. E. Bose, D. D. Lingelbach, R. L. Lowery, and P. A. McCollum, I extend my thanks for their guidance, critiques, and patience. Especially their patience while I worked on the dissertation without losing touch with my other engineering and my military interests.

To Velda Davis I extend my sincere appreciation for her expert assistance which insured that a "rough" manuscript turned into a professional looking document.

I thank the following personnel who were extremely helpful though their association with the Fluid Power Research Center (FPRC): Jim McBurnett and Roger Elliott for their assistance in establishing the FPRC Acoustical Laboratories; William Adams, Randy West, and Greg Snyder for their help during the data acquisition phase of the study; Lynn Alger, Joel Moore, and Gary Flesher whose professional drafting assistance enhanced the appearance of the dissertation.

To my colleagues, Leonard Bensch, Ram Iyengar, Gary Roberts, and Dick Tessmann, I extend my sincere appreciation for their untiring counsel, confidence, and honest, objective criticism. I especially thank Dick Tessmann for our long discussions of cavitation and wear, which assisted greatly in the formulation of several of the concepts presented in the manuscript.

I thank my mother and father for the opportunity. I thank my mother for her inexhaustible faith and encouragement.

Most of all I thank Vivian, Angie, and Shane, who tolerate my "adventures" (which ofttimes must seem to them quixotic) and are my "oasis".

I am extremely grateful to my many associates in government and industry who have provided financial support during my graduate studies. In particular I thank the members of the Basic Fluid Power Research Program and the Components and Systems Branch of U. S. Army MERDC, whose support helped make this study possible.

I am grateful to all of the monitors of my research efforts during the past decade whose continued support, thoughts, encouragement, and criticism not only made this study possible but hopefully assured that it has a high degree of practicality.

TABLE OF CONTENTS

Chapter Page

LIST OF TABLES

LIST OF FIGURES

NOMENCLATURE

a	constant
a	radius of piston (m)
a	radius of sphere (m)
abn	airborne noise (P_a)(W)
A*	air/liquid volume ratio (stp)
A	area (m^2)
A_i	complete amplitude
b	constant
B	stress strain constant
c	cycle
c	constant
c	constant defining stress
c	sonic velocity (m/sec)
c_i	sonic velocity in the ith medium (m/sec)
C	wear law constant
C_d	discharge coefficient
C_1	noise without wear (W)
C_2	wear coefficient (N/sm^2)
C_3	wear rate coefficient (N/m^2)
d	constant
d	derivative operator
dB	decibel
e	constant (2.718)

f	frequency (c/s)
f	harmonic (c/s)
F_{EF}	conversion function, energy to fluidborne noise
F_{ES}	conversion function, energy to structureborne noise
F_{FS}	conversion function, fluidborne to structureborne
F_{SA}	conversion function, structureborne to airborne
F_{SS}	conversion function, structureborne to structure-borne noise
g	grams
g*	contamination level
H	hardness (N/m^2)
Hz	Hertz (cycles/s)
i	index
I	intensity (W/m^2)
I_o	intensity at reference position, $x = 0 (W/m^2)$
I_R	gear polar moment of intertia (kgs^2m)
I_r	pinion polar moment of intertia (kgs^2m)
j	index
j	index for the harmonic number
k_i	wavelength constant (rad/m)
K	constant defining load/area relation
ℓ	thickness of the second medium (m)
ℓ	thickness, length (m)
ℓ	position
L	the data matrix
L	distance traveled during wear (m)

L	normal load (N)
L_a	acceleration level (dB)
L_d	displacement level (dB)
L_i	noise level of ith harmonic (dB)
L_{ij}	the level associated with the jth harmonic of the ith sample (dB)
L_v	velocity level (dB)
m	constant in fatigue failure criteria
m	integer, index
m	meter
M'	the modified data matrix
M_{ij}	the curve fit estimate of the noise level at the jth harmonic at the ith time (dB)
n	number of wear sheets
n	index defining work-hardening
n	integer, index
n	total number of harmonics
n	total number of samples
n_o	the initial particles concentration (particles/m^3)
N	constant for fixed mass of particular gas (N(m)/k)
N	pinion speed (rev/s)
N	speed (rev/sec)
N	Newton
N_i	the noise wear index for the ith sample
p_∞	pressure in liquid (Pa)
p_i	pressure, incident (Pa)

p_o	pressure, atmospheric (101.3 kPa)
p_r	pressure, reflected (Pa)
p_t	pressure, transmitted (Pa)
p_v	vapor pressure (Pa)
P	pressure (Pa)
P	normal load (N)
Pa	Pascal
P_e	equilibrium pressure (Pa)
P_i	pressure, inlet (Pascals)(absolute)
P_1	system pressure (Pa)
P_o	tooth load factor
P_o	pressure, outlet (Pa)
q_m	flow rate, mth component (m^3/s)
Q*	equal to Q/Q_R; equal to normalized flow
Q/Q_R	flow performance index
Q_R	rated flow
$\overline{Q}$	mean flow rate (m^3/s)
Q	flow rate (m^3/s)
Q	the flow at time t in the lab. (m^3/s)
Q_f^*	final Q^k associated with N_k
Q_o	the initial flow (m^3/s)
r	constant
r	air/liquid volume ratio
r	distance from piston along x-axis (m)
r	pinion pitch radius (m)
r	radius from source (m)
r	radius from sphere (m)

rad	radian
R	instantaneous bubble radius (m)
R	radius (m)
R	angular speed
R_o	gear pitch radius (m)
R_o	initial bubble radius (m)
s	second
s	solubility constant
S_o	distance slid to create n wear sheets (m)
t	time (s)
t	index defining wear particle size
t_f	final time associated with N_k
T	absolute temperature (k)
T	transmitted torque (NM)
T_ℓ	system temperature (°A)
T_o	standard temperature (273°A)
T_p	period (s)
u_o	velocity amplitude of spherical surface (m/s)
U	velocity (m/s)
V	total wear volume (m^3)
V	velocity (m/s)
V_a	volume of air (standard temperature and pressure) in system (m^3)
V_{ec}	volume of air (standard temperature and pressure) entrained and contiguous in system (m^3)
V'_{ec}	actual volume of entrained and contiguous air at system temperature and pressure (m^3)

V_d volume of gas at standard temperature and pressure that could dissolve in the liquid at equilibrium (m^3)

V_ℓ volume of liquid (m^3)

V_s tooth sliding velocity (m/s)

w pinion speed (rad/s)

w angular velocity (rad/s)

W watts

W tooth wear (m)

W total wear (m^3)

$\dot{W}$ wear rate (m^3/s)

W^e frictional work done (Nm)

x variable, distance (m)

X tooth contact point on line of action (in)

y variable

$\bar{y}$ mean displacement (m)

y_m displacement, mth component (m)

Greek Letters

α attenuation factor

α contaminant wear coefficient ($\frac{.6}{(\text{particles})^2 s}$)

α_t power transmission coefficient

β area ratio

β radius of asperity

γ constant defining particle size

$\bar{\epsilon}_i$ strain to failure in one loading cycle

η line distribution of asperities

θ	angle (rad)
λ	constant defining size to single contact
λ	wavelength (m)
μ	liquid viscosity (Pa(s))
μ	coefficient of friction
π	constant (3.1416)
ρ	density
ρ	liquid density (kg/m^3)
ρ_i	density of the ith medium (kg/m^3)
σ	standard deviation of ordinate distribution
σ	surface tension (N/m)
τ	time (s)
τ	time constant of particle destruction process (s)
χ	cavitation number
ω	angular frequency (rad/s)

CHAPTER I

INTRODUCTION

The proper analysis of the noise emitted by any system provides two important data sets. First, society's estimate of the overall potential of the machine to cause hearing damage can be determined. Second, knowledgeable simultaneous interpretation of the noise levels at individual frequencies yields information about the past and present operational status of the system. The former helps to monitor the "quietness" of the environment, the latter provides a viable diagnostic technique to assist in the achievement of quieter, more reliable systems.

The Problems

High-pressure hydraulic rotary pumps are the primary source of power in high-horsepower fluid power systems. Because a great deal of energy is transferred through the pump as it converts mechanical power to hydraulic power, its acoustical performance is an important consideration in the design of quiet systems. National test codes are available to assess the sound generated by hydraulic pumps and motors (1) (2). An international test code for measuring the sound emitted by hydraulic pumps has been prepared and

is being processed by the International Organization for Standardization (3). The adequacy of the constraints in the test codes have not been documented. There are several physical interactions that could affect the repeatability and reproducibility of the test codes (4) (5).

Current techniques used for the performance evaluation of fluid power systems and components in the field and laboratory require installing transducers in the system. When the installation of transducers in the field is impractical, components are disassembled for visual inspection, or they are shipped to a laboratory for performance evaluation. These techniques are time consuming and expensive. The fluid power industry needs viable non-intrusive diagnostic techniques.

Although not obviously related, two problems facing the fluid power industry are:

1. the sensitivity of pump sound to test parameters needs to be more fully documented
2. the possibility of developing non-intrusive diagnostic techniques for fluid power systems needs to be fully explored.

The Thesis

The analysis of component noise signatures is an effective indicator of machine performance (6), and machine wear (7). In the laboratory non-intrusive diagnostics, in the form of acoustical signature analysis, provides the "eyes"

with which experimenters "see" cavitation in low pressure systems (8), and monitor other physical phenomena (9).

The proposition examined in this dissertation is that acoustical signature analysis has the potential for becoming a viable non-intrusive diagnostic technique for high-pressure fluid power systems. It is further proposed that the use of this technique and the subsequent theoretical explanations of the signature variations associated with system parameter changes will lead to a better understanding of the phenomena involved in pump sound generation. Ultimately this knowledge should lead to quieter, more reliable fluid power pumps and systems.

The Objective

In all of the cases where acoustical signature analysis is a viable technique, the acoustical diagnostician understands how to "read" the "noise". The proper interpretation of any data set requires prior knowledge of what to observe and the possible meanings of the observations. For acoustical signature analysis to become a viable technique for fluid power systems, both experimental and theoretical bases are needed.

The principal objective of this dissertation is to provide theoretical and experimental bases which will (1) allow the evaluation of acoustical signature analysis as a non-intrusive diagnostic technique for high-pressure fluid power pumps and (2) provide a better understanding of the

process of pump sound generation.

The Study

Non-fatigue failures of hydraulic pumps can be attributed to normal wear, contaminant induced (accelerated) wear, vaporous cavitation, and gaseous cavitation. These phenomena can occur in all pumps. High-pressure gear pumps were chosen for this study because they are prevalent in the industry, therefore appropriate for diagnosis and relatively inexpensive as test specimens.

Previous Investigations

Although acoustical signature analysis information for gears is available (7) (10), and low-pressure centrifugal pump acoustical signatures have been studied (8) (11), very little has been published about the use of acoustical signature analysis of high-pressure pumps as a diagnostic technique. There are only two recent publications available in the fluid power literature on fluid power pump airborne sound modeling or signature analysis (5) (12). Both of these articles are the result of this study.

The literature is replete with case histories of how a particular hydraulic system or pump was modified to reduce the system noise level. Basic theories are available to assist in the control of noise, such as the reduction of pump pressure ripple (13). But the author was not able to locate any published articles which dealt in depth with pump

airborne noise levels as a function of the numerous test variables: time, inlet pressure, fluid viscosity, entrained air, contamination level, etc. To attain the objective of the study, the scope of the research provides a means for determining the sensitivity of pump sound to pump test parameters.

The Scope

To gain a better understanding of pump sound sensitivity to operating parameters and to study acoustical signature analysis as a fluid power diagnostic technique the scope of the research effort includes:

1. A review of basic theory which could provide a rational explanation for gear pump acoustical signature variations due to pertubations of the test parameters.
2. The design of the experiments, the procurement of components, the selection and procurement of data acquisition instrumentation, and the design and construction of special test facilities and equipment to meet the study objectives.
3. The acquisition and analysis of the acoustical signatures of high-pressure gear pumps operating normally, normally as a function of time, with contaminated fluid, normally after wear, and with cavitation. The cavitation studies

include data obtained with low and high air/ liquid volume ratios.

4. The correlation of the results of simple and factorial designed experiments as related to one another, the basic theory, and the results of experiments in low pressure hydraulic systems.

Principal Results

The results of this study indicate that the acoustical signatures of high-pressure gear pumps operating in "real" systems could provide useful information about the past and present operating conditions of the pumps. The consistency of the qualitative trends obtained in this study imply that they can be applied to other gear pumps. Further, the results show that acoustical signature analysis has excellent potential as a non-intrusive diagnostic technique for fluid power systems.

The principal results of this study are:

1. A noise wear index which can be used to determine if a pump should be replaced because it is worn beyond acceptable limits. The index is calculated using the results of a near field pump noise measurement.
2. A simple test for a new system design to determine if the system is cavitating.

The test requires making near-field noise measurements while the pump speed is varied. If the pump has a fixed speed the inlet pressure is varied.

3. Pump noise levels are sensitive to contamination level. Contamination levels during pump noise measurements should be controlled.

4. Proper design of the pump inlet system and proper control of the system's entrained air could reduce a pump's noise level, at maximum speed, over 2 dBA. During pump noise tests air/liquid volume ratios should be controlled.

5. A cavitation potential index (CPI) is proposed for high-pressure fluid system. The number has a value of zero at cavitation inception and increases as cavitation potential increases. It is proposed that the bubble pressure for air be included as one of the critical cavitation inception pressures for high-pressure systems. The resultant CPI has the form:

$$\Psi = 1 - \frac{p\ S}{r\ p_o}$$

6. Near-field noise measurements represent an excellent means for assessing the operational characteristics of a component.
7. The hydraulic system test parameters which should be specified and controlled during a pump noise test are speed, inlet pressure, air/liquid volume ratio, liquid, temperature, outlet pressure, and contamination level.
8. The all-pass noise level of pumps varies a great amount as a function of time. This variation is due to the standard deviation of the noise levels of the pumping harmonics. All-pass pump noise level measurements should be averaged (sampled) for a reasonable length of time (e.g., 30 seconds).

The next chapter discusses some basic acoustical theory and theory which is applicable to known and suspected noise generation processes that occur in fluid power pumps. Chapter III is devoted to discussions of the pertinent experimental considerations that preceded testing. The experimental program is outlined in Chapter IV. Chapter V presents the experimental results. A discussion of the correlation between the experimental results and the basic theory are included in Chapter VI. Specific conclusions and recommendations for further studies are made in Chapter VII.

The appendicies contain definitions, selected experimental results, and discussions of pertinent mathematics, instrumentation, test systems, and fluid properties.

CHAPTER II

THEORETICAL CONSIDERATIONS

The design of engineering experiments and the interpretation of experimental results should reflect consideration of the project objectives, applicable theories, test specimen characteristics, test facility limitations, and data analysis constraints.

The purposes of this chapter are (1) to examine the basic characteristics of high pressure pumps and their operational environments, since both could significantly affect their acoustical signatures, (2) to present theories in the areas of acoustics, wear, and cavitation, which appear directly applicable to acoustical signature analysis of high pressure pumps, and (3) to summarize how various system variables might affect pump sound generation.

The Gear Pump

The basic operation of a spur gear pump is illustrated in Figure 1. During operation of the gear pump volumes of low pressure fluid are transported in the spaces between the gear teeth to the high pressure region which is sealed radially by the tooth tip to housing clearnace, and the contact of the gears as they mesh. Axially the high pressure

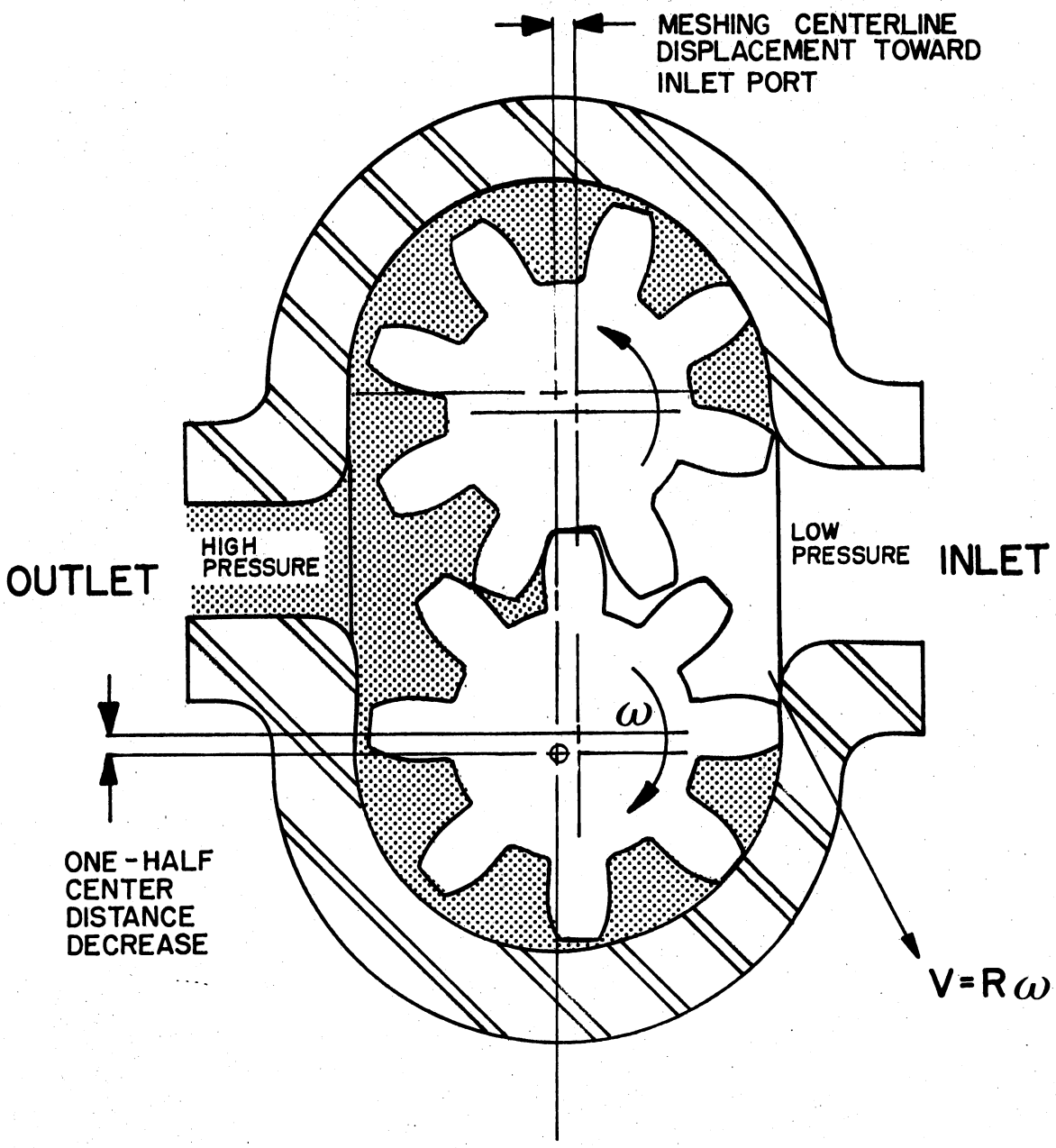

Figure 1. Gear Pump Section Illustrating Basic Operation, Exaggerated Meshing Offset Due to High Pressure, and Gear Tooth Tip Velocity

region is sealed by the gear face to housing clearances. The gear face to housing clearances are frequently controlled with pressure-compensated wear plates. The gear shafts are usually supported with journal bearings. Besides the fluid leakage paths, from the high pressure region to the inlet, associated with the sealing areas there is some controlled lubrication flow through the bearings.

The pressure differential across the gears causes a displacement of the gear centerlines. This displacement is controlled by several interactions, but generally allows the gear teeth tips to seal at the housing wall. The velocity of the gear teeth tips relative to the housing wall is directly proportional to the angular velocity of the input shaft.

The fluid introduced to the pump inlet will be some mixture of gas and liquid. The system fluid will be contaminated. Among the contaminants there will be some amount of particulate contaminant. The pump and the system fluid temperatures can be expected to vary from less than $-50^{\circ}C$ to greater than $100^{\circ}C$. The fluid viscosity will normally vary significantly as the system temperature varies.

Acoustical Theory

Noise is an erratic, intermittent, or statistically random oscillation (14). Noise is also defined as any undesired sound (14). For this study, both definitions are appropriate. The ensuing discussions consider the

characteristics or changes of intermittent oscillations. The study also considers how undesired sound changes due to variations of operational parameters. The context used with the word provides the distinctions.

Sound is defined in the following ways:

1. Sound is an oscillation in pressure, stress, particle displacement, particle velocity, etc., in a medium with internal forces (e.g., elastic, viscous), or the superposition of such propagated oscillations.
2. Sound is an auditory sensation evoked by the oscillation described above.

For this study "sound" means "an auditory sensation", while noise refers to either any parametric oscillation or undesired sound.

Noise is temporal. During a sample interval (time) with steady operation most machine noise can be considered periodic. A great deal of machine noise is best examined by considering the noise as complex periodic data, which can be expanded in the Fourier series according to the following formula (15):

$$x(t) = \frac{a_o}{2} + \sum_{n=1}^{\infty} (a_n \cos 2\pi n f_1 t + b_n \sin 2\pi n f_1 t) \qquad (2.1)$$

where:

$$f_1 = 1/T_p$$

$$a_n = 2/T_p \int_o^{T_p} x(t) \cos 2\pi n f_1 t \, dt \qquad n = 0, 1, 2, \ldots$$

$$b_n = 2/T_p \int_0^{T_p} x(t) \sin 2\pi n f_1 t \, dt \qquad n = 1, 2, 3, \ldots$$

T_p = period (time required for one full fluctuation) (seconds)

Bendat and Piersol (15) show an alternate expression for Equation (2.1):

$$x(t) = x_o + \sum_{n=1}^{\infty} x_n \cos(2\pi n f_1 t - \theta) \qquad (2.2)$$

where:

$$x_o = a_o/2$$

$$x_n = \sqrt{a_n^2 + b_n^2} \qquad n = 1, 2, 3, \ldots$$

$$\theta_n = \tan^{-1}(b_n/a_n) \qquad n = 1, 2, 3, \ldots$$

Equation (2.2) indicates that complex periodic data consists of a static component, x_o, and an infinite number of sinusoidal components (harmonics with amplitude, x_n and phase θ_n). The harmonic component frequencies are integral multiples of f_1. Thus, complex periodic machine noise can be described with a graph of the magnitude of the various harmonics (a plot of level versus frequency).

Given a definition of noise and the basic mathematics for discussing noise it is practical to consider the sound and noise generation processes in high pressure gear pumps, the transmission of noise in structures, airborne noise radiation, and the "near-field".

Sound Generation

A simplified illustration of the sound generation process for a hydraulic pump is shown in Figure 2. Sound occurs in the sound field which is excited by the component or noise source. The component excites the sound field through surface vibrations (structureborne noise). Structureborne noise in the component may be due to other structureborne noise or fluidborne noise. For a hydraulic pump all of the inherent noise can ultimately be traced to the energy conversion process and associated component interactions. For mechanical noise sources only structureborne noise must be considered in the generation process.

This illustration, Figure 2, of the sound generation process is extremely simplified. Willekins (16) presents a more complete illustration of the interactions associated with noise generation in hydraulic pumps in his paper "Fluidborne Noise in Hydraulic Systems". The fact that this study is directed toward airborne noise as opposed to sound is reflected in Figure 3, which outlines the basic relationship between the energy conversion process and component airborne noise.

Noise Generation

Figure 2 implies that given an analytical description of the energy conversion process in a hydraulic pump and five functional relationships the airborne noise emitted by a pump can be described. One objective of this chapter is

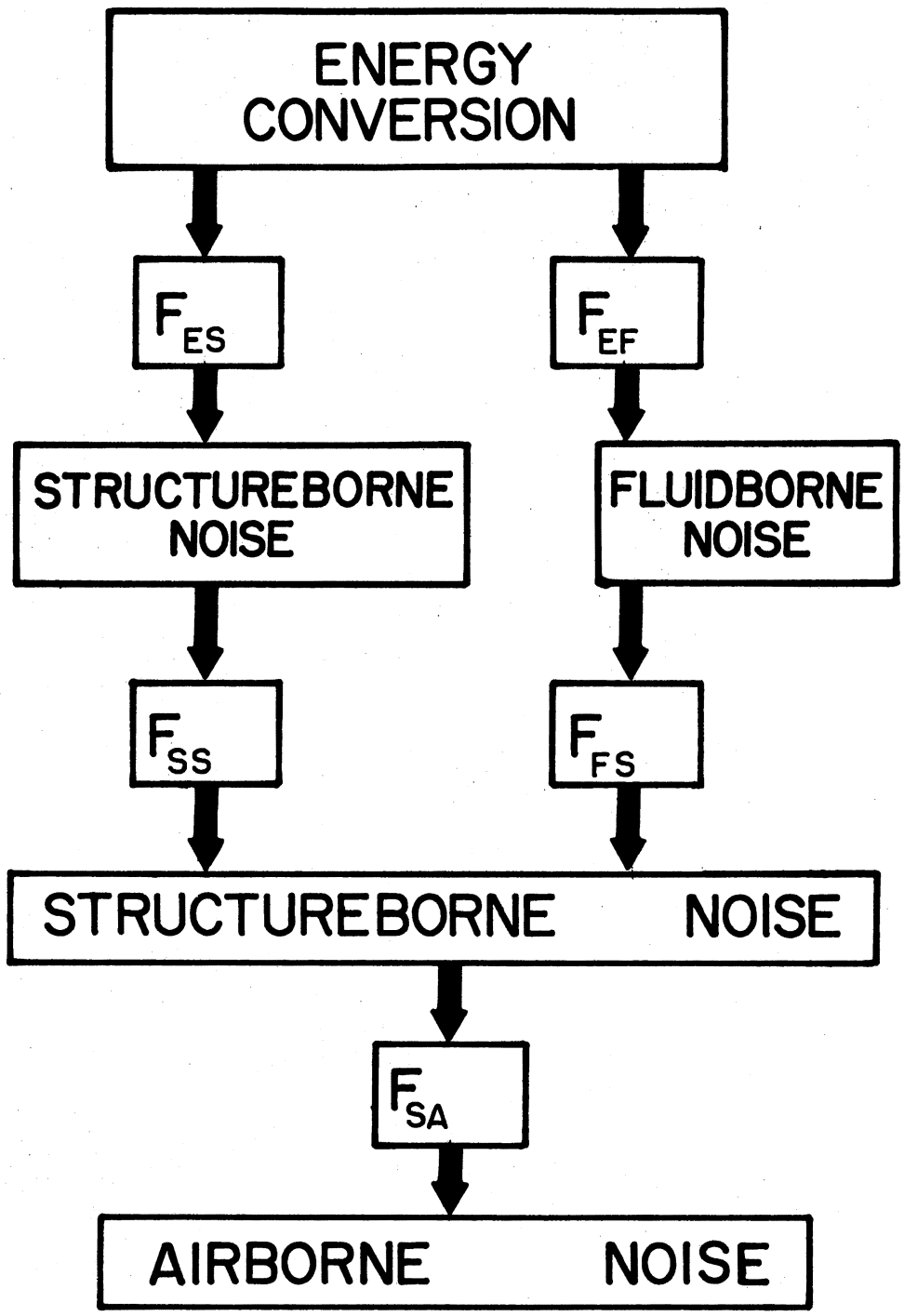

Figure 2. Block Diagram of Functional Relationship Between Airborne Noise and the Energy Conversion Process. (The sound field exists where the airborne noise can be detected.)

to qualitatively discuss the functional relationships necessary to relate pump airborne noise to the energy conversion process (F_{ES}, F_{EF}, F_{SS}, F_{FS}, F_{SA}). Although it is not practical or necessary at this time to consider a complete mathematical relation between the total component sound power level and the energy conversion process, it is practical and necessary to consider qualitatively how the airborne noise at some point on a component is related to the noise generation process.

Ichikawa and Yamaguchi (17) proposed a model for the flow of a hydraulic gear pump:

$$Q = \overline{Q} + \sum_{m=1}^{\infty} q_m \cos m\omega t \qquad (2.3)$$

where:

$\overline{Q}$ = mean flow rate (m^3/s)

q_m = amplitude of the mth component (m^3/s)

ω = angular frequency (rad/s).

This model is a first step toward defining the fluidborne noise which occurs in the inlet or outlet of a pump. It is reasonable to consider a structural noise model similar to Equation (2.3):

$$y = \bar{y} + \sum_{m=1}^{\infty} y_m \cos m\omega t \qquad (2.4)$$

where:

$\bar{y}$ = mean displacement (m)

y_m = amplitude of the mth displacement component (m)

Equation (2.4) would be a multiplier for the function F_{ES} (Figure 3).

The airborne noise being emitted by the component can be traced to at least two significant flow ripple sources and three major mechanical displacement sources. The flow ripple sources are the inlet and outlet fluid regions. The mechanical sources are the meshing area and the two areas where the gears interact with the component walls. The fluidborne noise in a hydraulic pump can be described by coupling Equation (2.3) with other physical characteristics of the pumps and the fluid systems that are connected to the pump inlet and outlet. A model such as proposed in Equation (2.4) could be used to describe structural vibrations in a pump, if the equation were coupled with the proper pump characteristics. Thus a simplified equation which describes the airborne noise, abn, of a pump in terms of the energy conversion process has the form (Figure 3):

$$\begin{aligned} abn_m = F_{SA}(&F_{FS1}\, F_{EF1}\, q_{m1} \cos m\omega(t - \tau_{q1}) \\ &+ F_{FS2}\, F_{EF2}\, q_{m2} \cos m\omega(t - \tau_{q2}) \\ &+ F_{SS1}\, F_{ES1}\, y_{m1} \cos m\omega(t) \\ &+ F_{SS2}\, F_{ES2}\, y_{m2} \cos m\omega(t - \tau_{y2}) \\ &+ F_{SS3}\, F_{ES3}\, y_{m3} \cos m\omega(t - \tau_{y3})) \end{aligned} \qquad (2.5)$$

where:

F_{--i}, q_{mi}, y_{mi}, τ_{qi}, τ_{yi}, $i = 1, 2, 3$, is associated

with the ith noise transmission path originating with either flow or displacement variations. τ_{-i} provides the phase relationship between the resultant noise and the source.

Fluid and Structural Noise Transmission

The airborne noise emitted by any portion of a component is a function of specific interactions and the manner in which the noise of those interactions is transmitted to the emission point. More specifically, the noise is a function of the parts of Equation (2.5), F_{FS1}, F_{EF2}, ..., F_{ES3}.

The amount of energy transmitted through a fluid or solid medium is related to the impedances in the transmission mediums. For example, consider Figure 3, plane wave transmission across two boundaries into an anechoic termination. For the case illustrated in Figure 3 the complex ratio of the incident pressure wave to the final pressure wave is (18):

$$\frac{A_1}{A_3} = \frac{(\rho_3 c_3 + \rho_1 c_1) \cos k_2 \ell}{2\rho_3 c_3} + j \frac{(\rho_2^2 c_2^2 + \rho_3 c_3 \rho_1 c_1) \sin k_2 \ell}{2\rho_3 c_3 \rho_2 c_2} \qquad (2.6)$$

where:

ρ_i = density of the ith medium (kg/m^3)

c_i = sonic velocity in the ith medium (m/sec)

ℓ = thickness of the 2nd medium (m)

k_2 = ω/c_2, wavelength constant of 2nd medium (radians/m)

Kinsler and Frey (18) further show that the noise power transmission coefficient can be expressed in terms of the physical parameters as:

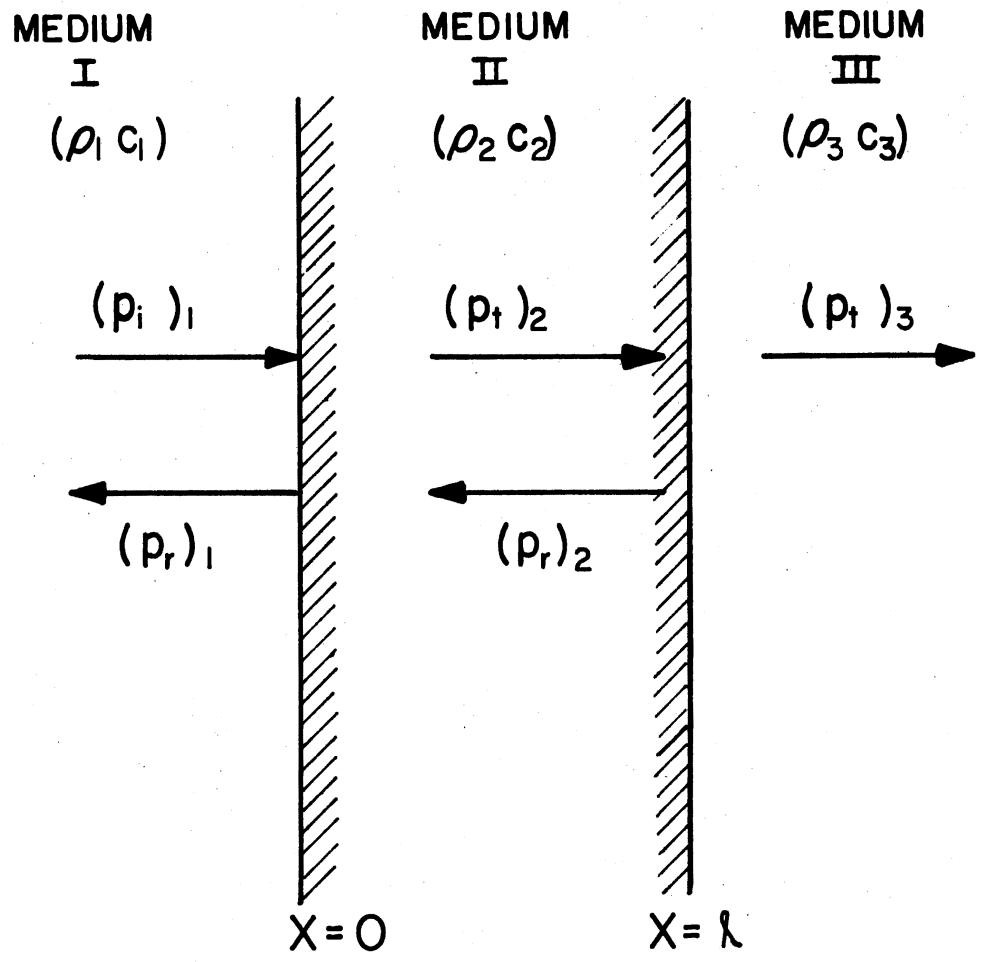

$$\alpha_t = \frac{4\rho_3 c_3 \rho_1 c_1}{(\rho_3 c_3 + \rho_1 c_1)^2 \cos^2 k_2 \ell + \left(\rho_2 c_2 + \frac{\rho_3 c_3 \rho_1 c_1}{\rho_2 c_2}\right)^2 \sin^2 k_2 \ell}$$

Figure 3. Transmission of Plane Waves Across Two Boundaries Into an Anechoic Termination (18)

$$\alpha_t = \frac{4\rho_3 c_3 \rho_1 c_1}{(\rho_3 c_3 + \rho_1 c_1)^2 \cos^2 k_2 \ell + (\rho_2 c_2 + \rho_3 c_3 \rho_1 c_1 / \rho_2 c_2)^2 \sin^2 k_2 \ell} \tag{2.7}$$

where:

$$\alpha_t = \rho_1 c_1 A_3^2 / \rho_3 c_3 A_1^2.$$

Equation (2.6) allows the determination of the actual pressure ratio amplitudes and the phase angle by which the incident wave at $x = 0$ leads the transmitted wave at $x = \ell$. Equation (2.7) allows determination of the amount of energy that is transmitted into the third medium. It is important to note that the noise power transmission is a function of lengths, sonic velocities, frequencies, and material densities. If test parameter variations do not significantly alter the lengths, frequencies, or material properties then according to Equation (2.7) the noise power transmission coefficient is a constant.

Equation (2.6) does not account for any absorption of energy as the waves travel through the various mediums. Absorption occurs in fluids due to structural relaxation, chemical relaxation, viscous losses, heat conduction, molecular energy exchange, and scattering (18). Scattering absorption occurs because of fluid inhomogeneities such as suspended particles or bubbles. Since air bubbles can occur in hydraulic system liquids (9), pump noise levels can be affected by absorption changes associated with test parameter variations.

The intensity, I_ℓ, at some position, ℓ, can be related to the intensity at $x = 0$, I_o, by the following equation (18):

$$I_\ell = I_o e^{-\alpha \ell} \tag{2.8}$$

where:

e = constant (2.718, base of natural system of logarithms)

α = attenuation factor

The attenuation factor is generally a function several parameters such as frequency, area, density, sonic velocity, or the coefficient of shear viscosity. Even though the exact absorption characteristics of hydraulic fluids are not known it is reasonable to expect significant changes in α as test system parameters are varied. If the absorption factor is insignificant then the term $e^{-\alpha \ell}$ is approximately 1 and does not alter the transmitted power. However, as the attenuation factor, α, increases then the term $e^{-\alpha}$ becomes less than 1 and the transmitted power decreases. In the latter case less power is available at the component surface to be radiated as airborne noise.

Radiation

The final factor that describes the airborne noise in terms of the energy conversion process in the component is the term F_{SA} in Equation (2.5). This is the term that relates how the structural vibrations are radiated into the sound field.

Baranek (19), during his discussion of the radiation field of a sound source uses a classic illustration such as the one shown in Figure 4. This figure shows qualitatively how the sound pressure level varies as a function of the radius from the noise source. The near-field may exhibit large variations of sound pressure level at the same radius from the source. The far-field is divided into two regions, the free-field and the reverberant field. When it exists, the free-field exhibits approximately 6 db drop of the sound pressure level for a doubling of the radius from the source. The reverberant field exhibits large variations of the sound pressure level at the same radius from the source.

Both McCandlish et al. (20) and Chan et al. (21) correlated free-field pressure level measurements with structure-borne measurements. Their interest in this correlation was prompted by the basic relationship between intensity, pressure level, and surface velocity which for a pulsating sphere is (18):

$$I = \frac{P^2}{2\rho_o c} = \frac{\rho_o c\, k^2\, a^4\, u_o^2}{2\, r^2} \qquad (2.9)$$

where:

a = radius of pulsating sphere (m)

P = pressure at radius r from sphere (N/m^2)

ρ_o = equilibrium density of medium (kg/m^3)

u_o = velocity amplitude of spherical surface (m/s)

r = radius from sphere (m)

As noted by McCandlish equations of the form of Equation

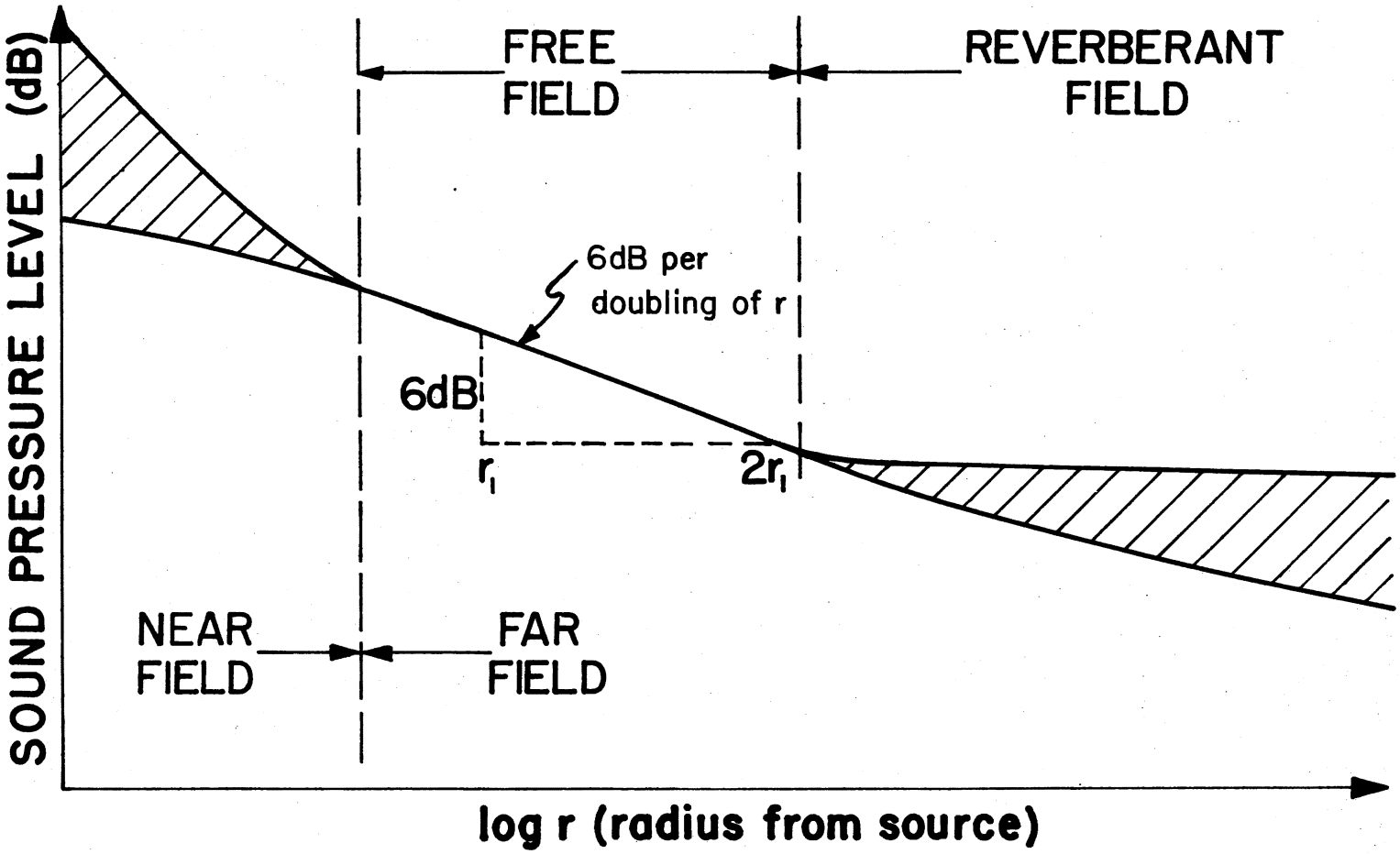

Figure 4. Sound-Pressure Level Variation in an Enclosure Along a Radius, r, From a Noise Source. (Shaded Areas Indicate Regions Where Sound Pressure Level Fluctuates Most With Distance.)

(2.9) imply that for normal ambient conditions pressure level is proportional to surface velocity. McCandlish et al. (20, p. 46) stated the following regarding the correlation they found between pressure level and surface velocity:

> The spectral correlation of sound pressure level and surface vibration velocity for both the No. 1 pump and the No. 2 pump was very good, provided the accelerometer was located at a suitable point on the pump casing. The optimum point can only be found empirically by testing the pump in an anechoic chamber.

Chan et al. (21, p. 266) after analyzing their data on an engine and a heading machine, drew the following conclusion:

> The mean square sound pressure radiated is proportional to mean square vibration acceleration below 400 Hz and proportional to mean square vibration velocity above this frequency, for structures with surface areas in the range 1000 to 4000 in^2.

The "mean" vibration measurements referred to by Chan were compiled from over a hundred individual structureborne measurements. Thus, there is enough correlation between pressure levels and surface velocity measurements to indicate that on the "average" the trend of Equation (2.9) is valid in the free-field above 400 cycles/second.

The existence of the free-field is dependent on the environment having quasi-anechoic boundaries. Although it is possible to test pumps in an "anechoic" environment in the laboratory, there is little probability that they will operate in "anechoic" environments in the field.

Most acoustical field environments for hydraulic pumps will be reverberant. It should be noted that the pressure

level in both the free and the reverberant field is less than or equal to the pressure level in the near-field. Thus, the pressure measurements in the far field are more susceptible to background noise changes than measurements in the near-field.

Since the free-field cannot be guaranteed, both the near and reverberant fields might exhibit large measurement standard deviations, and the near-field is less susceptible to background noise, the near-field is the best candidate for airborne noise measurements "in-situ".

The Near-Field

An examination of the radiation characteristics of a flat piston provides a basic understanding of the behavior of the near-field. The radiation equations shown below were derived assuming a rigid circular piston which is mounted flush with the surface of an infinite baffle. The piston is assumed to be vibrating with simple harmonic motion, $u = u_o \cos \omega t$ (18). Figure 5 illustrates the critical dimensions associated with the vibrating piston. Anticipating the manner in which near-field measurements might be used it is reasonable to make the angle θ equal to zero and, r, the distance from the source along the x-axis very small. For these assumptions the axial intensity can be expressed as (18):

$$I_o = 2\rho_o c\, u_o^2 \sin^2 \frac{k}{2} \left(\sqrt{r^2 + a^2} - r\right) \qquad (2.10)$$

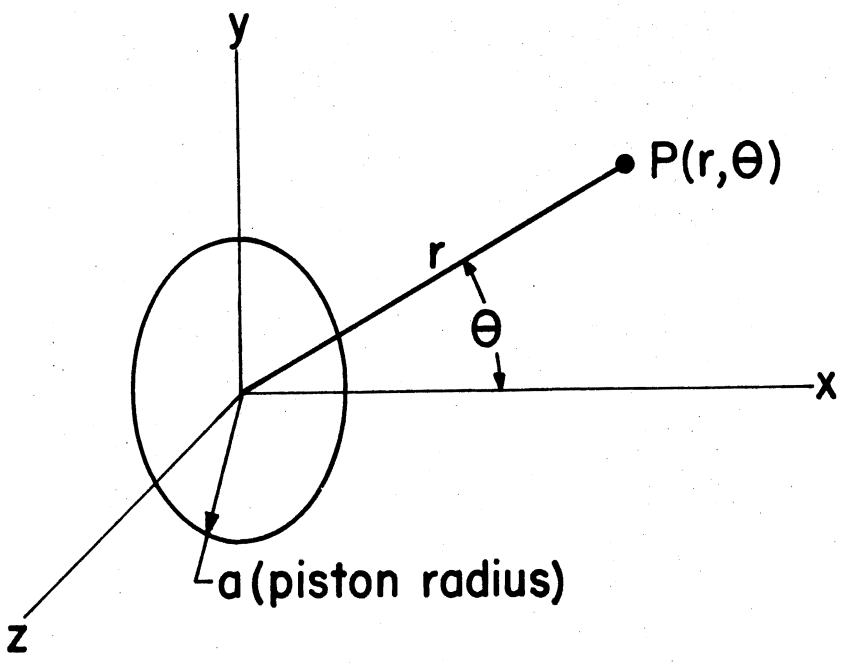

Figure 5. Coordinate System and Critical Dimensions Associated With Radiating Piston and Measurement Point, P (18)

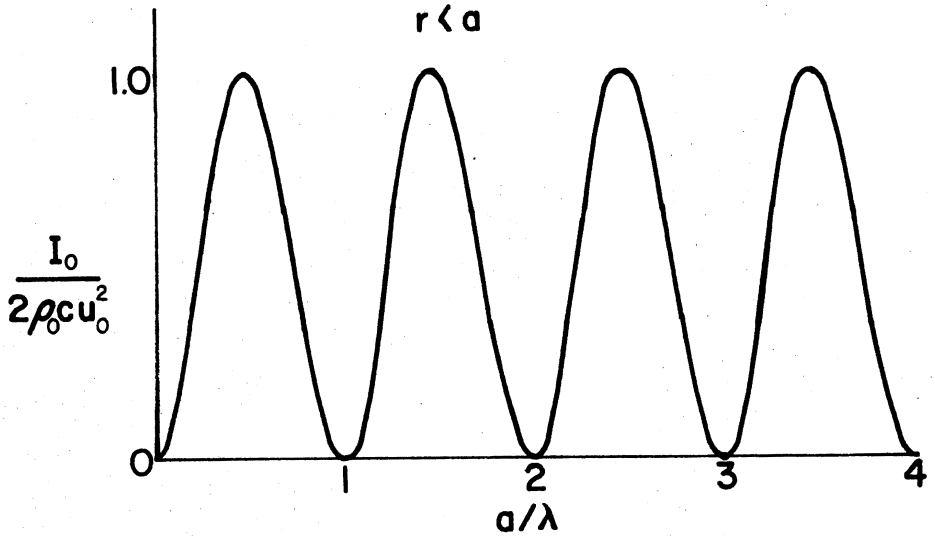

Figure 6. Axial Intensity Ratio at a Fixed r as a Function of Piston Radius Divided by Wave Length Showing Zero Intensity Frequency

where:

u_o = velocity amplitude of the piston surface (m/ second)

r = distance from piston along x-axis (m)

a = radius of piston (m)

k = $2\pi/\lambda = \omega/c$

λ = wavelength, f/c (m)

When $r < a$ or $r \approx 0$ and when k in Equation (2.10) is replaced by $2\pi/\lambda$ the result is:

$$I_{o(r=0)} = 2\rho_o c\, u_o^2 \sin^2 \frac{a\pi}{\lambda} \qquad (2.11)$$

Consistent with Equation (2.11) Figure 6 shows that on the x-axis of the hypothetical piston, at a fixed distance, r, there are frequencies at which the intensity will be zero. This theoretical zeroing of the intensity, due to interactions between waves radiated from different portions of the piston, occurs at discrete points in space.

It is interesting to consider those piston radii or the first few frequencies at which Equation (2.11) predicts the intensity along the piston axis goes to zero. The basic relationship to be considered is a/λ. This can be rewritten as af/c. Thus, for a sonic velocity in air of 340 m/second and a frequency of 100 Hz the critical radius is 3.4 m. Likewise for 10,000 Hz the critical radius is 34 mm. If the piston radius is given as 0.1 m then the first critical frequency is 3400 Hz, the second is 6800 Hz, the third is 10,200, and the fourth is 13,600 Hz. For any specific

configuration the critical frequencies can readily be estimated.

After completing their discussion of pressure along the piston axis, Kinsler and Frey (18, pp. 176-177) discourage the use of near-field measurements:

> As a result of the fluctuations in intensity that occur in the immediate vicinity of any extended radiator, measurements of the acoustic radiation from a loudspeaker or sonar transducer should not be made with the measuring microphone placed close to the vibrating surface.

This is probably good advice when the capital is available to insure that all acoustic measurements of the source can be obtained in a controlled laboratory environment. But it is poor advice in general since it may discourage the use of near-field noise measurements in cases where they are the only practical means of obtaining meaningful information.

There are two reasons why near-field measurements may provide a viable measurement technique. First, there is nothing in the equations that implies that at a fixed radius on the piston axis the measurement technique will increase the measurement standard deviation. The equations do imply that the measurements in the near-field are more sensitive to deviations of the displacement than measurements in the free-field. Second, the principle reason that the mathematics only considered the intensity along the piston axis is:

> . . .the general case of the pressures and intensities at a point near a piston source is too difficult for mathematical analysis, and our discussion will therefore be limited to points on the axis of a circular piston (18, p. 775).

The arguments which warn against near-field measurements because of predicted zero pressure levels on the piston axis would seem more significant if microphones were infinitely small. However, since microphones (the transucer for near-field measurements) have a finite diameter they sense the overall effect of various pressures acting over their entire surface. Thus, a microphone of finite diameter should detect, at every location in the near-field of a piston, the existence of any finite acoustic intensity, because even if the acoustic intensity is zero at a point on the piston axis, the pressure transducer integrates the effects of the energy radiated through the measured medium to the measurement surface.

It is not an objective of this study to mathematically or statistically defend the general utility of near-field airborne noise measurements. After reviewing the literature and successfully using near-field measurements for this study, it is apparent to this writer that the area of near-field measurements deserves further exploration, both experimentally and mathematically. A discussion of near-field airborne measurements was necessary in this chapter because such measurements were made during the experimental phase of this study. Airborne near-field noise measurements were used because they exhibited satisfactory repeatability and reproducibility for system diagnostic purposes.

Acoustical Signatures

Equation (2.5) is based on the premise that an

identifying characteristic noise spectrum or acoustical signature of a particular pump operating at specified test conditions in a known environment is related to the energy conversion process. The identifying spectrum of level versus frequency may be associated with an inlet pressure, an outlet pressure, a structureborne measurement, or an airborne noise level. Several noise signatures of pressure level, displacement level, velocity level, and acceleration levels are shown in Appendix F, Selected Experimental Results. The filters used for the signatures in Appendix F were 10 hertz, 100 hertz, and 1/3 octave, which is discussed more fully in Chapter III. But, it should be noted that the spectra are also a function of the instrumentation used for recording level versus frequency.

The remaining objectives of this chapter are to discuss wear and cavitation theories that appear directly applicable to pump acoustical signature analysis and summarize what system variables are expected to affect pump noise generation.

Wear

Hydraulic component inefficiencies manifest themselves as heat, wear, and noise (22). Flow ripple, structural impacts, and wear are all prime suspects as noise generators. Flow ripple probably will not alter the form of mechanical parts, although it may accelerate fatigue. Impacting will alter the shape of the mechanical parts. Wear,

by definition, will remove material, thus altering the configuration of mechanical parts. Since noise at a given time is directly related to the shapes of the mechanical structures and the manner in which they interact (4), then as the mechanical structure changes so will the noise.

Wear Versus Time

Wear rate as a function of component operating time follows a curve of the form shown in Figure 7 (23), (24). The wear rate is high during the "break-in" period and decreases to an essentially constant value until normal wear-out begins. During the wear-out period the wear rate increases until the component is taken out of service or experiences catastrophic failure. The three sketches in Figure 8 show hypothetical gear profiles during "break-in", normal operation, and normal wear-out. These gear profiles are probably more representative of forged gears than shaped gears such as those used in gear pumps, but the profiles serve the purpose of illustrating the basic wear surfaces. The high wear rate during the first hours of operation may be due to surface asperities being worn from the original profile. During normal, relatively quiet, operation a finite amount of material is constantly being removed because of normal wear processes. During normal wear-out profile changes probably cause an increase in the wear rate because gear profile ireegularities will increase the sliding action between the gears.

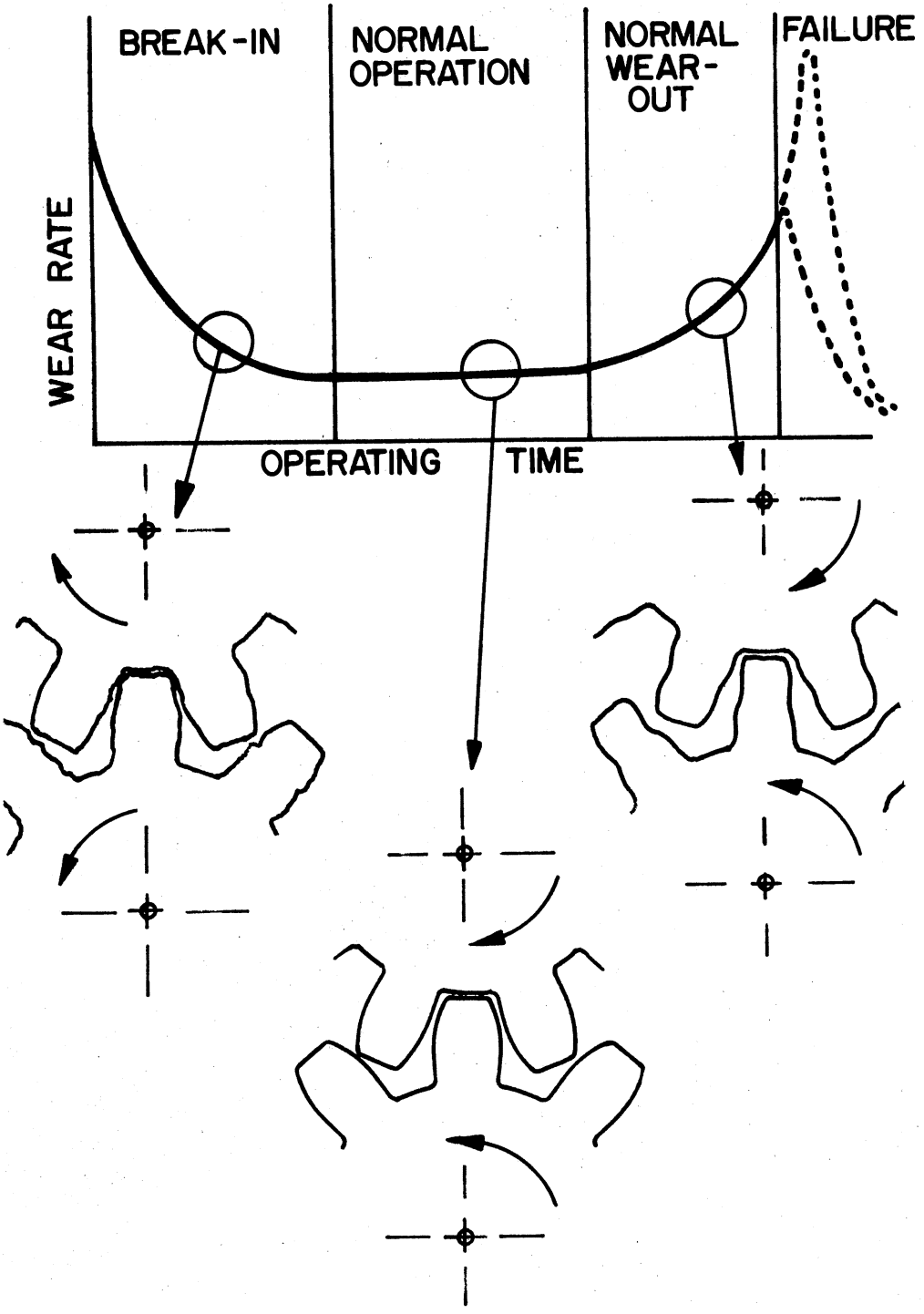

Figure 7. Wear Rate Curve as a Function of Operating Time

Given that the wear rate versus time behaves as shown in Figure 8, what does this mean about noise versus time? The correlation of noise and wear should help answer this inquiry.

Noise Versus Wear

Lavoie (24) cites a case where surface abnormalities were introduced in the outer races of a bearing so that noise measurements with and without the surface damage could be compared. The noise trace of the bearing with the damaged race is significantly noisier than the bearing's acoustical signature without the damaged race.

Downham and Woods (25) show that increased noise levels from operating machinery can be associated with increased machine wear. For two cases discussed in their paper, "The Rationale of Monitoring Vibration on Rotating Machinery in Continuously Operating Process Plant", they present data which shows that worn machinery has higher than "normal" noise levels. For one machine, allowed to fail without repair, the noise level continued to increase until failure. When noise monitoring indicated excessive wear in another machine, the machine was repaired, and the noise level returned (decreased) to a "normal" level.

These examples indicate that worn machinery has higher than "normal" noise levels. More specifically, intentionally damaged machinery and worn machinery, allowed to operate while damaged, exhibit higher than "normal" noise levels.

Examination of Figure 8 shows that the wear rate is high during the normal wear-out period. Integration of the wear rate curve reveals that the wear is approaching a maximum during the normal wear-out period. Hence, during wear-out high noise levels occur simultaneously with both high total wear and high wear rates. During the break-in period there is relatively little total wear and there is a higher than normal wear rate. If there were documented evidence that component noise levels were higher than "normal" during break-in then it could be concluded that noise levels are directly related to wear rate.

Since there is no known data relating noise and wear during component "break-in", it is necessary to base noise-wear theories partially on conjecture. Noise is related to the power generated by the source inefficiencies. The power being generated by component inefficiencies is directly related to the wear rate. Hence, it is reasonable to assume that the noise from a component is related to the wear rate.

As the component wears the mechanical parts will change. Leakage paths will increase, clearances will increase, part configurations will be modified. As these parameters change the noise level will also change. Thus, it is reasonable to hypothesize that the noise from a component is related to the total wear.

Combining the hypotheses that the noise level of a component is related to both the wear rate and the total wear leads to the following relation:

$$abn_m = C_1 + C_2 W + C_3 \dot{W} \qquad (2.12)$$

where:

abn_m = airborne noise at mth harmonic (watts)

C_1 = "normal" noise without wear (watts)

C_2 = wear coefficient (N/sm^2)

C_3 = wear rate coefficient (N/m^2)

W = total wear (m^3)

$\dot{W}$ = wear rate (m^3/s)

Equation (2.12) recognizes three terms which could dominate the noise being emitted by a component. If there is no wear occurring and none has occurred then the dominant term is C_1. If the wear rate is essentially zero, significant total wear has occurred, and the product $C_2 W$ has an absolute magnitude much greater than C_1, then the wear related term is dominant. When the wear rate is extremely high, such as during failure, the third term of the equation probably dominates the noise from the component.

Noise Versus Time

Assuming that the component noise level is related to the wear as indicated by Equation (2.12), the general behavior of the noise level as a function of time can be hypothesized. Generally, as a component wears the noise level at a given harmonic should decrease, then may or may not "level-off" and will ultimately increase during machine failure.

Figure 8(b) displays the hypothesized behavior of three

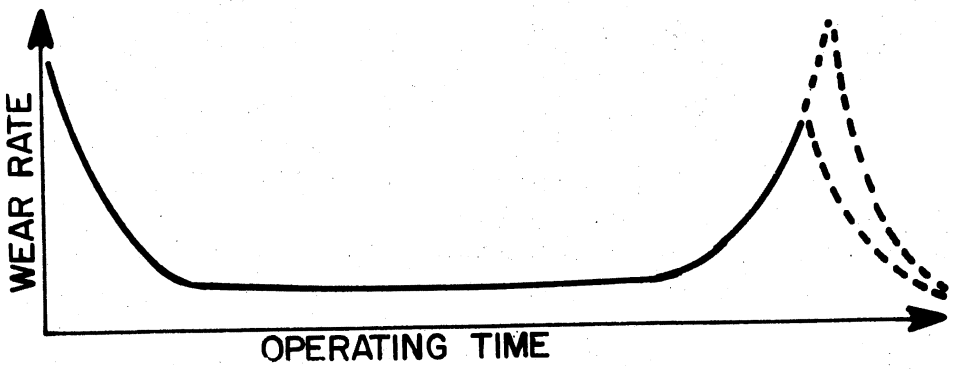

(a) Wear Versus Operating Time

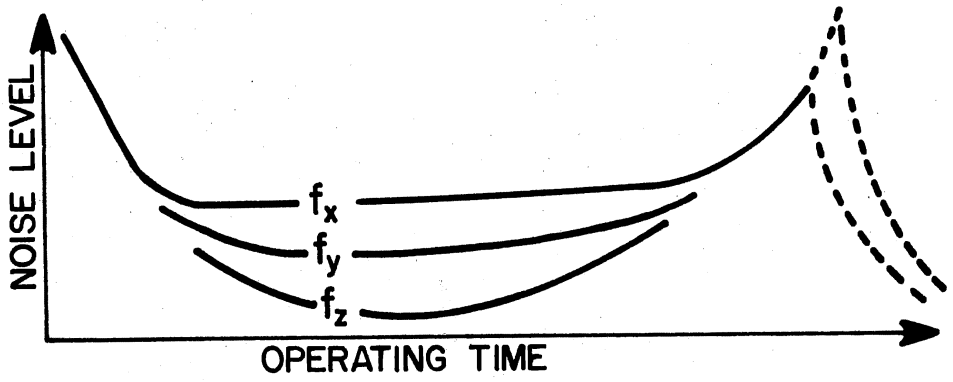

(b) Noise Level Versus Operating Time

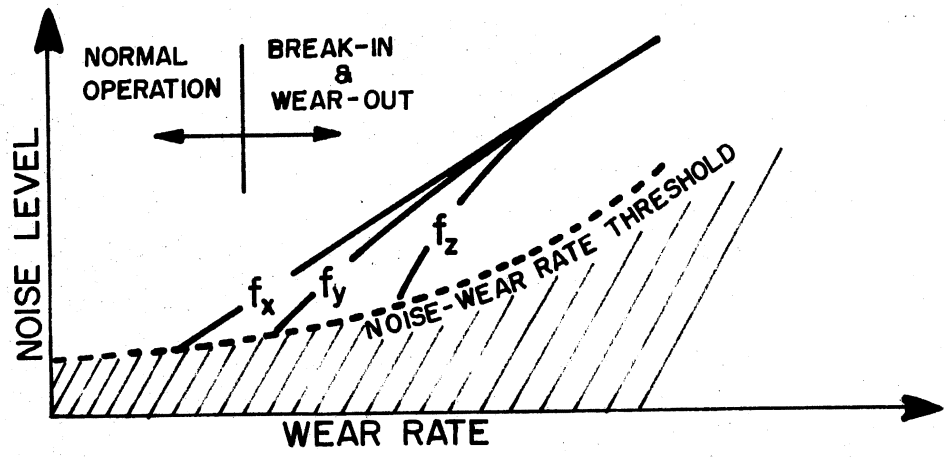

(c) Noise Level Versus Wear Rate

Figure 8. Hypothesized Noise Level Versus Operating Time at Arbitrary Pumping Harmonics and Noise Level Versus Wear Rate

harmonics (f_i, i = x, y, z) of the noise signal as a function of time. If some of the harmonics behave much like the wear rate there will be a one-to-one relation between the wear rate and the noise level of those harmonics, as illustrated by the curve for f_x in Figure 8(c).

The hypothetical model for noise level versus wear rate, shown in Figure 8(c), indicates that at a given wear rate for the ith harmonic the noise level could be used as an indication of incipient failure. Noise levels below the noise-wear rate threshold are not necessarily indicative of a particular wear rate because the region below the threshold is dominated by the first two terms of Equation (2.12). In other words, noise levels above the threshold are dominated by wear rate factors. General Electric successfully monitored incipient failure of ball bearings using noise measurements (24).

In summary the noise versus time behavior of a wearing component is hypothesized to follow qualitatively the trends indicated in Figure 8(b). This hypothesis is supported by experimental evidence obtained during normal operation, normal wear-out, and failure (24) (25).

Wear Models

Since the noise and thus the acoustical signatures of pumps is dependent on wear, a review of wear models should isolate parameters to be considered in noise studies. Wear models can be divided into three categories, Force Models,

Energy Models, and Contaminant Models.

Force Model. The force model for wear has the basic form (22) (26):

$$\frac{V}{L} = C \frac{P}{H} \tag{2.13}$$

where:

V = total wear volume (m^3)

L = distance traveled during wear process (m)

C = wear law constant (non-dimensional)

P = normal applied load (newton)

H = hardness (flow pressure, newton/m^2)

This model indicates that the ratio of the total wear volume to the distance traveled is directly related to the applied load. In a high pressure pump the load is related to the torque, or the system pressures, both inlet and outlet. The distance traveled would be related to the shaft speed and the total component operating time.

Halling (26) gives the following expression for C in Equation (2.13):

$$C = \frac{0.001^n \eta\gamma}{\pi \bar{\epsilon}_1^m} \frac{(\sigma\lambda)^{(t-n+m-2)/2}}{\beta^{(2+m-n+t)/2}} \left(\frac{K}{\pi B_c}\right)^{(m+t)/n-1} \frac{(\frac{m+t}{2})!}{(1+\frac{n}{2})!} \tag{2.14}$$

where:

C = wear law constant

n = index defining work-hardening

η = line distribution of asperities

γ = constant defining particle size

$\bar{\epsilon}_1$ = strain to failure in one loading cycle

m = constant in fatigue failure criteria

σ = standard deviation of ordinate distribution

λ = constant defining size of single contact

t = index defining wear particle size

m = constant in fatigue failure criteria

β = radius of asperity

K = constant defining load/area relation

B = stress/strain constant

c = constant defining stress

All of the terms in Equation (2.14) are related to material properties and material surface descriptions. Halling's complex force model for wear implies that pump speed, total operating time, and system pressures are the only operating and environmental parameters that will affect wear.

Thompson and McCullough present a dynamic model for gear wear relative to pinion speed (7). They refer to the model as being "coupled", because the model incorporates the concept that the dynamic loads resulting from wear perturb the wear rate. The coupled wear equation is (7):

$$\frac{dW}{dN} = C\ p_o\ V_s\left[T + \frac{2\ I_R\ I_r\ r_o^2\ \omega^2}{I_R\ r_o^2 + I_r R_o^2}\ \frac{d^2W}{dX^2}\right] \qquad (2.15)$$

where:

W = tooth wear (m)

N = pinion speed (rev/s)

C = wear constant (s/N)

p_o = tooth load factor

V_s = tooth sliding velocity (m/s)

I_R = gear polar moment of inertia (kg s^2 m)

I_r = pinion polar moment of inertia (kg m s^2)

r_0 = pinion pitch radius (m)

ω = pinion speed (rad/s)

X = tooth contact point on line of action (in)

T = transmitted torque (Nm)

R_0 = gear pitch radius (m)

According to Equation (2.15) the only operating parameters that will affect wear, and thus noise, are speed and torque. Thus, all of the force models for wear considered in this section imply that on a hydraulic pump the operating and environmental parameters that will affect pump noise are speed, pressure, and total operating time.

Energy Model. Suh and Sridharan consider the frictional work done during the wear process in their paper, "Relationship Between the Coefficient of Friction and the Wear Rate of Metals" (27). In terms of operating and environmental parameters the important result in equation form is:

$$W^e = \frac{L\ S_o \mu}{n} \qquad (2.16)$$

where:

W^e = frictional work done (Nm)

L = normal load (N)

S_o = distance slid to create n wear sheets (m)

μ = coefficient of friction

n = number of wear sheets

This model implies that parameters affecting the coefficient of friction will affect the wear process. Since the fluid viscosity will affect the coefficient of friction, viscosity changes will influence the wear process. In terms of operating and environmental parameters the type of fluid and its temperature will determine the viscosity and thus are important parameters to monitor in noise studies. Note that the energy model also includes, by implication, the pump speed, total operating time and system pressures as critical wear parameters.

Contaminant Model. The importance of contaminant wear in hydraulic systems was recognized by the fluid power industry and the Fluid Power Research Center long before the "center" began formal studies of contaminant wear control in 1962 (28). Several contaminant wear models have been proposed by the "Center" during the past decade. The most apropos and neoteric contaminant wear model is (29):

$$Q_L = Q_0 e^{-\alpha \tau n_0^2 (1 - e^{-2t/\tau})} \qquad (2.17)$$

where:

Q_L = the flow at time t in the laboratory (m^3/s)

Q_0 = the initial flow (m^3/s)

α = contaminant wear coefficient $\left(\frac{m^6}{(particles)^2 s}\right)$

τ = time constant of particle destruction process (s)

n_0 = the initial particle concentration ($particles/m^3$)

t = time (s)

Equation (2.17) provides an estimate of the flow rate of a hydraulic pump while operating in a controlled contaminated environment at rated speed and pressure. Indirectly this equation provides the flow degradation due to the initial particle concentration or system contaminant level. This flow degradation is attributed to wear processes which are accelerated by the presence of particulate contaminant (30). Therefore, the fluid contamination level is an environmental parameter that should be monitored during pump wear and noise tests.

The three wear models considered in this section indicate that the following operational and environmental parameters should be monitored during pump wear and noise tests: pump speed, pump inlet pressure, pump outlet pressure, fluid viscosity (fluid and temperature), fluid contamination level, and operating time.

Accelerated Wear

Fitch (29, p. 131) states, when referring to Equation (2.17):

> Pump tests have shown that the time constant (tau) for the particle breakdown process is approximately equal to nine minutes, regardless of the type of pump or size of contaminant.

This fact suggests that if it is desired to evaluate the effectiveness of noise monitoring to determine the total wear of a component then an accelerated test, normally used to evaluate the contaminant wear coefficient, could be used in the laboratory to greatly reduce the total time required

to reach a given state of wear for a hydraulic pump.

Since the evaluation of acoustical signature analysis as a wear monitoring technique would require several samples, the use of a standard, repeatable test procedure would reduce the variation between samples. Fitch (29, p. 128) makes the following statements about the standard test procedures for measuring component contaminant sensitivity:

> These formal tests for pumps, motors, valves, cylinders and linear seals provide repeatable and reproducible methods for accurately assessing the components' contaminant tolerance. . . . The test procedure for a pump has been shown to be equally effective on all high-pressure types-gear, vane, and piston.

The contaminant test for pumps to which Fitch refers is currently being used by industry and is a proposed national standard test procedure (32). Certainly, for controlled, accelerated wear tests the test code (32) should be used to achieve the best practical repeatability.

Noise Wear Index

It has been hypothesized that the noise emitted by a component is related to the total wear and the wear rate of the component. It has been shown that the noise from a component will be greater during wearout and failure. Since noise monitoring offers the potential of indicating incipient failure, a critical question is: "If acoustical signature analysis can indicate the wear state of a hydraulic pump, how might the 'signature' be interpreted to provide a Noise Wear Index?"

Figure 8(b) suggests that the ratio of the pumping harmonic levels will vary during the life of the component. The following paragraphs define a Noise Wear Index (NWI) based on variations of the pumping harmonic noise levels with time (wear).

James V. Shott (31) introduced a technique for acoustical signature analysis which ratios the frequency of the noise level at each frequency to the first order shaft frequency. The resultant ratio is called a Signature Ratio (31). Noise levels are then plotted versus a Signature Ratio (31) rather than frequency. Since the dominant noise energy emitted by a hydraulic pump is usually associated with the pumping fundamental (5) and its harmonics (which are also harmonics of the first order shaft frequency), it seems more practical for the development of a pump Noise Wear Index to reference the harmonic noise level frequency to the fundamental pumping frequency. Such normalization will mask small variations in speed between tests, since only frequency ratios are reported. In other words, the fundamental pumping frequency will always be reported as one. Large variations of speed could significantly affect the noise levels. Therefore, data associated with large speed variations from the specified test speed should initially be excluded from the Index. In the future it might be desirable to determine if the NWI is independent of test speed.

While using frequency ratios may obscure the actual

frequencies associated with a test, the concept of using level ratios or referencing one level to another is desirable since the latter could act to minimize the effects of minor environmental changes, slight calibration variations, and small transducer location deviations. This approach suggests that all levels at a given time be referenced to the noise level at one frequency, the fundamental for instance. Since the objective is to monitor the percent wear or the flow degradation, then any change in a level at a given harmonic could be noted by comparing the level at some ith sample time to the level of the same harmonic at an earlier time. Since there will undoubtedly be a noticeable standard deviation in the component noise measurements at individual frequencies (33), any Noise Wear Index should provide a means for "smoothing" the data to minimize the effects of data scatter.

The following paragraphs outline the procedure for obtaining a Noise Wear Index for hydraulic pumps. At each sample time there will be a noise vector, L_i', composed of m noise levels, where m is the number of harmonics being studied. After several acoustical signatures have been recorded there will be a data matrix of the form:

$$L' = \begin{matrix} L_{11} & \cdots & L_{1m} \\ \vdots & & \vdots \\ L_{n1} & \cdots & L_{nm} \end{matrix} \qquad (2.18)$$

where:

L' = the data matrix

L_{ij} = the level associated with the jth harmonic of the ith sample (dB)

i = index for the sample number, i = 1, 2, 3, ..., n

j = index for the harmonic number, j = 1, 2, 3, ..., m

n = total number of samples

m = total number of harmonics

This "raw" data set should be "smoothed" by relating the data with an equation to the significant variable (time or flow degradation). Associated with the ith sample there is a corresponding amount of wear. This wear of the pump can be related to the flow, Q_i, at some sample time, t_i, relative to the rated flow, Q_r, measured when the pump was new. Field use of a noise wear index is dependent on monitoring noise as a function of time. The analysis of a noise wear index is accomplished by relating the noise to component wear, or in the case of a pump, relating the noise to flow degradation. For analysis purposes the best estimate of the noise level at a given harmonic as a function of Q_i/Q_r, (Q^*), is not the experimental data, but the value of the level calculated using an equation developed from the experimental data. For monitoring purposes the best estimate of the noise level at a given harmonic as a function of operating time is a level calculated using an equation based on the field data. Thus, for monitoring or analyzing, the data matrix can be modified to:

$$M' = \begin{matrix} M_{11} & \cdots & M_{1m} \\ \vdots & & \vdots \\ M_{n1} & \cdots & M_{nm} \end{matrix} \qquad (2.19)$$

where:

M' = the modified data matrix

M_{ij} = the curve fit estimate of the noise level at the jth harmonic at the ith time (dB)

The M_{ij} are estimated using a curve fit (34), (35) to an appropriate equation for analyzing or monitoring. For instance, for monitoring the equation form might be:

$$M_{ij} = Z \log_{10}\left[a_{ij} (t_i)^{b_{ij}} + c_{ij} + d_{ij} (t_i)^{f_{ij}}\right] \qquad (2.20)$$

where:

a_{ij} = constant based on all data for the jth harmonic, i = 1, ..., n

b_{ij} = coefficient based on all data for the jth harmonic, i = 1, ..., n

c_{ij} = constant based on all data for the jth harmonic, i = 1, ..., n

d_{ij} = constant based on all data for the jth harmonic, i = 1, ..., n

f_{ij} = coefficient based on all data for the jth harmonic, i = 1, ..., n

t_i = equivalent operating time at specified test conditions for the ith sample

Z = an appropriate constant dependent on the

noise variable

For analysis the equation for M_{ij} might be:

$$M_{ij} = Z \log_{10} \left[a_{ij} \left(Q_i / Q_r \right)^{b_{ij}} \right] \qquad (2.21)$$

The next step in developing the proposed Noise Wear Index is to reference each harmonic value at the ith sample to the value at the fundamental pumping frequency for the ith sample. This process produces a matrix with zeros in column one:

$$R' = \begin{matrix} 0 & r_{12} & \cdots & r_{1m} \\ \cdot & \cdot & \cdots & \cdot \\ 0 & r_{n2} & \cdots & r_{nm} \end{matrix} \qquad (2.22)$$

where:

$$r_{ij} = M_{ij} - M_{i1} \qquad i = 1,n \; ; \; j = 1,m$$

Since the M_{ij} are in dB, the r_{ij} are also in dB and represent $Z \log_{10} (m_{ij}/m_{i1})$, where the m_{ij} are values of the noise in appropriate units with Z being the appropriate multiplier for the noise variable. The point to be noted is that the subtraction of the matrix entries in dB does represent taking a ratio as was deemed desirable. The seeming chicanery of using matrix values in dB should appear rational after considering the chapters which discuss experimental considerations and the analysis of experimental results. Next the data for each harmonic is referenced to the first level recorded for the jth harmonic. The new matrix is:

$$S' = \begin{matrix} 0 & 0 & \cdots & 0 \\ 0 & s_{22} & \cdots & s_{2m} \\ . & . & \cdots & . \\ . & . & \cdots & . \\ 0 & s_{n2} & \cdots & s_{nm} \end{matrix} \qquad (2.23)$$

where:

$$s_{ij} = r_{ij} - r_{1j} \qquad j = 1,m \; ; \; i = 1,n$$

Each s_{ij} represents an estimate of the deviation at the ith sample of each of the m harmonics from the initial value of the respective harmonic. This S' matrix can be further refined by curve fitting the s_{ij} in a manner similar to that used to obtain M' with Equation (2.20) or (2.21). The resultant matrix:

$$T' = \begin{matrix} 0 & 0 & \cdots & 0 \\ 0 & t_{22} & \cdots & t_{2m} \\ . & . & \cdots & . \\ . & . & \cdots & . \\ 0 & t_{n2} & \cdots & t_{nm} \end{matrix} \qquad (2.24)$$

is composed of t_{ij} which replaced the s_{ij} with best estimates based on the appropriate monitoring or analysis curve fit. The Noise Wear Index is defined as:

$$N_i = - \sum_{j=1}^{m} |t_{ij}| \qquad (2.25)$$

where:

N_i = the Noise Wear Index for the ith sample

The first index, N_1, will always be zero. The use of the absolute value of t_{ij} insures that the Noise Wear Index accounts for any changes in the noise level. The negative sign provides the Index with a sign which is consistent with a degradation of performance.

The general trend of the wear versus time curve (Figure 8(a)) and the hypothesized similarity of the noise versus time curve for the pumping harmonics suggests that during normal wear-out the proposed Noise Wear Index could approach zero. See Figure 9. This possible zeroing of N_i leads to the consideration of a Cumulative Noise Wear Index (CNWI) as a more meaningful diagnostic device. The CNWI is defined as:

$$C' = \sum_{k=1}^{p} N_k \, \Delta\beta_k \qquad (2.26)$$

where:

$\Delta\beta_k$ = increment of the independent variable (t or Q*)

k = index for samples of N for CNWI

p = total number of samples of N for CNWI

To provide an accurate estimate of C' the interval between samples of N for the CNWI should be kept "small" when N is changing rapidly as a function of the independent variable. Keeping the sample interval "small" requires apriori knowledge of the behavior of the Noise Wear Index or curve fitting the experimental data. Curve fitting the experimental data would allow integration of the Noise Wear Index with respect to the independent variable. This procedure involves

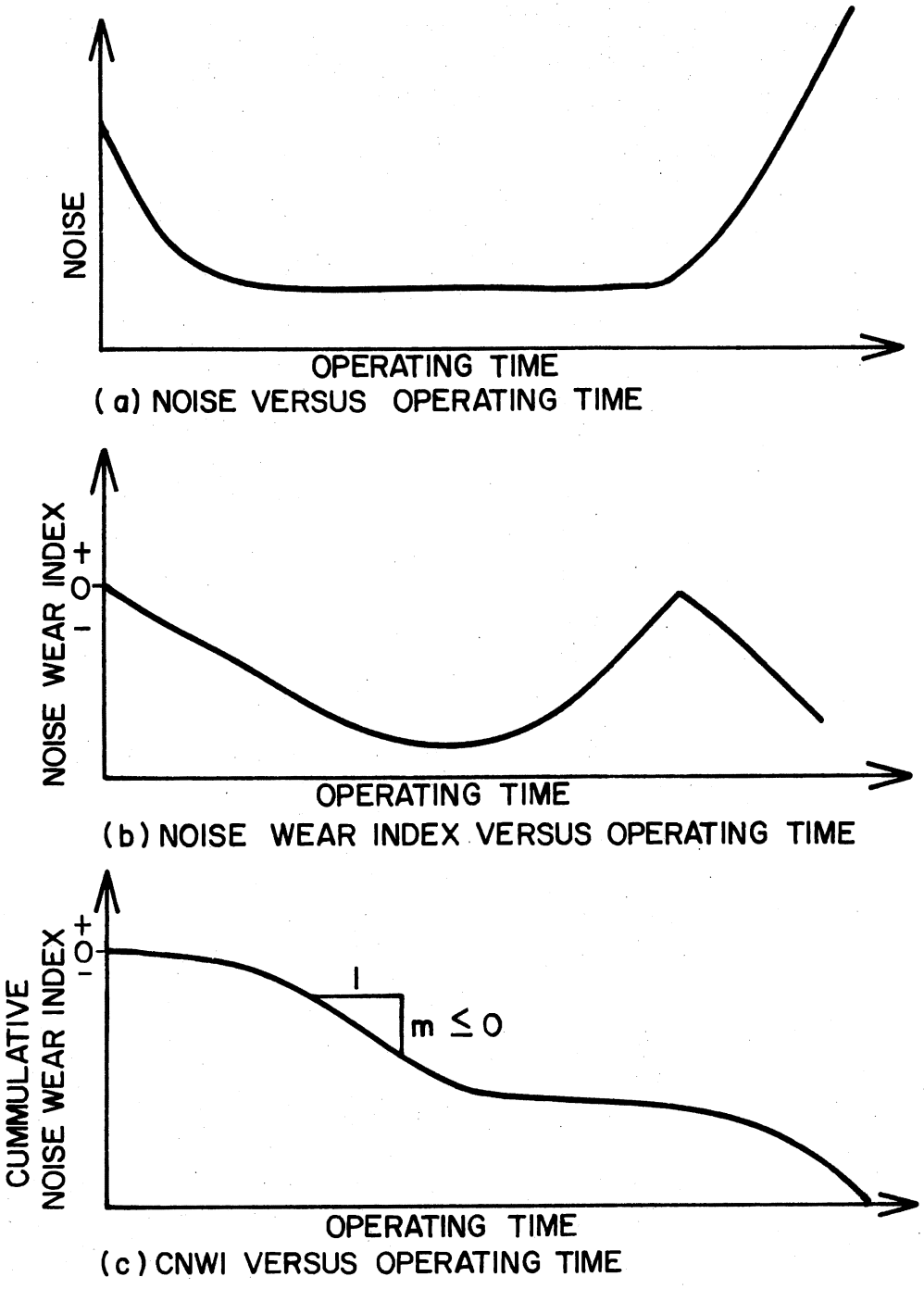

Figure 9. Noise Wear Index and Cumulative Noise Wear Index Versus Time Showing Slope of CNWI Curve Always ≤ 0.

obtaining an expression for N as N(t) or N(Q*) and finding C′ with:

$$C' = \int_0^{t_f} N(t)dt \tag{2.27}$$

or with:

$$C' = \int_0^{Q_f^*} N(Q^*)dQ^* \tag{2.28}$$

where:

t_f = final time associated with N_k

Q_f^* = final Q* associated with N_k

The conjectured behavior of noise versus time and its relationship with N and C′ are summarized in the curves of Figure 9. It should be noted that in general N can have the same value three times during the life of the component. C′, however, will usually be decreasing in value during the life of the component.

The Noise Wear Index and the Cumulative Noise Wear Index are potential diagnostic aids which could be used to monitor the amount of wear of a component. Hypothetically, either of these indices could be used to indicate when further pump diagnostics is warranted or when a pump is badly worn and should be replaced.

Cavitation

The reason for discussing cavitation in this dissertation is to provide a broad fundamental understanding of the cavitation process which will help insure that the design of

the experiments and the interpretation of the test results includes the most significant variables and their anticipated effects on high pressure pump noise.

It should be noted that cavitation does, indeed, affect component noise (36), (8). Knapp et al. (36) lists several methods for detecting the presence of cavitation. Summarized, the detection methods involve monitoring one of the following: component performance, system pressure distributions, light, and noise. Sevestyèn et al. (8) and Varga et al. (37) have shown that cavitation can be detected in low pressure hydraulic pumps by vibration and airborne noise measurements. Discussions of how cavitation does or might affect system performance and noise follows sections on a cavitation theory, the critical processes, dynamics, and cavitation numbers.

A Cavitation Theory

Knapp, Daily, and Hammitt (36) prepared what is certainly one of the best modern treatises on the subject of cavitation. But even their work does not include a succinct view of cavitation theory, which is so desirable if one wishes to isolate the critical system parameters necessary for studying cavitation related phenomena. The following paragraphs present a cavitation theory which evolved after pursuing the observations of Knapp et al. (36), and Schweitzer and Szebehely (38), as supported by others (39), (40), (41), (42).

The Cavitation Process. Figure 10 schematizes the basic cavitation process. The fluid system shown contains a liquid and a gas solute (air), similar to a typical high pressure hydraulic system. If the system fluid is sufficiently heated or decompressed, gas bubles will form (36), (38), (41), (42). The bubble formation may be due to solute diffusion (36), (38), liquid vaporization (36), (38), (41), (42), or a combination of these (36), (38). When the entrained solute, vapor, or solute and vapor mixture is sufficiently cooled or compressed the bubbles collapse (36), (38), (41), (42). Bubble collapse occurs because the solute dissolves, the vapor condenses, or both. The process of bubble growth and collapse is dynamic (36), (38), (39), (40), (41), (42). Both the solute in question and vapor are gases (43). Therefore, cavitation is the dynamic process of gas cavity growth and collapse in liquid. This definition of cavitation will be used throughout this study.

Formerly cavitation has been used to describe: a pressure reduction, a process, and a form of wear (36). Any pressure reduction associated with the cavitation process is adequately described with the word decompression. But, what terminology can be used to describe the wear that can be associated with the cavitation process?

Implosion Wear. Knapp et al. (36, p. 323), when discussing the wear associated the cavitation process, states:

> Experimenters who studied cavitation damage in fluid flow systems reached the consensus that the damage occurred at the downstream end of the

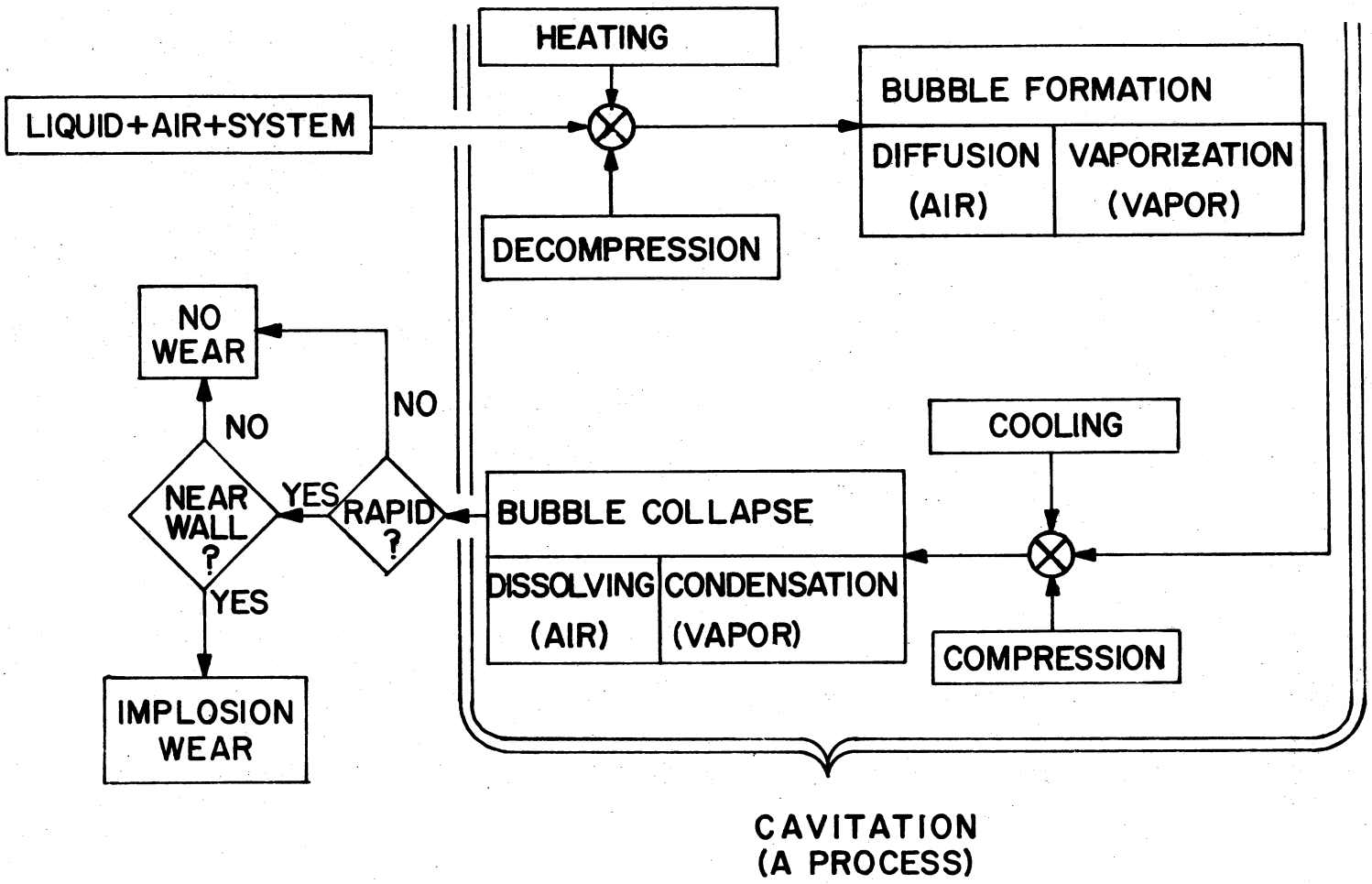

Figure 10. Diagram Schematizing Cavitation Process and Implosion Wear

> cavitation zone. Also, experiments . . . clearly demonstrated that the . . . high stresses . . . definitely coincided with the collapse and not the initiation phase.

Once it became apparent that the wear associated with the cavitation process had concomitance with bubble collapse, investigators attempted to define the mechanism for the resultant damage (36).

Both Bose (39) and Knapp et al. (36) discuss the work of Kornfeld and Suvorov, and others who attribute the bubble collapse damage to microjets that attack adjacent surfaces when the gas cavities collapse. This concept that cavitation associated damage is caused by microjets formed during bubble implosions is supported by Lichtarowicz (44). To achieve the energy necessary to damage a system surface it is apparent that the bubble collapse must be rapid, or must be an implosion. A gradual compression of entrained solute and liquid could result in bubble collapse without implosion and certainly without damage to the system structure.

The wear associated with cavitation occurs during bubble collapse. For wear to occur the bubble must implode adjacent to a system surface. This wear process may be defined as implosion wear:

> Implosion Wear...a diminution of material due to inward burst(s).

Figure 11 schematizes the implosion wear that may be concomitant with cavitation.

Cavitation Categories. A clear picture of cavitation

categories emerges if two additional facts are considered. First, for cavitation to occur there must be an interface between the liquid and a gas or the liquid and a void (36), (38). Second, liquids have tensile strength (36), (38).

Schweitzer et al. (38, p. 1222) clearly state the requirement for an interface: "Evaporation takes place when liquid in the vapor phase leaves the liquid in the liquid phase. This requires an interface." For evaporation to occur it is also necessary that the pressure in the cavity be lower than the vapor pressure of the liquid (38).

During their discussions of the static tensile strength of liquids, Knapp et al. (36, p. 51) state the following:

> . . .we define the vapor pressure as the equilibrium pressure, at a specified temperature, of the liquid's vapor which is in contact with an existing free surface . . . if a cavity is to be created in a homogeneous liquid, the liquid must be ruptured, and the stress required to do this is not measured by the vapor pressure but is the tensile strength of the liquid at that temperature. . . . Measurements have been made by several different methods and are too numerous to report completely.

Table I, adapted from (36), shows some of the liquid tensile strength values obtained by various investigators for different fluids. Knapp et al. (36) more thoroughly discusses the data scatter of liquid tensile strength than does Schweitzer et al. (38). However, enough data is available to establish statistical confidence that "qualitatively" liquids have tensile strength, even if exact "quantitative" information is not known.

Since a cavity, which also provides an interface for vaporization, is needed for cavitation to occur, it is

TABLE I

LIQUID TENSILE-STRENGTH MEASUREMENTS WITH BERTHOLET TUBES
(Adapted from Knapp et al. (36, p. 51))*

	Investigator	Liquid	Tensile Strength (atm)
A. Glass Bertholet tubes	Bertholet (4)	Water	50
	Dixon (15)	Water	50-150
	Dixon (16)	Sap	50-200
	Meyer (38)	Water	34
	Meyer (38)	Alcohol	39
	Meyer (38)	Ether	72
	Vincent (55)	Oil (heavy mineral)	119
	Vincent (55)	Water	157
B. Steel Bertholet tubes	Rees and Trevena (43a, 43b)	Water	13
	Rees and Trevena (43a, 43b)	Carbon Tetrachloride	15
	Rees and Trevena (43a, 43b)	Aniline	21
	Rees and Trevena (43a, 43b)	Liquid Paraffin	22-29

*Reference Numbers in Table are From Reference (36).

essential to examine how a cavity might be obtained in a fluid system. There are three ways which are of interest for this study. First, if the liquid contains a gas solute, adequate decompression will allow the gas solute to form cavities by diffusion. Second, if the liquid contains a gas solute which diffuses, at a given temperature, at a pressure above the liquid vapor pressure, when the liquid vapor pressure is reached by decompression, the liquid will vaporize into the solute filled cavity. Third, if no gas solute exists in the liquid, the systems wetted surfaces are hydrophillic, and the pressure is reduced below the tensile strength of the liquid a void will be created when the liquid fractures. This fracture created void provides an interface. Since the vapor pressure of the liquid is above the liquid tensile strength, the void will fill with vapor.

It now appears that there are three cavitation categories associated with three areas of cavitation dynamics. The three areas of dynamics are: bubble dynamics, solute dynamics, and vapor dynamics. Figure 11 diagrammatically relates these three dynamic areas so that it illustrates their relationship to the three categories of cavitation. When a cavity is formed by solute diffusion and no vapor exists in the cavity, the associated process is solute-cavitation. When a solute filled cavity subsequently acquires vapor, the associated process is solute-vapor-cavitation. If the liquid is free of solute influences and a cavity is formed by liquid tensile fracture the resultant

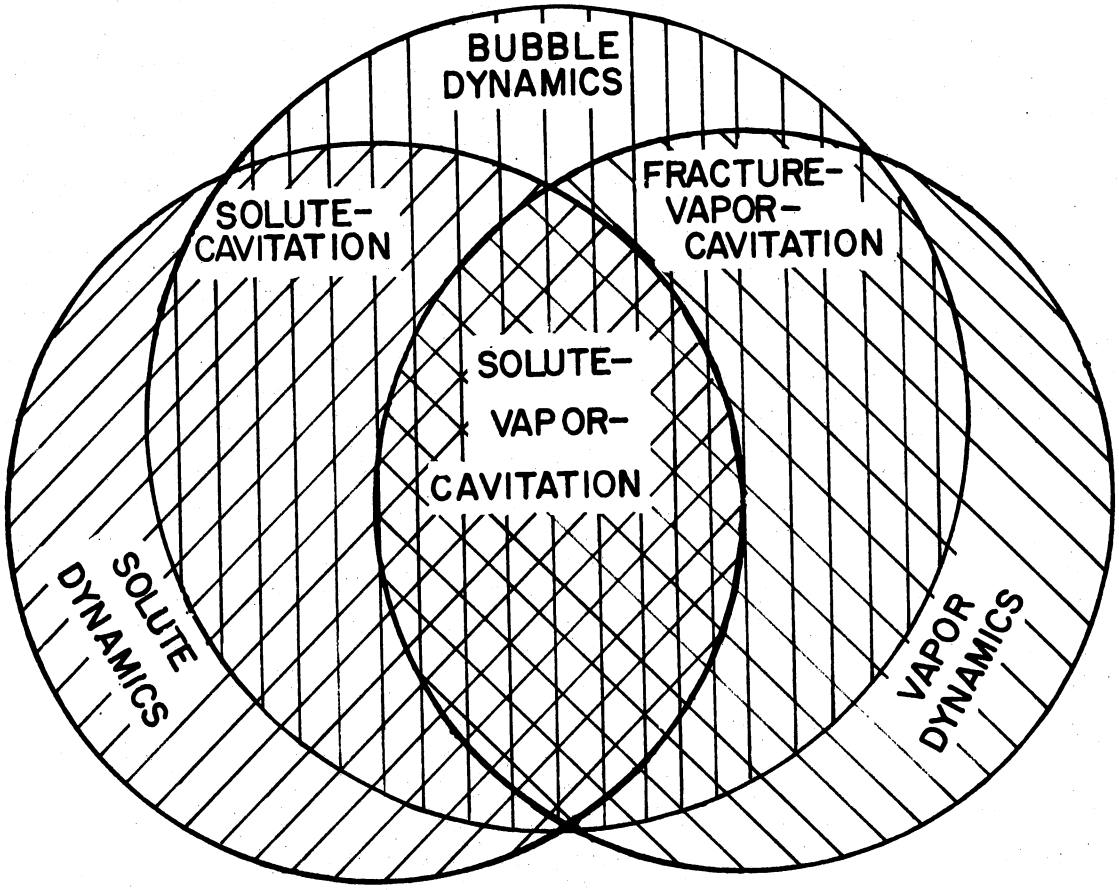

Figure 11. Modified Venn Diagram of Gas Dynamics Affecting Cavitation Showing Three Categories of Cavitation

cavity fills with vapor and the associated process is fracture-vapor-cavitation.

The Critical Categories

Now that an overview of cavitation categories exists it is possible to isolate those cavitation processes which can normally be expected in high pressure fluid power systems. It is certainly reasonable to expect that solute-cavitation will occur in practical systems (36), (38). Since system pressures could be below the vapor pressure of system liquids and the liquids are expected to contain gas solute, solute-vapor-cavitation will probably occur in practical systems (36), (38). Since practical systems will most likely: (1) contain gas solute, (2) contain hydrophobic materials, and (3) have system pressures above liquid tensile strengths, it does not seem reasonable, in this study, to entertain the thought that practical systems will experience fracture-vapor-cavitation. Thus, for the remainder of this study only solute-cavitation and solute-vapor-cavitation will be discussed.

Solute-Cavitation. The only significant gas solute to be considered when discussing cavitation in fluid power systems is air (9), (36), (37), (38), (41). The gas solute in the system will be dissolved in the liquid, entrained in the liquid, or contiguous to the liquid. The amount of air that will dissolve in the liquid can be determined by using Henry's (Henry-Dalton's) law (38):

$$V_d = S \frac{p_e}{p_o} V_\ell \qquad (2.29)$$

where:

V_d = volume of gas at standard temperature and pressure that could dissolve in the liquid at equilibrium (m^3)

S = solubility constant

p_e = equilibrium pressure (Pa)

p_o = atmospheric pressure (Pa)

V_ℓ = volume of liquid (m^3)

The volume of air that can actually dissolve in the liquid must be less than or equal to the total amount of air that is in the system with the liquid:

$$V_d' \leq S \frac{p_e}{p_o} V_\ell \qquad V_d' \leq V_a \qquad (2.30)$$

where:

V_d' = volume of gas at standard temperature and pressure actually dissolved in the liquid at equilibrium (m^3)

V_a = volume of air (standard temperature and pressure) in system (m^3)

Given the system conditions, (p_e, V_a, and V_ℓ) V_d and V_d' can be determined if the solubility constant, S, is known. Magorien (45) presents a linear plot of air content (%, based on volume at standard conditions) versus saturation pressure (psia) for MIL-H-5606. Using Magorien's plot, the estimated solubility constant, S, for MIL-H-5606 is 0.088.

Table II shows the summary of Schweitzer and Szebehley's (38) experimental results which include the solubility constant (%) for various fluids, including oils. Appendix G contains information showing that MIL-L-2104 Hydraulic Oil has a kinematic viscosity of 100 centistokes at 21°C (70°F). Fluid number 9 in Table II has a viscosity of 88.7 cSt, which is the closest to that of MIL-L-2104 at 21°C, with a corresponding S of 0.092. The National Engineering Laboratory (46) derived an empirical relationship between the solubility constant of oil and its viscosity as shown in Appendix G. Using the National Engineering Laboratory relationship and a viscosity of 100 cSt the corresponding solubility constant is approximately 0.086.

It is informative to assume a value for S and calculate the resultant V_d/V_ℓ. If it is assumed that MIL-L-2104 has a solubility constant of 0.09 (disregarding temperature variations), at atmospheric pressure (101.4 kPa) the resultant V_d/V_ℓ is equal to 0.09. If the absolute pressure is 50 kPa, V_d/V_ℓ is only 0.044. But if the absolute pressure is 20.7 MPa (3000 p.s.i.), then V_d/V_ℓ is 18.4 or 1840 percent. High pressure hydraulic oil is capable of dissolving a great volume of air relative to the system fluid volume.

The volume of entrained and contiguous air can be determined with the following equation:

$$V_{ec} = V_a - V'_d \qquad V_a \geq V'_d \tag{2.31}$$

where:

TABLE II

SUMMARY OF SCHWEITZER AND SZEBEHLEY'S (38, p. 1223) EXPERIMENTAL RESULTS, r IS THE GAS-LIQUID VOLUME RATIO, V_a/V_ℓ

Liquid	Solubility Constant (%)	Evolution (seconds)	Solution (seconds)	Kinematic Viscosity at 70°F (Centistokes)
1. Heavy Lubricating Oil	7.75	51.4	414.	823-974
2. Heavy Lubricating Oil	8.14	43.0	292.	823-974
3. Heavy Lubricating Oil	8.15	45.0	386.	762-974
4. Heavy Lubricating Oil	8.24	48.2	396.	762-974
5. Heavy Lubricating Oil	8.61	37.2	244.	762-974
6. Heavy Lubricating Oil	8.62	34.8	252.	562-670
7. Heavy Lubricating Oil	9.05	31.0	125.4	325-411
8. Heavy Lubricating Oil	9.11	17.9	50.2	249-346
9. Heavy Lubricating Oil	9.18	11.6	32.7	88.7
10. Light Lubricating Oil	9.70	4.74	10.22	17.5
11. Light Lubricating Oil	9.95	4.18	9.77	17.5
12. Light Lubricating Oil	10.72	3.56	6.14	13.5
13. Light Lubricating Oil	11.30	7.63	9.46	17.5
14. Diesel Fuel	11.98	0.301	3.08	4.4
15. Aircraft Engine Fuel	17.20	0.236	2.595	1.67
16. Aircraft Engine Fuel	22.80	0.128	1.214	0.6350
17. Aircraft Engine Fuel	25.14	0.137	1.344	0.6350
18. Distilled Water	1.84	3.86	7.930	1.0

NOTE: Evolution and Solution Times are Half-lives for $r = 4$.

V_{ec} = volume of air (standard temperature and pressure) entrained and contiguous in system (m^3)

Pockets of contiguous air may exist in the system after a pressure change, the removal of system air, or the ingestion of air into the system. Eventually the contiguous air should be dissolved or become entrained. It may require a significant amount of time for the air "pockets" to be eliminated. The problem of solute dynamics is discussed in a later section.

The actual volume of the system occupied by the entrained and contiguous air can be calculated by using the Boyle-Charles' Law (47):

$$V'_{ec} = V_{ec} \frac{p_o}{p_\ell} \frac{T_\ell}{T_o} \qquad (2.32)$$

where:

V'_{ec} = actual volume of entrained and contiguous air at system temperature and pressure (m^3)

p_ℓ = system pressure (Pa)

T_ℓ = system temperature (°A)

T_o = standard temperature (273°A)

Given the necessary system parameters, Equations (2.29) through (2.32) make it possible to discuss the status of the air in a high pressure hydraulic system operating at "steady-state" conditions. Figure 12 illustrates how the "entrained" air varies in a given system as a function of the air volume in the system and the system pressure. At a

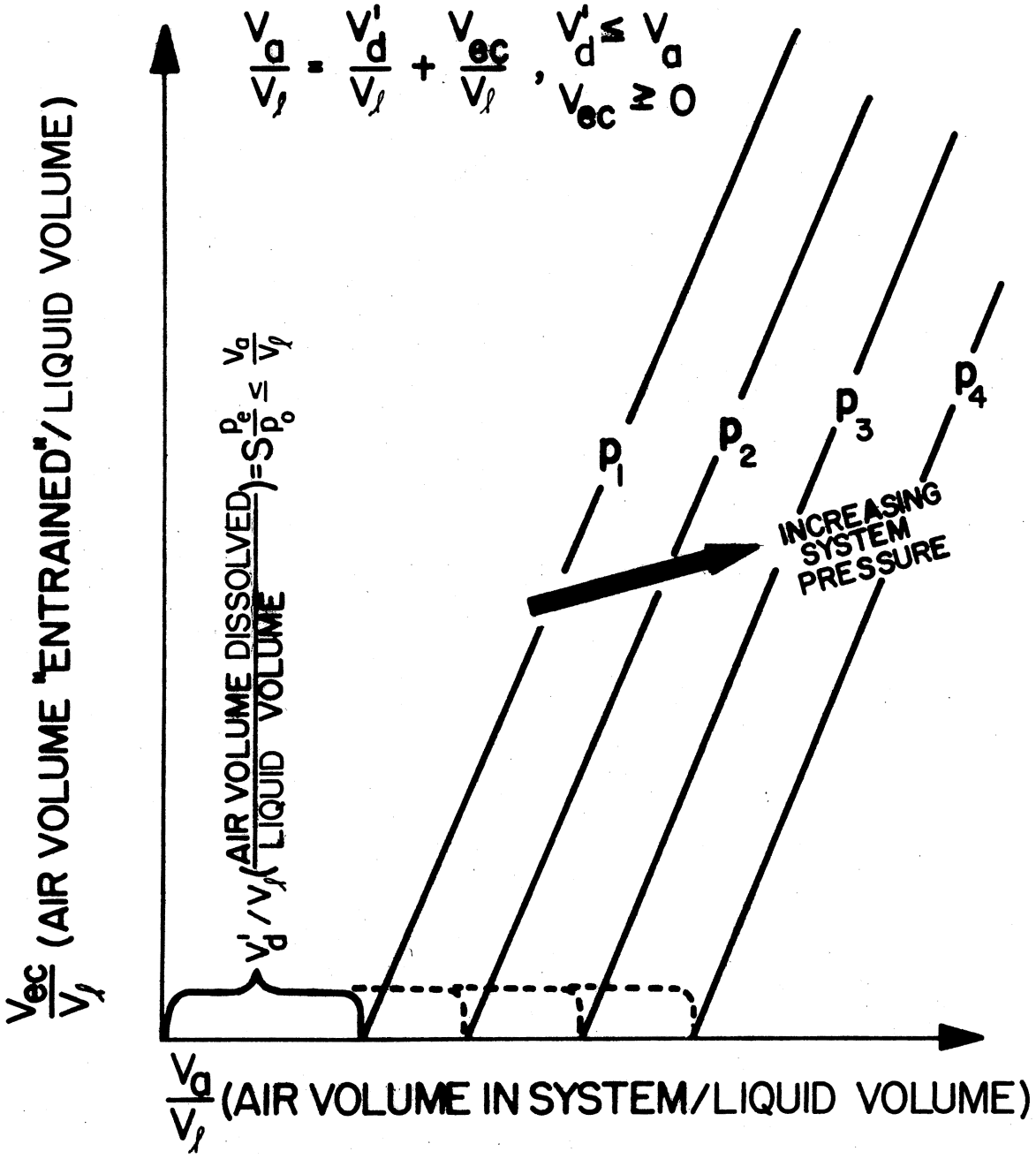

Figure 12. Illustration of Relationship Between "Entrained" and Dissolved Air

given pressure the air volume in the system must increase above the amount of air the system liquid will dissolve before any air becomes "entrained". For a given volume of air in the system, with a specified amount of "entrained" air, if the system pressure is increased, some (or all) of the "entrained" air will be dissolved and the entrained air volume will decrease.

The nomograph in Figure 13 quantifies the relationships between system air, dissolved air, and "entrained" air. The nomograph was constructed for MIL-L-2104 assuming a solubility constant of 0.09. It is clear from Figure 14 that if a "typical" hydraulic system has an open reservoir then V_a/V_ℓ is going to be 0.09. Thus, for an open reservoir system without air removal devices, if there is any pressure drop between the reservoir and the inlet to the pump, there will be "entrained" air in the system. Since pressure drops do exist between reservoirs and system pumps (due to pipe friction), the previous assumption that solute-cavitation occurs in practical hydraulic systems is supported.

Solute-Vapor-Cavitation. Since solute-cavitation exists in practical hydraulic systems, solute-vapor-cavitation could exist if the vapor pressure of the system liquid is reached. The following paragraphs examine: (1) the vapor pressures of two liquids, oil and water, used in hydraulic systems, and (2) the possibility that their vapor pressures are attained in practical systems.

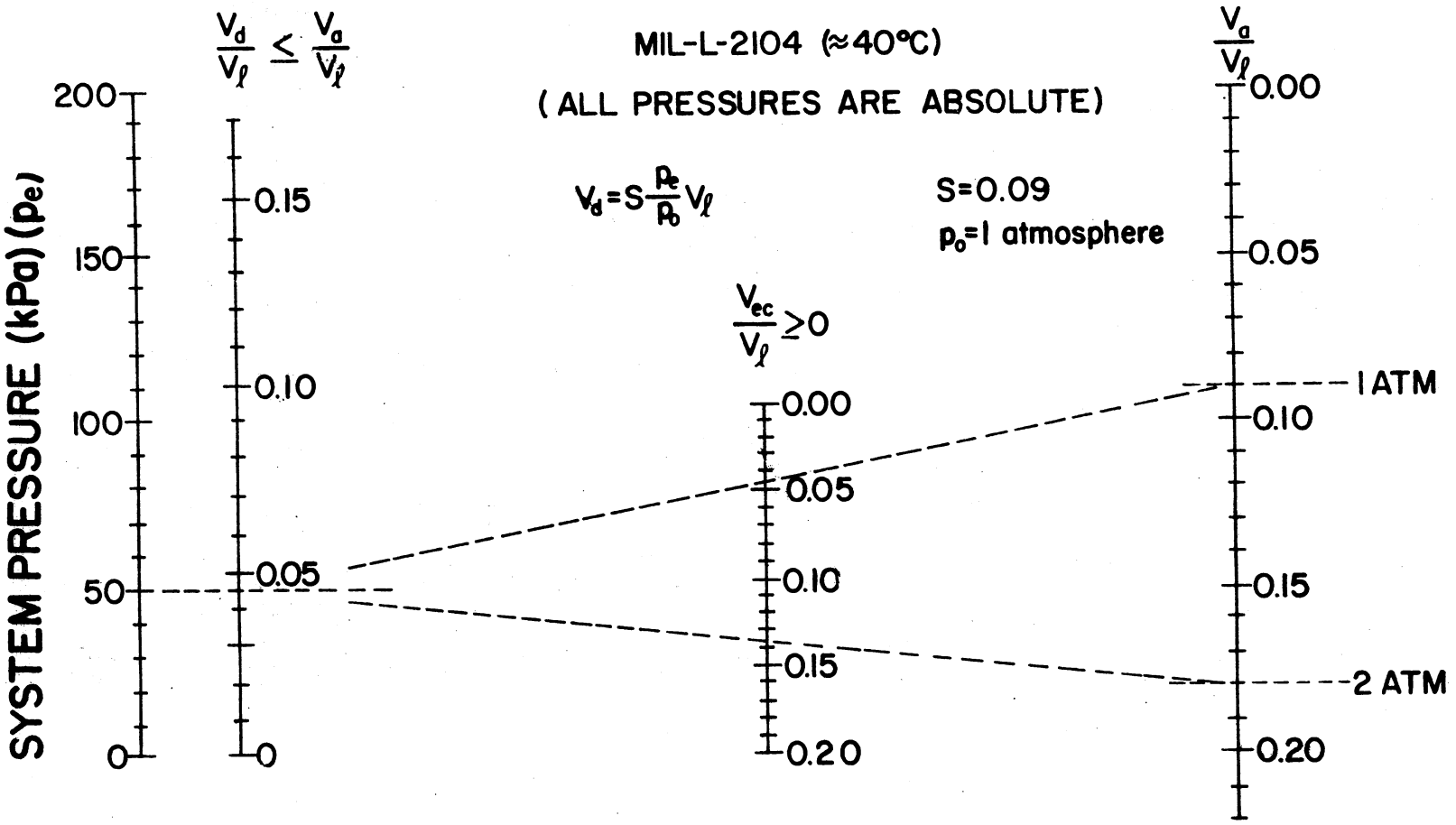

Figure 13. Nomograph Showing Relationship Between System Liquid Volume, V_ℓ; Air Volume in System, V_a; Dissolved Air Volume, V_d; and Volume of Entrained and Contiguous Air, V_{ec}

Appendix G shows that the vapor pressure of water is 25.6 kPa at 66.0°C and 79.2 kPa at 93°C. It is reasonable to expect either of these pressures in an operating fluid power system. It is also reasonable to expect fluid temperatures to be between 66°C and 93°C simultaneous with pressures low enough to cause vaporization of water (37).

It is shown in Appendix G that a typical hydraulic oil like MIL-L-2104 has a vapor pressure of less than 0.27 Pa (0.002 mmHg) at 93°C (200°F). It is not obvious that this pressure will be reached in a typical hydraulic system. To determine if vaporization of hydraulic oil occurs in typical systems there are two system areas that should be examined: (1) the low pressure region in a hydraulic pump; and (2) the high velocity, low pressure region downstream of a load valve or orifice.

For this study the low pressure region inside of a hydraulic pump is of prime interest. The minimum pressure in a hydraulic pump can be estimated, to a first approximation, by using the Bernoulli Theorem (49). Assuming no significant difference in heights between the pressure measurement point and the point where the pressure is calculated the equation becomes:

$$P_a + (0.5)\rho U_a^2 = p_b + (0.5)\rho U_b^2 \qquad (2.33)$$

where:

p_a = pressure at measurement point "a" (Pa)

p_b = pressure at point of interest "b" (pa)

ρ = fluid density (g/m^3)

U_a = velocity at the measurement point "a" (m/s)

U_b = velocity at point of interest "b" (m/s)

The location in the pump where the pressure is likely to be the lowest is in the region between the gear teeth tips and the wall of the pump housing adjacent to the suction port (see Figure 1). Considering the case of a pump with 60 mm outside diameter gears, an inlet pressure of 50 kPa, a speed of 50 (2π) rad/s, and an inlet velocity of 3.0 m/s (10 ft/s): Equation (2.33) becomes:

$$p_b = 50 \text{ kPa} + (0.5)\ (0.86)\ \text{Mg/m}^3\ (U_a^2 - U_b^2) \qquad (2.34)$$

$$p_b = 50 \text{ kPa} + 430 \text{ Kg/m}^3\ (9.0 - (50(2\pi)(30)\ 10^{-3})^2)\text{m}^2/\text{s}^2$$

$$p_b = 50 \text{ kPa} + 430\ (9 - 88.8) \text{ Pa}$$

$$p_b = 50 \text{ kPa} - 430\ (79.8) \text{ Pa}$$

$$p_b = 50 \text{ kPa} - 34.3 \text{ kPa} = 15.7 \text{ kPa} = 15{,}700 \text{ Pa}$$

The maximum vapor pressure anticipated for MIL-L-2104 is 0.3 Pa which is five orders of magnitude less than the minimum pressure calculated in the example pump. The typical hydraulic pump will not be operated 317 times faster than 50 (2π) rad/s. Typically pump manufacturers recommend that the inlet pressure for pumps be greater than 74.3 kPa (50), (51). The typical pump shaft seal would probably leak air profusely if the inlet pressure were anywhere close to 1 Pa. Therefore, it is not reasonable to expect solute-vapor-cavitation to be initiated in high pressure oil hydraulic

system pumps.

It might be possible for solute-vapor-cavitation to be initiated elsewhere in the system and the solute-vapor bubbles transported to the pump inlet. This possibility can be examined by considering the minimum pressure downstream of a high pressure hydraulic restriction (orifice) such as a metering valve.

There are two equations of interest for examining the minimum pressure downstream of an orifice-type restriction. First, there is the orifice equation (52):

$$Q_a = \frac{C_d A_2}{\sqrt{1 - \beta^2}} \sqrt{\frac{2}{\rho} (p_1 - p_2)} \qquad (2.35)$$

where:

Q_a = actual flow rate (m^3/s)

C_d = discharge coefficient

β = area ratio, A_2/A_1

A_2 = orifice cross section area (m^2)

A_1 = conduit cross section area (m^2)

p_1 = pressure upstream of orifice (Pa)

p_2 = pressure in vena contracta (Pa)

For a given flow rate through a specific orifice, Equation (2.35) gives the pressure difference between the high pressure region and the pressure in the vena contracta (see Figure 14). The pressure downstream of the vena contracta, p_3, is usually greater than the pressure in the vena contracta. The pressure difference between the high pressure

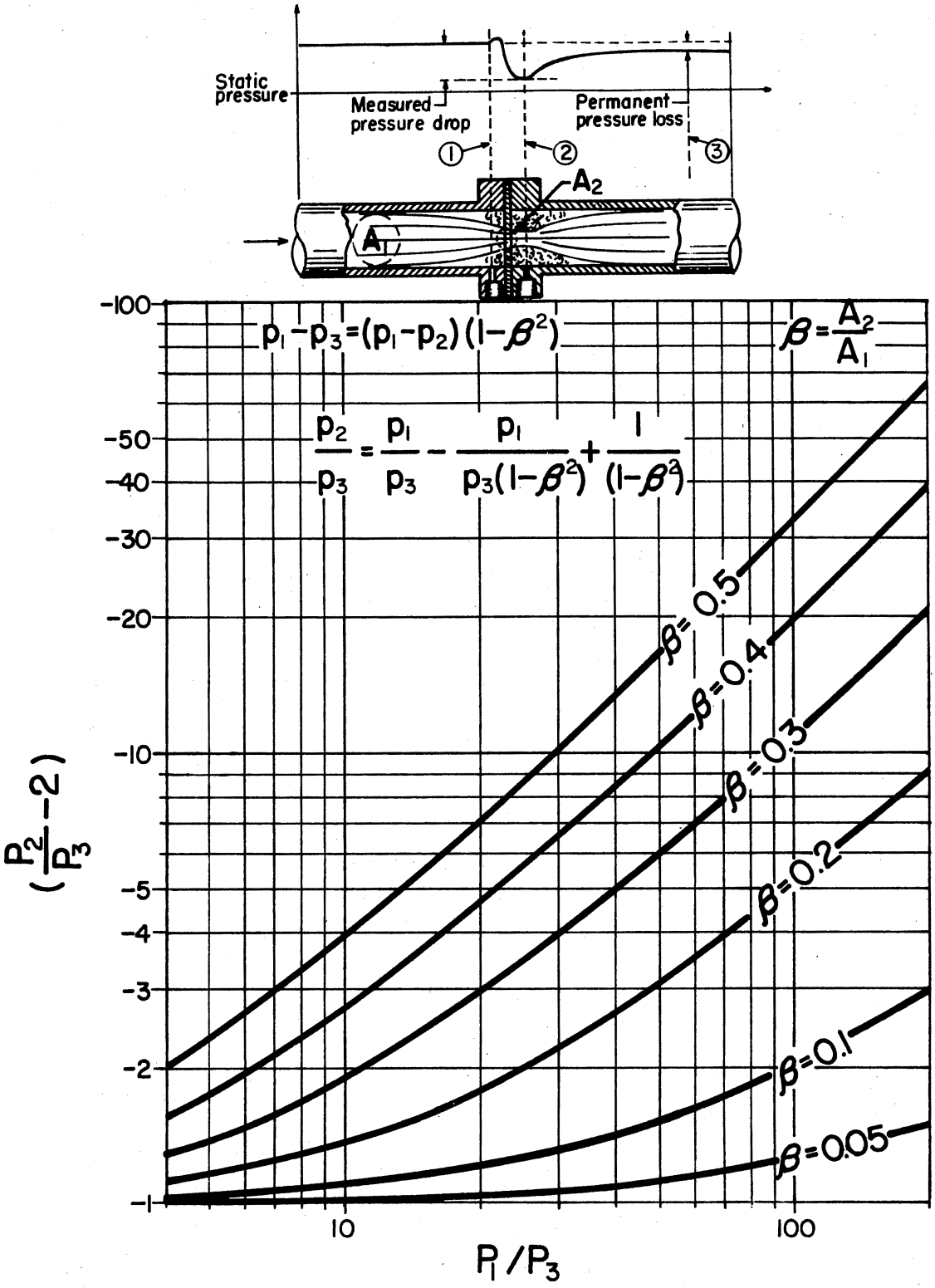

Figure 14. Plot of Non-dimensional Permanent Pressure Loss Equation Parameters With Orifice Figure

region and the pressure downstream of the vena contracta is the actual pressure loss for the orifice, which can be approximated by (52):

$$p_1 - p_3 = (p_1 - p_2)(1 - \beta^2) \tag{2.36}$$

Equation (2.36) can be re-arranged and nondimensionalized to obtain:

$$\frac{p_2}{p_3} = \frac{p_1}{p_3} - \frac{p_1}{p_3(1-\beta^2)} + \frac{1}{(1-\beta^2)} \tag{2.37}$$

Using Equations (2.35) and (2.37) it is possible to hypothesize regarding the existence of solute-vapor-cavitation initiated by fluid power system orifices.

Figure 14 is a plot of the relationship between the nondimensional permanent pressure loss equation parameters where the ordinate, $(p_2/p_3) - 2$, was used to allow plotting the equation on a log-log graph to examine the critical region of the equation.

Figure 15 is a plot of the orifice equation assuming a C_d of 0.65, a conduit velocity less than or equal to 6.1 m/s (20 ft/s), and a fluid specific gravity of 0.86. The assumed velocity is consistent with, but slightly higher than, accepted design practice (53). The specific gravity is comparable to that of MIL-L-2104.

Doebelin (52) indicates that disturbances upstream of an orifice will tend to reduce β. If a system has conduits or flow passages which increase the fluid velocity above

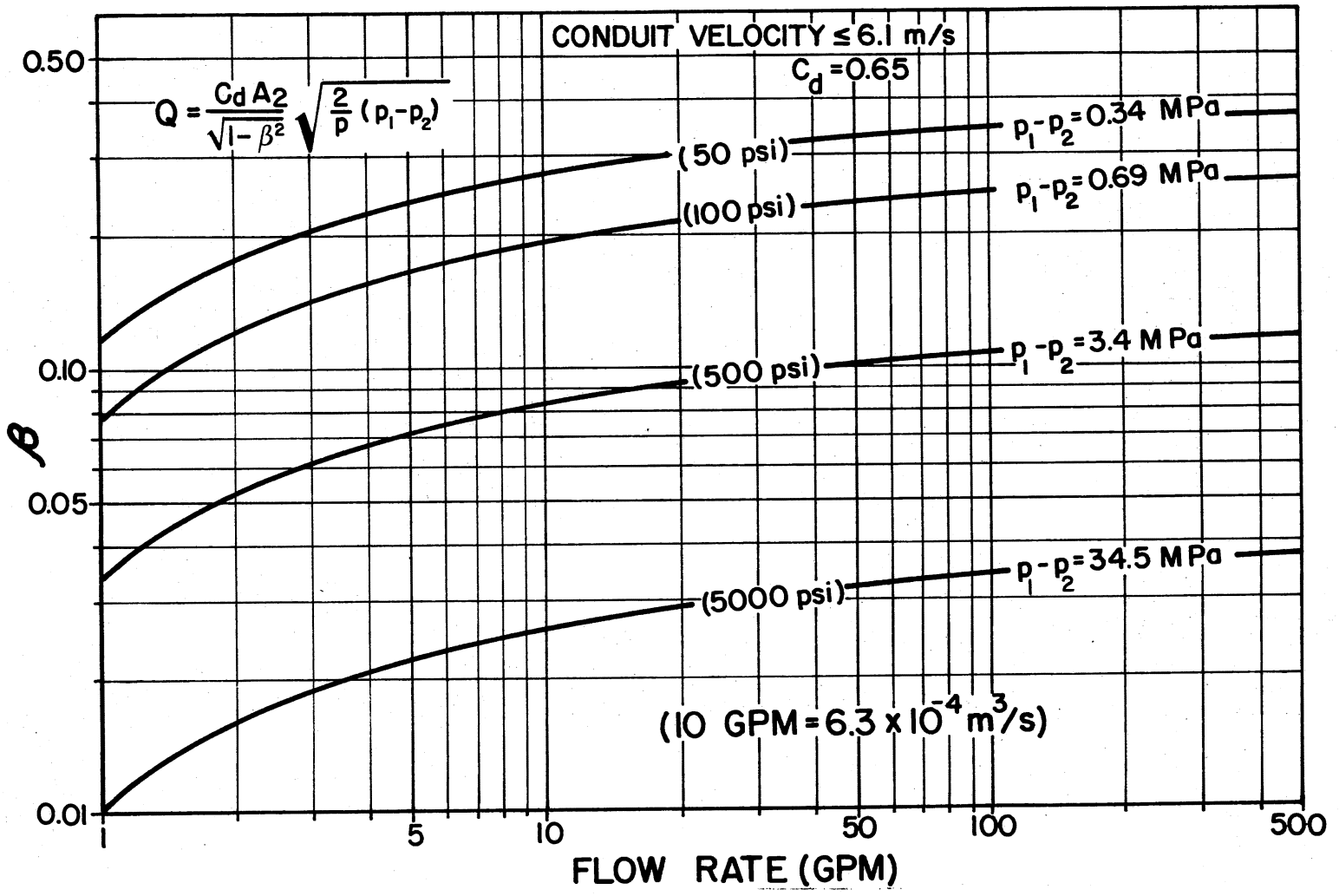

Figure 15. Plot of Orifice Equation Showing β for Various Flow Rates and Pressures

accepted design values, the effective conduit diameters are smaller than those used to develop Figure 15, thus β is larger than the values shown in Figure 15.

Since field system reservoirs are operated at pressures greater than or equal to atmospheric, and some additional pressure is required to force the fluid from the location of p_3 to the reservoir, p_3 will be greater than or equal to atmospheric pressure.

Because the vapor pressure of hydraulic oil is so close to zero, for a qualitative discussion of whether or not vaporization will occur the vapor pressure can initially be assumed zero, and if the analysis shows it is zero or less than zero then vaporization can occur. However, if the analysis shows that p_2 must be significantly greater than zero then vaporization cannot occur. If p_2 is zero, since p_3 will be finite, then the quantity $(p_2/p_3) - 2.0$ must be equal to -2.0. If $(p_2/p_3) - 2.0$ cannot become approximately -2.0 or less than -2.0 then vaporization will not occur.

Assuming p_2 is zero, p_1 is 34.5 MPa (from Figure 15), p_3 is atmospheric (101.3 kPa), and β is ≈ 0.04, then p_1/p_3 is 345.0. If p_1/p_3 is 345.0 and β is 0.04 then, extrapolating from Figure 15, $(p_2/p_3) - 2.0$ will not be less than approximately -1.5, which means p_2 is actually about 50 kPa and no vaporization will occur.

Since it does not appear that vaporization will occur at high values of p_1, perhaps it will occur if p_1 is low. This possibility can be examined by assuming p_3 is

atmospheric; selecting p_1 (greater than or equal to p_3) as 0.34 MPa; noting on Figure 16 that with these conditions β is less than or equal to 0.35; noting on Figure 15 that for a β of 0.35 and $p_2 = 0.0$, that p_1/p_3 is about 8.0; and determining that p_1 has to be about 0.8 MPa. This means that β would actually be $\approx$0.2 and again vaporization cannot occur. So even for a low pressure upstream of the orifice $(p_2/p_3) = 2.0$ is not small enough for vaporization to occur. This examination can be continued adnausem, but leads to the same conclusion, vaporization cannot occur.

The foregoing analyses lead to the conclusion that there is little possibility that a reasonably well designed oil hydraulic system with MIL-L-2104 type fluid will experience solute-vapor-cavitation. A more comprehensive analysis, supported with experimental evidence is needed to conclusively establish the absence or presence of solute-vapor-cavitation in oil hydraulic systems.

It may be concluded, based on the foregoing discussions and analyses, that solute-vapor-cavitation is not likely to occur in practical oil hydraulic systems, while it can readily occur in water hydraulic systems.

Dynamics

The dynamics of a cavitation process depend on the interactions of three fluids, the liquid, vapor, and any gas solute(s) in the system. Figure 16 illustrates the relationships between these three fluids. The Venn diagram

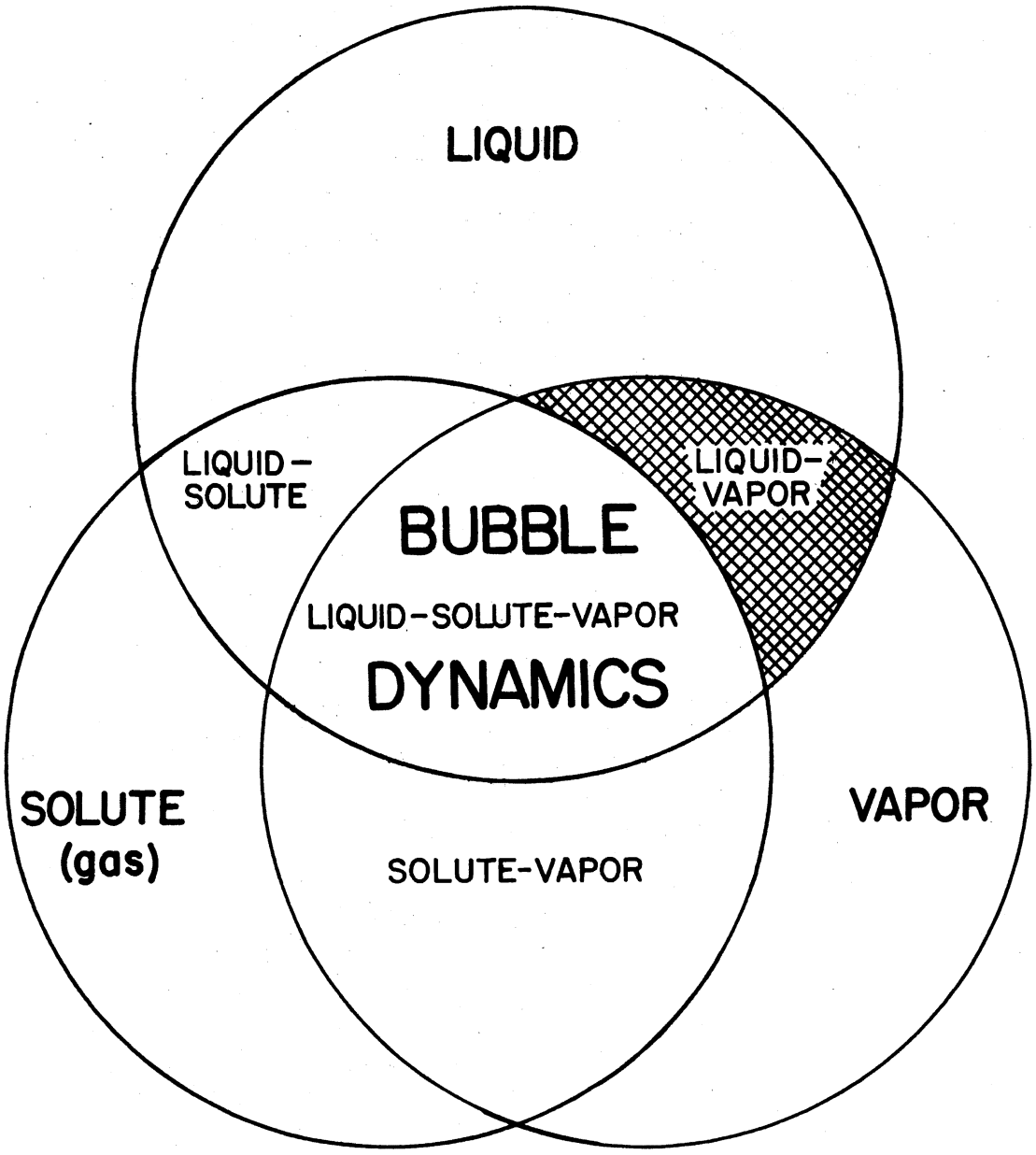

Figure 16. Venn Diagram (54) Showing Fluid Interactions Associated With Bubble Dynamics for Hydraulic Systems. (Note that the liquid-vapor interaction is not considered to be important for hydraulic systems.)

of Figure 17 isolates the four possible combinations of the three fluids that could be of interest when studying the cavitation process. The liquid-vapor interaction is not discussed in this section because it is associated with fracture-vapor cavitation, which is unlikely to occur in typical hydraulic systems. The solute-vapor interaction is a critical part of the interaction labeled "bubble dynamics", thus solute-vapor dynamics are not discussed independently.

The two fluid interaction areas of Figure 16 which are significant to the cavitation dynamics problem in fluid power systems are: (1) liquid-solute dynamics; and (2) bubble dynamics. The times required for these processes, evolution (diffusion), solution (dissolving), and bubble growth and collapse could have a significant affect on the acquisition and interpretation of data. Also, a study of the dynamics of cavitation could reveal new variables which might influence hydraulic pump noise.

Bubble Dynamics. Knapp et al. (36) outline several techniques for describing bubble-wall motion and indicate that the total equation for the motion of the wall of a gas filled bubble in an incompressible liquid, consistent with Poritsky's (55) treatment, is:

$$0 = -\sigma(R_o^2 - R^2) + \frac{(p_i - p_\infty)\,(R_o^3 - R^3)}{3} + \frac{\rho}{2} R^3 \left(\frac{dR}{dt}\right)^2 + 4\mu \int_0^t R\left(\frac{dR}{dt}\right)^2 dt + N\,T(\ell n R_o - \ell n R) \tag{2.38}$$

where:

σ = surface tension (N/m)

R_o = initial bubble radius (m)

R = instantaneous bubble radius (m)

p_i = pressure exerted by interior gas on bubble wall (Pa)

p = pressure at infinity in liquid (Pa)

ρ = liquid density (kg/m^3)

μ = liquid viscosity (Pa(s))

t = time (s)

N = constant for fixed mass of particular gas (N(m)/K)

T = absolute temperature (K)

Poritsky's integration of a modified form of Equation (2.38), which still included the viscosity and surface tension terms, was adapted by Knapp, Daily, and Hammitt to yield Figure 17. Figure 17 graphically illustrates the influence of viscosity and surface tension on both the growth and collapse of spherical bubles in an incompressible liquid.

Although Equation (2.38) provides some insight regarding the variables that affect bubble growth and collapse, it does not provide a straightforward clue to the time involved in bubble growth and collapse. Equation (2.38) also does not provide, without a significant amount of evaluation, any guidance concerning the importance of its numerous variables. Some insight into the time associated with the cavitation process

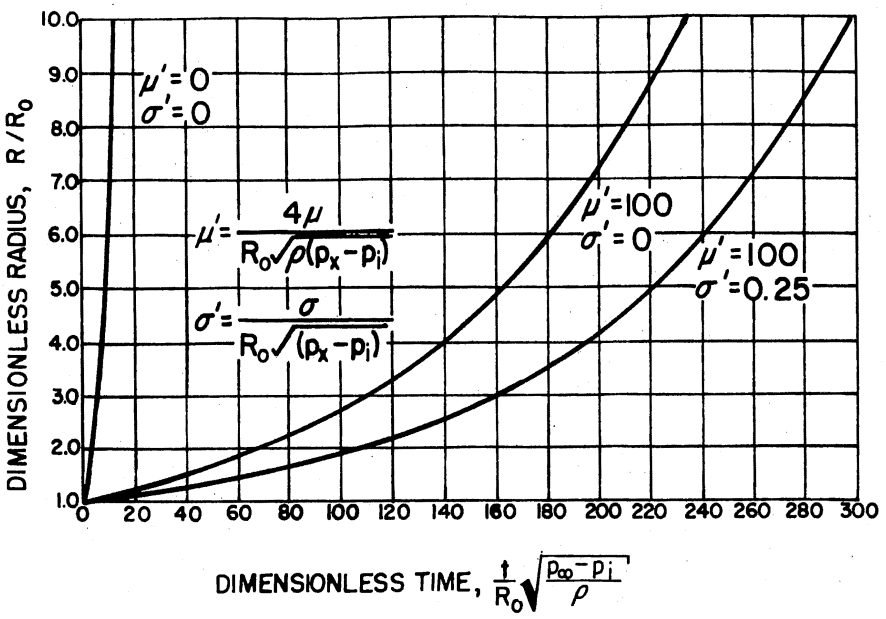

(a) Growth of a Spherical Bubble in an Incompressible Liquid With and Without Viscosity and Surface Tension (36)

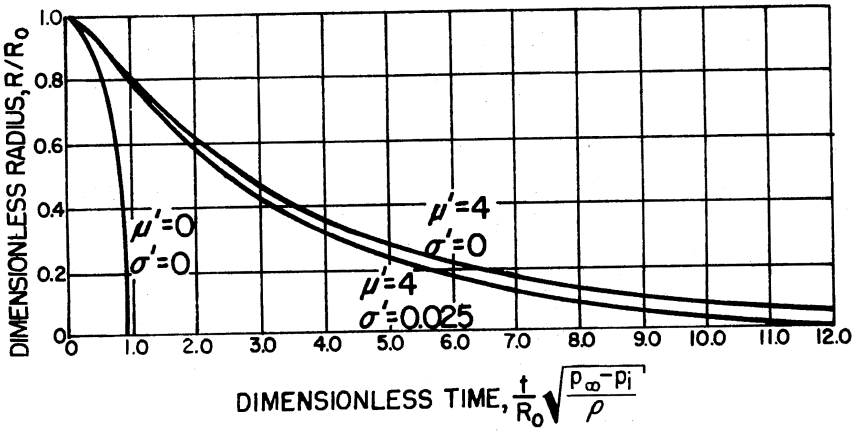

(b) Collapse of a Spherical Bubble in an Incompressible Liquid With and Without Surface Tension (36)

Figure 17. Growth and Collapse of a Spherical Bubble in an Incompressible Liquid (36)

and the significance of the numerous variables in Equation (2.38) is gained by considering an equation derived by Lord Rayleigh. In a 1917 discussion "On the Pressure Developed in a Liquid During the Collapse of a Spherical Cavity", Lord Rayleigh (36), (42) presented an equation which describes the radial velocity of a bubble-wall in an inviscid, incompressible liquid, assuming the radial flow is irrotational:

$$U^2 = \frac{2\ p_\infty}{3\rho}\ \left(\frac{R_o^3}{R^3} - 1\right) \qquad (2.39)$$

where:

U = wall velocity (m/s)

Figure 18 shows a comparison between the Rayleigh solution and experiments for bubble collapse in an incompressible liquid with a constant pressure field. The results shown in Figure 19 indicate that the Rayleigh solution is reasonably accurate, considering it is significantly simplier than Equation (2.38). It appears that liquid density, bubble radius, and liquid pressure are the dominant factors controlling bubble growth and collapse. It is important to note that the time required for the bubble collapse in Figure 19 is less than a millisecond.

Knapp et al. (36) also discuss the vapor cavity in an incompressible liquid with surface tension and a variable pressure field. During this discussion they refer to the work of Plesset (56) and his correlations between theory and

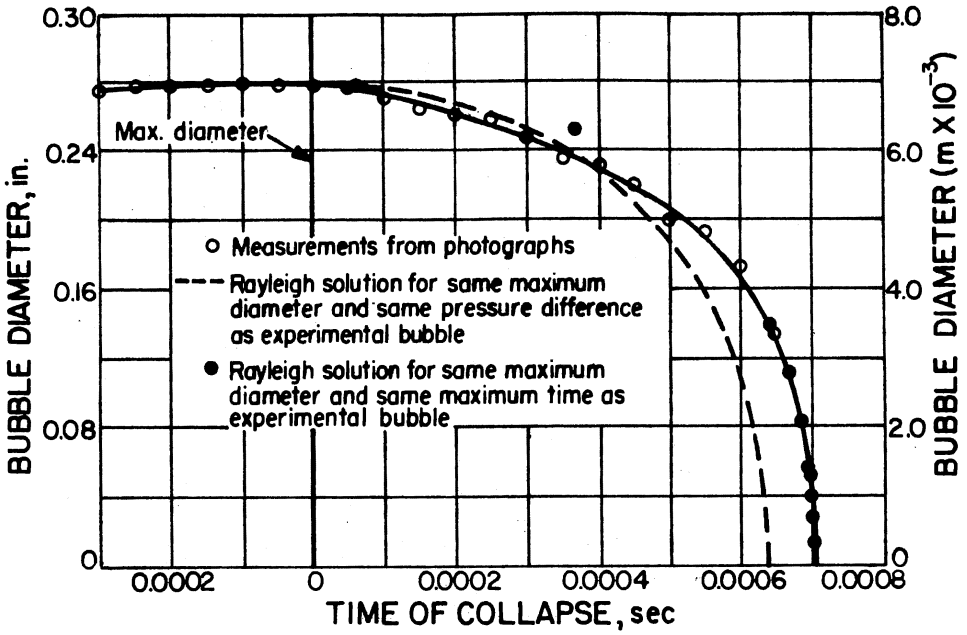

Figure 18. Comparison of Measured Bubble Size With the Rayleigh Solution for an Empty Cavity in an Incompressible Liquid With a Constant Pressure Field (Knapp et al. (36))

experiment. Figure 19 shows correlations by Plesset for two bubbles with constant cavity vapor pressure and temperature, in an incompressible liquid with a variable pressure field. These figures show that with a pressure difference of 0.69 kPa (10 p.s.i.), the total time for bubble growth and collapse is approximately 2 milliseconds. The millisecond-type lag between the pressure input and the bubble radius response is also indicative of the response characteristics associated with the process of bubble growth and collapse.

Liquid-Solute-Dynamics. Liquid-solute-dynamics involves the response characteristics, during evolution and solution, of entrained solute and contiguous solute. Fortunately studies have been conducted with air and oil which provide information about evolution and solution during vigorous agitation, and quiescent solution. With information from both ends of the spectrum inferences can be made regarding liquid-solute-dynamics in fluid power systems.

Schweitzer and Szebehely (38, p. 1220) reached the following conclusion regarding the rate of evolution (diffusion) and the rate of solution (dissolving) of air in liquids: ". . . The conclusion was clear: the rate of evolution is proportional to the supersaturation (the rate of solution to the undersaturation) and represents, therefore an exponential function of time." Their model for the amount of gas still dissolved in a system's liquid, during evolution, is:

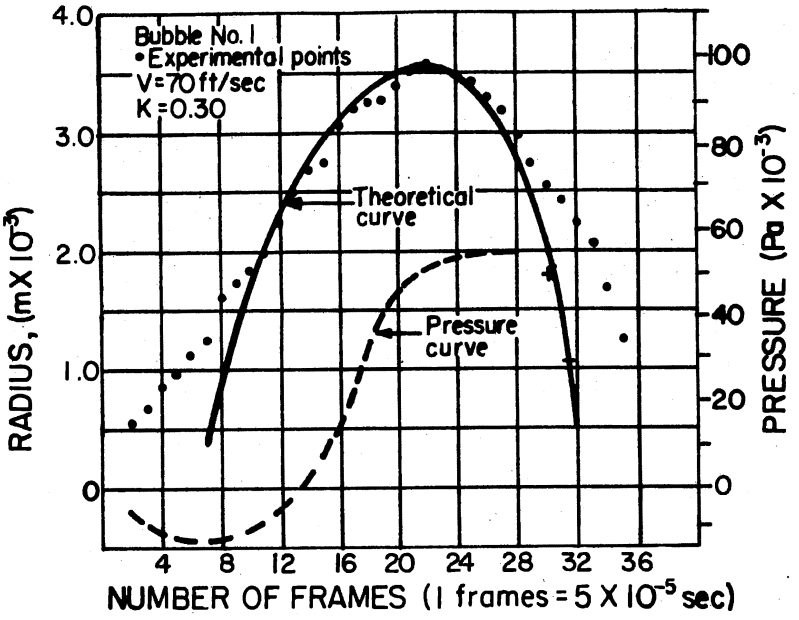

(a) Comparison of Measured Bubble Size With the Solution for a Cavity of Constant Vapor Density and Temperature in an Incompressible Liquid With a Variable Pressure Field. Bubble No. 2. (Plesset (56))

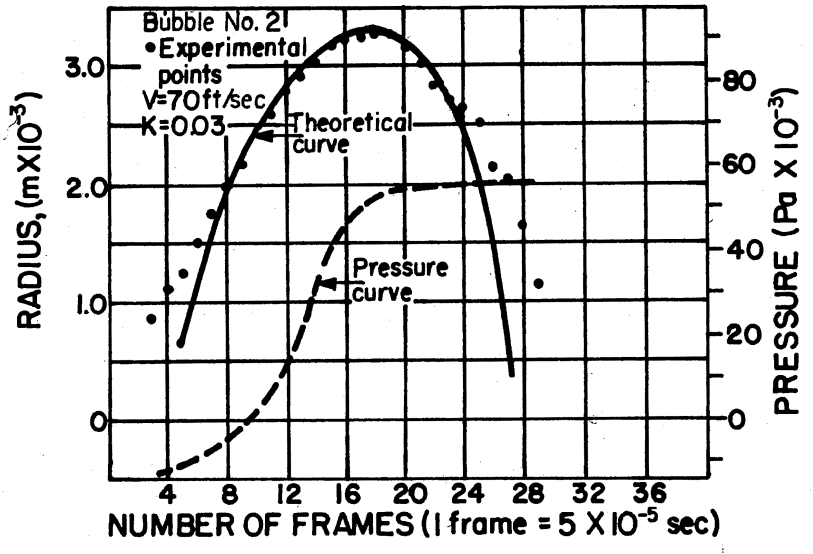

(b) Comparison of Measured Bubble Size With the Solution for a Cavity of Constant Vapor Density and Temperature in an Incompressible Liquid With a Variable Pressure Field. Bubble No. 1. (Plesset (56))

Figure 19. Comparison of Measured Bubble Size and Experimental Results for Two Bubbles (36)

$$V'_d = \frac{S}{\frac{V_a}{V_\ell} + S} \frac{V_\ell}{p_o}\left[S\ p_e + \frac{V_a}{V_\ell}\ p_i + \frac{V_a}{V_\ell}\ (p_e - p_i)\ \exp(-0.693\ \frac{t}{T_{0.5}})\right] \tag{2.40}$$

where:

p_i = initial gas pressure before evolution or solution (Pa)

$T_{0.5}$ = half-life of evolution (s)

Schweitzer and Szebehely (38) also present a model for the amount of gas that has evolved from the liquid during the agitated evolution process:

$$\Delta V_{ae} = \frac{S\ (V_a/V_\ell)}{S + (V_a/V_\ell)} \frac{p_e - p_i}{p_o} V_\ell\left[1 - \exp(-0.693\ \frac{t}{T_{0.5}})\right] \tag{2.41}$$

where:

ΔV_{ae} = volume of gas evolved

Schweitzer and Szebehely (38) conducted experiments by supersaturating the oil with air and then carefully reducing the pressure to avoid bubble formation. Once the pressure was reduced to one atmosphere, agitation and evolved air measurements were initiated. The agitation apparatus operated at 6.7 cycles per second (400 cycles/minute) with a stroke of 25.4 mm. The half-lives obtained during their testing, using a V_a/V_ℓ of 4.0, are summarized in Table II (p. 66). It can be seen from studying Table II that the half-life of evolution and solution for oils appears to correlate well with the liquid viscosity.

The half-life with agitation (38) can be converted to

the time constant τ with:

$$0.5 = 1 - \exp(T_{0.5}/\tau) \tag{2.42}$$

$$\ln(0.5) = -T_{0.5}/\tau = -0.693$$

$$\tau = 1.443\ T_{0.5}$$

where:

τ = time constant, time required for the process to be 63% complete (s)

After five time constants, the evolution or solution process will be 99% complete (57). Using the data from Table II for oil number 9, which is similar to MIL-L-2104 the following dynamic times result:

agitated evolution	$5\tau_{ae}$ = 83.7 seconds	(2.43)
agitated solution	$5\tau_{as}$ = 235.9 seconds	

where:

τ_{ae} = time constant for evolution with agitation (s)

τ_{as} = time constant for evolution with agitation (s)

Schweitzer and Szebehely (38, p. 1221) state the following about the relation between evolution and solution:

> After the foregoing detailed discussion of the evolution process, the solution process can be settled shortly. In the solution process a disturbed undersaturated liquid is approaching to an equilibrium condition. The analogy between evolution and solution processes is complete, therefore the same letters and steps can be used in deriving the same formula.
>
> The experiments performed showed that without exception the half-life for evolution was always shorter than that for solution, which means that

the evolution process is quicker than the solution process.

Hayward (58), (59) studied the solution of air in oil under quiescent conditions. Hayward took a mixture of oil and air bubbles in a cylinder at atmospheric pressure, and pressurized the mixture by loading the cylinder piston. The displacement of the piston versus time was converted to the percent of bubbles dissolved versus time. McCloy (41) presents and discusses some of Hayward's data. Figure 20 is an adaptation of McCloy's presentation of Hayward's data (58).

A plot of the 1.4 MPa (200 p.s.i.) solution curve in Figure 20 as log(100 - %dissolved) versus time yields essentially a straight line. This confirms that the basic process of quiescent solution can be modeled as suggested by Schweitzer and Szebehely (38). Figure 21 shows a plot of Hayward's data with several extrapolated solution curves based on Equation (2.41). These plots illustrate how the solution time changes as a function of the solution equilibrium pressure. Note that the plots are for one value of the air volume to liquid volume ratio. This set of curves vividly illustrates the long times required for solution when the equilibrium pressure is only slightly greater than the initial gas pressure.

Data such as Hayward's can be used to obtain the half-lives for the quiescent solution process with a particular fluid by using a rearranged form of Equation (2.41):

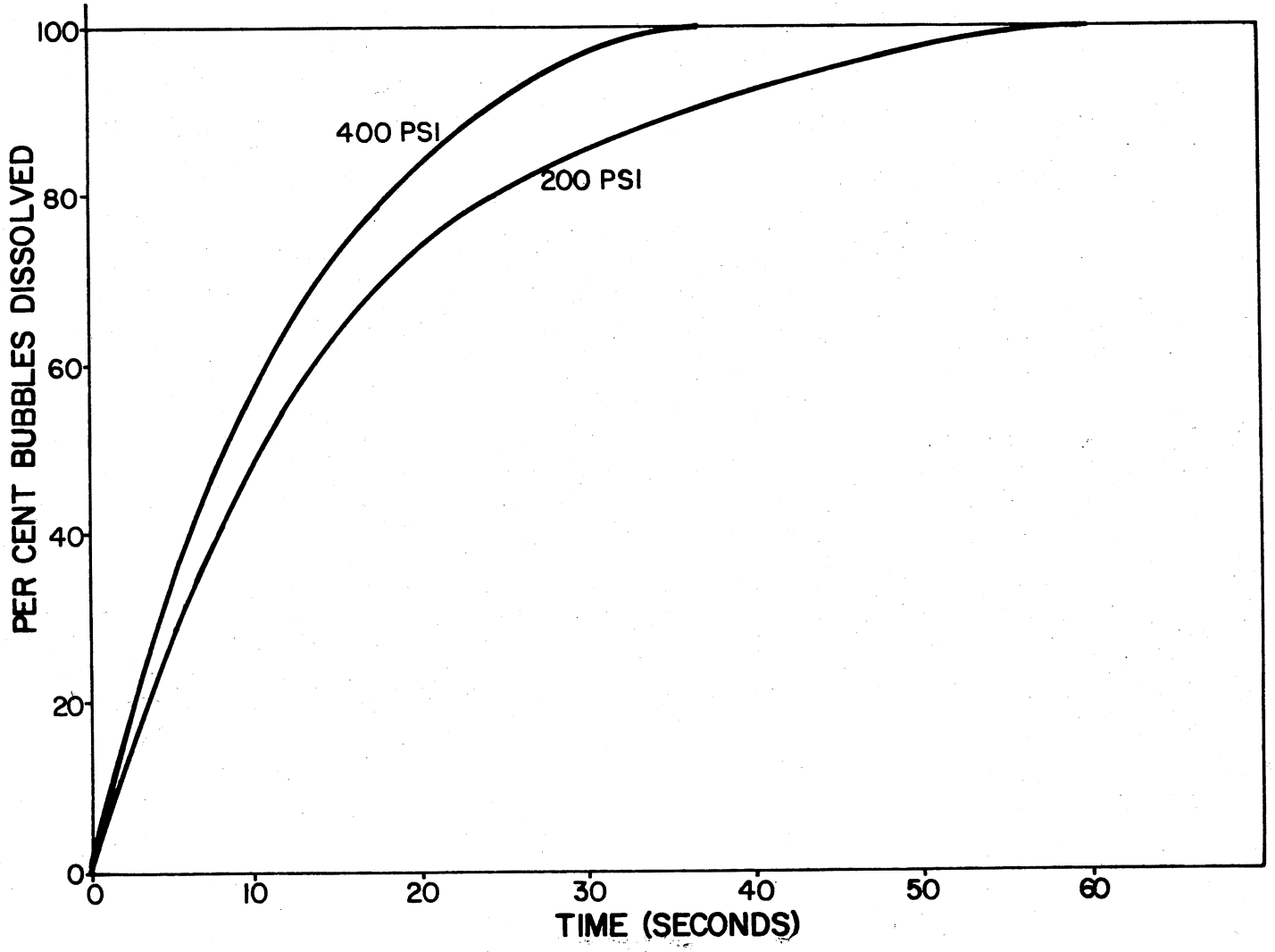

Figure 20. Solution of Air Into Hydraulic Oil for Quiescent Conditions. V_a/V_ℓ Approximately 21%. (McCloy (41), Hayward (58))

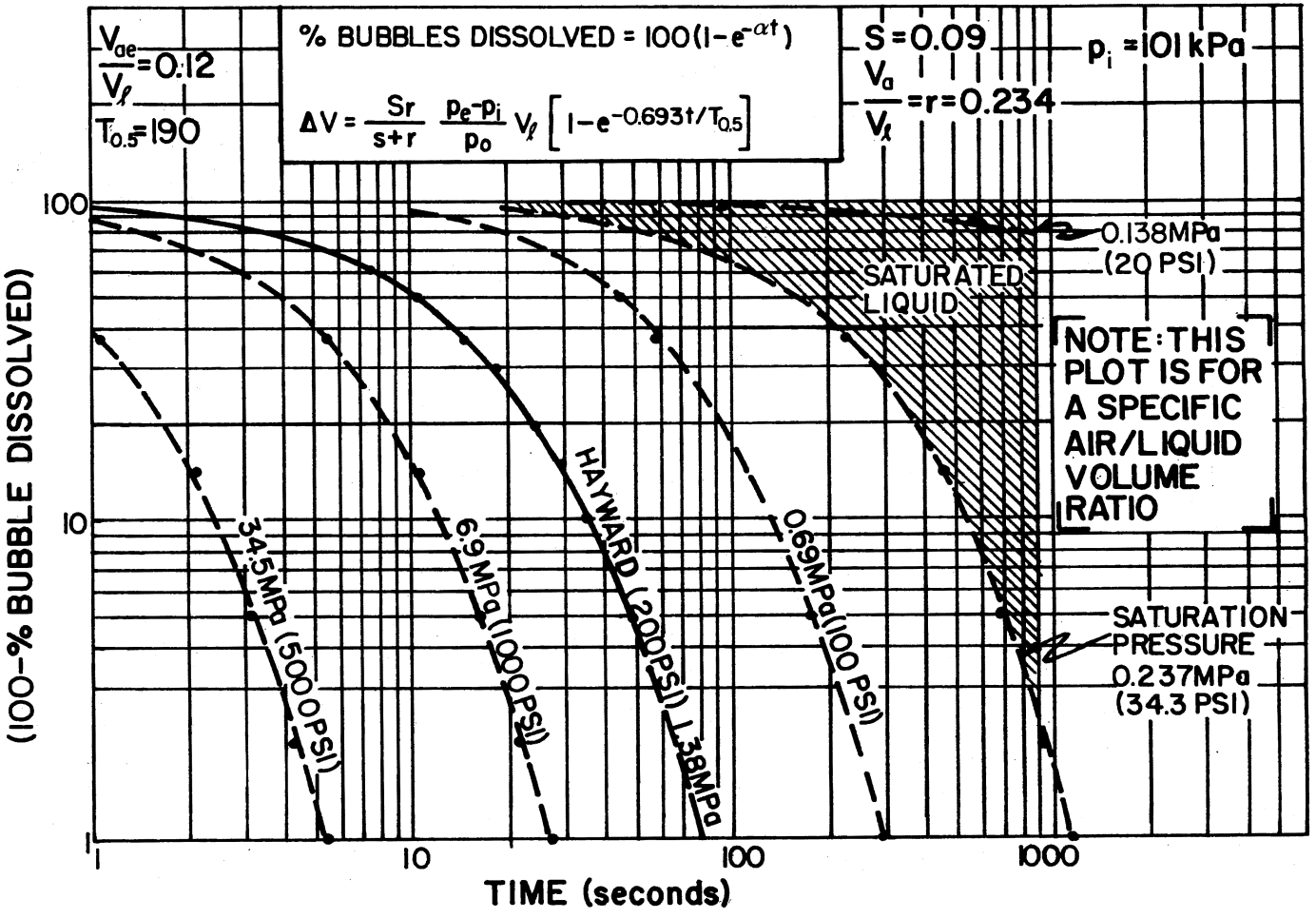

Figure 21. Transformed Plot of Hayward's Data (58), (59), on Bubbles Dissolved as a Function of Time. Extrapolated Data (dashed lines) Based on Hayward's Data and Schweitzer et al. (38) Equation.

$$T_{0.5} = \frac{-t(0.693)}{\ln\left(1 - \frac{\Delta V}{V_\ell}\,\frac{str}{sr}\,\frac{p_o}{p_e - p_i}\right)} \qquad (2.44)$$

where:

$r = V_a/V_\ell$

Using Hayward's description of the test apparatus and Equation (2.44) the average half-life for the two curves in Figure 20 is 190 seconds. This half-life for quiescent solution can be converted to five time constants to obtain:

$$\text{quiescent solution} \qquad 5\tau_{qs} = 1370 \text{ seconds} \qquad (2.45)$$

where:

τ_{qs} = time constant for quiescent solution (s)

An appreciation of the length of time required for quiescent solution is further enhanced by considering an example that could easily occur in a typical fluid power system. If $S = 0.09$, $r = 0.07$, $p_o = 101$ kPa, $V_d/V_\ell = 0.03$ at 34 kPa, and the pressure is increased to 48 kPa; then V_d/V_ℓ can increase to 0.0429. The time required for this process to be 99% complete is 3790 seconds, a little over an hour.

The observations of Schweitzer et al. and Hayward can be related to practical fluid power systems by considering entrained air to be agitated during system operation and contiguous air to be quiescent. This implies that entrained air will complete the evolution or solution process much more rapidly than contiguous air. Inference allows the estimation of a time constant for quiescent evolution. By

relating the ratio of agitated evolution and solution time constants to the quiescent solution time constant an estimate for five quiescent evolution time constants is:

$$\text{quiescent evolution} \qquad 5\tau_{qe} = 490 \text{ seconds} \qquad (2.46)$$

where:

τ_{qe} = time constant for quiescent evolution

Since the bubble growth and collapse times are orders of magnitude less than the corresponding evolution and solution times, the latter will be the dominant consideration for experimental and correlative purposes. Equations (2.40) through (2.46) provide the information necessary to make estimates of the times required for the evolution and solution process given variations of the operational parameters in a specified field or laboratory fluid power system.

Figure 23 provides a simplified illustration of the interactions of several of the more dominant parameters which influence the cavitation process in an oil hydraulic system. Two important points emphasized by the illustration are: (1) vapor can only exist if there is entrained air; and (2) viscosity acts to retard the evolution and solution processes.

Cavitation Numbers

Cavitation numbers were developed to provide indices which defined the dynamic flow conditions from two viewpoints:

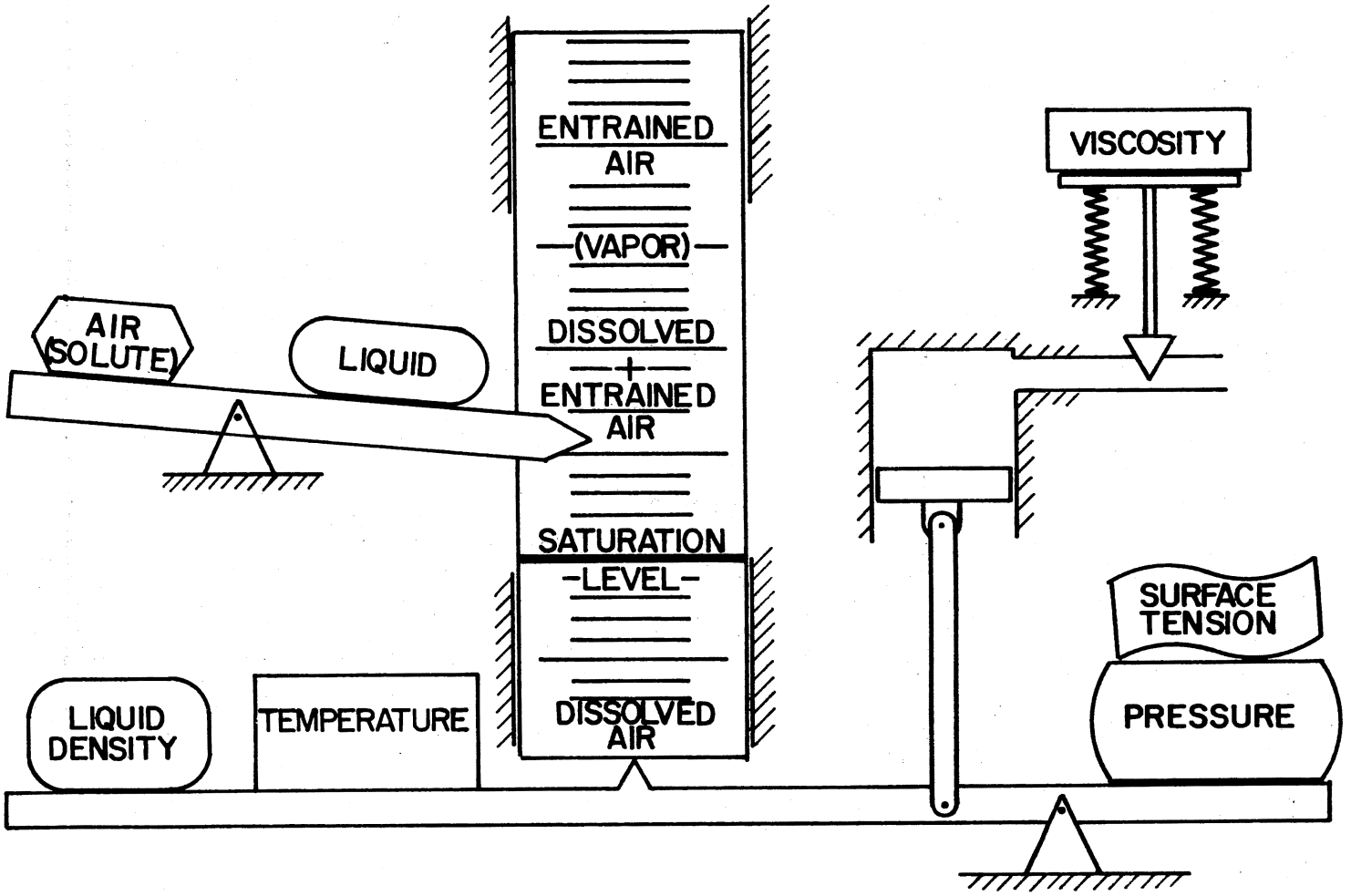

Figure 22. Simplified Illustration of the Influences of Several Cavitation Parameters on the Cavitation Process in an Oil Hydraulic System. (Note that vapor only exists when there is entrained air (solute).) (36) (38) (41) (42)

1. A parameter that would assume a unique value for each set of dynamically similar cavitating conditions.

2. An index or parameter to describe the flow conditions relative to those conditions for cavitation to be absent, incipient, or at various stages of development (36, p. 41).

This section discusses classic type cavitation numbers, Thoma type cavitation numbers, the critical cavitation pressures, and a Cavitation Potential Index.

Classic Type. Cavitation numbers were originally formulated for flow in large conduits around stationary objects. The resultant cavitation numbers, which ignore gravitational effects, are of the form (11), (36), (60):

$$K = \frac{p_o - p_v}{\rho \, V_o^2 \, (0.5)} \qquad (2.47)$$

where:

K = cavitation number

p_o = pressure of undisturbed liquid (Pa)

p_v = liquid vapor pressure (Pa)

ρ = liquid density (kg/m^3)

V_o = velocity of undisturbed liquid relative to object (m/s)

There are several variations of Equation (2.47), which are obtained by substituting other pressures or velocities in the equation. For instance, p_o is sometimes replaced with p_∞ (60); p_b, the "bubble pressure" is sometimes used in lieu of p_v (36); and for centrifugal pumps V_o is sometimes replaced with the impeller velocity, U_2 (11).

Thoma Type. When the classic type cavitation number proved inadequate for discussing cavitation in low pressure centrifugal type hydraulic pumps, Thoma (61), (62) introduced a new cavitation parameter (36):

$$\sigma_T = \frac{H_a - H_s - H_v}{H} \qquad (2.48)$$

where:

σ_T = Thoma cavitation parameter

H_a = baraomtric-pressure head (Pa)

H_s = static draft head defined as elevation of runner discharge above surface of tail water (Pa)

H_v = vapor-pressure head (Pa)

H = head produced (pump) or absorbed (turbine)

The Thoma cavitation parameter was expanded by others to included more pressure terms (36). The intent of these Thoma type cavitation numbers is to define a parameter for each installation. Thus, each installation has a definite value of σ, known as the plant σ_p. As long as the plant σ_p is greater than the critical σ_c no cavitation exists.

Critical Pressures. Cavitation parameters attempt to account for the critical system pressure at which cavitation inception occurs. There are three pressures which are directly related to cavitation inception. The three pressures are: vapor pressure, evolution pressure, and the critical nucleation pressure.

As previously noted in this chapter, the vapor pressure is probably of major concern for hydraulic systems which use water or water-oil emulsions. But, it is highly improbable that the vapor pressure of oils used in high pressure hydraulic systems plays a significant role in cavitation inception.

The evolution pressure, or "bubble" pressure, appears to be a critical pressure for all hydraulic systems. The evolution pressure is the pressure at which dissolved solutes evolve into the liquid and initiate the cavitation process. Equation (2.30) provides a means for determining the pressure at which air in solution will begin evolution, p_b.

A critical nucleation pressure can be defined based on the existence of free solute nuclei in the liquid and solute nuclei in the interstices of system walls and system particulate contaminant (36). Knapp et al. (36, p. 63) state the following:

> Apparently large numbers of small elements of undissolved gas can remain distributed throughout the liquid. . . . Two mechanisms have been suggested to account for undissolved gas elements existing stably within the body of liquid. Harvey et al. (63) proposed that the undissolved gas nuclei could exist as pockets in submicroscopic, hydrophobic cracks and interstices in container walls or in microscopic solid particles. Fox and Herzfeld (64) proposed that small nuclei do not dissolve because the bubbles are surrounded by organic skins.

The equilibrium conditions for "gas pockets" in interstices is described by (36):

$$p_g + p_v - p_\infty = - \frac{2\sigma}{R} \qquad (2.49)$$

where:

p_g = gas partial pressure in cavity (Pa)

p_v = vapor pressure (Pa)

p_∞ = pressure in liquid (Pa)

σ = surface tension (N/m)

R = radius of curvature of interface (m)

Since the radius of the equivalent solute bubble in the interstice approaches zero as R approaches zero, a first approximation of a critical pressure due to vapor and solute in the interstice, p_{ci}, is:

$$p_{ci} = p_g + p_v + \frac{2\sigma}{r_{ci}} \qquad (2.50)$$

where:

p_{ci} = critical pressure due to interstice solute and vapor (Pa)

r_{ci} = effective radius of solute-vapor volume in interstice (m)

If r_{ci} is 10^{-6} m., p_v = 0.0, p_g = 33 kPa, σ = 27 10^{-3} N/m (65), then Equation (2.50) yields a p_{ci} equal to 87 kPa. If the pressure in the example increases above 87 kPa then some of the gas will dissolve and the effective bubble will decrease in size. A decrease of the liquid pressure would allow the bubble size to increase and the solute to evolve into the bubble.

The equation which describes the equilibrium radius of

a free solute nuclei in the system liquid can be rearranged to obtain the critical pressure for a given equilibrium radius (36):

$$p_{c\ell} = \left[p_v - \frac{2\sigma}{R} + \frac{NT}{R^3}\right]_{R=R_e} \qquad (2.51)$$

where:

$p_{c\ell}$ = critical pressure due to free nuclei in the liquid (Pa)

R = bubble radius (m)

R_e = bubble equilibrium radius (m)

N = constant for fixed mass of particular gas (N(m)/K)

T = temperature (K)

Considering an example where $p_{c\ell}$ = 87 kPa, σ = 27 10^{-3}N/m, R_e = 10^{-6}m, and p_v = 0.0, then Equation (2.51) indicates that the quantity NT is equal to 141 10^{-15}Nm. If the pressure is increased to 180 kPa then the equilibrium radius decreases to 0.05 10^{-6}m.

Equation (2.51) is based on the assumption that the gas nuclei associated with the cavitation process are merely small free bubbles. Equation (2.50) is based on the Harvey et al. (63) hypothesis regarding "gas pockets" in material interstices. Knapp et al. (36, p. 67) make the following comments about Harvey's mechanism and the organic skin model as explanations of undissolved gas elements existing stably within the body of liquid:

> In general, however, Harvey's mechanism is more satisfactory. His model will explain all observed behaviors without postulating improbable fluid properties. . . . The combination of physical properties required for the organic-skin model is not known to exist.

An appreciation for the number of solid particles that exist in a typical oil hydraulic system can be gained by referring to references (66) and (67). There are 144 particles greater than 10μm in diameter in a 1 g/m^3 mixture of oil and AC Fine Test Dust (66). The results of a field survey of the contamination level of farm tractors revealed that the average tractor hydraulic system sampled had an equivalent gravemetric level of 233 g/m^3 (67). This means that in every cubic centimeter of the average tractor hydraulic system fluid there are 33,617 particles capable of functioning as gas nuclei. In other words, in a typical tractor hydraulic system that contains 38×10^{-3} m^3 of fluid there are 1,300,000,000 particles capable of "hosting" gas pockets.

Cavitation Potential Index. In general the pressure at which cavitation ceases (desinent pressure) is greater than the pressure at which it starts (incipient pressure). Generally, in high pressure oil hydraulic systems, the cavitation incipient pressure is of more interest than the desinent pressure. The incipient pressure can be reached when an inlet pressure decreases too much, a pump speed is increased too much, or perhaps when too much air becomes entrained in the system fluid. While the potential for

implosion wear in a hydraulic pump is associated with the pressure difference between the inlet and the outlet, the potential for cavitation is associated with the low pressure regions in the system, such as the pump inlet. In a high pressure hydraulic pump the inlet and outlet ports do not communicate as they do in low pressure pumps, therefore the outlet pressure has less effect on the conditions at the inlet of a high pressure pump.

For a given pump in a given system there is one critical pressure at which cavitation will be initiated. The critical pressure may be the vapor pressure, the bubble pressure, or a critical nucleation pressure. The critical pressure will manifest itself on a plot of cavitation potential versus pump inlet pressure in a manner similar to that shown in Figure 23. The region of interest in Figure 23 is from zero pressure to the critical pressure.

For cavitation discussions it would be desirable to have an index which concentrated on the region between zero pressure and the critical pressure. Preferably the index would start at zero when there was essentially no cavitation potential and increase as the potential for cavitation increased. And finally it would enhance comparisons of cavitation data sets if the index normalized the region from zero pressure to the critical pressure. One index which meets these requirements is the Cavitation Potential Index.

$$CPI = \Psi = 1 - \frac{p}{p_c} \qquad (2.52)$$

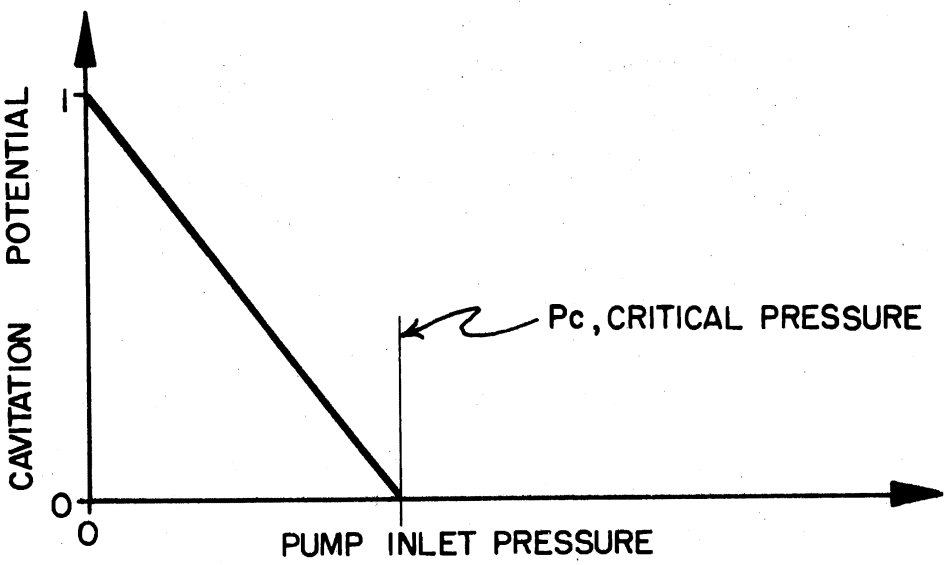

Figure 23. Cavitation Potential as a Function of Pump Inlet Pressure

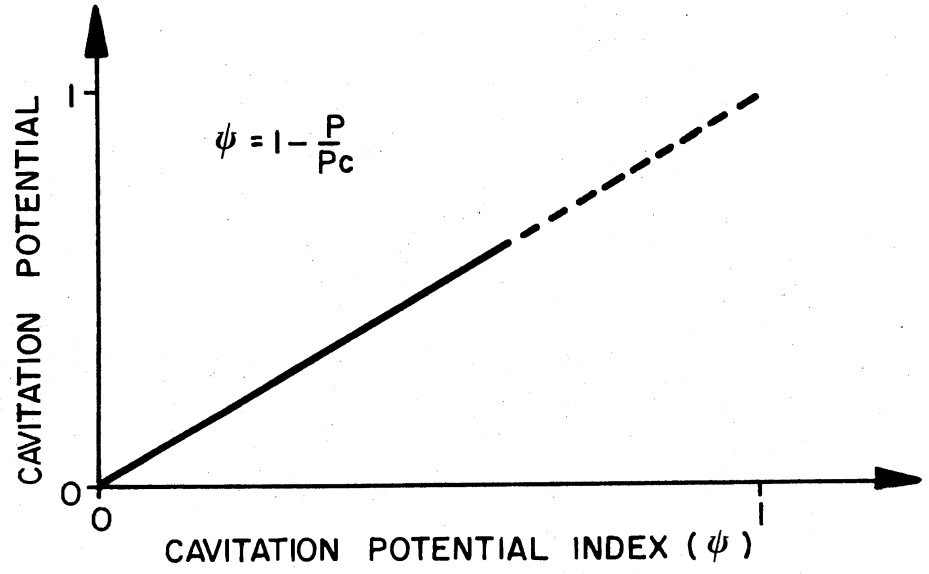

Figure 24. Cavitation Potential as a Function of Cavitation Potential Index

where:

CPI = the cavitation potential index

Ψ = the cavitation potential index

p = minimum pressure in area of interest (Pa)

p_c = critical pressure for area of interest (Pa)

Figure 24 shows a hypothetical plot of the cavitation potential in a hydraulic system versus the Cavitation Potential Index. Negative values of the CPI are ignored.

If a particular system has a critical pressure associated with the "bubble" pressure, then combining Equations (2.30) and (2.52) yields the appropriate CPI:

$$\Psi = 1 - \frac{p\ S}{r\ p_o} \qquad (2.53)$$

where all of the terms have been previously defined. Other critical pressure descriptions can be substituted into Equation (2.52) as desired to obtain the correct Cavitation Potential Index for a specific location in a particular system.

Performance Degradation

The presence of solute-cavitation in a high pressure oil hydraulic pump causes the output flow rate of the pump to decrease compared to the pump's output flow rate in the absence of solute-cavitation. Minor deviations of the pump's output flow rate can be monitored using standard measurement techniques. Major deviations of the output flow

rate are usually accompanied by significant system instabilities and necessitate terminating system operation at those conditions.

Standard test procedures have been formulated which test the ability of a pump to deliver "rated" flow when the inlet pressure of the pump is reduced below atmospheric pressure (68). Reference (68), a Method for Evaluating the Filling Characteristics of a Fixed Displacement, Fluid Power Pump, compares the output flow rate of a pump with atmospheric pressure at the inlet to the output flow rate when the inlet pressure is reduced to 67.6 kPa. The test is conducted at "rated" speed and an outlet pressure of 3.4 MPa. In essence the procedure determines if the pump is susceptible to solute-cavitation at "rated" conditions when the inlet pressure is reduced below atmospheric.

A similar type of test could be conducted with fixed inlet and outlet pressures, but with varying speed. As the pump's speed increased the output flow would increase linearly (essentially) with speed until cavitation occurred. When cavitation occurred the output flow rate would depart from the established linear relationship. This procedure would establish the maximum acceptable speed for a given pump operating at a given inlet pressure in a system with a fixed air/liquid volume ratio.

Cavitation Noise

There are four important topics relative to what is known or suspected about the manner in which cavitation will affect high pressure pump noise. These four topics are: (1) noise attenuation due to solute-cavitation; (2) noise level increase due to cavitation; (3) cavitation noise in low pressure hydraulic pumps; and (4) cavitation effects in high pressure hydraulic pumps.

Noise Attenuation. Knapp et al. (36, p. 367) stated the following about the effect of injected air on the damage rate due to implosion wear:

> The effect of injected air was also investigated. . ., and it was shown that substantial quantities of air produced a large reduction in damage rate, presumably because of its cushioning effect upon bubble collapses.

Kinsler and Frey (18) point out that the presence of inhomogeneities in a fluid, such as suspended bubbles in oil, cause excess attenuation of acoustic waves due to additional absorption mechanisms and scattering. Consistent with this comment they note that extremely high attentuations of acoustic waves are produced in water which contains suspended gas bubbles. In one illustration they note that in the wake of a destroyer the attenuation at $40\pi k$ rad/s is 1.2 db/m. This attenuation is 2000 times greater than the attenuation in bubble free sea water.

Knapp's et al. (36) comments about reduced damage rates with air in the liquid and Kinsler's et al. (18) comments

about increased acoustic attenuation with gas bubbles in the sea water both indicate that it is reasonable to expect that solute bubbles in hydraulic oil will tend to reduce implosion wear rates and the associated noise.

Noise Level Increase. Increasing the cavitation potential of a high pressure hydraulic pump will ultimately cause an increase in the cavitation level in the pump, and thus an increase in the implosion wear rate. As the wear rate increases it seems reasonable to expect the noise generated by the source to increase. Thus, as the cavitation in a hydraulic pump increases, in spite of any attenuation that exists due to bubbles, the noise level of the pump should eventually increase.

Low Pressure Hydraulics. Varga and Sebestyèn (37, p. 292) made the following comment regarding the correlation between noise and cavitation intensity in low pressure hydraulic systems: "The noise level curves of cavitation are in an unequivocal and definite correlation with the erosion intensity curves of cavitation."

Figure 25 (11) shows how the noise level of a centrifugal pump changed as a function of the cavitation parameter χ.

$$\chi = \frac{p_2 - p_v}{0.5\rho\ U^2} \qquad (2.54)$$

where:

χ = cavitation parameter

p_2 = delivery pressure (Pa)

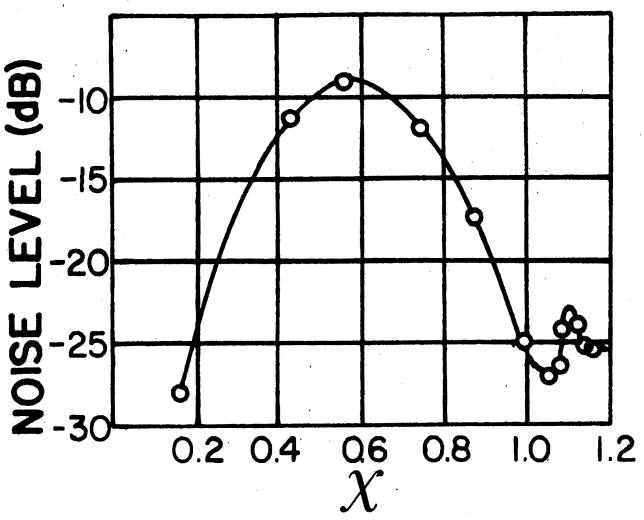

Figure 25. Centrifugal Pump Noise Level (40π k rad/s) as a Function of the Cavitation Parameter, χ (11)

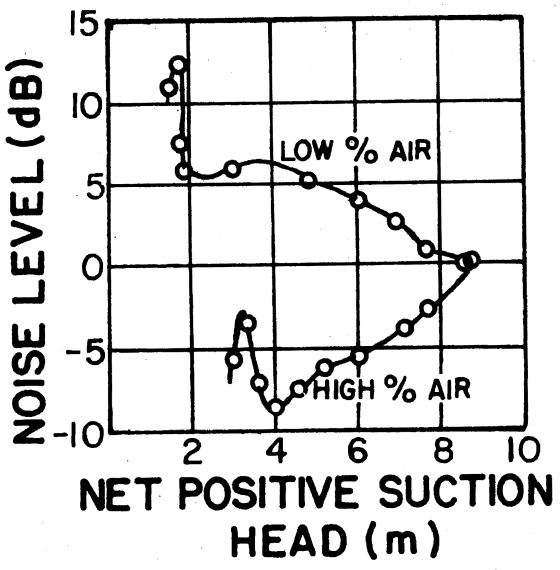

Figure 26. Centrifugal Pump Noise Level (40π k rad/s) Variation Due to Increased Air/Liquid Volume Ratio (11)

p_v = vapor pressure (Pa)

ρ = liquid density (kg/m^3)

U = impeller velocity (m/s)

Figure 25 illustrates that the 40πk rad/s noise level of the pump being tested exhibited two distinguishable peaks as the cavitation parameter decreased. Because of the significant variation of the noise level of the pump between $\chi = 1.0$ and $\chi = 0.2$, Varga et al. (11) concluded that measurements of a pump's noise level at a single frequency could be used to effectively detect the presence of cavitation in a low pressure pump.

Varga et al. (11) also conducted low pressure pump noise measurements with varying air/liquid volume ratios in the hydraulic system. Some of their test results are shown in Figure 26 which vividly illustrates how the presence of air in the liquid can decrease the high frequency noise associated with low pressure hydraulic pumps.

High Pressure Hydraulics. The literature contains qualitative information about the relationship between pump cavitation and pump noise (69), (70). Becker (69) indicates that the presence of air bubbles in the hydraulic system oil increases the sound level of high pressure pumps. Tessmann (70) conducted tests on gear pumps with varying "aeration", "cavitation" conditions. Although Tessman was not able to aurally detect any variation of the sound level during the various tests, his comments regarding the pump's performance

and internal pump damage are noteworthy.

Tessmann's test results are summarized in Table III. Before each test new "pressure plates" were installed in the test pump. The only time during the tests that a measurable amount of flow degradation occurred was when the maximum amount of air was injected into the pump inlet. This result supports the idea that output flow rate can be used as an indicator of "cavitation". The second important point is that the cavitation damage was either reduced or immeasurable when air was injected into the pump inlet. This latter observation supports the comments of Knapp et al. (36) who indicated that air in the liquid tends to reduce the damage rate associated with the cavitation process.

Tessmann's qualitative observation that every test was "loud" does not refute the hypothesis that significant noise level changes were occurring, at high frequencies, due to the changes of cavitation conditions between tests. Varga et al. (11) found that cavitation caused significant changes in high frequency noise levels (16π-40π k rad/s). Even significant changes in the 16π-40π k rad/s frequency band would probably go aurally undetected, because these high frequency sounds would probably be masked by the high intensity, lower frequency sounds of the pump. The ear is more sensitive to the lower frequencies emitted by a hydraulic pumping system than to the higher frequencies emitted (5), (71).

TABLE III

SUMMARY OF TESSMANN'S TEST RESULTS (70) SHOWING QUALITATIVE EFFECTS OF AIR ON SYSTEM AND HYDRAULIC PUMP "PRESSURE PLATES." SYSTEM FLUID CONTAINED ADDITIVES. NEW "PLATES" INSTALLED FOR EACH TEST

Test No.	Total Test Time (s)	Air Injected (m^3/s) STP	Pump Inlet Pressure (kPa) Absolute	Pump Outlet Pressure (MPa)	Remarks					
					Noise	Fluid Aeration	System Operation	Flow Degradation %	"Plate" Condition After Test	Cavitation Damage
1	1,800	0.59	101	10.3	Loud	Severe	Erratic	6-7	"Burnt" (100° Arc)	None
2	14,400	0.29	101	10.3	Loud	Severe	Erratic	0	"Burnt" (360° Arc)	None
3	4,500	0.00	27	3.4	Loud	Medium Severe	Erratic	0	"Burnt" (100° Arc)	Yes
4	4,500	0.15	27	3.4	Loud	Severe	Erratic	0	"Burnt" (100° Arc)	Yes (Less Than Test 3)
5	14,400	0.00	27	3.4	Loud	Medium	Erratic	0	"Burnt" (Dark) (360° Arc)	Yes (More Than Test 3)

Pump Noise Generation

During the early stages of this study a high pressure pump sound model was formulated which describes, to a first approximation, the manner in which speed and outlet pressure affect the overall noise emitted by a hydraulic pump. The objectives of this section are: (1) to discuss the pump noise model; and (2) to summarize how known, "critical" variables do affect, or might affect the noise emitted by a high pressure oil hydraulic pump.

Basic Pump Noise Model

Two variables that are generally accepted to significantly affect pump noise levels are speed and outlet pressure. Maroney et al. (72) noted that, with minor deviations, the speed, outlet pressure sound power surfaces of most hydraulic pumps behave as shown in Figure 27. Using data plots for an example pump, Maroney et al. (72, p. 1660), observed the following:

1. The sound power is approximately linear as a function of pressure on semi-log paper.
2. The sound power is approximately linear as a function of speed on log-log paper.

Using this information they proposed the following pump noise model:

$$W = K\, N^{\alpha}\, 10^{\beta P} \qquad (2.55)$$

where:

W = sound power (watts)

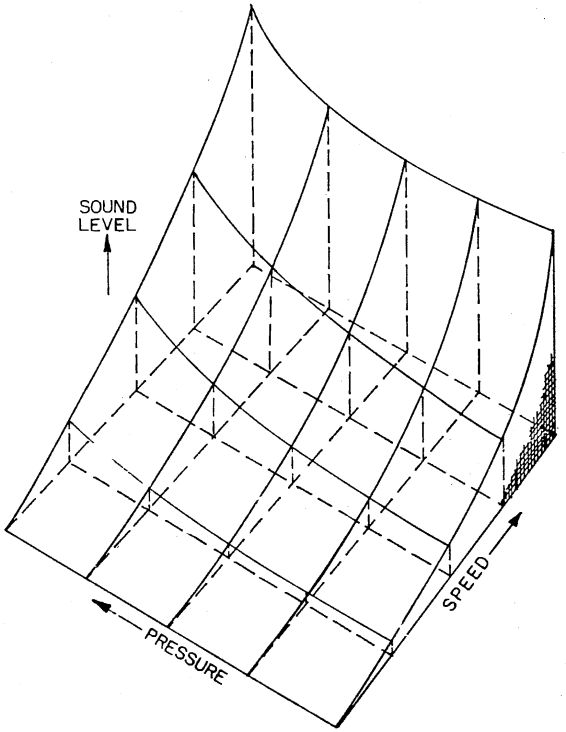

Figure 27. Monotonically Increasing Sound Power Surface to Describe Pump Noise as a Function of Speed and Pressure

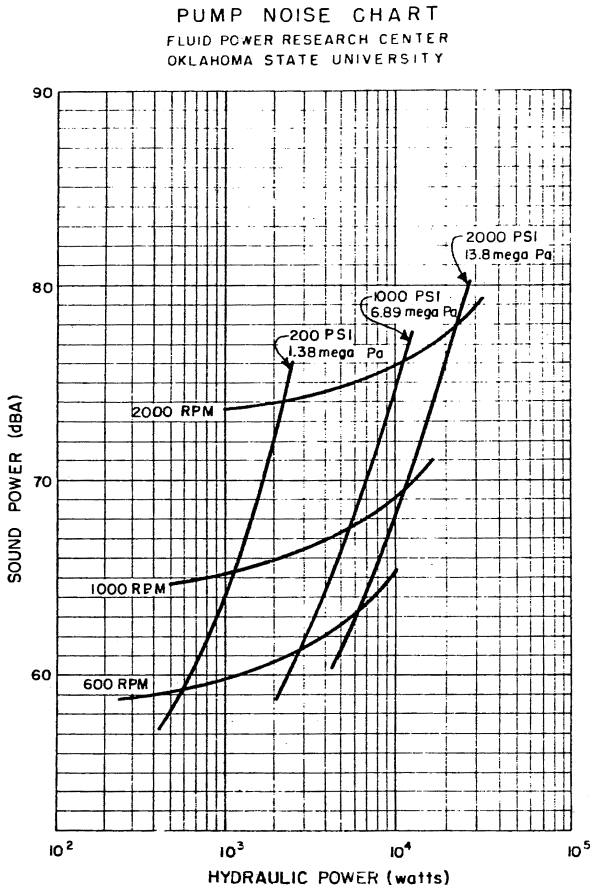

Figure 28. Predicted Pump Airborne Sound Power Versus Pump Hydraulic Power for Various Speeds and Pressures

N = speed (rad/s)

α = constant

β = constant

K = constant

P = outlet pressure (Pa)

Figure 28 shows plots of the predicted sound power level of a hydraulic pump as a function of speed and pressure. The plots in Figure 28 show the relative sensitivity of the pump's sound power to speed and outlet pressure. It is readily apparent that the pump's sound power is more sensitive to speed changes than to outlet pressure changes. To date, over thirty high pressure hydraulic pumps have been tested for sound power level at the Fluid Power Research Center. The sound power speed sensitivity for all of these pumps was greater than the sound power outlet pressure sensitivity.

Critical Variables

Figure 29 summarizes the "expected" effects of known "critical variables on the noise "emitted" by a high pressure oil hydraulic pump. The variables are categorized by environments: the acoustic environment and the hydraulic environment. The hydraulic system variables are further sub-divided into operational parameters and the system fluid. It is recognized (4) that mechanical and hydraulic system interactions can significantly influence the noise produced by a hydraulic pump. However, a detailed discussion of

CRITICAL VARIABLE			SYMBOL	"EXPECTED" EFFECT ON "EMITTED" NOISE
HYDRAULIC ENVIRONMENT	OPERATION	TIME	t	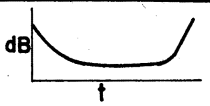
		pressure, inlet	p_{in}	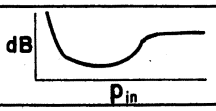
		pressure, outlet	p_{out}	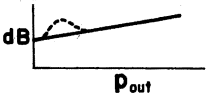
		speed	ω	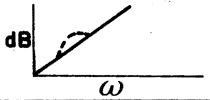
		temperature (viscosity)	T	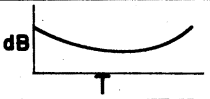
	FLUID	AIR/LIQUID VOLUME RATIO	r	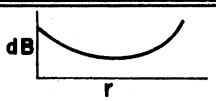
		VISCOSITY	μ	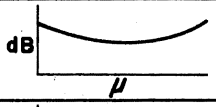
		LIQUID SURFACE TENSION	σ	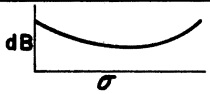
		CONTAMINATION LEVEL	g*	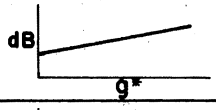
		LIQUID SOLUBILITY CONSTANT	s	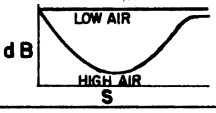
		LIQUID SONIC VELOCITY	c	ESSENTIALLY CONSTANT
		LIQUID VAPOR PRESSURE	p_v	USUALLY NEGLIGIBLE
		LIQUID DENSITY	ρ	ESSENTIALLY CONSTANT
		LIQUID TENSILE STRENGTH	σ_T	USUALLY NEGLIGIBLE
ACOUSTIC ENVIRONMENT	MEASURED MEDIUM	TEMPERATURE	T_e	NEGLIGIBLE (< 0.5 dB VARIATION)
		PRESSURE	p_e	
		HUMIDITY	h_e	

Figure 29. Chart Summarizing "Expected" Effects of Known "Critical" Variables on Noise "Emitted" by a High Pressure Oil Hydraulic Pump

their influence is beyond the scope of this study. The effects of mechanical and hydraulic system interactions are minimized using techniques outlined in the next chapter, Experimental Considerations. The effects shown for any single variable in Figure 29 were obtained by interpretation of the discussions in this chapter, assuming that the other variables were constant and that the pump was operating at "normal" operating conditions.

The comments about the negligible effects of the acoustic environment can be verified using any good reference on noise measurements (71), (73). The comments are predicated on laboratory measurements using modern instrumentation, which has low sensitivities to all parameters other than the measured quantity. It is recognized that the physical configuration of the acoustic environment and the proximity of other noise sources will influence acoustical measurements. Experimental techniques to account for these acoustic variables are discussed in the next chapter.

The summary in Figure 29 and the associated discussions in this chapter provide a comprehensive base for the development of an experimental program for the study of the acoustical signatures of high pressure fluid pumping phenomena. The next chapter discusses experimental considerations, including the influence of the critical variables on the design and implementation of a test program.

CHAPTER III

EXPERIMENTAL CONSIDERATIONS

The objectives of the study, the preliminary examination of the specimens, and the theoretical base provide the information needed to simultaneously select: (1) test facilities, (2) data acquisition and reporting techniques, and (3) specific test specimens.

The objectives of the study require non-intrusive measurement of pump noise as a function of time, wear, and cavitation. These objectives necessitate the use of a "typical" pump performance test system, a pump contaminant sensitivity test system, and a pump cavitation sensitivity test system. The objective of measuring hydraulic pump noise means that noise measurement instrumentation is required in addition to the usual hydraulic and mechanical measurement instrumentation required for pump tests.

The selection or construction of the test systems and the selection of instrumentation is predicated on the characteristics of the test specimens. The specimen characteristics establish requirements for the test system and its instrumentation, as well as noise measuring instrumentation.

This chapter establishes specific constraints for the test specimens, considers four data categories and their

relative merits, delineates the characteristics of the test systems, and discusses the measurements and associated instrumentation necessary to meet the study objectives.

Specimen Characteristics

The basic characteristics of the test specimens, high pressure hydraulic pumps, are discussed in Chapter II. A prominent gear pump manufacturer, who requested to remain anonymous, agreed to furnish specimens for the study. It was decided to limit the power requirements for the pumps to 74.6 kW (100 hp). This arrangement was satisfactory to the pump manufacturer and well within the test system capabilities of the Fluid Power Research Center, where the tests were conducted. It was previously determined (33) that such test specimens would acoustically represent typical pumps available in the fluid power industry.

To establish a frequency range for the noise measurements, the number of teeth per gear in the pump had to be established, as well as the maximum pump speed. It was decided that the specimens would have 10 teeth per gear, operate at a maximum speed of 42 rev/s, and have a displacement per revolution of approximately 50.0×10^{-6} m^3.

The number of teeth for the drive gear and the maximum operation speed of 42 rev/s means that the maximum fundamental pumping frequency for the specimens is (74):

$$f_{1p} = n \cdot N = 10\ (42) \text{rev/s} = 420 \text{ Hz} \qquad (3.1)$$

where:

f_{1p} = fundamental pumping frequency (Hz)

n = number of teeth on drive gear

N = pump drive shaft speed (rev/s)

It was decided to limit the minimum test speed to 10 rev/s which means that the minimum fundamental pumping frequency is equal to or greater than 100 Hz.

Data Categories

It is essential at the outset of an experimental program to establish the categories of data necessary to meet the project objectives. Four data categories are considered in this study: "accurate", relative, single-factor, and multi-factor.

"Accurate"

F. K. Willenbrock (75, p. 141), National Bureau of Standards, indicated that measurement methods should be "relevant, unambiguous, reproducible, accurate, simple, and inexpensive." According to reference (43) accurate means precise, and precise means definite or without variation. Roberts (76, pp. 8-11) noted the following: "Some confusion exists regarding the use of the terms accuracy and error. While both of these words describe very real quantities, both are in fact unknowable." Roberts discusses the fact that data should be discussed in terms of the reporter's confidence in a value of uncertainty. He points out that

increased confidence and decreased uncertainty mean a more expensive data acquisition procedure. The manufacturer of the noise analysis instrumentation used for this study discusses the "confidence" and "uncertainty" of their instrumentation using confidence levels and confidence intervals (77).

High confidence in small confidence intervals between the observed and actual value of a measured parameter is important for reporting the characteristics of components and systems to purchasers, and it is extremely important when establishing fundamental scientific data such as the speed of light, etc. In both of these cases, elaborate care must be taken to isolate the measured quantity. It is questionable, however, that the expense of achieving high confidence in small confidence intervals is justified for most of the data needed to achieve the objectives of this study. First, it would require isolating all of the mechanical and hydraulic system interactions necessary to correct the measured quantities. Second, it would require elaborate, time consuming, and expensive development and measurement efforts to obtain some of the unknown fundamental characteristics of the fluids. Third, since the fluid power industry has been unable to converge on "acceptable" techniques for reporting data (76), it is certainly beyond the scope of this study to use anything other than standard laboratory practices for calibration, data acquisition, and data reporting.

Relative

It is sufficient for the purposes of this study that the reported data has high relative confidence levels in small relative confidence intervals. This means that even though the measurement systems are calibrated and it is possible to study and discuss high confidence in small confidence intervals, it is not necessary for this study. The objective of this study is to determine the sensitivity of pump noise to various parameters. This objective is satisfied by conducting each series of tests with the same test system and recording observed parameter values with the same instrumentation as the variables of interest are changed.

As noted in Chapter II pump speed will affect the noise frequency and amplitude. Tests conducted at essentially constant speed will only reflect a pump's noise sensitivity to mechanical and hydraulic factors, if the speed happens to correspond to one of the systems natural frequencies. The possibility of the latter occurring was carefully considered during the design of the test systems to minimize the increased measurement standard deviation that would occur if the pump happened to force the systems at one of their natural frequencies. However, system resonance induced variations due to small-random speed changes do not affect the observation of significant changes in the relative values of the measured variable, even though the measurement standard deviation may be higher.

For this study differences between test systems are noted and those variations are considered when analyzing the test data on a relative basis.

The acquisition, reporting, and analysis of data for this study does not dwell on the "exact" answers, but on the significant relative changes in a pump's noise level due to operating parameter changes.

Single-Factor

The single-factor experiment, traditional with engineers (78), consists of recording values of the measured quantity while only one test parameter is known to be changing. The advantage of this approach to data acquisition is its simplicity, relative to both conducting the test and analyzing the data. The disadvantage is that single-factor experiments provide no information about significant interactions that occur between the test parameters (79).

Multi-Factor

Multi-factor experiments provide information about the output variable effects due to interactions that occur between the operating parameters. If the variables of interest are not linearly independent then the multi-factor experiment will show that an interdependence exists. As implied by the discussion, the multi-factor experiment consists of recording values of the variable of interest while several operating parameters are changing simultaneously.

References (78), (79), and (80) have excellent discussions of the multi-factor experiment. Multi-factor experiments are generally larger and more complex than single-factor experiments (79).

In spite of their complexity, multi-factor experiments can provide two important pieces of information for any study. First, the multi-factor experiment indicates the possible existence of operating parameter interactions, uncontrolled operational parameters, or both. Second, a multi-factor experiment is an efficient way to determine whether a given set of operational parameter control limits is satisfactory. One multi-factor experiment is included in this study to obtain the two pieces of information described in this paragraph.

Pump Test Systems

The objectives of this study require three test system capabilities: provide normal pump operation versus time, provide pump operation with controlled accelerated wear, and provide pump operation with controlled air/liquid volume ratios.

Performance

Any "typical" pump performance test system can be used to obtain information about the noise level of pump as a function of time with "normal" operating conditions. Either the pump contaminant sensitivity test system or the pump

cavitation test system described below can be controlled to serve as a "typical" pump performance test system.

Contaminant Sensitivity

Pump contaminant sensitivity test systems are well defined (81). Appendix C contains a schematic of the hydraulic pump contaminant test system currently being proposed by The National Fluid Power Association (81). The test system is a direct result of extensive studies conducted at the Fluid Power Research Center (FPRC). The FPRC Pump Contaminant Sensitivity Test System was used for the controlled pump contaminant sensitivity tests reported in this study. The basic procedure for pump contaminant sensitivity tests is outlined in Reference (81) and is not repeated here.

Since the pump contaminant sensitivity test procedure is well defined and the tests are well controlled (81), it affords an opportunity to measure pump noise levels as a function of contamination levels as well as after controlled accelerated wear.

When system flow rate is directed through the system filters, the pump contaminant sensitivity test system is capable of functioning as a "typical" pump performance test system.

Cavitation Sensitivity

To achieve the necessary air/liquid volume control for

this study the FPRC Acoustics Laboratory Hydraulic Test System was modified. The resultant system allows control of the system air/liquid volume ratios as described by Elliott (82). A schematic of the system is shown in Appendix C. It is sufficient to note here that the system's vacuum pump with the average test circuit is capable of attaining a system pressure of approximately 34 kPa (absolute) which is used to reduce the air/liquid volume ratio. An injection chamber for air allows up to 2.07×10^{-3} m^3 of air at 721 kPa (absolute) to be injected into the hydraulic system to attain air/liquid volume ratios as high as 0.42. By properly controlling the air/liquid ratio the system is capable of functioning as a "typical" pump performance test system.

Measurements

Given the characteristics of the specimens for acoustical signature analysis, the type of data required, and the test systems it is possible to select the measurement instrumentation necessary to achieve the objectives of the study. This section considers the selection and use of acoustical, hydraulic, and mechanical instrumentation.

Acoustical

The purpose of acoustical instrumentation is to isolate the magnitude noise energy within desired frequency bands. Typically the results are presented as noise levels versus

frequency (see Appendix D). Knowing the characteristics of the test specimens and the fact that cavitation noise is present above 10 kHz allows establishing a frequency range for the noise instrumentation of 100 Hz to 50 kHz. Table IV shows the relationship between the elements of a typical measurement system (52) and the noise measurement systems used for this study. The decision to usually report relative information eliminates the need to report noise measurements in absolute terms with characteristic impedances.

The remainder of this section considers several important topics regarding noise measurements in fluid power systems: measurement units, measurement environments, sensing elements, analyzers, recorders, and calibration.

Units. There are three forms of noise associated with fluid power systems: hydraulic pressure ripple, structural vibrations, and the resultant airborne noise. For this study the magnitude of these physical parameters is referred to in decibels (dB) as defined below. The intensity level of airborne noise is defined as (14):

$$IL = 10 \log_{10} (I/I_r) \qquad (3.2)$$

where:

IL = intensity level of noise (dB)

I = intensity of noise (W/m^2)

I_r = reference intensity (10^{-12} W/m^2)

Since intensity is related to pressure squared the airborne noise pressure level, for atmospheric conditions, is (14):

TABLE IV

RELATIONSHIP BETWEEN MEASUREMENT SYSTEM ELEMENTS AND NOISE MEASUREMENT INSTRUMENTATION USED TO OBTAIN ACOUSTICAL SIGNATURES

Noise Type	Airborne Noise	Structureborne Noise	Fluidborne Noise
Measured Medium	Air	Solid	Fluid
Measured Quantity	Pressure	Acceleration	Pressure
Primary Sensing Element	Microphone	Accelerometer	Pressure Transducer
Variable Conversion Element	Amplifier		
Data Transmission Element	Sequential 1/3 Octave-Band Analyzer	OR	Tape Recorder
Variable Manipulation Element			Sequential Narrow-Band Analyzer
Data Presentation Element	Recorder		
Presented Data	1/3 Octave-Band Plot of Level Versus Frequency	OR	Narrow-Band Plot of Level Versus Frequency
	Observer		

$$ABN = 20 \log_{10} (P/P_r) \qquad (3.3)$$

where:

ABN = airborne noise level (dB)

P = rms measured pressure (Pa)

P_r = rms reference pressure (20μPa)

An equation similar to Equation (3.3) can be used to report pressure ripple, or fluidborne noise. For fluidborne noise measurements the level can be reported as FBN (dB) using the same reference as Equation (3.3). This procedure greatly facilitates discussions of attenuations between fluidborne noise levels and the resultant airborne noise levels. For this study the levels for acceleration, velocity, and displacement are:

$$L_a = 20 \log_{10} (a/a_o) \qquad (3.4)$$

$$L_v = 20 \log_{10} (v/v_o) \qquad (3.5)$$

and

$$L_d = 20 \log_{10} (d/d_o) \qquad (3.6)$$

where:

L_a = acceleration level (dB)

a = measured acceleration (m/s^2)

a_o = reference acceleration (10^{-5} m/s^2)

L_v = velocity level (dB)

v = measured velocity (m/s)

v_o = reference velocity (10^{-8} m/s)

L_d = displacement level (dB)

d = measured displacement (m)

d_o = reference displacement (10^{-11} m)

Environment. The selection of the measurement environment and sensor locations in that environment are critical since the combination must provide repeatable information. The objectives of this study require selecting a measurement method that is non-intrusive, which means that the measurement technique must be practical for "field" use.

Fluidborne noise measurements must be made in the hydraulic fluid. This means that FBN measurements with stationary sensors are constrained to conduit walls and component cavities. FBN measurements are possible with moving transducers, but this procedure is even less practical in a "field" environment than measurements with stationary sensors. Even though preliminary measurements of pump FBN correlated well with pump ABN, (the pump outlet FBN over a 30 dBA range was approximately 120 dBA more than the ABN with a given hydraulic system), because FBN measurements are intrusive, it was decided to abandon FBN measurements as a feasible "field" diagnostic measurement at this time.

Structureborne measurements require placing a sensor in contact with the measured surface. The attachment of vibration pickups requires special techniques (71) which can introduce another variable into the measurement process. The attachment of the sensor and its associated mass to the measured surface has some effect on the response of the surface. Since vibration measurements have been used successfully for diagnostics (31), (60), preliminary vibration measurements were made for this study. The use of

structureborne measurements for this study was abandoned because of the unknowns associated with the mounting techniques. It was considered beyond the scope of this study to initiate a study of the standard deviations associated with mounting techniques for vibration transducers. Had it not been for the necessity of comparing test results between similar pumps the vibration sensor mounting study might have been avoided, and vibration measurements used to determine an individual pump's sensitivity to particular operational parameters variations.

ABN measurements are non-intrusive. Since the sensing element does not have to touch the component, the only effect it can have on the surfaces response is to cause a pressure feedback because of its presence in the acoustical field. If fixed coordinates for the microphone are selected relative to the component, then the only other coupling factor that may introduce measurement variation is the air, whose impedance does not normally change significantly from day to day.

Every acoustical environment can be plagued with standing wave problems. It is not a question of whether or not they will exist at certain frequencies, it is only a question of their magnitude. When looking for exact answers standing waves can be a significant problem. When looking for a relative change in a noise level the effect of standing waves can be minimized by always making measurements in the same carefully selected point.

Every acoustical environment has some background noise. When making noise measurements, it must be determined that the noise is from the source being studied and not a background source. Figure 5 indicates that the best way to minimize background noise effects when making ABN measurements is to take the measurements in the near-field of the source being examined.

Any combined effects, or interactions, of the transducer location and the environment on the noise level can be minimized by using fixed coordinates for the microphone and not changing the environment until the tests are completed.

Sensing Elements. The sensing elements for the noise measurements in this study are shown in Table IV and specified in Appendix B. Preliminary FBN measurements were made at the outlets of selected pumps. Since the effects of cavitation should be greatest in the low pressure region of the pump, the pump inlet was selected for vibration and ABN measurements.

A "pressure" microphone was selected for the ABN measurements, because the perpendicular-incidence response of a "pressure" or random-incidence microphone is much greater above 10 kHz than the perpendicular-incidence response of a similar free-field microphone. By using a random-incidence microphone with the microphone face parallel to pump's surface, the high frequency cavitation noise is amplified relative to the "lower" frequency noise associated with the normal fluid pumping phenomena. The microphone is shown in

"position" at the inlet of a typical high pressure pump in Appendix C.

The location of the microphone relative to the pump inlet was established by insuring that the microphone was no further from the pump than a quarter wavelength at the maximum frequency of interest. Since it was not considered necessary to measure frequencies above 50 kHz the distance between the face of the microphone and the pump's surface was selected to be less than:

$$\frac{\lambda}{4} = \frac{340 \text{ m/s}}{(4)\ 50{,}000 \text{ cycles/s}} = 1.7\ 10^{-3} \text{ m} \qquad (3.7)$$

where:

λ = wavelength (m)

A dimension of 1.0 mm was selected for the distance between the pump and the microphone.

Analyzers. As outlined in Table IV two techniques were implemented to obtain level versus frequency information for analysis. A commercially available 1/3 Octave analyzer was selected which has averaging times that provide 90% confidence intervals of less than or equal to 0.5 dB over the frequency range of interest. The 0.5 dB confidence interval is associated with the lower frequencies and the confidence interval decreases at higher frequencies.

Because of capital limitations, real-time data acquisition instrumentation with associated data manipulation equipment was not available for this study. As shown in Table IV,

a tape recorder was used in conjunction with a sequential narrow-band analyzer to obtain quasi-real-time narrow-band data. The use of the tape recorder also allowed making 1/3 Octave plots of quasi-real-time data.

The sequential narrow-band analyzer has 10 Hz and 100 Hz filters. Per the manufacturer's recommendation (83) the analyzer was operated at an analysis rate of less than or equal to 10 Hz/s with the 10 Hz filter and an analysis rate of less than or equal to 100 Hz/s with the 100 Hz filter. During preliminary tests it was determined that the use of 5 Hz/s with the 10 Hz filter from 100 Hz to 1000 Hz, the use of 10 Hz/s with the 10 Hz filter from 1000 Hz to 10 kHz, and the use of 100 Hz/s with the 100 Hz filter for 10 kHz and higher frequencies, gave repeatable data sets of pump noise. The total time required for each plot is 1230 s.

Recorders. Since the noise emitted by the pump could change significantly during 1230 seconds required for a narrow-band analysis it was necessary to record the noise data for analysis at a later time. The tape recorder was modified to "play" tape loops of approximately 6 s duration repeatedly during the narrow-band analysis. This procedure allowed making data tapes approximately every minute. The largest 90% confidence interval for data processed in this manner is estimated to be 0.6 dB.

The recorder for the two analyzers was a "common" unit which adapted to both analyzers. Typical data plots are

shown in Appendix D. The recorder-mainframe, common to both analyzers, also accommodates a pre-amplifier plug-in module which allows recording all-pass data while the tape recorder is being used to obtain quasi-real-time data. This procedure allows monitoring calibrations and major acoustical data variations.

Calibration. The calibrators for the ABN and SBN measurements are listed in Appendix B. Before and after each ABN test series the ABN calibrator was used to calibrate the instrumentation system and verify the calibration, respectively. For FBN measurements the reference voltage available with the ABN calibrator is used to set the instrumentation. The FBN sensors and amplifiers are factory calibrated. For SBN measurement the SBN calibrator is used to calibrate and verify the systems performance.

The stability of the tape recorder is periodically verified by comparing ABN measurements recorded with the 1/3 Octave analyzer while the noise signal is being taped, with the taped data which is subsequently "played-back" to the 1/3 Octave analyzer. This procedure insures that the deviations of relative measurements are due to variations of the measured quantity and not to "drift" of the tape recorder.

As indicated in Table V if the difference between the "before" and "after" calibrations exceeds 0.5 dB the data is rejected.

TABLE V

ALLOWABLE OPERATING CONDITION VARIATIONS: 1) PER ISO/TC 131/SC8 (WG1-1)84(3), 2) FOR SINGLE FACTOR STUDIES, AND 3) FOR MULTI-FACTOR STUDIES

Measured Quantity	ISO/TC 131/SC8 (WG1-1) 84 Maintain Within	Single Factor Studies Maintain* Within	Deviations (+ & -) During Multi-Factor Study	Multi-Factor Study Maintain Within
Low Pressure**	± 2%	± 2%	0.0	± 2%
High Pressure	± 2%	± 2%	3.3%	± 1.0%
Speed	± 2%	± 1%	3.3%	± 0.7%
Temperature	± 2°K	± 1°K	2.0°K	± 0.5°K
Noise	Calibration Before Test	Calibration Before & After Difference ≤ 0.5 dB	Calibration Before & After Difference ≤ 0.5 dB	Calibration Before & After Difference ≤ 0.5 dB

*Parameter values reported in study were maintained within limits shown in table.

**All reported pressures less than 0.5 MPa are absolute pressures.

Hydraulic and Mechanical

For this study hydraulic and mechanical measurements include the measurements of fluid parameters as well as operational parameters. Most of these measurements are made using standard laboratory techniques and are not discussed in this section.

Operational. Table V shows allowable observed operational parameter variations per the latest proposed ISO (International Organization for Standardization) hydraulic pump noise test code (3). During the single-factor tests during this study the allowed variations were constrained as shown in Table V. For the multi-factor tests even more stringent allowable variations were maintained, but as shown in Table V the deviations of the variables were not exceedingly large which necessitated the more stringent controls.

Since the inlet gauge was not located at the same height as the inlet of the pump, the difference in height was noted and the inlet pressures were corrected for the difference.

Fluid. The fluid properties of viscosity and vapor pressure were not measured during this study, but rather the data shown in Appendix G was considered reliable and used as required. Consistent with the data reported in Chapter II a solubility of air in oil of 0.09 was used for this study. MIL-L-2104 hydraulic oil was used as a system liquid for all

of the experiments reported in this study.

Visual observations of the entrained air at the pump inlet were made using a sight tube that was installed in the pump inlet. Appendices C and D, respectively, contain photos of the sight tube with stationary aerated fluid and the sight tube with aerated flowing fluid. Quantitative appraisals of the air/liquid volume ratio, r, were made using an aeration detection device described and discussed by Elliott (82) and Tessmann et al. (84). Briefly, the aeration detection devices consist of a scaled syringe, which is partially filled with the fluid to be measured, and a plunger, which is used to create a vacuum on the trapped fluid providing a resultant volume of air at standard temperature and pressure which is ratioed to the remaining liquid volume to estimate r.

Within the constraints defined in this chapter and consistent with the study objectives a formal test program was outlined. That program and the resultant experimental results are discussed in the next chapter.

CHAPTER IV

THE EXPERIMENTS

The experimental program proposed for this study was modified during execution to capitalize on the outcome of the initial tests and the availability of test facilities and test specimens. Table VI shows the expanded data acquisition program. The purpose of this chapter is to delineate the program depicted in Table VI.

During the study data acquisition period, which has spanned three years, over 600 plots of noise level versus frequency were recorded. Many of the data sets are narrow-band band plots, but the majority are 1/3 Octave-Band plots. Each of these plots covered the 100 Hz to 50 kHz frequency range. A 1/3 Octave-Band plot from 100 Hz to 50 kHz includes 28 center-frequencies. Thus, assuming the plots are all 1/3 Octave-Band information, there are well over 17,000 data points, associated with the study, that require examination, assimilation, digestion, and culling to insure presentation of the most meaningful information. It is simply impractical to discuss all of the tests in these pages or present all of the test results in this document. Therefore, only the most important tests are discussed in this chapter and only selected experimental results are

TABLE VI

DATA ACQUISITION PROGRAM FOR THE ANALYSIS OF PUMP ACOUSTICAL SIGNATURE SENSITIVITY TO OPERATIONAL PARAMETERS

	Pump Lot "A"						Pump Lot "B"		
Objectives	4321	4323	4324	4325	4326	4327	4351	4352	4353
Select Data Acquisition Technique	A		E						
Study Noise Level Stabilization	A 36ks	D 9ks	E 16ks	F 36ks	F 43ks	F 41ks	F 40ks	B 30ks	
Conduct Multi-Factor Experiment			E						
Select Cavitation Study Outlet Pressure		D							
Study Cavitation Effects	A*	D*	E	F	F		F	B	
Study Air/Liquid Ratio Effects	A*				F				
Study Speed Induced Cavitation								B	
Study Volumetric Efficiency Versus Cavitation Noise		D*		F	F		F	B	
Study Contamination Level Effects	B*				B			B	B
Study Wear Effects	B*				B		B*	B	B
Study Temperature Effects					F				

NOTES:
1. Letter in a cell indicates test system used for study.
2. Asterisk indicates data used for "trend" examination or verification.
3. Times are lengths of respective noise stabilization studies.
4. Underlined letter in a cell means some data for the associated tests are presented in Chapter V.

presented in Chapter V. In some cases unpresented data are summarized in the analyses in Chapter VI. A very small portion of the "raw" data is presented in Appendix D for illustrative purposes.

The test program is designed to provide experimental data from two sample lots of gear pumps to determine if pump acoustical behavior is consistent with theory and consistent between random samples of specimens from different distributions. It was originally proposed to have the major variable between pump "lots" be displacement per revolution. During discussions with the pump manufacturer it was determined that they produce pumps with essentially the same displacement, but with different gear configurations. It was decided to make the major variable between pump "lots" the gear configuration (and associated internal design) because it would be most beneficial to the company furnishing the pumps and would inhance the study. The gears in the lot "A" pumps have an outside diameter of 53.4 mm and the gears in the lot "B" pumps have an outside diameter of 61.0 mm.

The presence of a letter in a cell of Table VI indicates the accomplishment of the respective set of experiments on a particular specimen. The letter in the cell indicates the test system on which the tests were conducted. Test systems A, C, D, E, and F are all minor modifications of the FPRC Acoustical Laboratory Pump Cavitation Sensitivity Test System. These modifications involve small length changes,

always less than 25 cm., of the inlet and outlet conduits. Test system B is the FPRC Pump Contaminant Sensitivity Test System. During the experiments the test parameters were maintained within the limits discussed in Chapter III, Table V.

The experiments discussed in the remainder of this chapter are: data acquisition, noise level stabilization, multi-factor, cavitation, contamination, wear, and temperature.

Data Acquisition Technique

The selection of a diagnostic data acquisition technique was based on the results of numerous tests at the Fluid Power Research Center Acoustics Laboratory. As noted in Table VI, only two of the study pumps were used in the selection process. Some of the SBN measurements on unit 4324 are shown in Appendix D, Selected Experimental Results. The final decision to use ABN measurements for the data acquisition process is based on all of the previous studies and the studies of specimens 4321 and 4324. Selected data from these tests is presented in Chapter V. The reasons for selecting an ABN data acquisition technique are outlined in Chapters II, III, and VI.

Noise Stabilization

Sample standard deviations of 3.6 dBA have been observed for fluid-power pump noise levels (4). It was

conjectured that this deviation was due to either the characteristics of the components or to the measurement procedures (4). Since the reason for this deviation is important for the purposes of this study and for the rational comparison of pumps in the "market place", the noise level of pumps as a function of operating time is examined in this study. The data presented in this study was obtained using near-field ABN measurements. Although it was originally proposed to examine the noise stabilization characteristics of only two pumps, a total of eight pumps were monitored for noise level versus time. Individual pump noise stabilization study test lengths are listed in Table VI. The shortest test time is 9ks and the longest is 43 ks.

The test conditions for the experimental data discussed in Chapter V are presented with the data. Although the specific operation conditions for the tests varied, they were in the vicinity of the following: speed, 27.0 rps; outlet pressure, 10 MPa; inlet pressure, 150 kPa; and temperature, 38.0°C. During these experiments the microphone was moved frequently for calibration, which is an important consideration in the analysis.

Multi-Factor

A multi-factor experiment was conducted on specimen 4324 to obtain information about the sensitivity of high pressure pump noise levels to operating parameter variations. The operating conditions for the experiment were varied

about a speed of 25 rps, an outlet pressure of 10.3 MPa, and a temperature of 38.0°C. The deviations for speed, outlet pressure, and temperature are listed in Table V, Chapter III. The data for the experiment is listed in Appendix F, along with the analysis of variance tables. Appendix F also contains a brief summary of the significance of the results obtained with any analysis of variance. The summary of the results of the multi-factor experiment are presented and discussed in Chapter VI. In accordance with the original test plan only one pump from lot "A" was used for the multi-factor experiment. During the multi-factor experiment it was not necessary to move the microphone often for calibration.

Cavitation

Noise level versus cavitation condition studies were conducted on pumps from both lots "A" and "B". Preliminary studies were conducted to establish an outlet pressure for the remainder of the cavitation experiments. Subsequent cavitation studies were conducted by varying the air/liquid volume ratio, the inlet pressure and speed, or the reservoir pressure and the speed. Volumetric efficiencies of selected pumps versus cavitation noise levels were also studied. The remainder of this section discusses these various experiments. Most of the noise level versus cavitation experiments were conducted with a minimum number of movements of the microphone for verifying calibration.

Outlet Pressure. Unit 4323 was tested at a fixed speed of 25.0 rps, an inlet pressure of 142 kPa, a fluid temperature of 38.0°C, and two outlet pressures. The outlet pressures were 3.4 MPa and 10.3 MPa. Preliminary cavitation studies were conducted at both test pressures. The data for this study are not presented in the report, but the results and the decision to use high outlet pressure during the remainder of the cavitation studies are discussed in Chapter VI.

Inlet Pressure. Most of the noise level versus cavitation studies were conducted by controlling the air/liquid ratio, holding the pump speed constant, and varying the inlet pressure to induce cavitation. Some of the noise level versus inlet pressure experimental data for units 4324, 4325, 4326, 4351, and 4352 are presented in Chapter V and discussed in Chapter VI.

Air/Liquid Ratio. To determine the influence of the air/liquid volume ratio on the cavitation noise emitted by a fluid power pump, tests were conducted with units 4321 and 4326. Some of the "raw" data from the tests with 4321 are shown in Appendix D. Some of the results of the tests with unit 4326 are presented in Chapter V and discussed in Chapter VI. The air/liquid volume ratios were measured with the aeration detection device discussed in Chapter III. Aeration levels measured with the aeration detection device are reported as A*. Two test series were conducted with

different air/liquid volume ratios. The lower air/liquid ratio measured approximately 0.7% and the higher air/liquid ratio measured 7.0%. Since the results of the cavitation tests were so consistent with the expected results, consistent with the original experimental plan, air/liquid volume ratios were not varied for tests with pumps from lot "B".

Speed Induced. Since many practical fluid power systems operate without the facilities to directly control the inlet pressure (which would in turn control the cavitation conditions), but do have variable speed capability, it was considered desirable to study the possibility of detecting speed induced cavitation. This experiment was conducted using unit 4352 and monitoring expected output flow rate and pump noise level as the pump speed was increased with a constant system reservoir pressure. Part of the results of the test are shown in Chapter V and discussed in Chapter VI.

Volumetric Efficiency. Volumetric efficiency is the ratio of the actual output flow to the expected output flow rate at a given operating pump speed. A comparison of the volumetric efficiency and the noise level provides a means of relating a cavitation performance parameter to the noise emitted by a pump. During several tests the output flow rate was monitored for comparison to the pump noise level. The results of noise level-volumetric efficiency tests with units 4325, 4326, 4351, and 4352 are presented in Chapter V and discussed in Chapter VI.

Contamination

Particulate contamination levels are one of the basic operating parameters for hydraulic pumps. Although test codes frequently require that contamination levels be controlled with filtration consistent with the pump manufacturer's recommendations (3). This type of constraint may not provide adequate contamination control from an acoustical point of view. To determine the sensitivity of a pump's noise level to particulate contamination tests were conducted on four specimens.

Preliminary noise level versus contamination level experiments were conducted on unit 4321. One narrow-band spectrum for unit 4321 operating in a contaminated fluid environment is shown in Appendix D. Controlled noise level versus contamination level tests were conducted with units 4326, 4351, and 4352 using known levels of A C Fine Test Dust in the system fluid. The tests were conducted on the FPRC Contaminant Sensitivity Test System using recommended test procedures (81). During these tests the microphone was repositioned several times for calibration checks. Some of the test results are summarized and discussed in Chapter VI.

Wear

Acoustical signature analysis is frequently used to detect unusual or abnormal wear of a component (24), (25). The possibility of using non-intrusive diagnostics as a

viable means of detecting a "worn-out" pump is one of the major objectives of this study. Two preliminary tests and three carefully controlled wear tests were conducted on selected specimens using the test system and procedures used for the particulate contamination studies (81). Results of these studies are presented in Chapter V and discussed in Chapter VI. The Noise Wear Index is developed and discussed relative to the data that resulted from these tests. All of these controlled tests were conducted on the FPRC Contaminant Sensitivity Test System (81). During these tests the microphone calibration was checked frequently, which required repositioning the microphone.

Temperature

The results of the multi-factor experiment indicated temperature variations and temperature-speed interactions significantly affected the noise emitted by a high pressure hydraulic pump. To further examine this phenomena a single-factor temperature experiment was conducted on specimen 4326. The operating conditions for this test are reported in Chapter V with some of the experimental results. The data are discussed in Chapter VI. The microphone was stationary during this test series.

The next chapter presents selected samples of the more significant experimental results of the tests outlined in this chapter. The experimental results are summarized and discussed in Chapter VI.

CHAPTER V

SELECTED EXPERIMENTAL DATA

The purpose of this chapter is to present selected experimental results applicable to the discussions in Chapter VI. Both general trends and observed anomalies of the experimental results are presented in the following pages. To achieve objectivity the data is usually presented without conclusions or explanations for observable trends. The discussions in Chapter VI compare the results of this study with known theory and similar acoustical signature analysis results for low pressure hydraulic pumps.

In some cases coefficients of determination, r^2, are presented with the data plots. Where coefficients of determination are shown the corresponding curves are the result of "fitting" the data to an appropriate equation. If a curve for a given data set is shown without a coefficient of determination, the curve is "estimated" to assist in visualizing any apparent data trends.

Unless noted otherwise, the operating conditions for the experiments were controlled as outlined in Chapter IV. The following paragraphs relate experimental results associated with the following areas: selection of a data

acquisition technique, noise stabilization, cavitation, wear, and temperature.

Data Acquisition Technique

Preliminary tests of the noise level associated with a high pressure hydraulic pump were conducted while varying the distance of the measurement from the pump's surface. These tests produced the results shown in Figure 30 (5). The "all-pass" ABN levels shown in Figure 30 were obtained by increasing the radial distance from a selected pump surface on an axis perpendicular to the surface. Measurements were recorded both for increasing and decreasing radii. The acoustical environment for the measurements was the FPRC reverberation room.

Relative to Figure 30, the operating conditions for Unit 4321 were changed to obtain the data shown in Figure 31. The data in Figure 31 was obtained in the same manner as that of Figure 30 where the maximum radius was smaller. The data in Figure 31 was obtained with the same instrumentation operating in the same environment as that of Figure 30. The conclusion presented with Figure 31 is discussed in reference (5) and is also discussed in Chapter VI.

Noise Stabilization

Figures 32 through 36 present experimental results of noise level versus time for eight test specimens. "All-pass", narrow-band, and 1/3 Octave-Band pump noise level

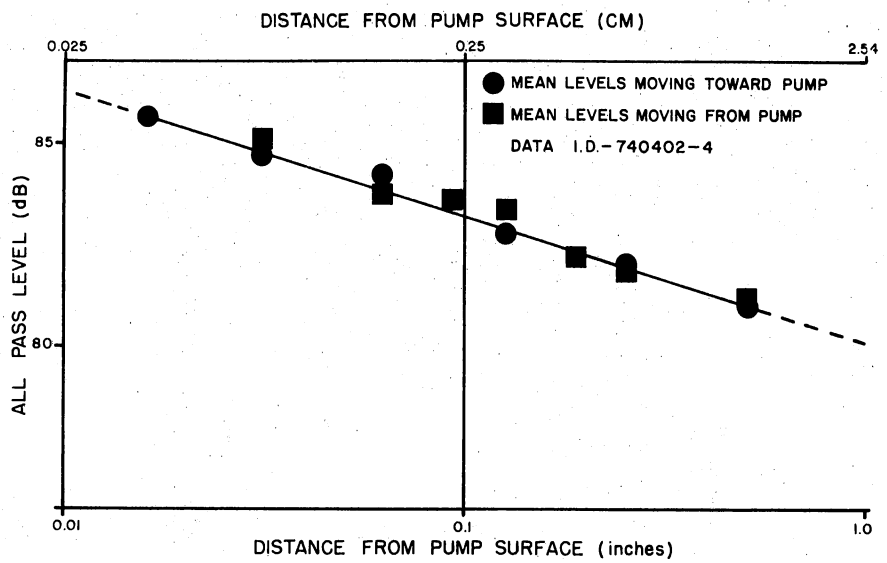

Figure 30. Variation of Average All-Pass Near-Field Noise Measurements as a Function of Distance From Selected Pump Surface, Unit 4321 (5)

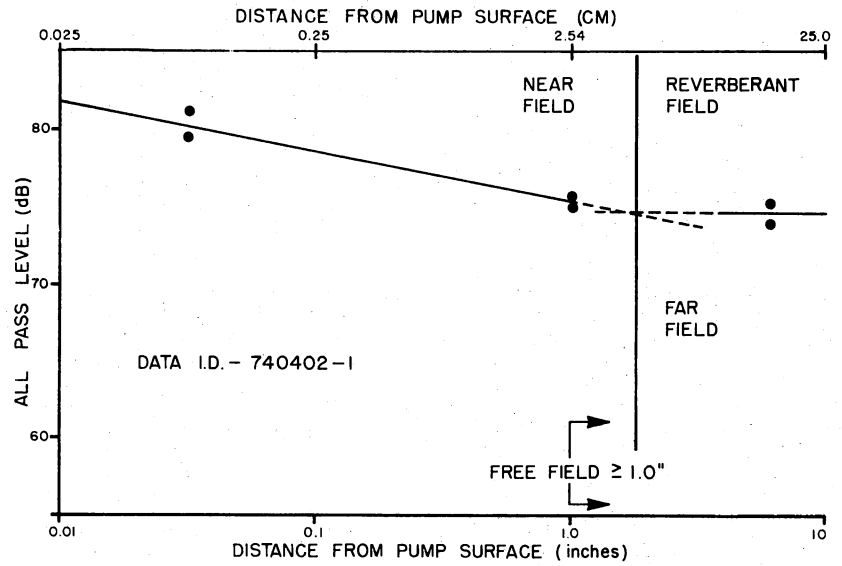

Figure 31. Pump Noise Levels Recorded in Reverberant Room Demonstrating That Averaged Measurements Within 2.5 cm of Selected Pump Surface Are in the Near-Field, Unit 4321 (5)

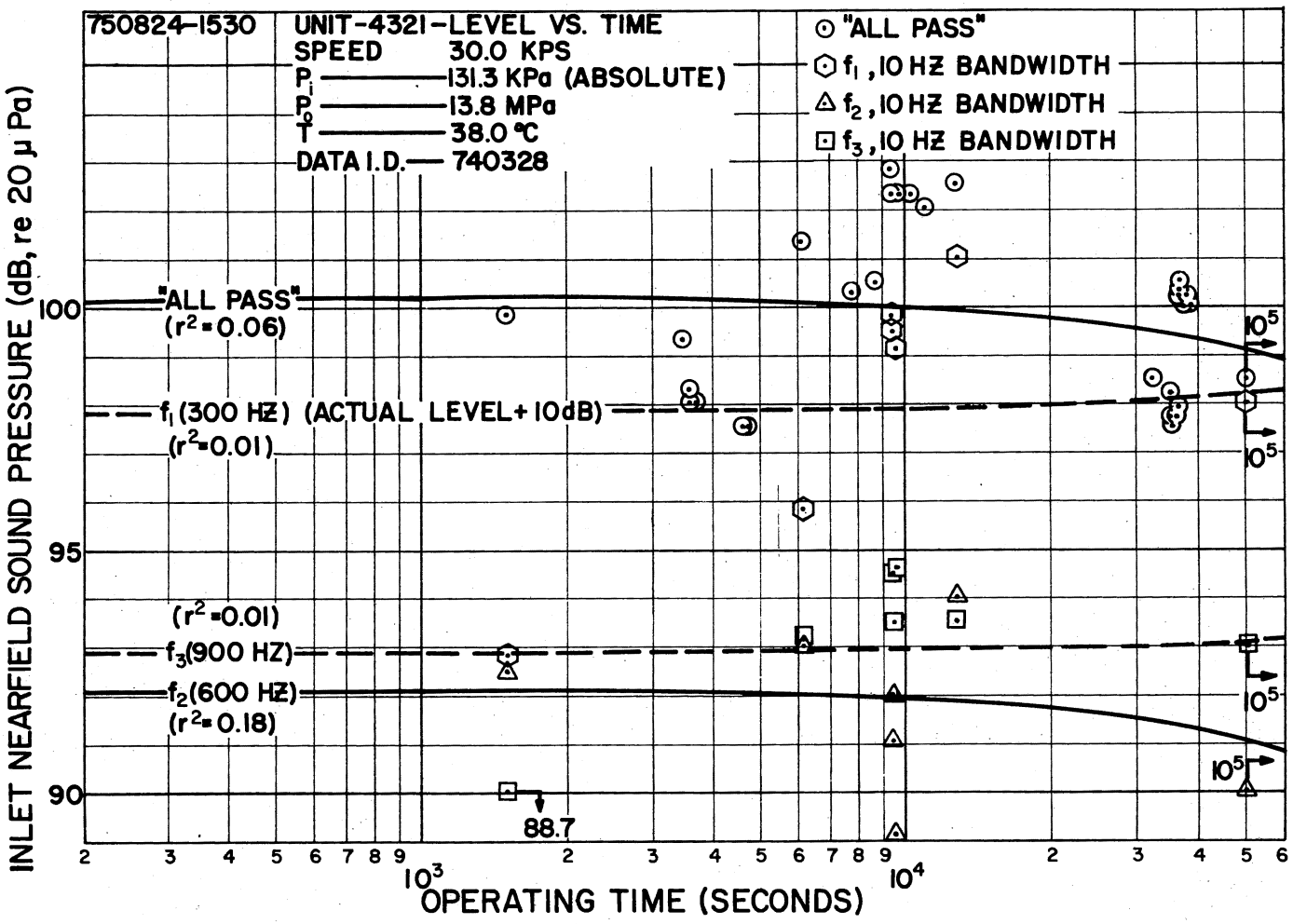

Figure 32. Inlet Near-Field Sound Level Versus Time for Unit 4321

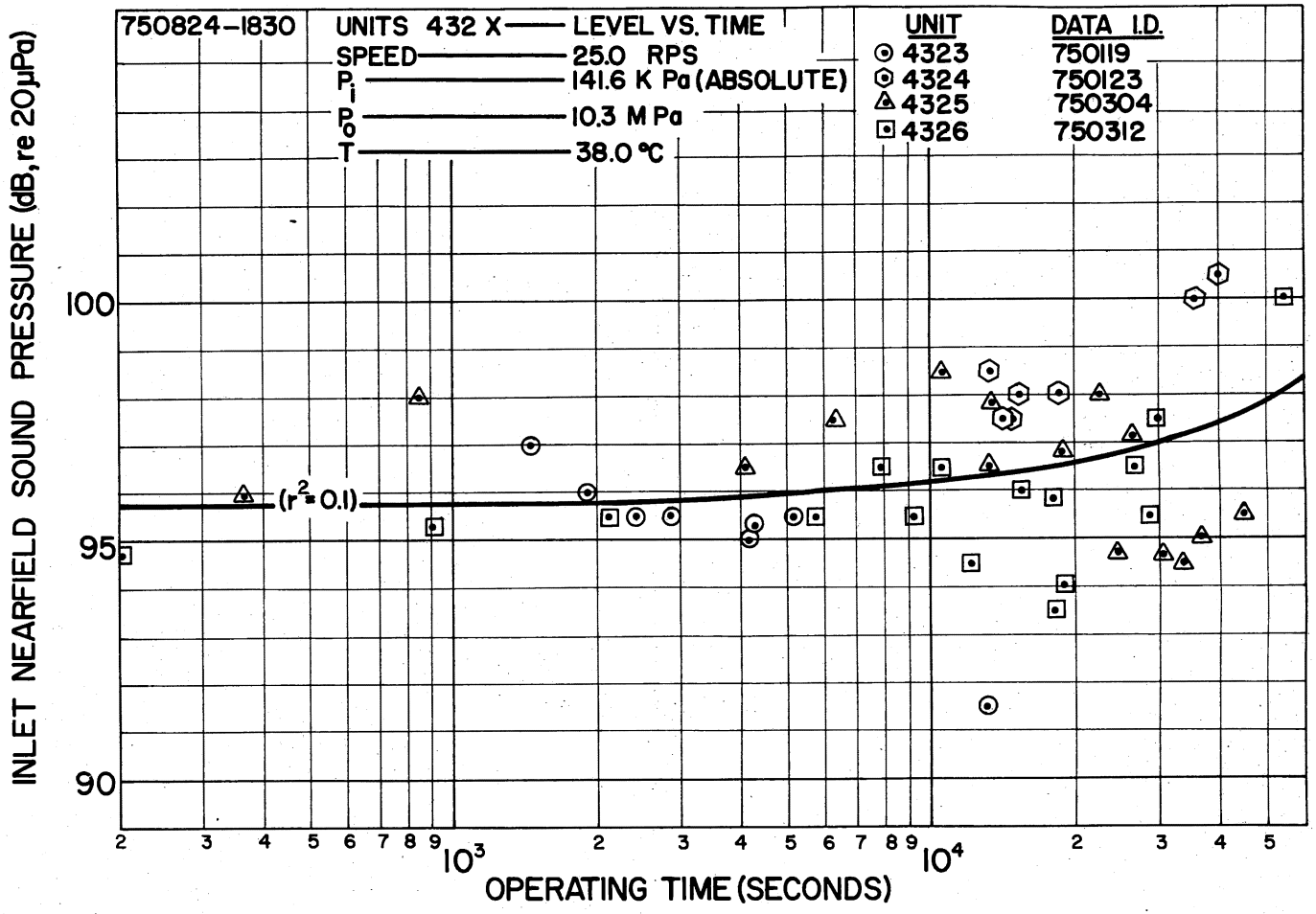

Figure 33. All-Pass Inlet Near-Field Sound Level Versus Time for Units 4323, 4324, 4325, and 4326

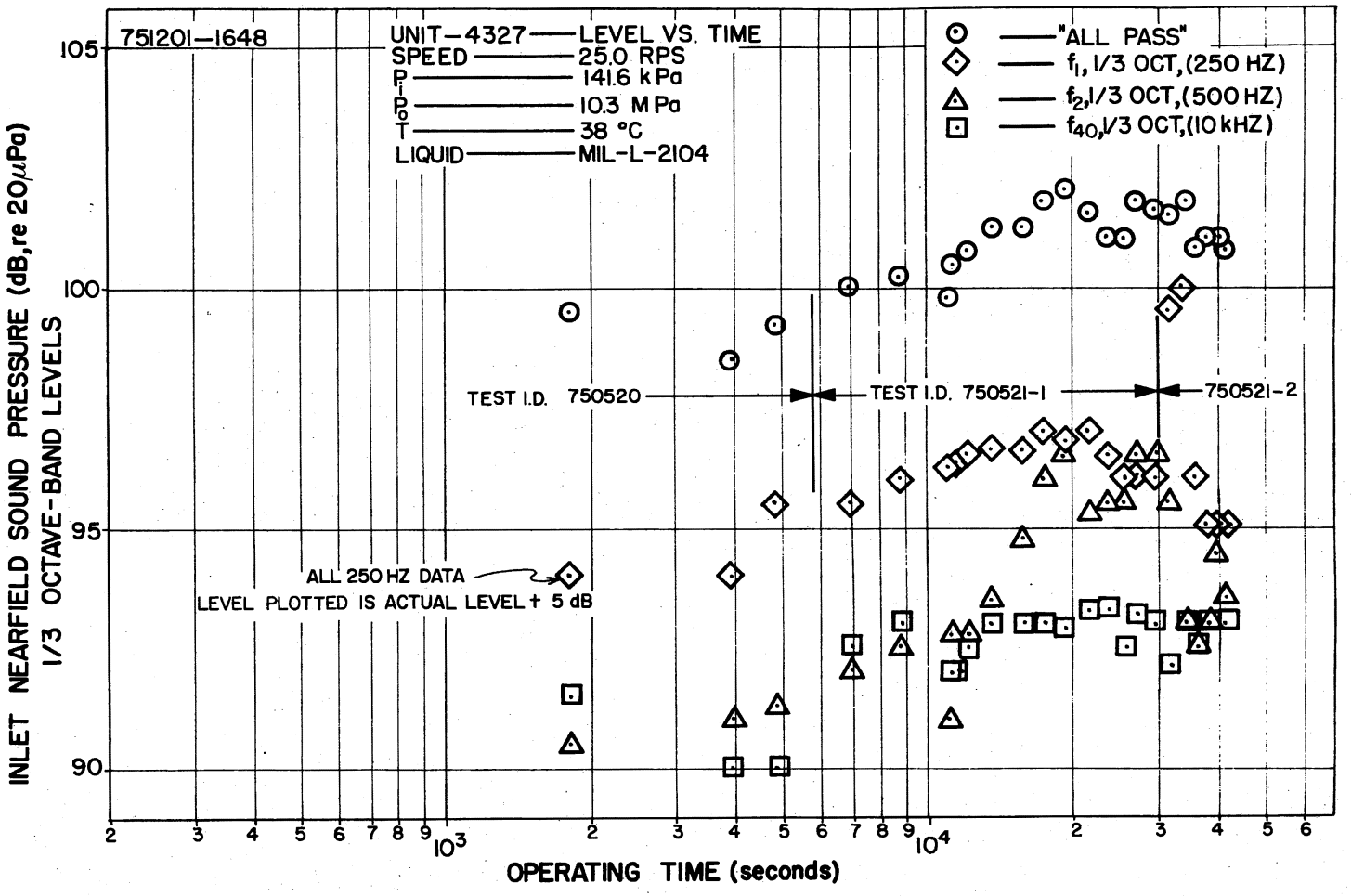

Figure 34. Inlet Near-Field Sound Level Versus Time for Unit 4327. Microphone 0.5 mm from Pump Surface

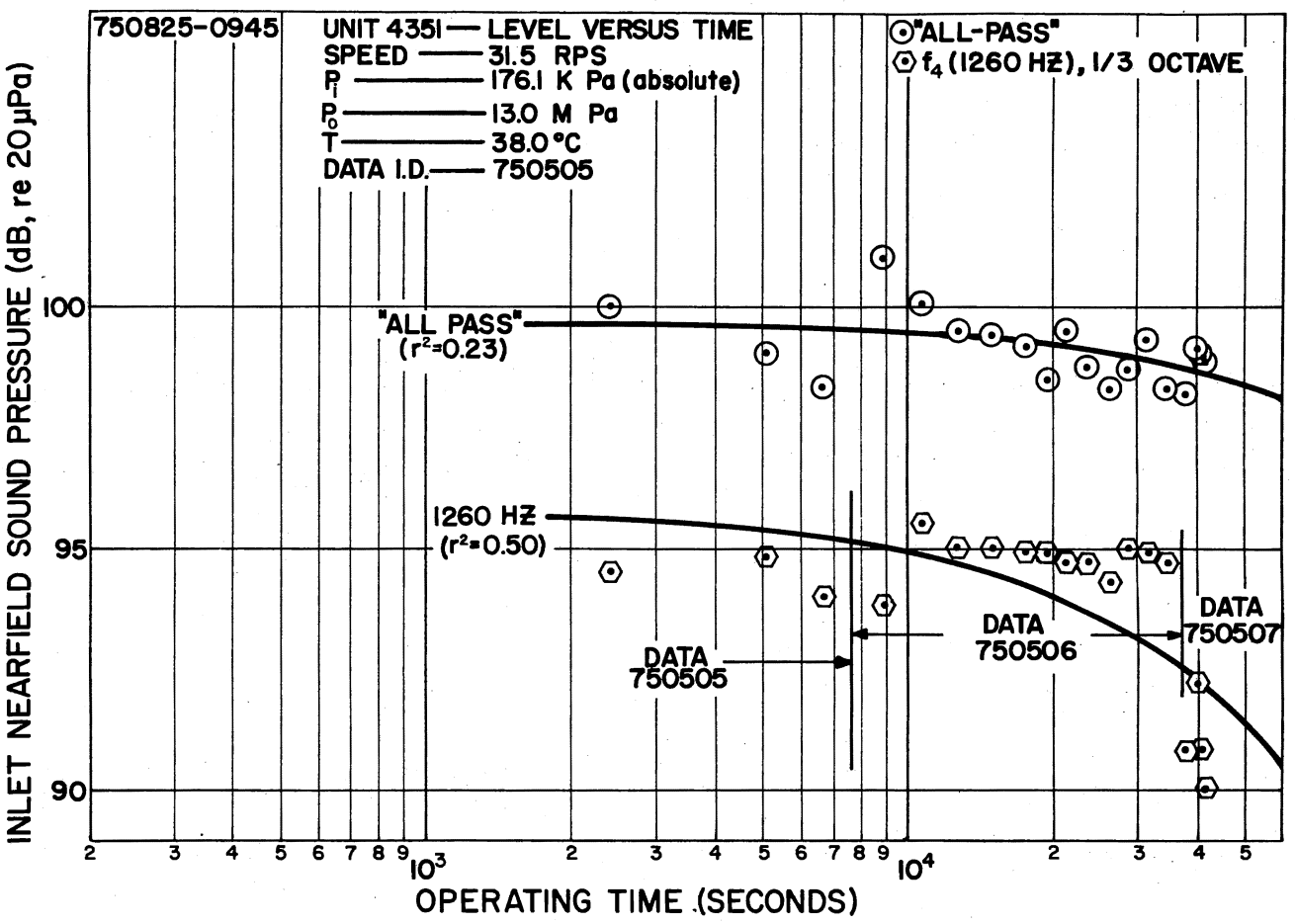

Figure 35. Inlet Near-Field Sound Level Versus Time for Unit 4351

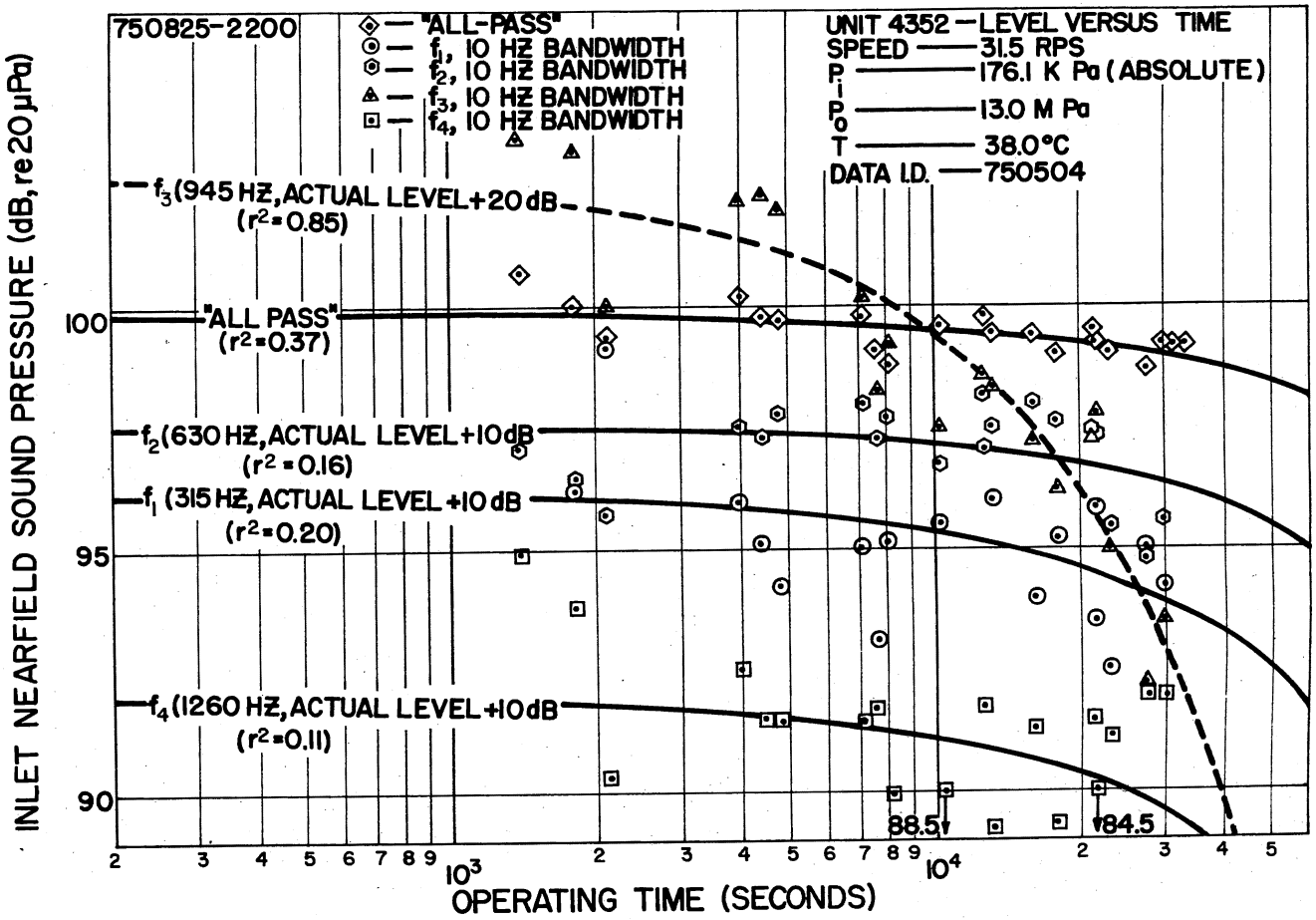

Figure 36. Inlet Near-Field Sound Level Versus Time for Unit 4352

data are used to present the noise stabilization data. In every case the operating conditions are shown with the corresponding data.

Units 432X

Figure 32 shows the pump inlet near-field sound pressure levels measured versus time for Unit 4321. The "all-pass" and 10 Hz bandwidth noise level curves are based on a linear regression of the data to an equation relating the noise level in dB with the time in seconds. The actual levels measured for the first harmonic, 300 Hz, can be obtained by subtracting 10 dB from the values shown in the plot.

Figure 33 is a composite plot of the "all-pass" noise levels of Units 4323, 4324, 4325, and 4326 versus time. As noted in Table VI the test systems were slightly modified between some of the experiments whose results are shown in Figure 33. The curve in Figure 33 is the result of a linear regression of noise level in dB versus time in seconds.

Noise level versus time data for Unit 4327 is shown in Figure 34. During the measurements for Figure 34 the microphone was located approximately 0.5 mm from the pumps surface. The test identification numbers in the figure indicate specific discontinuities in the testing. The actual levels for the 250 Hz data can be obtained by subtracting 5 dB from the levels shown in the plot.

Units 435X

Two sets of noise level data for Unit 4351 are shown in Figure 35. Both the "all-pass" and 1260 Hz 1/3 Octave-Band noise levels are shown as a function of time. Discontinuities in testing are indicated by the different data identification numbers. The curves are the result of a linear regression on the experimental data shown in the figure.

Four narrow-band noise levels and an "all-pass" noise level as a function of time for Unit 4352 are shown in Figure 36. The data was obtained during a continuous operation of the test specimen. However, periodically during the test, when data was not being recorded, the speed of the unit was reduced to zero rps and immediately increased to test speed on a random basis to simulate operational changes. The curves are all based on a linear regression (least squares fit) using the experimental results. Actual levels for the narrow-band data can be obtained by subtracting the amounts indicated in the figure.

Cavitation

Cavitation tests were conducted by varying inlet pressure, changing the air/liquid volume ratio, and changing pump speed. During some of the tests the volumetric efficiency of the pump was monitored. Part of the results of these tests are presented in the following paragraphs.

Inlet Pressure

Figure 37 shows the "all-pass" noise level for Unit 4324 as a function of inlet pressure, for a measured air/liquid volume ratio less than or equal to 1%. Each datum was recorded after decreasing the inlet pressure and waiting approximately five minutes for the system to stabilize. The data were recorded using the General Radio 1523-P1 Preamplifier Plug-In with the GR 1523 Mainframe Graphic Level Recorder identified in Appendix B.

Inlet near-field 1/3 Octave-Band noise levels for Unit 4325 as a function of inlet pressure are shown in Figure 38. The three sets of data represent different pump speeds. Each noise level curve is associated with the 16 kHz 1/3 Octave-Band. The data were obtained by decreasing the inlet pressure and recording the noise level after approximately five minutes had elapsed.

Figure 39 shows a comparison of the 16 kHz 1/3 Octave-Band inlet near-field noise levels for Units 4325 and 4326 as a function of inlet pressure. As indicated on the figure there was approximately eight days between the two tests. Visual observations of the inlet to the pump consistently indicated that for an A* of less than or equal to 1%, bubbles would begin to appear in a pump's inlet fluid stream at approximately 150 kPa. Although approximately five minutes were allowed to pass between data recordings, the importance of allowing time for inlet condition stabilization was not fully appreciated prior to the completion of

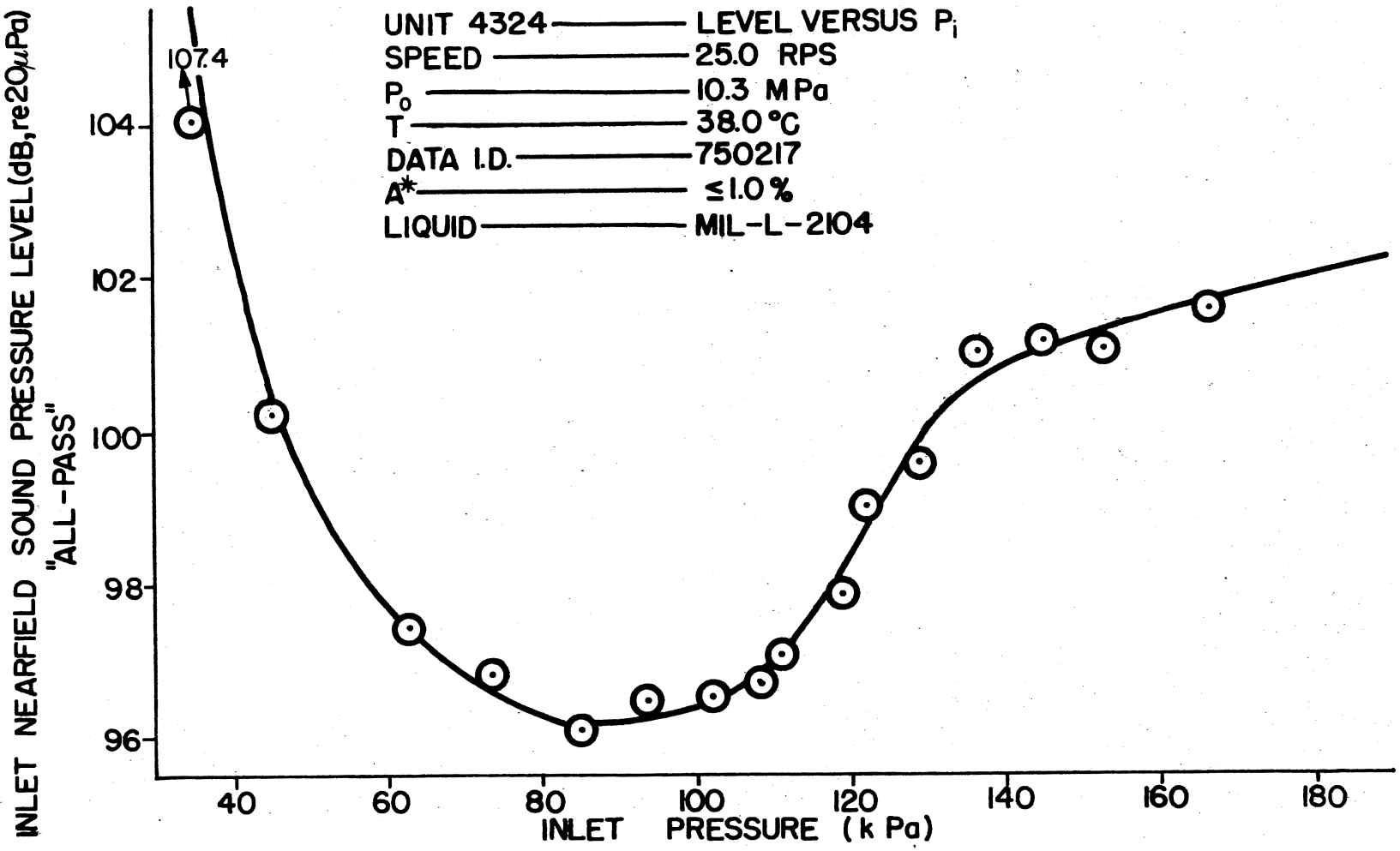

Figure 37. Inlet Near-Field "All-Pass" Noise Level Versus Inlet Pressure for Unit 4324

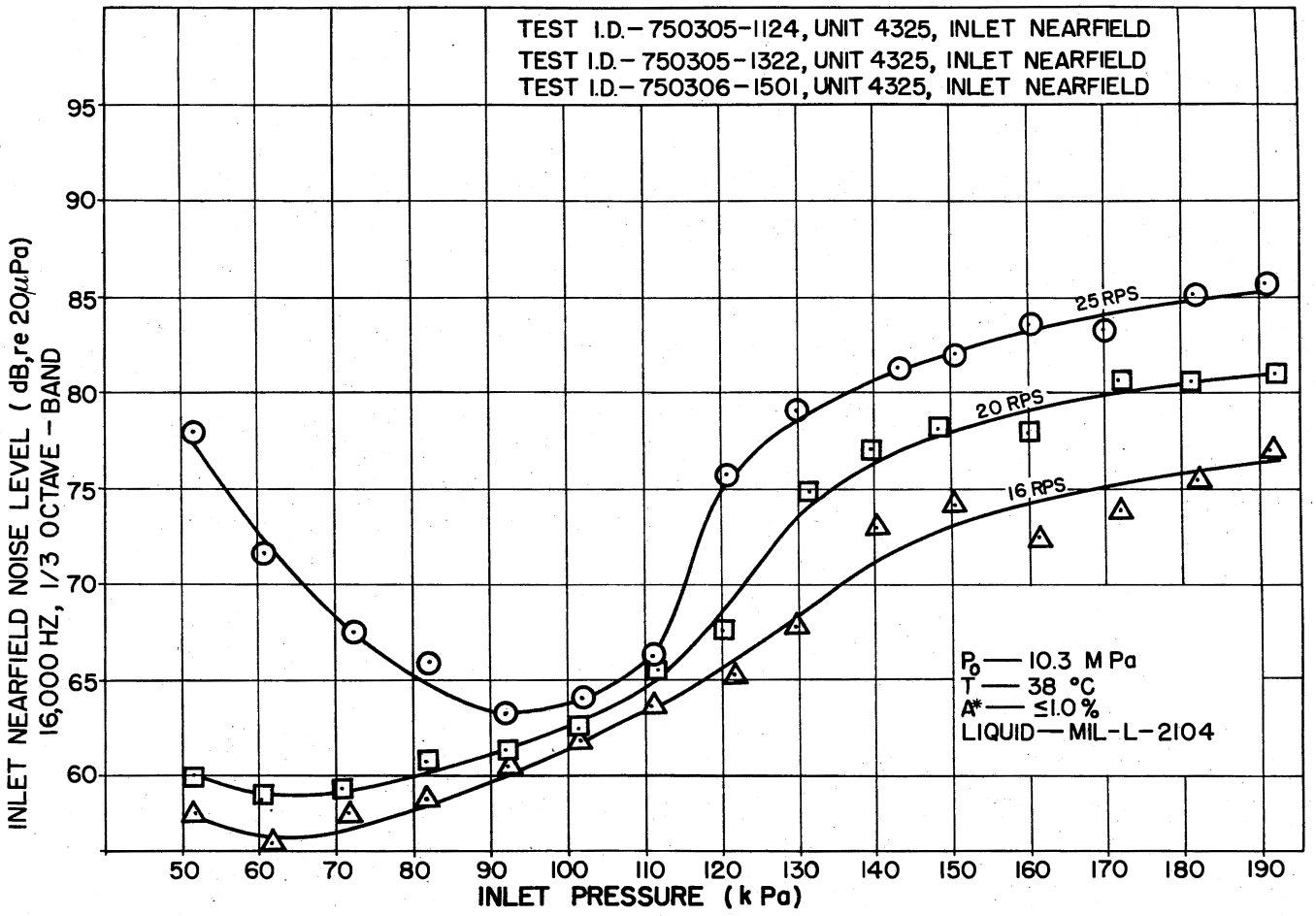

Figure 38. Inlet Near-Field (16,000 Hz, 1/3 Octave) Noise Level as a Function of Shaft Speed and Inlet Pressure. (A* $\leq$ 1%). Unit 4325

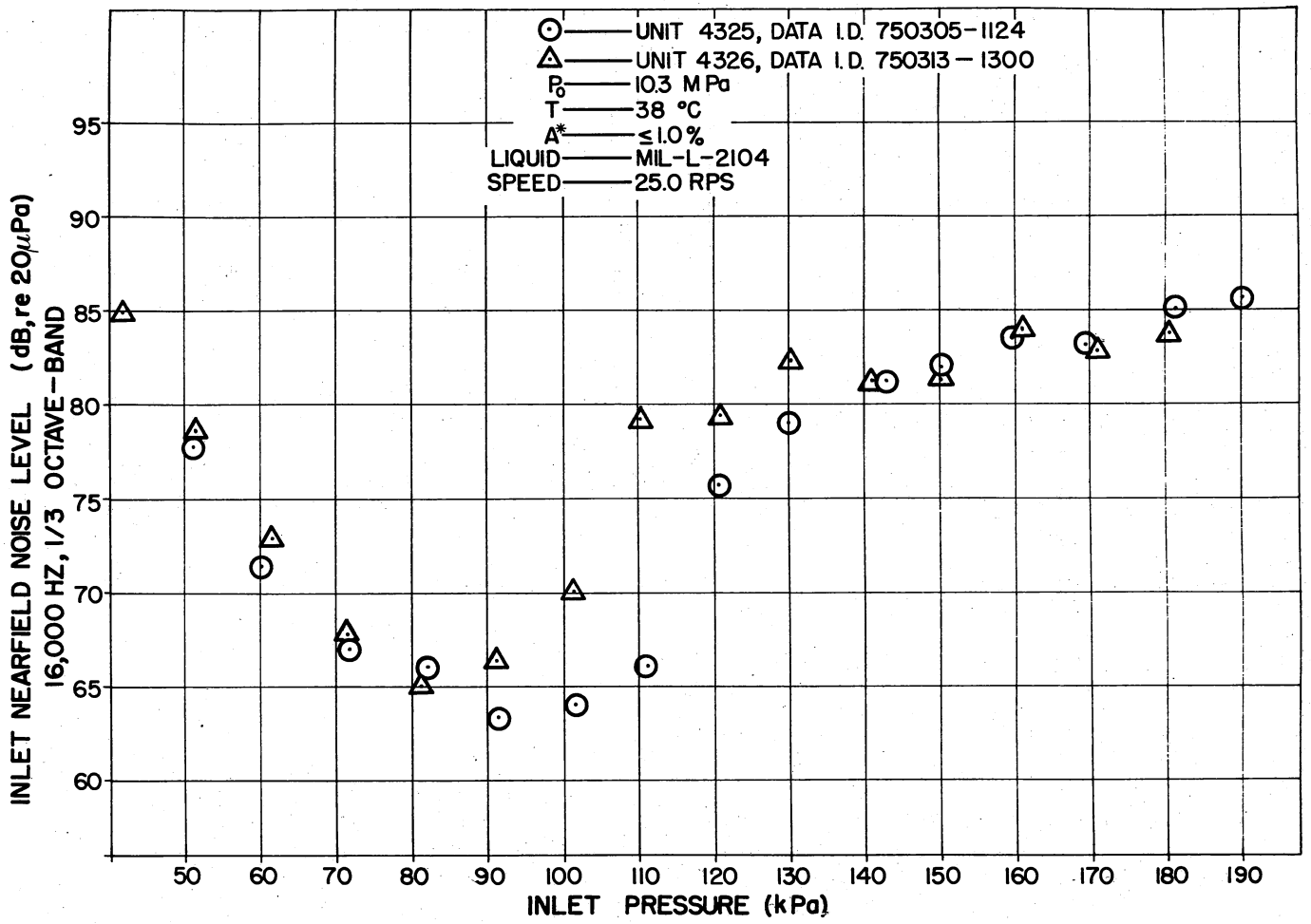

Figure 39. Comparison of Inlet Near-Field 16,000 Hz. (1/3 Octave-Band) Noise Levels as a Function of Inlet Pressure for Units 4325 and 4326

several experiments. Thus, the actual times between measurements were not recorded for Unit 4326 and could have varied considerably from those associated with Unit 4325.

A composite plot of the noise level versus inlet data obtained with Units 4325 and 4326 is presented in Figure 40. The data for 25.0 rps were obtained by averaging the results with the two units.

Figure 41 presents noise level versus inlet pressure for two 435X units. The times between recordings of data were greater than five minutes for both tests. Both the 16 kHz and the 40 kHz data are shown for Unit 4352, while only the 40 Hz data for Unit 4351 is shown. The two sets of 40 kHz data provide an indication of the standard deviation of results associated with different units. The 16 kHz data can be compared with similar results for the 432X units. The inlet pressure was decreased between data recordings.

Air/Liquid Ratio

The manner in which the air/liquid volume ratio affects high pressure pump noise levels is reflected in the data shown in Figure 42. The two curves of noise level versus inlet pressure for Unit 4326 are associated with different air/liquid volume ratios. The ratios varied by an order of magnitude as measured with the aeration detection device described in Chapter III. Both curves were obtained by decreasing the inlet pressure and recording data after a short stabilization time.

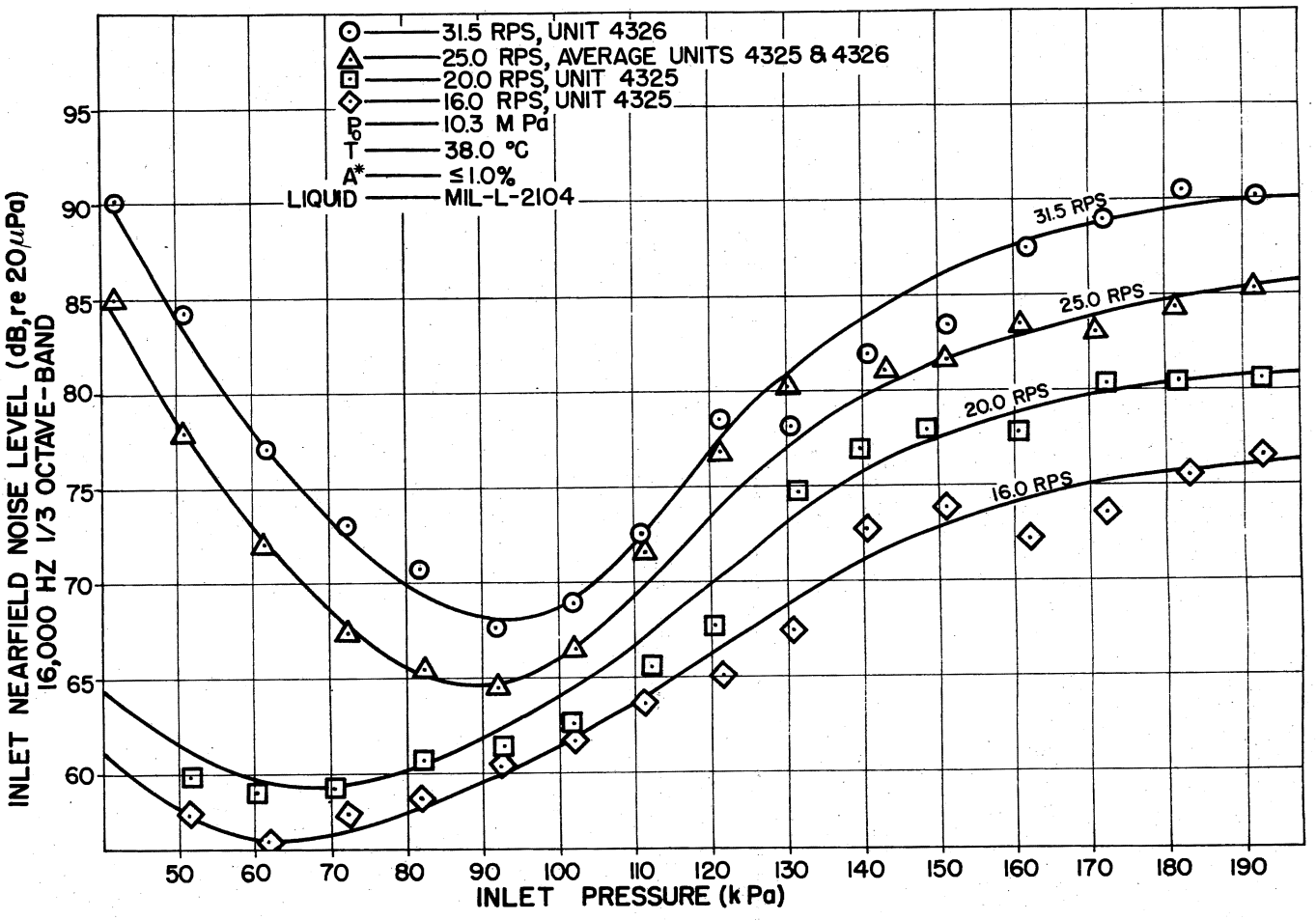

Figure 40. Composite Inlet Near-Field (16,000, 1/3 Octave) Noise Level as a Function of Shaft Speed and Inlet Pressure. Units 4325 and 4326

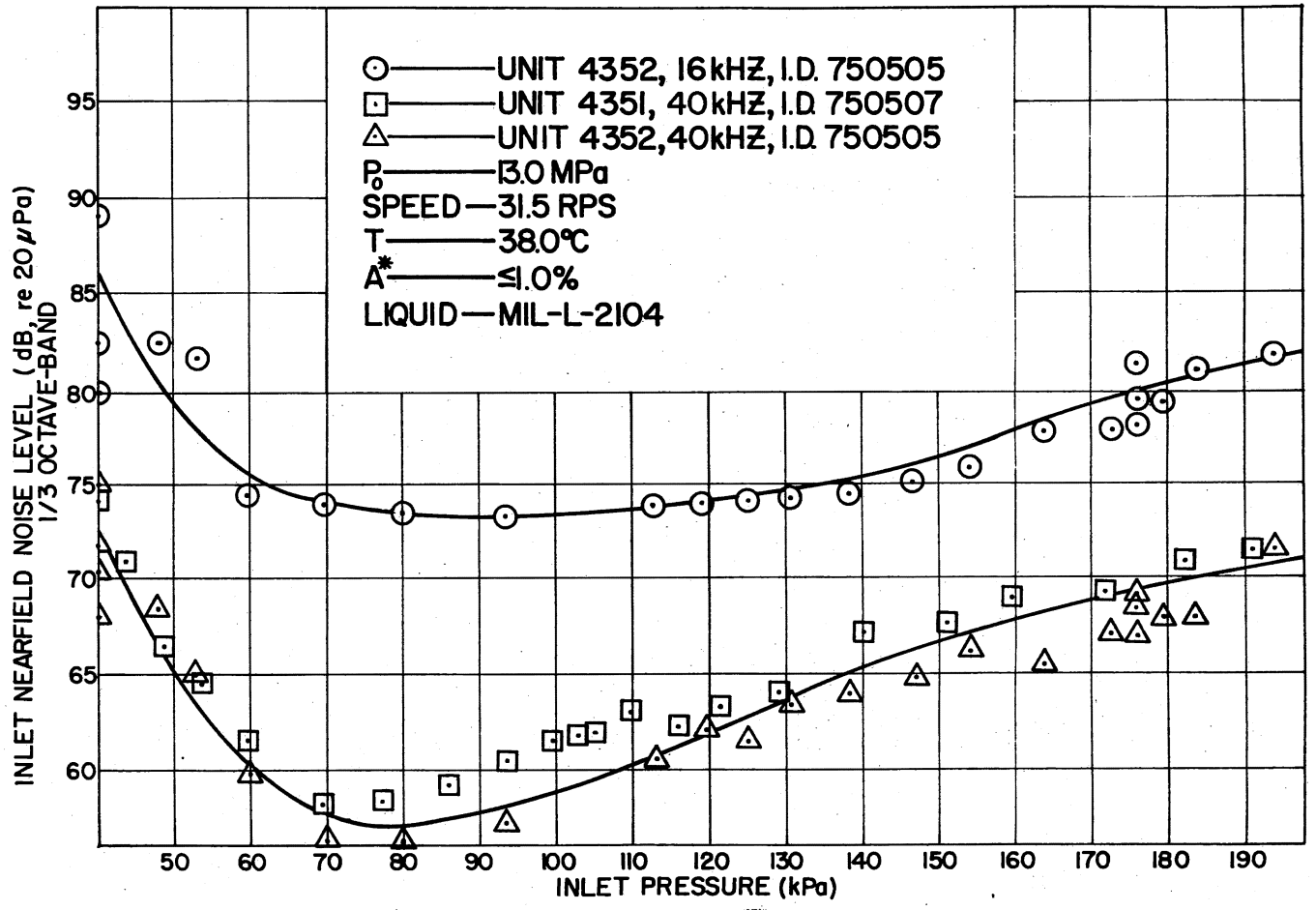

Figure 41. Inlet Near-Field Noise Level Versus Inlet Pressure for Units 4351 and 4352

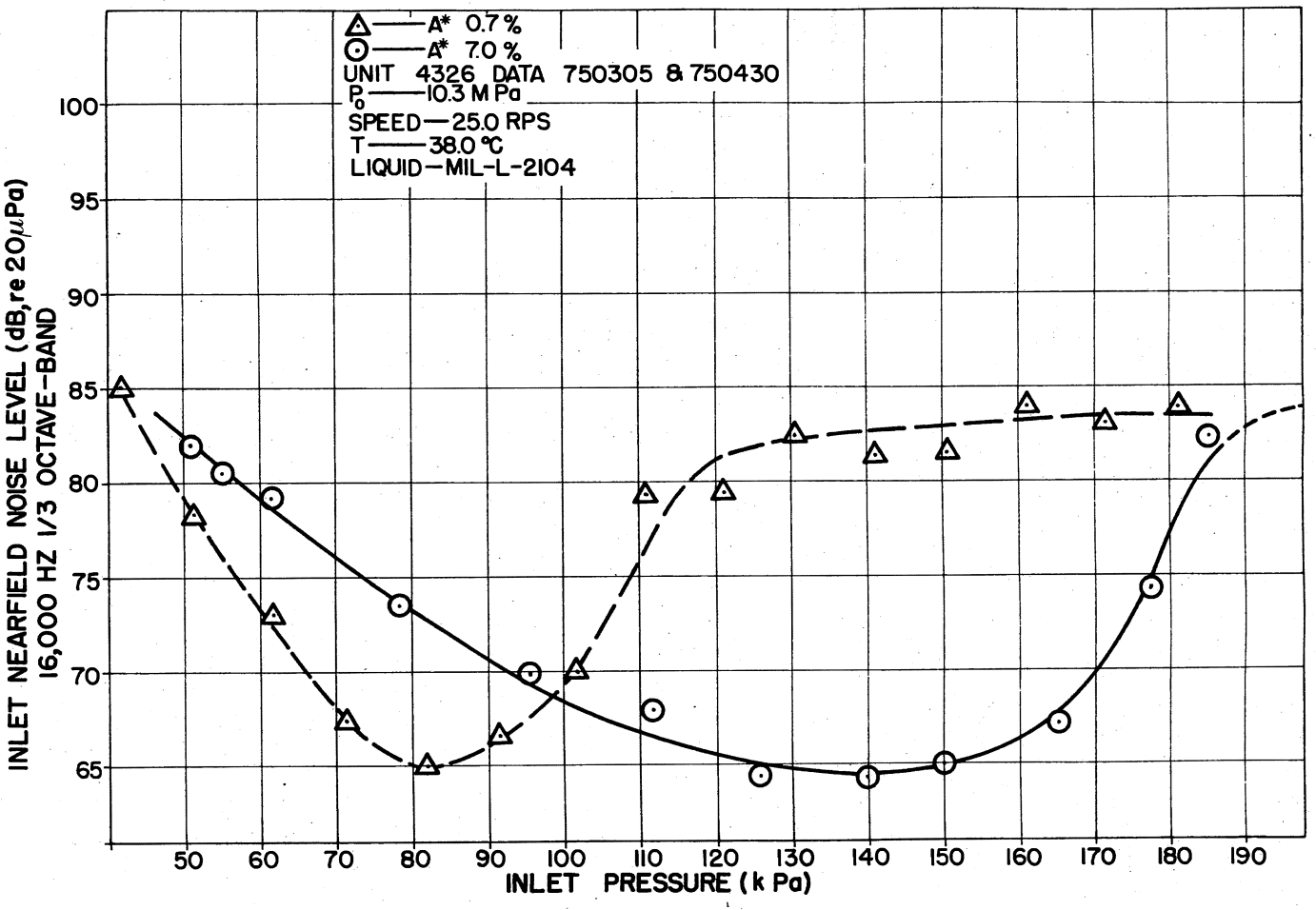

Figure 42. Inlet Near-Field (16,000 Hz., 1/3 Octave) Sound Level as a Function of Air/Liquid Volume Ratio and Inlet Pressure. Unit 4326

Speed Induced

The data in Figure 43 were obtained by varying the speed of the test pump while maintaining other operational variables "constant". The inlet pressure was controlled by maintaining the reservoir pressure constant, which means that the inlet pressure varied with increasing flow (pump speed). The near-field 1/3 Octave-Band and "all-pass" noise levels were obtained after increasing the pump speed. The hydraulic load on the pump was constant; therefore, the outlet pressure varied during the test, but was always less than or equal to 2.0 MPa.

Volumetric Efficiency

The volumetric efficiency data for Figure 44 was acquired during the noise tests reported in Figure 43. The flow rate measurement data shown in Figure 44 for the first six data points was used to project an estimate of the flow rate at the higher pump speed. The actual flow rate curve illustrates how the flow rate decreases at the highest pump speed. A linear regression of flow rate versus speed using the first six data points provides an estimate for the seventh data point that is 6% higher than the actual flow rate value obtained during the test.

Figures 45 and 46 show comparisons of the normalized flow rate versus 1/3 Octave-Band high frequency noise levels for 432X units and 435X units, respectively. The flow rates are plotted as normalized flow, Q*, which is the actual flow

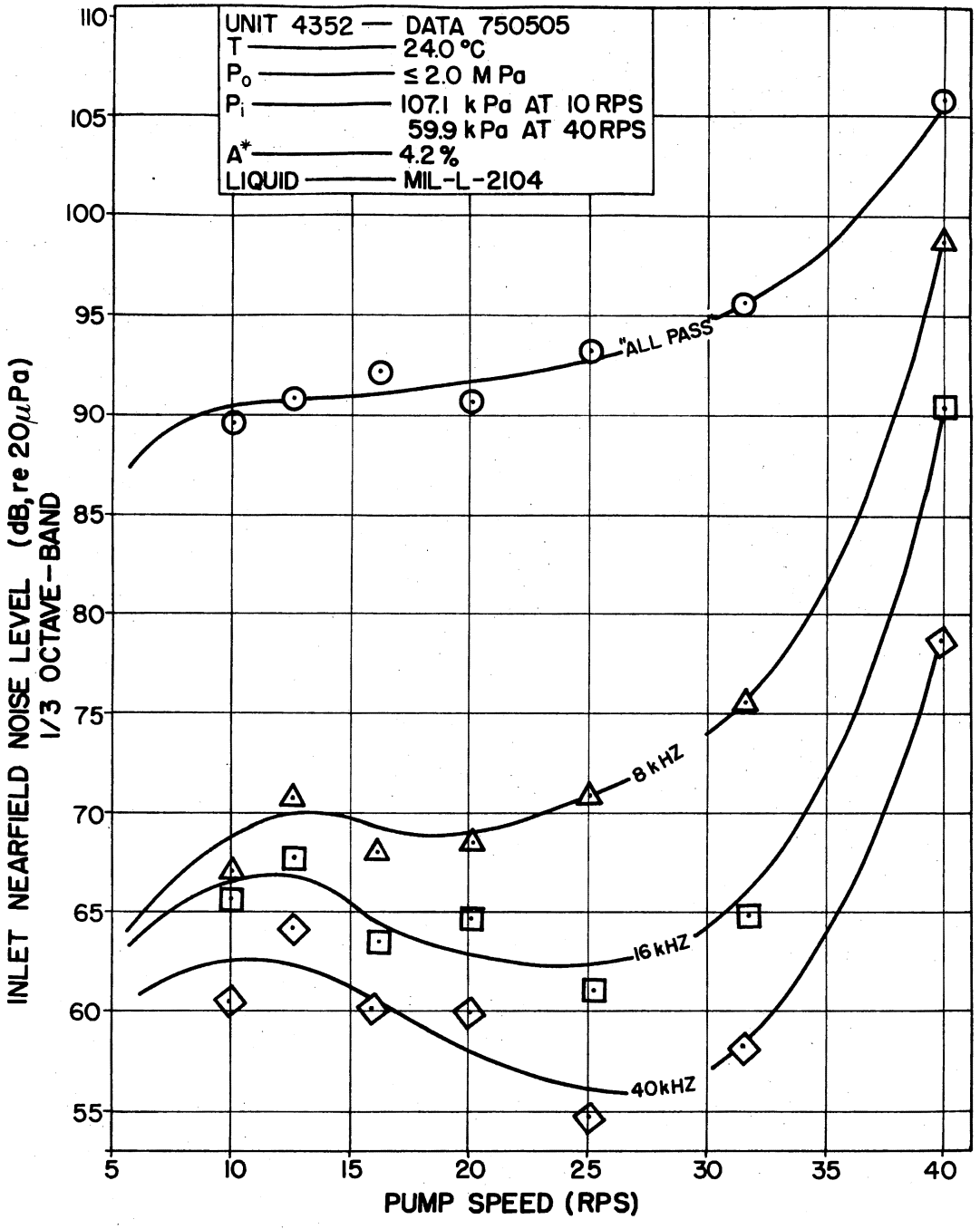

Figure 43. Inlet Near-Field Noise Level Versus Pump Speed, Unit 4352

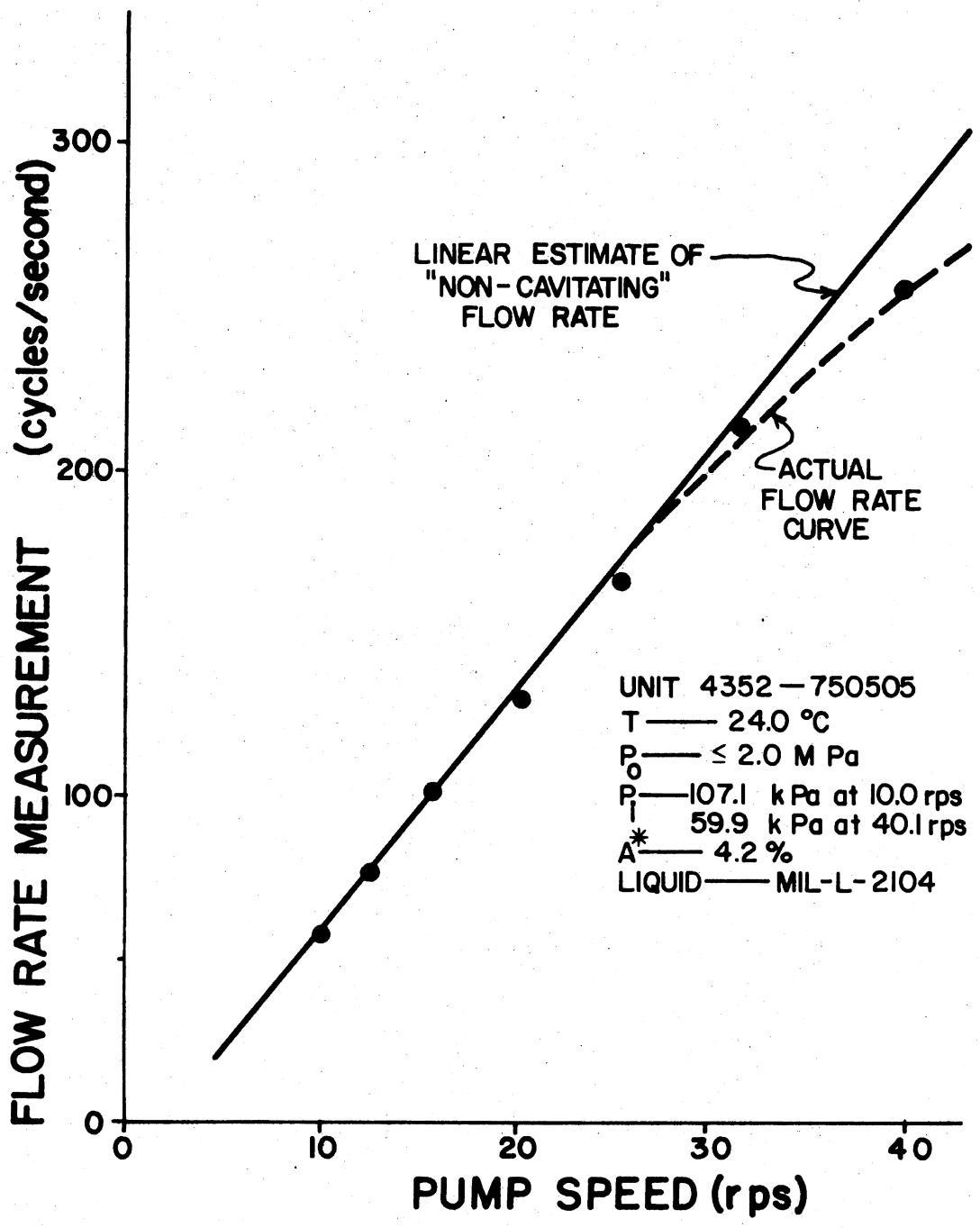

Figure 44. Decrease in Pump Flow Rate Due to Cavitation

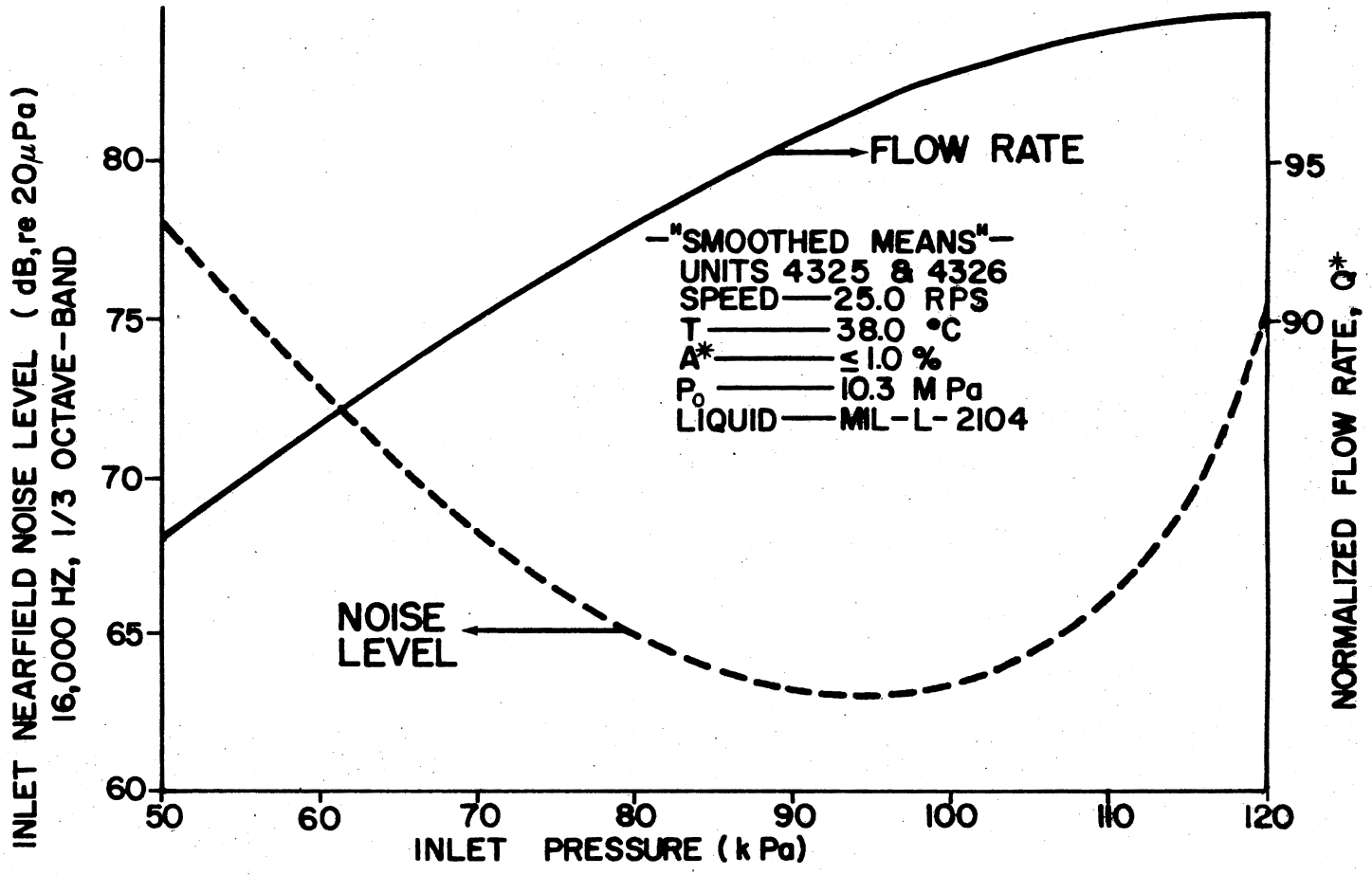

Figure 45. Normalized Flow Rate and Noise Level Versus Inlet Pressure, Units 4325 and 4326

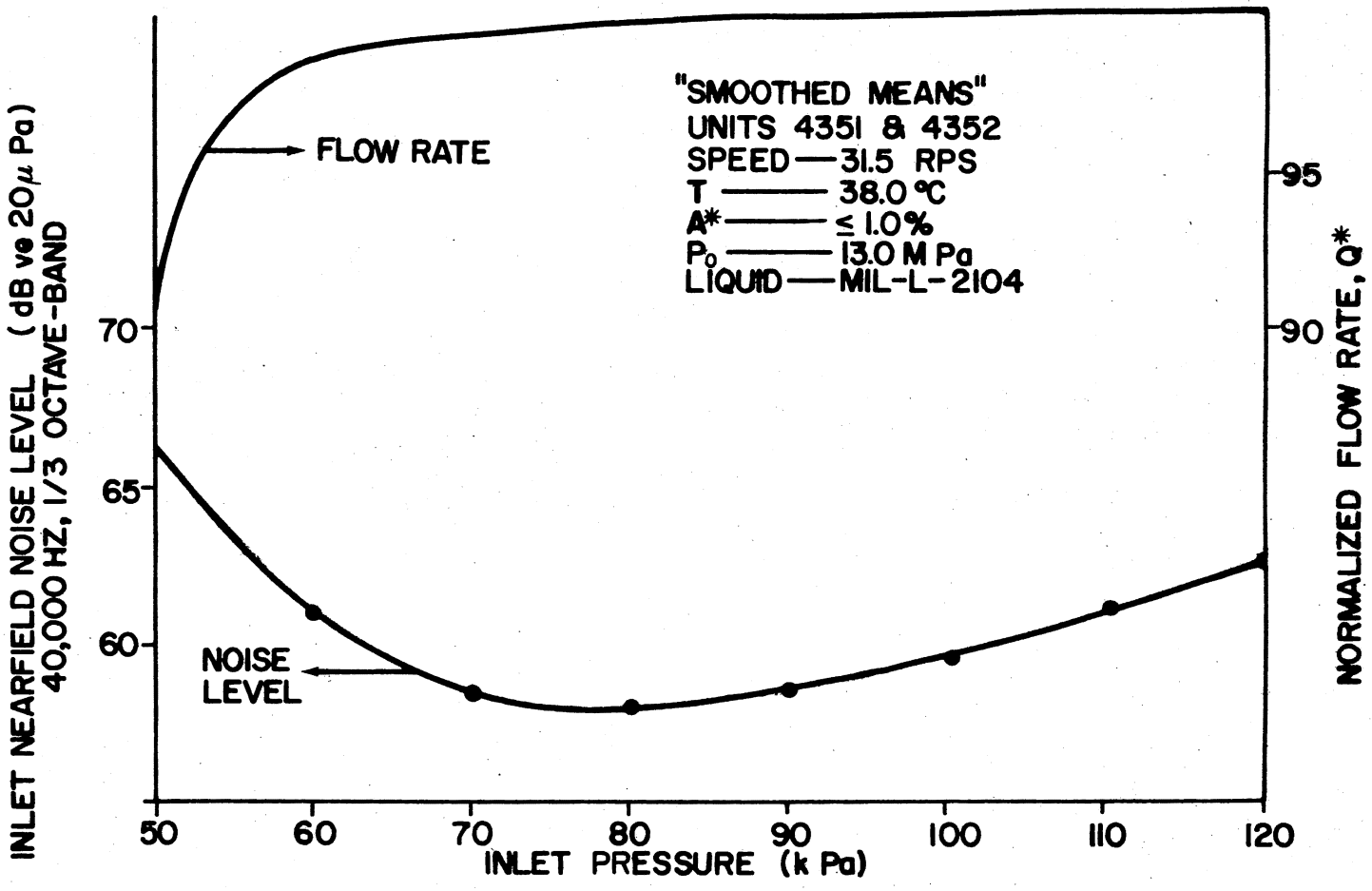

Figure 46. Normalized Flow Rate and Noise Level Versus Inlet Pressure, Units 4351 and 4352

rate divided by the rated flow. The plots in each figure are flow rate and noise level versus inlet pressure. The curves in both figures were obtained by averaging experimental data.

Wear

The results of the wear experiments were plotted as noise levels versus a flow performance index. The noise levels were recorded after the indicated "wear" with "clean" system fluid. The flow performance index Q/Q_r in percentage is used in Figures 47, 48, and 49. Figure 47 presents the results for Unit 4326, Figure 48 the results for Unit 4352, and Figure 49 the results for Unit 4353. All of the harmonic noise levels are 10 Hz narrow-band data. In terms of real-time, the higher Q/Q_r values occurred prior to the lower Q/Q_r values.

Temperature

Plots of 1/3 Octave-Band noise levels versus fluid temperature are contained in Figure 50. The data recorded during the test were obtained by increasing temperature as a function of time, allowing the system to "stabilize", and then noting the noise level. The three data points for each 1/3 Octave-Band at 38°C can be used to estimate the standard deviation associated with the repeatibility of the test data for a specific frequency band.

The experimental results presented in this chapter are discussed and analyzed in the next chapter.

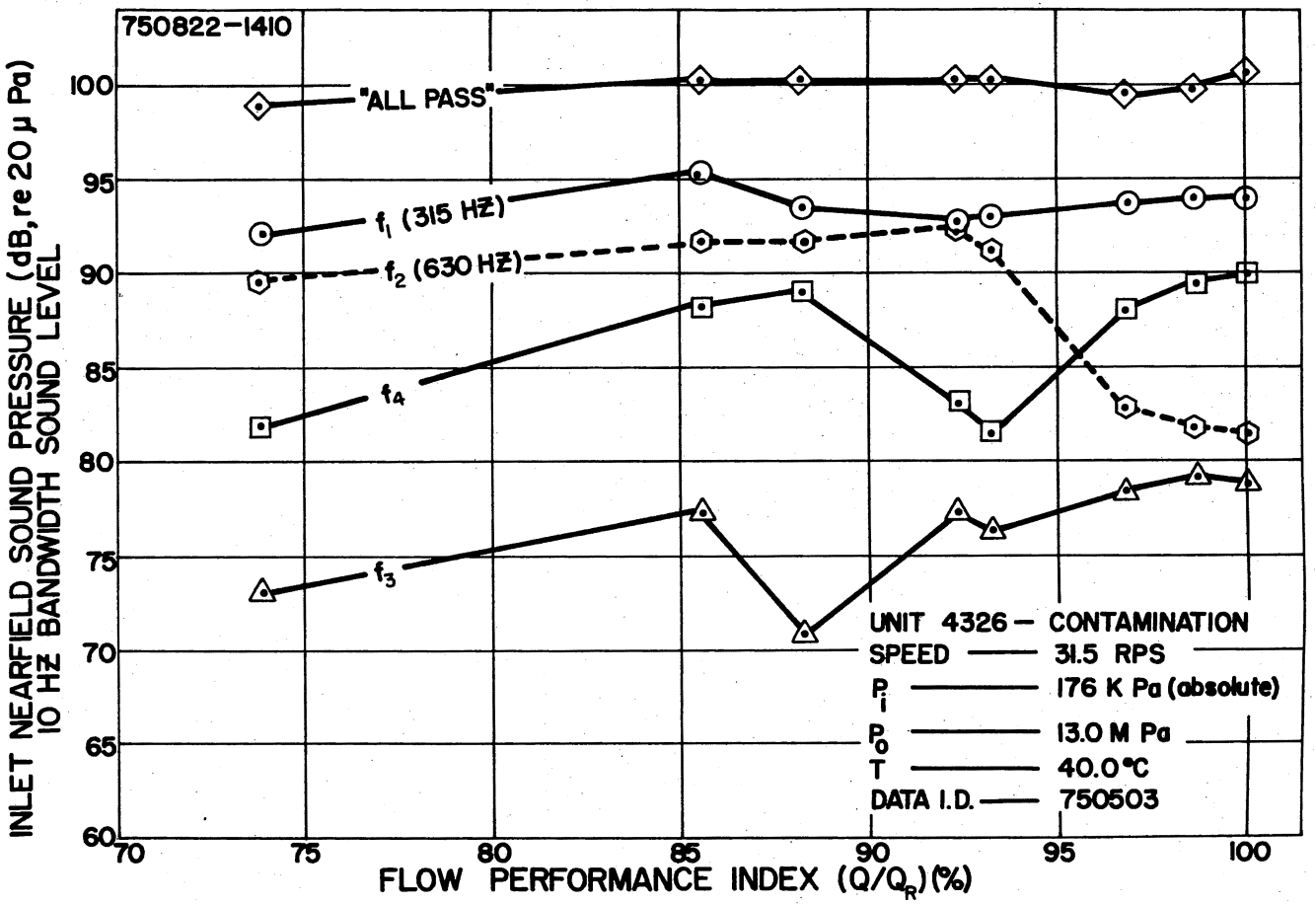

Figure 47. Near-Field Sound Level of Unit 4326 as a Function of Contaminant Induced Wear Manifested by Degradation of Pump Flow Performance Index (Q/Q_R)

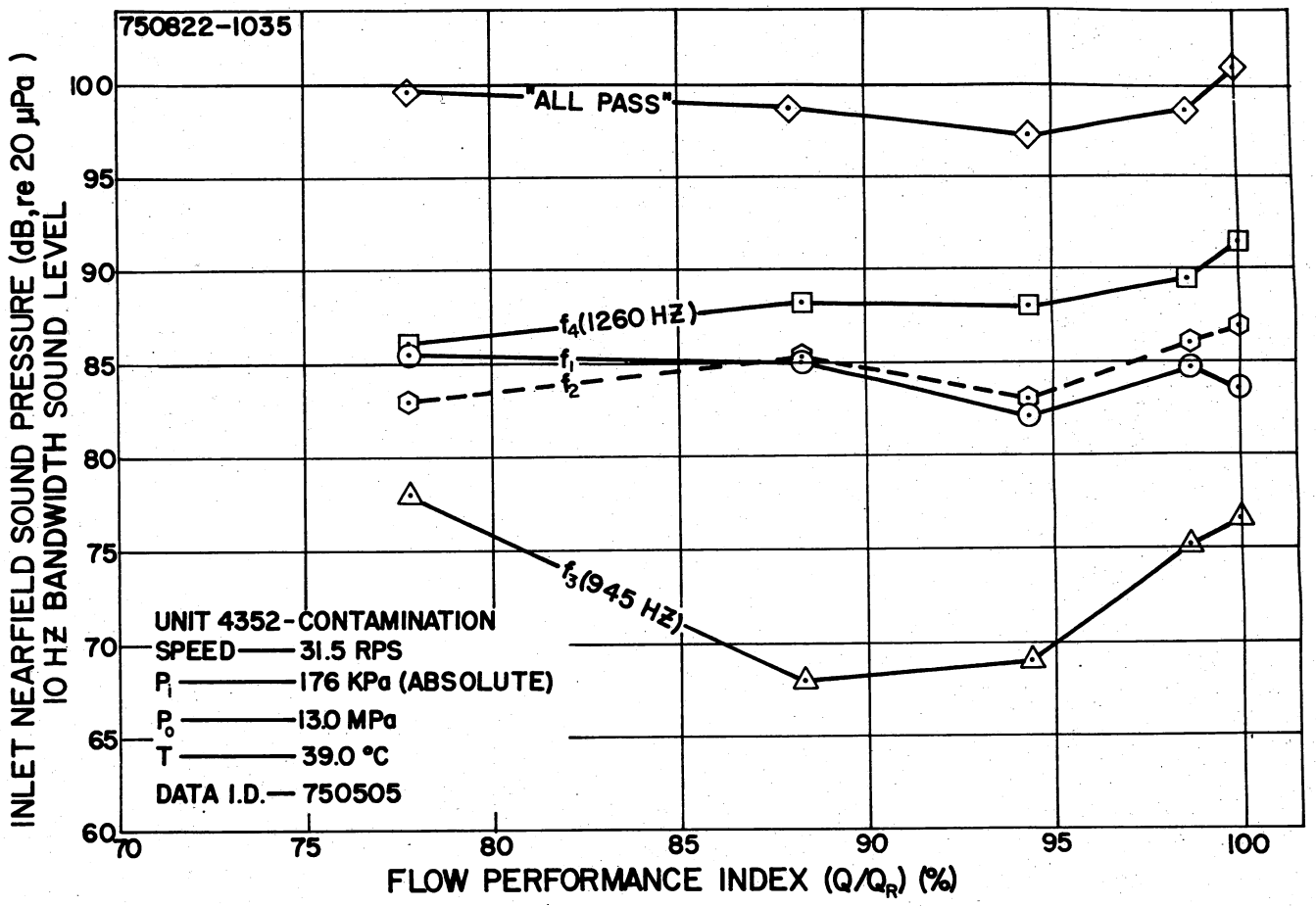

Figure 48. Near-Field Sound Level of Unit 4352 as a Function of Contaminant Induced Wear Manifested by Degradation of the Pump Flow Performance Index (Q/Q_R)

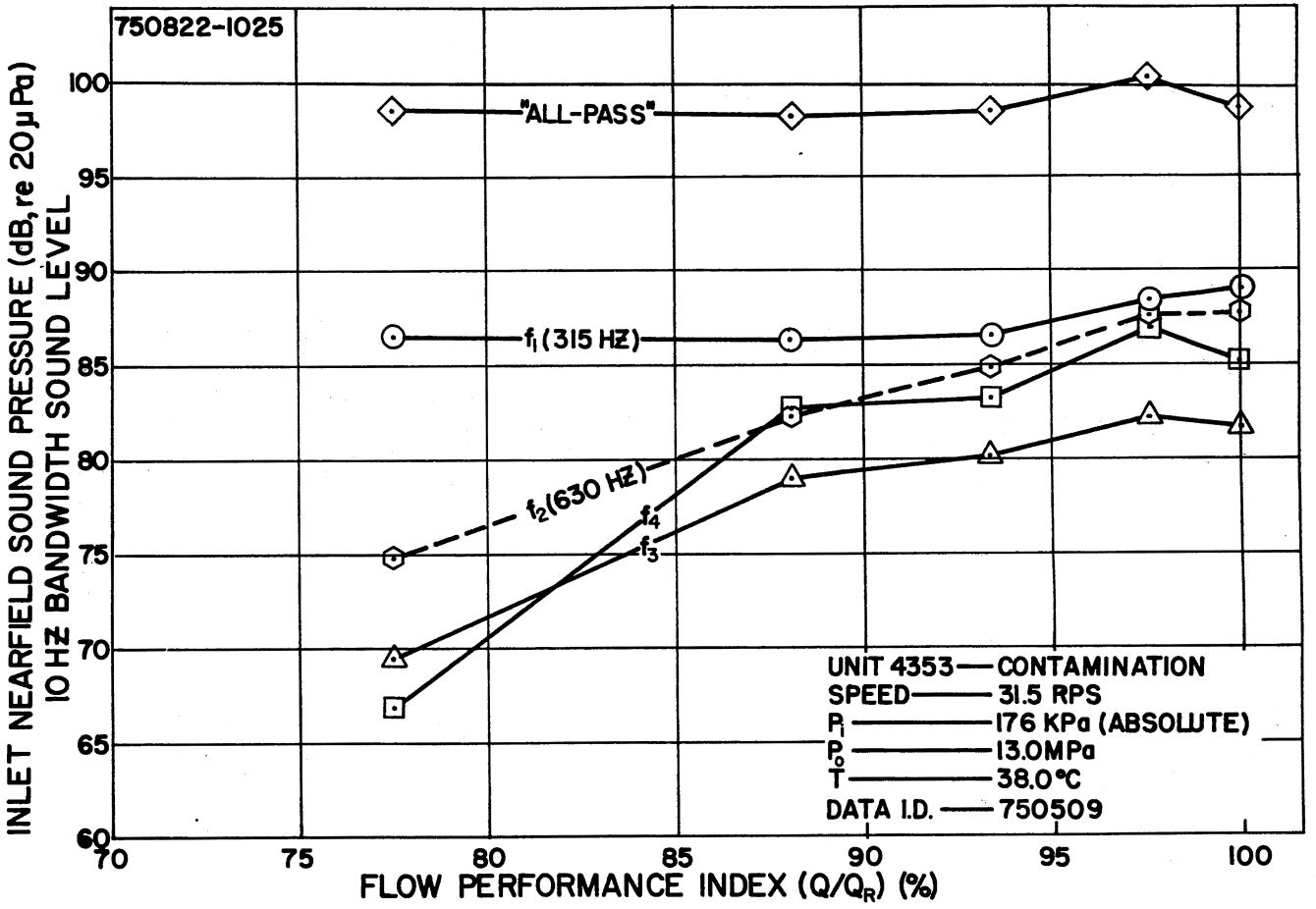

Figure 49. Near-Field Sound Level of Unit 4353 as a Function of Contaminant Induced Wear Manifested by Degradation of the Pump Flow Performance Index (Q/Q_R)

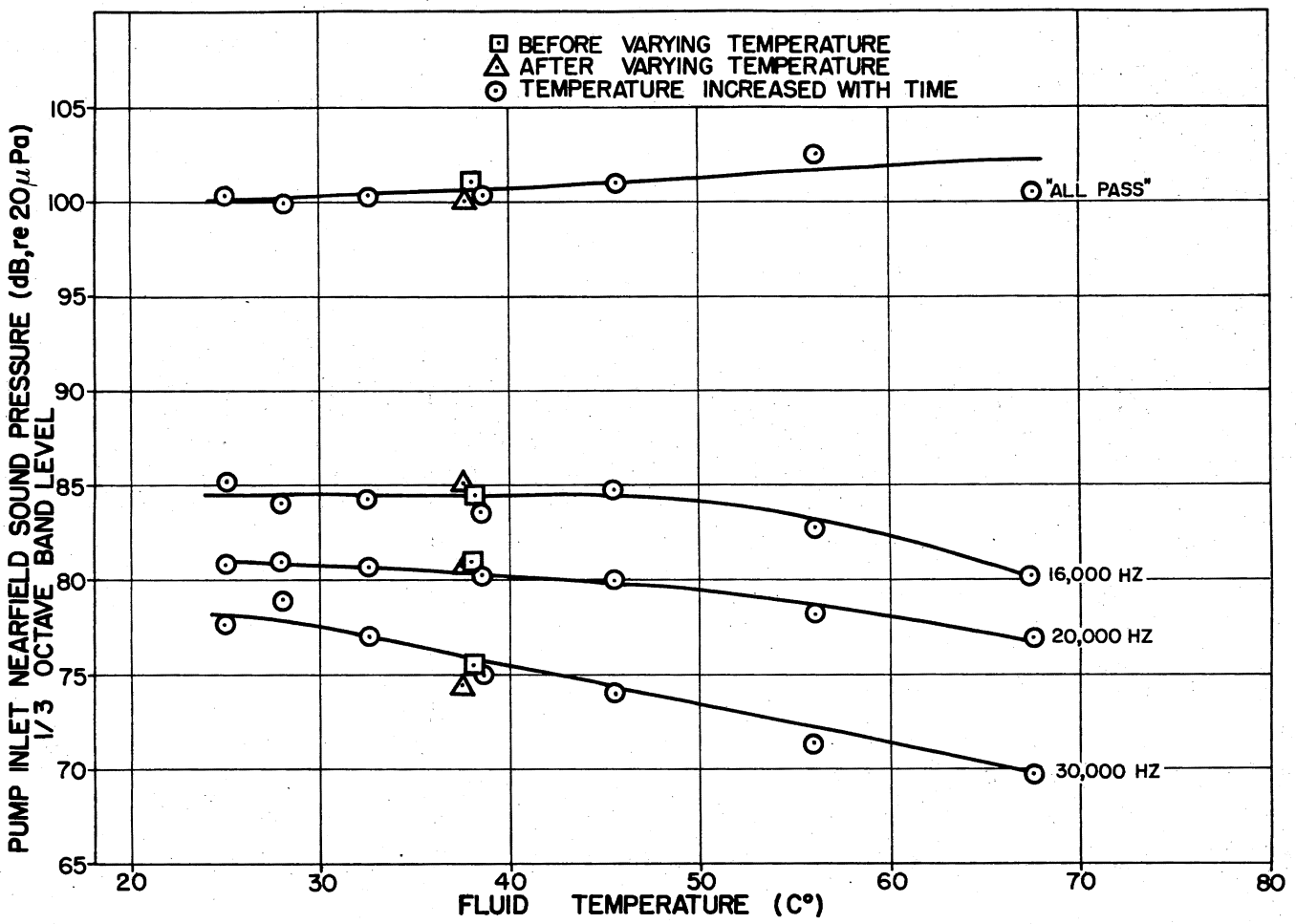

Figure 50. Sound Level Versus Temperature, Unit 4326, I.D. 750435-53, 25 RPS, 10.3 MPa Outlet Pressure, 141,5 kPa Inlet Pressure. (A* $\leq$ 0.7%) Liquid, Mil-L-2104

CHAPTER VI

ANALYSIS OF EXPERIMENTAL RESULTS

The objective of this chapter is to discuss the results of the experimental studies of high pressure pump acoustical signatures with respect to the theory presented in Chapter II and the results of acoustical signature analysis of low pressure hydraulic pumps. The topics discussed in the following pages include: the data acquisition technique, pump noise level stabilization, the multi-factor experiment, cavitation, contamination, wear, and temperature.

Data Acquisition Technique

The selection of a noise measurement technique was significantly influenced by the desire to utilize a non-intrusive acoustical diagnostic method. Fluidborne noise measurements require placing a transducer into a fluid passage either at the component or in a conduit. Structure-borne noise measurements require attaching a transducer on the surface of the test specimen. Since preliminary tests indicated that near-field ABN measurements provide a viable diagnostic measurement technique, near-field ABN measurements were utilized from the outset of the study. From the beginning of the test program the repeatability of the ABN

measurements was carefully monitored to insure that the technique was satisfactory.

Figure 30 illustrates that, on an "all-pass" basis the near-field ABN measurement technique has acceptable repeatability. Theory indicates, as shown in Equation (3.7), that an ABN measurement distance of less than 1.7 mm should provide repeatable data. Figure 31 coupled with the general behavior of acoustical fields shown in Figure 4, indicates that measurements at 1.0 mm or less are within the near-field boundary for the test specimen (432X).

Both Figures 30 and 31 provide an indication of the sample standard deviation, S, associated with measurements in the near-field of specimen 4321. Other sample standard deviation information obtained with Unit 4321 indicated the following: re-positioning the microphone, on reference centerline, at a radius of 1.0 mm, S is 0.27 dB; vertical displacement of the microphone ±1.3 cm, radius of 1.0 mm, S is 0.38 dB; operating the diffusers in the reverberant environment, microphone on reference ceterline, radius of 1.0 mm, S is 0.36 dB; encircling the measurement area with aluminum backed acoustical absorbant material, microphone on reference centerline, radius of 13.0 mm, S is 0.212 dB.

Most of the sample standard deviation estimates with Unit 4321 were based on three samples. A short time elapsed during the acquisition of the three samples. The total time required to obtain the data in Figures 30 and 31 was much greater than the time required to obtain the standard

deviation estimate data. Thus, the deviation of the noise level of the test specimen as a function of time has a much greater influence on the results in Figures 30 and 31 than measurement technique repeatability. Using the information in Table VII and the range of measurements in Figures 30 and 31 the sample standard deviation of the pump noise "all-pass" level is estimated to be 2.0 dB. Clearly, the sample standard deviation, σ, of the pump "all-pass" noise level with time exceeds by an order of magnitude the sample standard deviations due to repositioning the microphone, moving the microphone vertically over small distances, or altering the acoustical environment. For a normal distribution approximately 67% of the observations are within one σ of the mean, 95% of the observations are within two σ of the mean, and 99.5% of the observations are within three σ of the population mean (79). This means that in repeated sampling of the pump "all-pass" noise level at the same operating conditions there is a 2.5% chance that the observed value will be 4 dB above or below the population mean.

A perusal of the experimental results presented in Chapter V indicates that, in general, over short time intervals, the sample standard deviation of the pump noise level as measured with the ABN near-field measurement technique provides usable diagnostic information. In particular, the "all-pass" noise level versus time measurements for unit 4352 and the repeatability of the noise levels versus temperature indicate that the ABN near-field measurement

TABLE VII

RATIO OF POPULATION STANDARD DEVIATION, σ, TO RANGE IN SAMPLES OF n FROM THE NORMAL DISTRIBUTION. (EFFICIENCY OF RANGE AS ESTIMATION OF σ (79))

n	$\frac{\sigma}{\text{Range}}$	Relative Efficiency*
2	0.886	1.000
3	0.591	0.992
4	0.486	0.975
5	0.430	0.955
6	0.395	9.933
7	0.370	0.912
8	0.351	0.890
9	0.337	0.869
10	0.325	0.850

*Relative to calculating $S = \sqrt{\frac{\Sigma d^2}{n-1}}$ where d is the deviation of an observation from the sample mean.

technique provides good experimental information.

Noise Level Stabilization

Figure 32, which is the noise level of Unit 4321 versus time, shows that the "all-pass" level as a function of time has a coefficient of determination of 0.06. This indicates that (see Appendix E) 94% of the variance of the noise level is independent of time. Therefore, the large standard deviation of the pumps' noise levels, observed for most units, must be an inherent function of the components or due to some uncontrolled operational parameter. The narrow-band noise levels likewise have very "weak" correlation with time.

The coefficient of determination of the data shown in Figure 33 indicates that in general the "all-pass" noise level for units 432X may have some finite correlation with time, but the variation in noise level is primarily due to an inherent characteristic of the component or some uncontrolled variable.

The significance of the correlation of the 432X noise levels with time in Figure 33 can be evaluated by use of the "t" statistic (see Appendix E), the correlation coefficient, and the number of degrees of freedom. This procedure is greatly simplified by using the "Significance of Correlation" graph in Appendix E. Reference to Figure 33 and the Significance of Correlation" graph shows that the significance of the correlation is 95%. This means that statistically there

is a 5% chance that no correlation exists between the pump noise levels and time. In other words, this means that the null hypothesis of no correlation between the pump noise level and time is rejected at the 95% confidence level.

The linear regression curve in Figure 33 was obtained using the following equation:

$$y = a + b\,t \tag{6.1}$$

where:

y = noise level (dB)

a = coefficient

b = coefficient

t = time (seconds)

Equation (6.1) was also used to correlate the data in Figure 32.

The data in Figure 33 can be analyzed using a linear regression equation of the form:

$$y = a + b\,\log_{10}(t) \tag{6.2}$$

A regression of the data in Figure 33 with Equation (6.2) yields a coefficient of determination of 0.0112, which has an associated significance of correlation of 50%.

A regression analysis of the "all-pass" data in Figure 34 using Equation (6.1) yields a coefficient of determination of 0.37, which means that the corresponding significance of correlation is greater than 99.5%. Using Equation (6.2) for a regression analysis on the "all-pass" data for Unit 4327 in Figure 34 yields a significance of correlation over

99.9%. The fact that the "all-pass" noise level for Unit 4327 is higher than the other 432X pumps is partially due to the microphone being closer to the pump during the testing of Unit 4327. It was also noted that there was more high frequency energy associated with Unit 4327. The presence of the high frequency energy may have been due to a variation of A* between the earlier tests of other 432X units and the tests with Unit 4327.

The "all-pass" levels for both 435X units with respect to time have a significance of correlation of 95% or better. All of the regression analyses for the 435X units were accomplished with Equation (6.1). The significance of correlation for f_4 in Figure 37 is approximately 82%. If Equation (6.2) is used for the regression analysis of f_4 in Figure 36, with respect to time, the coefficient of determination is 0.24 and the associated significance of correlation is approximately 96%.

The narrow-band plots in Appendix D indicate a significant noise level component at 240 Hz occurred during the "normal" tests of Unit 4321. This frequency is below the pumping fundamental of 300 Hz for the indicated test conditions. The 240 Hz component is attributed to a coupler which was used for all of the tests in the reverberation facility, but not used during the tests on the contamination stand. It should be noted that the energy level at 240 Hz is greatly reduced in the noise signature for the pump when it was examined on the contamination test stand. Some 240 Hz

energy is expected since 240 Hz is a harmonic of the fundamental shaft frequency, but in general the 240 Hz level would not be expected to be as large as the noise level at the pumping fundamental.

If Equation (6.2) is a better expression for pump "all-pass" noise level with time, then there is little indication that the 432X unit noise levels are changing with time and a high probability that the 435X units noise levels are decreasing with time.

There is a strong possibility that the large amount of variance occurring in the "all-pass" pump noise levels with respect to time is due to variations of r, the air/liquid volume ratio.

Multi-Factor

Table VIII summarizes the results of the factorial experiments on Unit 4324. The analysis of variance for the factorial study is presented in Appendix F. As expected, based on the pump noise model, Equation (2.55), the hypothesis that speed affects the noise level could not be rejected at the 95% confidence level. After completing the analysis it was noted that the same table would result if a 99% confidence level were used for rejecting the null hypothesis. It is also apparent that the deviations in pressure during the factorial experiment were large enough to be significant. The most interesting result, not fully anticipated, was the significance of temperature and the temperature-speed interaction.

TABLE VIII

SUMMARY OF ANALYSIS OF VARIANCE UNIT 4324, 750217.
ONE-THIRD OCTAVE SOUND PRESSURE (db).
(Table is same for 99% confidence)

Effect-Interaction	Reject with 95% confidence Hypothesis: ith Treatment has no Effect				
	ALLPASS	250 Hz	500 Hz	10 kHz	20 kHz
Temperature	No	No	No	Yes	Yes
Speed	Yes	Yes	Yes	Yes	Yes
Pressure	No	No	No	Yes	No
Temperature-Speed	Yes	Yes	Yes	No	No
Temperature-Pressure	No	No	No	No	No
Speed-Pressure	No	No	No	No	No
Temperature-Speed-Pressure	No	No	No	No	No

The significant temperature-speed interaction means that the noise level of the pump is not linearly independent of the temperature and speed. Since the temperature-speed interaction and the temperature are significant at the 95% level, there is a good possibility that the proposed allowable operational parameter variations for the ISO/TC 131/SC8 (WG1-1) 84 pump airborne noise test procedure need to be further constrained to insure reproducibility of pump ABN tests.

Cavitation

The cavitation studies provided repeatable results that were consistent between the two sample lots. Figures 37 through 46 and other study results relative to cavitation are discussed in the following paragraphs.

Outlet Pressure

Unit 4323 was tested at both low and high outlet pressures to select a suitable pressure for cavitation studies. The test results did not show any significant trends due to the outlet pressure changes other than the normal increase in noise level when the outlet pressure is increased. Since there was no significant, unexpected, noise level variations due to outlet pressure, the high outlet pressure was selected for the cavitation studies because it is more realistic, it increases the signal to electrical "noise"

ratio, and minimizes the effects of background acoustical noise.

Inlet Pressure

A statistical analysis of the data in Figures 37 through 43 is not necessary to conclude that varying the inlet pressure of a high pressure hydraulic pump has a significance influence on the pump's noise level. Some comments are appropriate, however, about the general repeatability of the test data, the trends of the high inlet pressure portion of the noise level curves, the behavior of the data in the region where the noise level is a minimum, and the fact that pump noise levels can be reduced by controlling the inlet pressure.

Figure 39 compares the 16 kHz noise level of pumps 4325 and 4326. The variation in the noise levels between the two units at this frequency is probably due to variations of the air/liquid volume ratios and a variation of the stabilization times allowed before recording data. It is noteworthy that both the high and low inlet pressure ends of the curves are in good agreement.

During several of the cavitation tests, conducted by varying the inlet pressure, test data was recorded both for decreasing and increasing values of pressure with respect to time. The recorded values of noise level after increasing the inlet pressure showed the same trends as observed with decreasing inlet pressures; however, the resultant curves

with increasing inlet pressures were transposed toward the higher inlet pressure end of the graphs. This data is consistent with the conclusions in Chapter II that the rate of solution is slower than the rate of evolution.

The 40 kHz noise levels of Units 4351 and 4352 in Figure 41 demonstrated excellent reproducibility between units. The trend of approximately a 15 dB drop in the noise level far exceeds any expected standard deviation of the nose level. The repeatability of the data excludes the possibility of the noise reduction being a random occurrence. The distinct difference in the manner in which the 435X and 432X units respond to the variation of inlet pressure are consistent with the better "filling" characteristics exhibited by the 435X units during all tests.

The general trend of the noise level curves versus inlet pressure at the high inlet pressure portion of the curves seems to support the hypothesis that air exists in the fluid stream in the form of small bubbles that grow as the pressure is reduced. In fact, the 435X unit noise levels never exhibited the sharp decrease in noise level versus inlet pressure exhibited by the 432X units. The gradual decrease in the noise levels could easily be due to the air bubbles increasing in size and, therefore, increasing the diffusion of the high frequency noise thus causing a reduction of the near-field noise level of the pumps.

The noise level versus inlet pressure curves for the 432X units exhibit what could be construed as a noise level

drop associated with rapid diffusion of air bubbles. This region occurs after a gradual decrease of the noise level with a reduction of inlet pressure. For both sets of pumps the noise attenuation becomes inadequate with reduced inlet pressure compared to what may be an increased noise level due to cavitation. Thus, a hypothesis emerges. First, as the inlet pressure is reduced, gradual bubble growth (due to entrained air) attenuates the noise from the pump. Subsequently (depending on the pump), there may be rapid release of air due to diffusion and a further decrease of the noise level. In either case the presence of air induced cavitation noise (or increased noise levels due to a decrease of lubricity) causes the noise level to increase again as the inlet pressure is further reduced. Finally, at some inlet pressure the noise level becomes as high or higher than it was with a high inlet pressure and the hydraulic system becomes unstable because of the large amount of entrained air.

The presence of a minimum point in the noise versus inlet pressure curves indicates that for noise control purposes it may be optimal to operate a hydraulic system with a controlled amount of entrained air in the system. It is also interesting to recall Tessman (9) found that a small amount of air in the pump's inlet fluid reduced the pump damage attributed to cavitation. The approximate 6 dB drop of the noise level for Unit 4324 shown in Figure 37 is an indication that controlled aeration could reduce the noise

level emitted by a pump. Table IX and X are an analysis of the noise emitted by Unit 4323 to determine the relation between the minimum "all-pass" noise level point and the dBA noise level of the pump.

Table IX shows that 4.7 dBA decrease of the 8 kHz Octave-Band noise level occurred when the pump inlet (4323) was aerated as compared to the case where there was no visible entrained air in the pump inlet. A more complete comparison of the "normal" and "aerated" inlet noise levels is contained in Table X which indicates that over the frequency range of 100 Hz to 10 kHz there was approximately a 3 dB decrease in the "all-pass" noise level and 2.4 dBA decrease in the noise level. It is also interesting to note that the pumping fundamental and first harmonics noise levels are reduced by approximately 5 dBA, which is an appreciable reduction in the "pure-tone" signals produced by the unit.

The cavitation test results with the high pressure gear pumps are consistent with the test results obtained by investigators who studied the acoustical signatures of low pressure pumps.

Air/Liquid Ratio

Figure 42 shows the significant change in the pump's noise level due to a variation of the air/liquid volume ratio. The basic behavior of the noise level versus inlet pressure does not change. The point of system instability seems to be little affected by the air/liquid volume ratio.

TABLE IX

COMPARISON OF OCTAVE BAND dBA PRESSURE LEVELS
SHOWING HIGH FREQUENCY DECREASE
WITH AERATED FLUID

Octave Band Center Frequency (Hz)	"Normal" (750119-1539) (dBA)	Aerated (750119-1529) (dBA)	Difference (dBA)
1000	84.5	84.8	+0.3
2000	84.5	82.8	-1.7
4000	82.8	81.7	-1.1
8000	80.6	75.9	-4.7

TABLE X

COMPARISON OF "A" WEIGHTED NEAR-FIELD PRESSURE LEVELS
SHOWING NOISE LEVEL DECREASE WITH
AERATED LIQUID.
Q* ≈ 100% for Both Cases

Frequency (Hz)	"Normal" (750119-1539)			Aerated (750119-1529)		
	Measured (dB)	dBA Correction (dB)	A Weighted (dBA)	Measured (dB)	dBA Correction (dB)	A Weighted (dBa)
100	65.5	-19.1	46.4	64.0	-19.1	44.9
125	64.5	-16.1	48.4	63.5	-16.1	47.4
160	73.5	-13.2	60.3	72.5	-13.2	59.3
200	86.5	-10.8	75.7	85.5	-10.8	74.7
250	91.0	- 8.6	82.4	86.5	- 8.6	76.9
315	77.5	- 6.5	71.0	75.0	- 6.5	68.5
400	81.0	- 4.8	76.2	79.5	- 4.8	74.7
500	91.0	- 3.3	87.7	86.0	- 3.3	82.7
630	78.5	- 1.9	76.6	76.5	- 1.9	74.6
800	79.5	- 0.8	78.7	80.0	- 0.8	79.2
1000	82.0	0.0	82.0	82.0	0.0	82.0
1250	77.5	0.5	77.0	77.5	0.5	78.0
1600	80.5	1.0	81.5	80.0	1.0	81.0
2000	77.0	1.2	78.2	74.0	1.2	75.2
2500	77.5	1.2	78.7	74.0	1.2	75.2
3150	74.0	1.2	75.2	73.0	1.2	74.2
4000	79.5	1.0	80.5	78.5	1.0	79.5
5000	76.2	0.5	76.7	74.5	0.5	75.0
6300	74.2	-0.2	74.0	70.5	-0.2	70.3
8000	78.0	-1.1	76.9	72.5	-1.1	71.4
10,000	78.5	-2.4	76.1	74.0	-2.4	71.6
ALLPASS	96.2			93.1		
dBA			92.5			90.1

The "width" of the minimum noise level portion of the curve increases considerably with a higher A*. This latter observation is based on the fact that with an A* of 7.0% the noise level is below 67 dB over a range of 55 kPa while with an A* of 0.7% the noise level is below 67 dB over a range of only 20 kPa. This, of course, means that the noise level is less sensitive to changes of inlet pressure with a higher air/liquid volume ratio.

The use of any cavitation index should account for the presence of air in the system liquid. The proposal for a CPI is predicated on the availability of accurate descriptions of the fundamental behavior of air in hydraulic systems. This requires a means of accurately measuring the air/liquid volume ratio. Unfortunately, the aeration detection device, discussed in Chapter III, is an excellent "relative" measurement device, but not acceptable in its present form as an "absolute" measurement device.

These comments about the ADD are based on the following observations. The amount of air measured with the ADD depends on the minimum pressure attained when a vacuum is created with the plunger in the syringe. The procedure may be repeatable but there is no way of ascertaining that a pressure of absolute zero was attained during the de-gassing of the system liquid sample in the syringe. In fact (36, p. 65) there are arguments that indicate that all of the air in solution and in the liquid could not be extracted unless the pressure is reduced to absolute zero because the surface

tension of the liquid will hold air to the interstices of the particulate contaminant in the liquid. The amount of air that will go back into solution during agitation of the ADD has not been determined, but certainly some amount will return to solution, before the measurement is taken.

Assuming that the same minimum pressure is reached during each degassing and the same percent by volume returns to solution, the resultant measurement is an indication of the actual air/liquid volume ratio minus the air that was not diffused and minus the amount of air that returned to solution.

Suppose, as an example, that the minimum pressure reached with the ADD is 30 kPa. Knowing that air has a solubility constant of 0.09 in hydraulic oil leads to the conclusion that the oil retains a volume of air equal to 3% of the volume of liquid. If some of the diffused air returns to solution then any number obtained with the ADD would be in absolute error by the 3% plus whatever air/liquid volume ratio redissolved. This should not discourage experimenters from using the ADD for measurements, but the results with the ADD should not be considered absolute until the measurement technique is more thoroughly examined and perfected.

The problem of making accurate measurements of the air/liquid volume ratio could be approached using densitometer techniques or some of the measurement techniques developed by the Seaton-Wilson Manufacturing Co., Inc. (85).

The trend of the noise level versus inlet pressure curves with an increased air/liquid volume ratio does not clarify whether the increase in noise level at lower inlet pressures is due to solute cavitation or reduced lubricity. It is apparent, however, that at an inlet pressure above atmospheric, (101 kPa), the higher air/liquid ratio provides the quietest 16 kHz noise level and below atmospheric inlet pressure the lower air/liquid volume ratio provides the quietest noise level prior to the system becoming unstable.

If the noise level curve transition point, where the noise level begins to rapidly decrease as the inlet pressure is decreased, is associated with diffusion of air then those points allow the estimation of r. The estimates using the data in Figure 42 are 11 percent and 18 percent. It is also possible that the first major decrease in noise level as the inlet pressure is reduced for unit 4326 is some function of the design of the pump, since the same phenomena was not observed with the 435X units. The section on volumetric efficiency shows that the 432X units do not "fill" as well as the 435X units.

The results of the noise level tests where cavitation was induced with reduced inlet pressure are consistent with the results obtained by other investigators studying low pressure hydraulic pumps (Chapter II).

Speed Induced

The results of the tests to detect cavitation by

monitoring noise level versus increasing pump speed, and the associated reduction in Q*, indicate that acoustical signature analysis can be used to monitor cavitation inception. The test results are consistent with experimental results obtained when cavitation is induced by reducing the inlet pressure and detected by monitoring noise levels. The results indicate that operation of a pump at any speed prior to the high noise/speed slope portion of the curve will insure that the flow rate efficiency is satisfactory (see Figures 43 and 44). The noise level versus speed induced cavitation test is easy to conduct and provides a useful non-intrusive field technique for detecting the cavitation inception pump speed.

The behavior of the 16 kHz and 40 kHz noise levels of Unit 4352 during the speed induced cavitation study is consistent with their behavior during tests where cavitation was induced by varying the inlet pressure. The minimum noise level of the 40 kHz band preceded a significant drop of the flow rate efficiency.

Volumetric Efficiency

During both of the tests relating "filling" characteristics and noise level, the minimum noise level at a selected frequency preceded the point at which Q* was equal to 95%. A comparison of Figures 45 and 46 indicates that Units 435X are less susceptible to cavitation than Units 432X.

Contamination

There are two observed trends of the data acquired during the contamination tests that provide a diagnostic technique for monitoring the effects of contaminant. First, for both sample lots of pumps, the fourth harmonic of the fundamental pumping frequency appears to remain essentially constant with or without large amounts of contaminant in the system. Second, the fundamental pumping frequency noise level increases when contaminant is added to the system fluid. The significance of these trends is tested by using a parameter based on taking the difference (before adding contaminant) between the fundamental pumping frequency level, L_1, and the level of the fourth harmonic, L_4, which yields $(L_1 - L_4)_b$ and subtracting it from a similar difference when a given level of contaminant is present. For example with a 100 g/m^3 contaminant level the parameter is:

$$D_{100} = (L_1 - L_4)_{100} - (L_1 - L_4)_{b100} \qquad (6.3)$$

The resultant values of D are curve fitted to the equation:

$$y = a + b \log_{10}(g^*) \qquad (6.4)$$

where:

y = noise level difference, D_i, i = contaminant level

g^* = gravimetric level (g/m^3)

a = constant

b = constant

The results of evaluating values of D for several tests and the associated regression curves are shown in Figures 51 and 52. The significance of the data used to develop these figures can be evaluated using the null hypothesis: "contamination does not affect the noise level." The null hypothesis can be rejected at the 95% confidence level. This rejection of the null hypothesis means there is a high probability that the contaminant does affect the noise level.

Figure 51 shows the data for two test conditions with unit 4326. Although using all of the data points from both curves established that contaminant affects the noise level, the significance of the correlation of noise level as a function of contamination level is approximately 80% for both of the curves in Figure 51. The significance of the correlation for the data in Figure 52 is even less than that of the data in Figure 51. It is also important to note that the magnitude of the change of the noise level with contaminant in the liquid is, on the average, very small, being approximately 1.5 dB when 1000 g/m^3 of contaminant is present in the system.

In summary, the contamination level has a detectable influence on the noise level of a pump. However, the influence is small in magnitude and could easily be obscured by other variables. Hence, it is important to control the contamination level for noise tests, but it does not appear practical at this time to try using acoustical analysis for detecting the presence of contaminant in field systems.

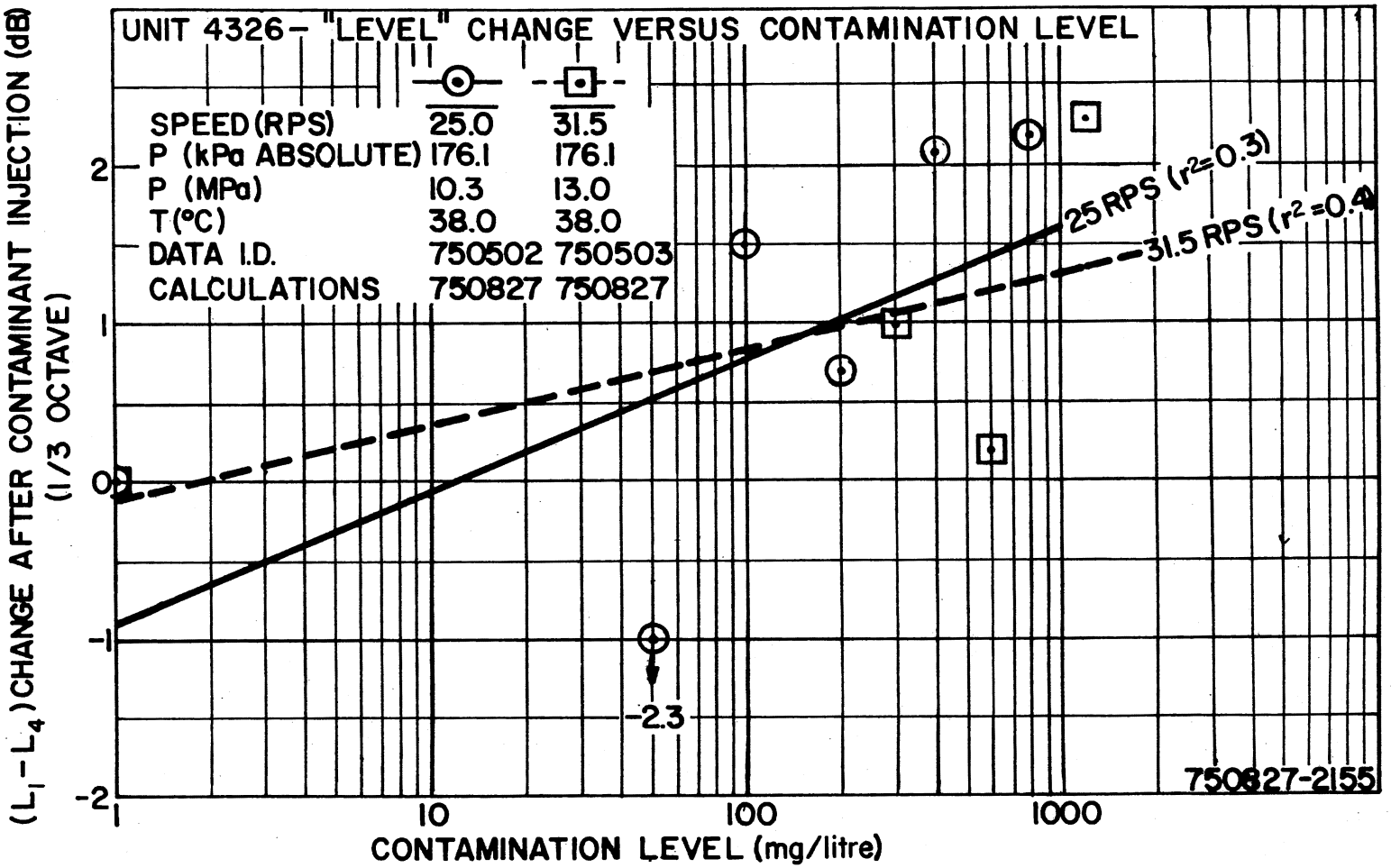

Figure 51. Near-Field Change of $L_1 - L_4$ After Injecting Contaminant Into Test Circuit Versus Contamination Level, Unit 4326

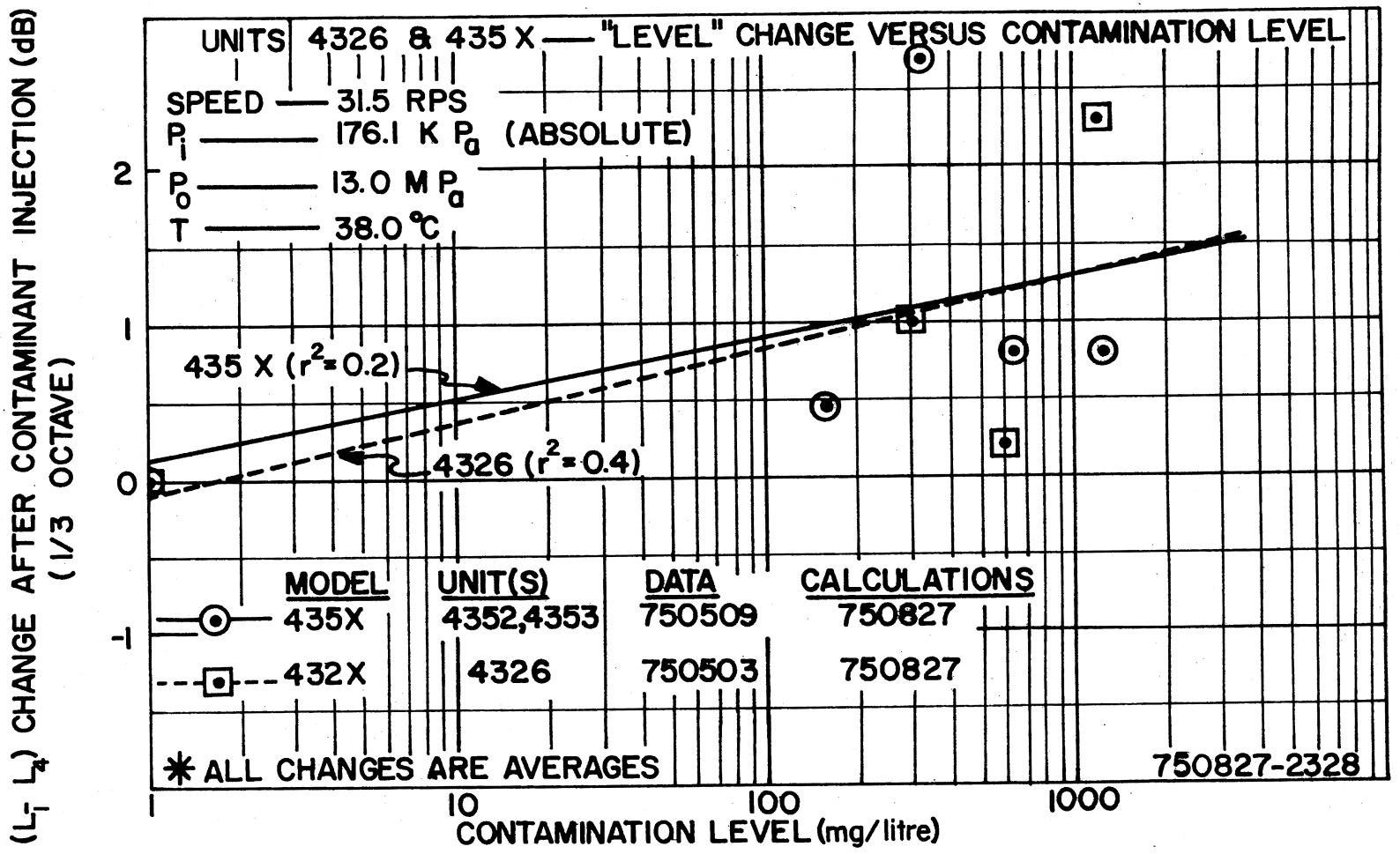

Figure 52. Near-Field Change of $L_1 - L_4$ After Injecting Contaminant Into Test Circuit Versus Contamination Level, Units 4326 and 435X

Wear

The results of the near-field noise level measurements after controlled wear of pumps was analyzed to determine if acoustical signature analysis could be used as a non-intrusive diagnostic method to determine if a given pump was worn beyond acceptable limits. The raw data of Figures 47, 48, and 49 were analyzed using the proposed noise wear index (Equation (2.25)). Table XI lists some of the variations of the noise wear index that were considered in the analysis.

Indicies were considered which used from two harmonics to four harmonics. For both pump lots attempts were made to use the first and third pumping harmonics for the noise wear index, but there was inadequate correlation with the resultant indicies. The coefficients of determination in Table XI are for the associated curve that describes the noise wear index as a function of pump performance degradation. The two basic equation forms used in the linear regressions are shown in Table XI. In some cases linear regression was employed on both the raw and normalized data of the matricies used for the development of the noise wear index (Equation (2.22) for instance).

Figures 53 through 56 present some of the more interesting results obtained during the investigations of the noise wear index. The results of line 1 in Table XI are shown in Figure 53. Figure 54 contains the results associated with line 2 of Table XI. Lines 4 and 8 of Table XI are associated with Figures 55 and 56, respectively.

TABLE XI

SUMMARY OF COEFFICIENTS OF DETERMINATION FOR EQUATIONS WHICH DESCRIBE THE EMPIRICAL RELATIONSHIP BETWEEN NOISE WEAR INDICIES AND THE PUMP FLOW INDEX

Line No.	Coefficient of Determination r^2	Noise Index N	Harmonics f_n	Equation Form "Level"	Equation Form "N"	Curve "Fitted" Raw Data	Curve "Fitted" Normalized Data	Calculation Identification
1	0.82	Σt_{ij}	f_1 f_2	$Y = ax^b$	$Y = ax^b$	No	Yes	750823-2100 750821-1055 750818-1700
2	0.75	Σt_{ij}	f_1, f_2	$\log Y = a+b\ X$	$Y = a\ X^b$	Yes	No	750821-1055 750820-0100
3	0.74	Σt_{ij}	f_1, f_2	*$\log Y = a+b\ X$	$\log Y = a+b\ X$	Yes	No	750820-0100 750821-1045
4	0.76	Σt_{ij}	f_1, f_2, f_4	$Y = a\ X^b$	$Y = a\ X^b$	No	Yes	750818-1700 750821-0925
5	0.73	Σt_{ij}	f_1, f_2, f_4	$\log Y = a+b\ X$	$\log Y = a+b\ X$	No	Yes	750818-1935 750821-0930
6	0.73	Σt_{ij}	f_1, f_2, f_4	*$Y = a\ X^b$	$Y = a\ X^b$	Yes	No	750819-1500 750821-0935
7	0.68	Σt_{ij}	f_1, f_2, f_4	$Y = a\ X^b$	$Y = a\ X^b$	Yes	No	750819-2020 750821-1105
8	0.67	$-\Sigma\lvert t_{ij}\rvert$	f_1, f_2, f_3, f_4	*$\log Y = a+b\ X$	$\log Y = a+b\ X$	Yes	No	750820-0005 750821-1000
9	0.65	Σt_{ij}	f_1, f_2, f_3, f_4	*$Y = a\ X^b$	$Y = a\ X^b$	Yes	Yes	750820-1100 750821-1120
10	0.65	Σt_{ij}	f_1, f_2, f_3, f_4	*$\log Y = a+b\ X$	$Y = a\ X^b$	Yes	No	750819-2200 750821-1115
11	0.61	Σt_{ij} $t_{ij} \leq 0$	f_1, f_2, f_3, f_4	*$\log Y = a+b\ X$	$\log Y = a + bX$	Yes	No	750820-0005 750821-1005
12	0.59	Σt_{ij}	f_1, f_2, f_3, f_4	$\log Y = a+b\ X$	$\log Y = a+b\ X$	Yes	No	750819-2120 750821-0945
13	0.56	Σt_{ij}	f_1, f_2, f_3, f_4	$\log Y = a+b\ X$	$\log Y = a+b\ X$	No	Yes	750817-1803 750821-0910

*First two data points averaged. Average level used at average Q/Q_r.

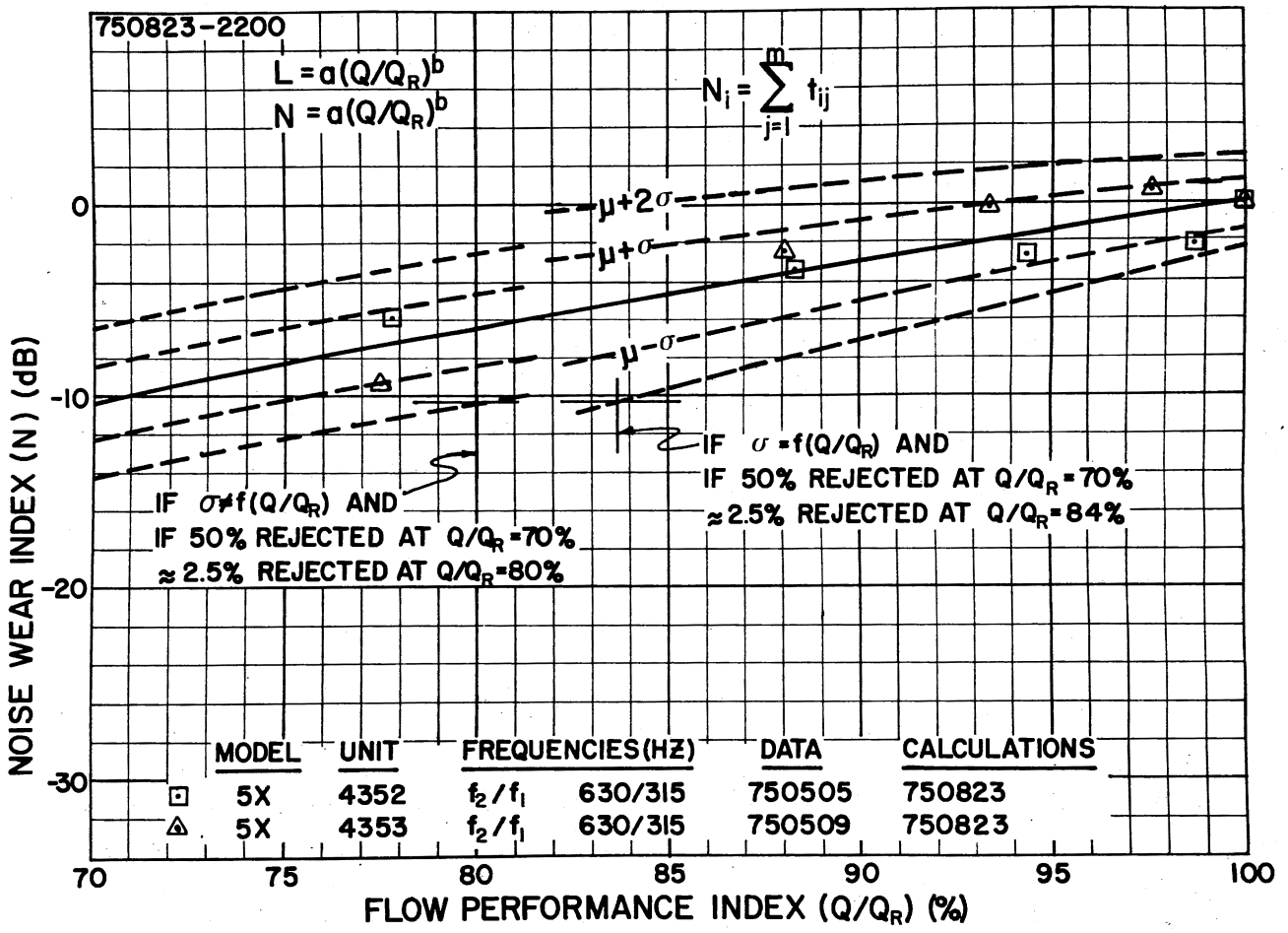

Figure 53. Noise Wear Index (N) Versus Flow Index for Units 4352 and 4353. (Index Based on Data for Two Harmonics. Graph shows influence of σ on % of units rejected at a given N.)

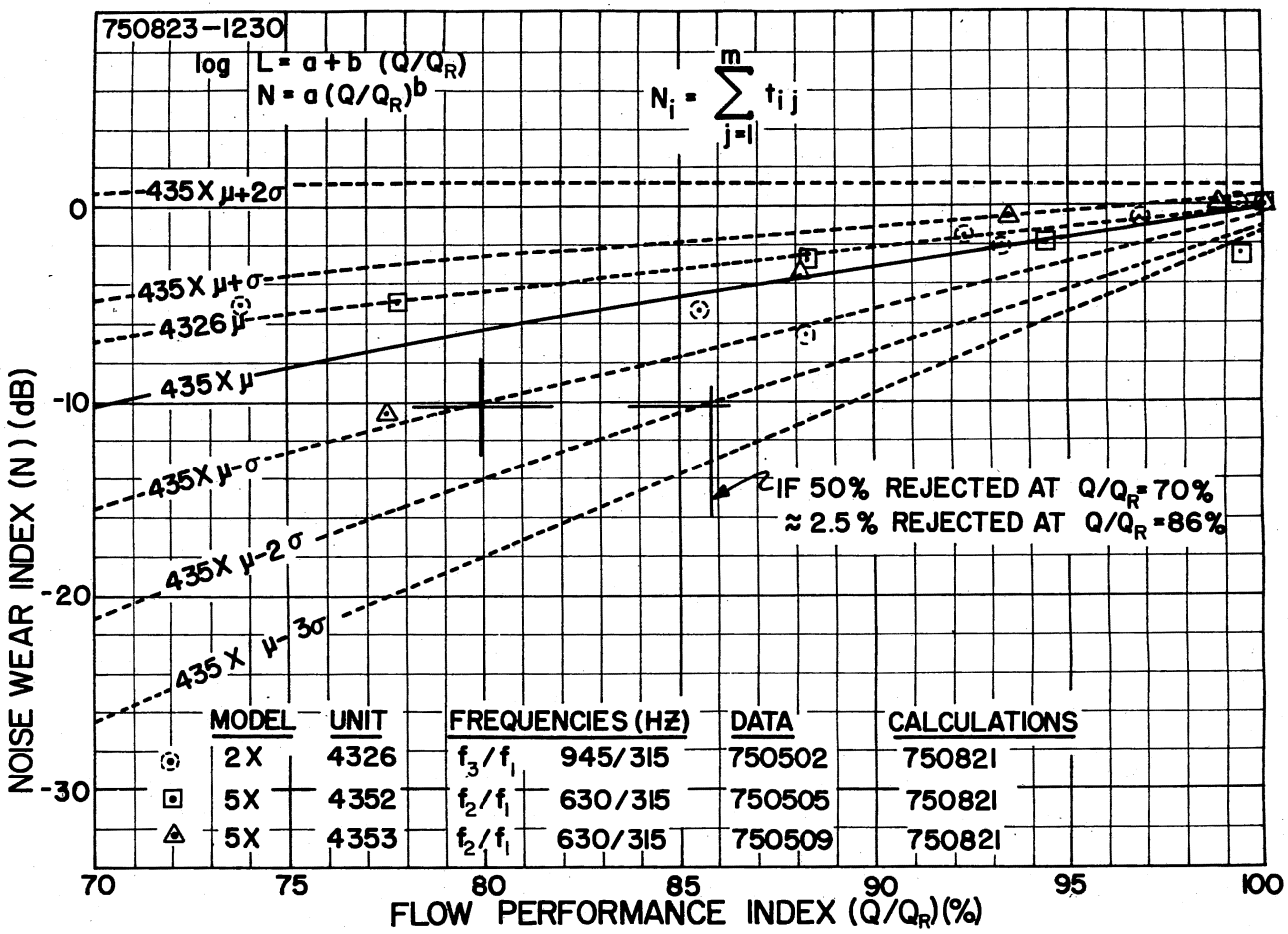

Figure 54. Noise Wear Index (N) Versus Flow Index for Units 4326, 4352, 4353. (Index based on data for two harmonics.)

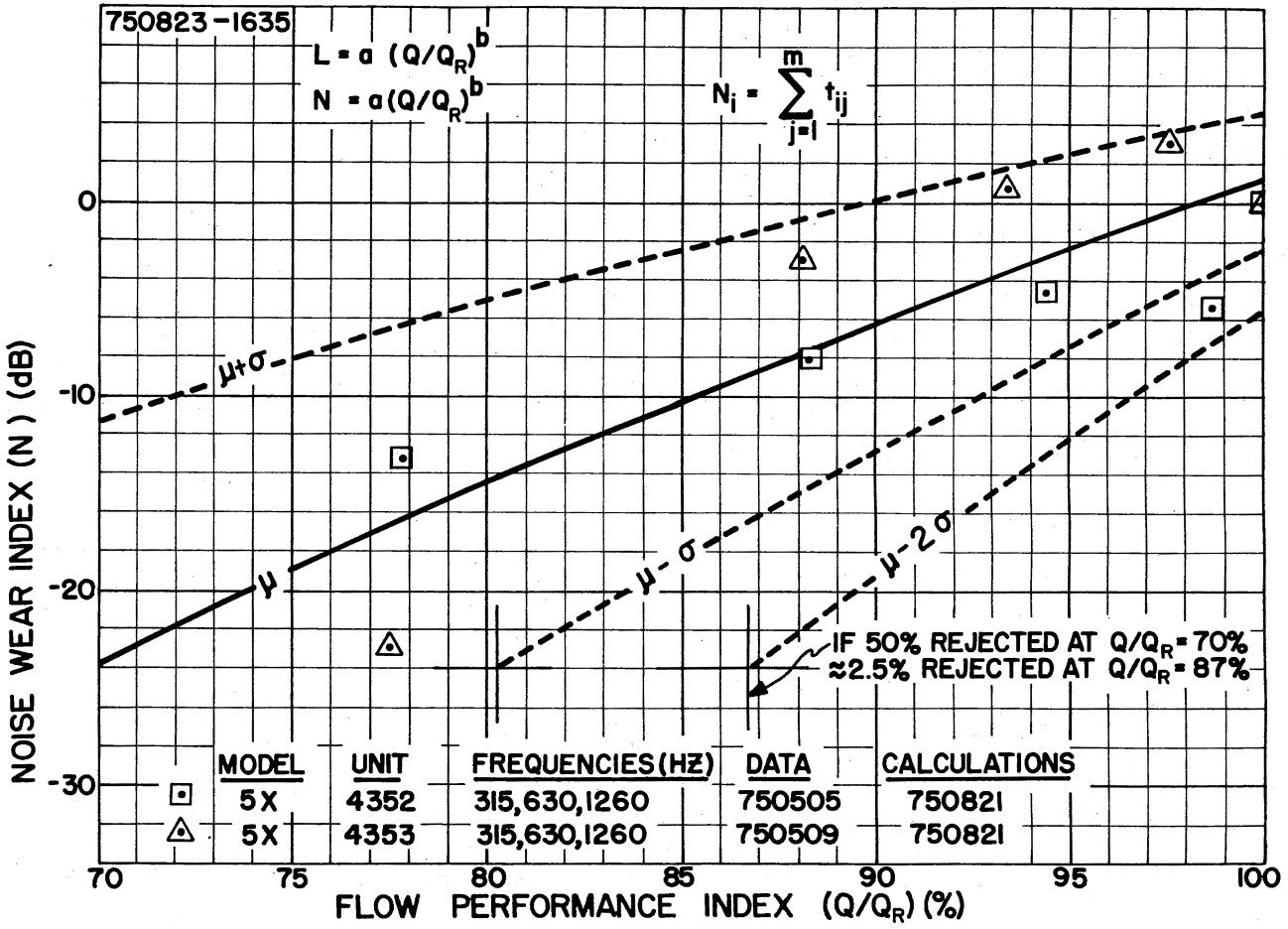

Figure 55. Noise Wear Index (N) Versus Flow Index for Units 4352 and 4353. (N based on data for three harmonics.)

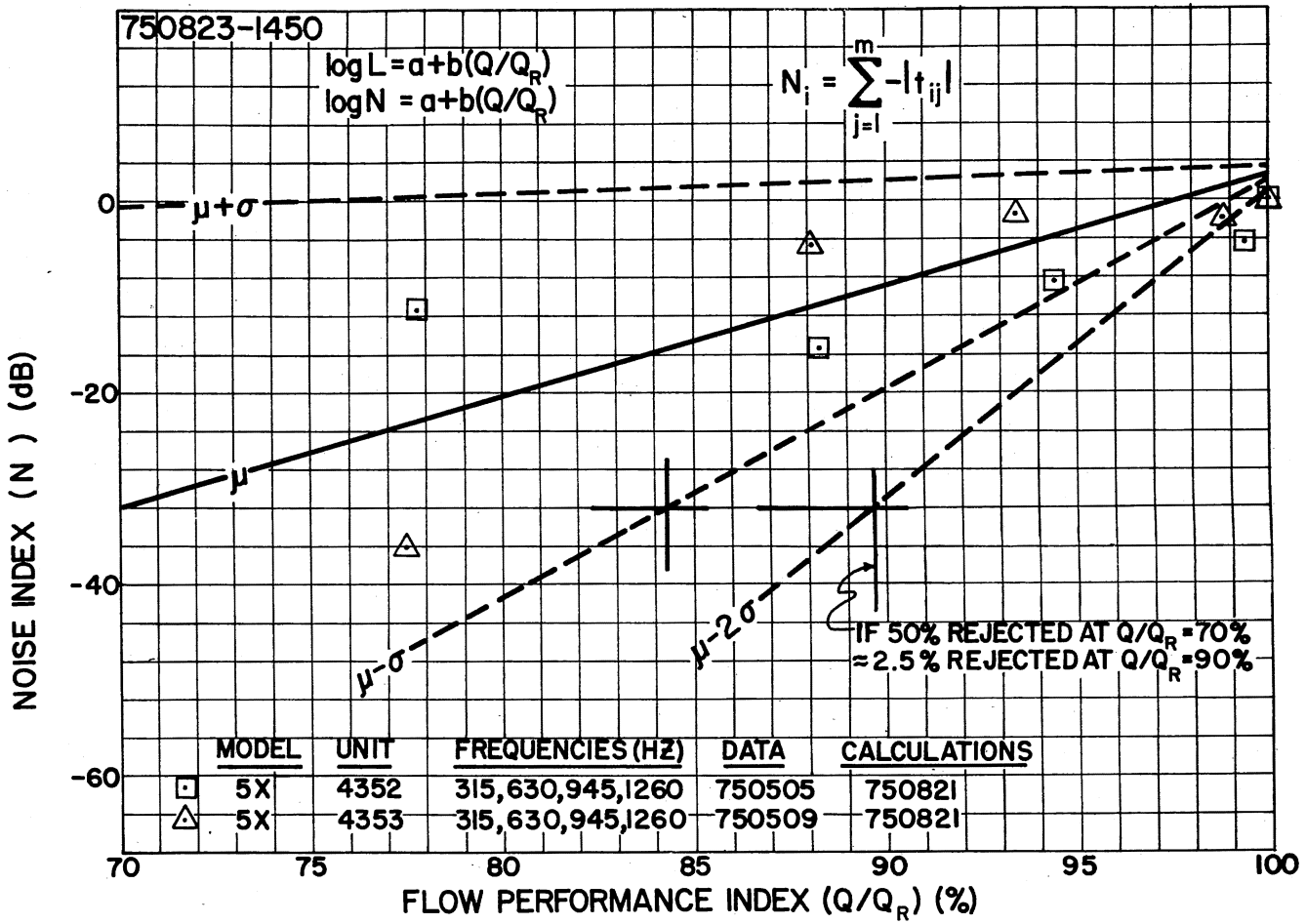

Figure 56. Noise Wear Index (N) Versus Flow Index for Units 4352 and 4353. (N based on $|t_{ij}|$ and data for four harmonics.)

The noise wear index for Figure 56 has a correlation significance of over 99.5%. The remaining correlation significances are greater than 99.9%. It appears that if the proper pumping harmonic noise level is ratioed to the pumping fundamental noise level and properly manipulated, a viable noise wear index can be formulated for any hydraulic gear pump. As more harmonics are included in the noise wear index the correlation coefficient becomes smaller. This observation is based on studies of the coefficients of determination in Table XI and by studies of the 2.5% rejection flow rate percentages in the figures.

Temperature

The results of the temperature experiments were consistent with expected behavior. Figure 50 shows that at the high frequencies the noise level decreased as the temperature increased. This reduction of the high frequency noise is hypothesized to be due to the release of air and the resultant "scattering" of the noise. The increase of the "all-pass" level is apparently due to an increase of the second pumping harmonic noise level. It is not readily apparent that the slopes of the noise versus temperature curves are significant enough to have caused the factorial experiment to show that temperature is a significant variable below 10,000 Hz over a four degree centigrade span.

The next chapter delineates specific conclusions and makes recommendations for further studies.

CHAPTER VII

CONCLUSIONS AND RECOMMENDATIONS

The "excursion into unexplored territory" reported in this dissertation provides specific information about the behavior of high pressure gear pump acoustical signatures in particular and high pressure pumping phenomena acoustical signatures in general. The study yielded many conclusions which are highly significant in both a statistical and engineering sense. Several "insights" that resulted from this study indicate the need for further exploration in areas related to acoustical signature analysis of high pressure pumping phenomena. Specific conclusions and recommendations are listed in the remainder of this chapter.

Conclusions

1. Near-field airborne noise measurements can be used in conjunction with acoustical signature analysis to provide a non-intrusive diagnostic technique for fluid power components. Near-field acoustical signatures of high pressure gear pumps are repeatable and reproducible.

2. The results of this study show that acoustical signature analysis of high pressure hydraulic gear pump noise provides specific information about past and present

component operating conditions. Cavitation and wear can be detected using acoustical signature analysis.

3. The Noise Wear Index developed during this study has a correlation significance of 99.5%. Since the proposed index is a function of gear pump flow degradation, it provides a non-intrusive means of assessing the performance of a gear pump.

4. Near-field noise monitoring and acoustical signature analysis of the 8 kHz to 40 kHz pump noise provides the cavitation inception speed of a gear pump operating with a variable speed power plant or the cavitation inception inlet pressure of a pump operating at constant speed.

5. The cavitation inception "bubble" pressure for practical oil hydraulic systems is determined by the system air/liquid volume ratio. It is independent of the vapor pressure of the oil.

6. The "filling" characteristics of hydraulic pumps are affected by the test system air/liquid volume ratio. Pump performance test codes must be changed to reflect this important fact.

7. With respect to air/liquid volume ratios, the "quietest" gear pump noise levels (dBA) occur when there is 3-4% entrained air at the pump inlet. Higher percents of entrained air cause higher noise levels and unstable system operation. The absence of entrained air at the pump's inlet also causes higher pump noise levels.

8. The null hypothesis that "contamination does not

affect pump noise levels" can be rejected at the 95% confidence level. The results of this study show that pump noise levels will not be affected more than 0.5 dB by test system contamination levels of 10 mg/l (A C Fine Test Dust).

9. The pump noise level versus time data "scatter" observed during this study cannot be attributed to a regression of the noise levels with time. The standard deviation of the data is due either to inherent pump instabilities or to some uncontrolled test variable. If the cause of the deviations is an uncontrolled test variable, a likely candidate is the system air/liquid volume ratio.

10. Based on the results of this study the factory "break-in" used on the test samples is satisfactory since the respective average values of the "all-pass" noise levels for the pumps remained within 1.0 dB during the first 6000 seconds of operation.

11. Noise measurements for an individual hydraulic pump should be an average of many samples to minimize the sample standard deviation associated with the measurement method.

12. The test parameters that should be controlled during noise tests of high pressure hydraulic gear pumps are: speed, inlet pressure, air/liquid volume ratio, liquid, fluid/temperature, outlet pressure, and contamination level.

13. The allowable variations of the test parameters in Reference (3) should be further constrained to insure repeatability suitable for an international standard. This

statement is based on two facts. First, it is practical to further constrain the speed and temperature allowable variations. Second, a null hypothesis of "speed and temperature variations have no effect on the noise level" can be rejected at the 99% confidence level.

Recommendations

1. Test procedures which require monitoring high pressure hydraulic pump performance should include constraints on the system fluid air/liquid volume ratio. These constraints should be placed on the entrained air/liquid volume ratio at the pump inlet.

2. To provide accurate assessments of the air/liquid volume ratios in hydraulic systems the use of densitometer, sonic velocity, and direct air volume measurement techniques should be investigated. These techniques should be studied with the objective of obtaining an "on-line" air/liquid volume ratio measurement device.

3. The Noise Wear Index should be investigated as a function of speed. This study developed the Noise Wear Index for one speed.

4. The use of large operational parameter changes between noise measurements should be studied to determine if this procedure will provide more realistic estimates of noise level sample standard deviations that occur in practice.

5. To obtain the best model for pump noise as a

function of time, models, such as $dB = a + b \log(t)$, should be investigated with respect to the fundamental characteristics of the components to establish fundamental bases for the models.

6. The relationship between wear and noise should be verified for high pressure pump type mechanisms, if not for high pressure pumps themselves.

7. A practical acoustical "field stethoscope" for component noise level data acquisition needs to be developed. The "stethoscope" could be an adaptor for a microphone. This technique should be considered as a means of decreasing the measurement standard deviation that could result from near-field acoustical measurements in the "field".

8. The actual behavior of air in hydraulic systems needs comprehensive examination. The influence of air on the operational performance of high pressure pumps is significant and its affect on system performance and reliability needs to be accurately assessed.

9. The behavior of pump side-band noise levels should be studied in detail to determine their correlation with variations of the operational parameters in fluid power systems.

10. A detailed study of near-field noise measurements as a function of frequency and measurement radius needs to be conducted.

11. The influence of various pump mounting techniques on the acoustical signatures of hydraulic pumps needs to be

carefully examined.

12. Investigations should be conducted to determine the relative significance of SBN and FBN on the noise level emitted by high pressure hydraulic pumps.

13. A study of the acoustical behavior of "new" pumps to determine how they behave acoustically during the "infant" portion of their life could provide information about the correlation between noise and wear.

14. The distribution of near-field pump noise level populations should be studied in detail to determine if they are adequately described by the normal distribution.

SELECTED REFERENCES

(1) Method for Measuring Sound Generated by Hydraulic Fluid Power Pumps. NFPA Recommended Standard T3.9.70.12. Theinsville, Wisconsin: National Fluid Power Association, Inc., April 19, 1970.

(2) Method of Measuring Sound Generated by Hydraulic Fluid Power Motors. NFPA Recommended Standard T3.9.14-1971. Thiensville, Wisconsin: National Fluid Power Association, Inc., May 9, 1971.

(3) Test Code for the Determination of Airborne Noise Level of a Hydraulic Pump. ISO/TC 131/SC 8 (WG1-1). Geneve, Suisse: International Organization for Standardization, August 8, 1974.

(4) Maroney, George E., and Dr. E. C. Fitch. "The Effects of Physical Interactions on Hydraulic Component Noise Measurement." Proceedings of the 3rd International Fluid Power Symposium. Sponsored and Organized by BHRA Fluid Engineering, Cranfield, Dedford, England, 1973.

(5) Maroney, George E. Acoustical Signature Analysis as a Non-Intrusive Field Diagnostic Tool. Stillwater, Oklahoma: Fluid Power Research Center, Oklahoma State University. Basic Fluid Power Research Program Report No. 74-4, Annual Report No. 8, 1974.

(6) Bannister, R. L., and V. Donato. "Signature Analysis of Turbe-machinery." Sound and Vibration (September, 1971), 14-21.

(7) Thompson, R. A., and J. R. McCullough. The Detection of Wear in Gears. 72-PTG-24. New York, N. Y.: The American Society of Mechanical Engineers, July, 1972.

(8) Sevestyen, G. et al. "Investigation of Cavitation in Pumps by Direct and Indirect Methods." Act Technica Academiae Scientiarum Hungaricae, 71 (3-4), (1971), 472.

(9) Tessmann, R. K. The Effect of Aerated Fluid on Hydraulic Pumps. 72-CC-15. Stillwater, Oklahoma: Sixth Annual Fluid Power Research Conference, Oklahoma State University, October, 1972.

(10) Frarey, J. L. An Investigation of Off-Road Vehicle Power Train Diagnostics Utilizing High Frequency Vibration Analysis. Contract Report for Contract DAAK02-74-C-0084. Ballston Lake, New York: Shaker Research Corporation. Submitted to U.S. Army Mobility Equipment Research and Development Center, Fort Belvoir, Virginia, March, 1974.

(11) Varga, J., and G. Sebestyen. "Noise Measuring as a Complementary and Checking Method for Pumps Testing." Separatum Periodica Polytechnica, Mechanical Engineering, Vol. 16, No. 2 (1972), 10.

(12) Maroney, G. E., and L. R. Elliott. An Acoustical Performance Appraisal Technique for Fluid Power Pumps. Peoria, Illinois: Society of Automotive Engineers, Earthmoving Industry Conference, 1974.

(13) Pillai, K. V. K. Noise in Axial Piston Pumps - A Literature Survey. Stillwater, Oklahoma: Eighth Annual Fluid Power Research Conference, Fluid Power Research Center, Oklahoma State University, October, 1974.

(14) USA Standard Acoustical Terminology. USAS S1.1-1960. New York: American National Standards Institute, 1960.

(15) Bendat, J. S., and A. G. Piersol. Random Data: Analysis and Measurement Procedures. New York: Wiley-Interscience, 1971.

(16) Willekens, F. A. M. Fluid-Borne Noise in Hydraulic Systems. East Kilbride, Glasgow: First European Fluid Power Conference, Birniehill Institute, National Engineering Laboratory, 1973.

(17) Ichikawa, T., and K. Yamaguchi. "On Pulsation of Delivery Pressure of Gear Pump (in the Case of a Long Delivery Pipeline)." Bulletin of Japanese Society of Mechanical Engineers, 14, 78 (1971), 1304-1312.

(18) Kinsler, L. E., and A. R. Frey. Fundamentals of Acoustics. 2nd ed. New York: John Wiley and Sons, Inc., 1962.

(19) Beranek, Leo L., ed. Noise and Vibration Control. New York: McGraw-Hill, 1971.

(20) McCandlish, D., and S. A. Petrusewicz. Assessment of Noise Generated by Hydraulic Pumps Using Accelerometers. London: Conference on Noise Emitted by Fluid Power Equipment-Its Causes and Control, The Institution of Mechanical Engineers, March 15, 1973, 43-50.

(21) Chan, C. M. P., and D. Anderton. "The Correlation of Machine Structure Surface Vibration and Radiated Noise." Washington, D. C.: Inter Noise 72 Proceedings, October 4-6, 1972, 261-266.

(22) Tessmann, R. K. "Component Wear," Chapter II in Fundamental Wear Concept. Stillwater, Oklahoma: Basic Fluid Power Research Program, Fluid Power Research Center, Oklahoma State University, Annual Report Number 5, Section 71-5, 1971.

(23) Tessmann, R. K. Contaminant Wear in Hydraulic and Lubrication Systems. Paper No. P75-4. Stillwater, Oklahoma: Fluid Power Research Conference, Oklahoma State University, October, 1975.

(24) Lavoie, Francis J. "Signature Analysis: Product Early-Warning System." Machine Design, 10 (January, 1969), 151-160.

(25) Downham, E., and R. Woods. The Rationale of Monitoring Vibration on Rotating Machinery in Continuously Operating Process Plant. ASME Paper No. 71-Vibr-96. Toronto, Canada: Vibrations Conference, September 8-10, 1971.

(26) Halling, J. "A Contribution to the Theory of Mechanical Wear." Wear, 34, 3 (October, 1975), 239-249.

(27) Suh, N. P., and P. Sridharan. "Relationship Between the Coefficient of Friction and the Wear Rate of Metals." Wear, 34, 3 (October, 1975), 291-299.

(28) Decontamination of Hydraulic Fluids. Technical Documentary Report No. TRD-TDR-63-4262 prepared for Air Force Systems Command, Wright-Patterson Air Force Base, Ohio. Stillwater, Oklahoma: Fluid Power Research Center, Oklahoma State University, December, 1963.

(29) Fitch, E. C. "Filter Requirements for Hydraulic Pumps." Hydraulics & Pneumatics, 28, 12 (December, 1975), 102.

(30) Fitch, E. C., and G. E. Maroney. A Fundamental Method for Establishing Contaminant Tolerance Profiles for Pumps. Guilford, England: 2nd International Fluid Power Symposium, British Hydromechanics Research Association, University of Surrey, January 4-7, 1971.

(31) Keller, A. C. "Real-Time Spectrum Analysis of Machinery Dynamics." Sound and Vibration, 10 (April, 1975), 40-48.

(32) Draft Recommended Standard Method of Establishing the Flow Degradation of Hydraulic Fluid Power Pumps When Exposed to Particulate Contaminant. Project 3.9.18. Theinsville, Wisc.: National Fluid Power Association, Inc., October, 1975.

(33) Elliott, L. R., G. E. Maroney, and E. C. Fitch. An Experimental Survey of Fluid Power Pumps. P75-AV-2. Stillwater, Oklahoma: Seventh Annual Fluid Power Research Conference, Fluid Power Research Center, Oklahoma State University. Also presented at the 29th National Conference on Fluid Power, Cleveland, Ohio, 1973.

(34) Davis, Dale S. Nomography and Empirical Equations. London: Reinhold, 1962.

(35) HP-55 Owner's Handbook. Cupertino, Calif.: Hewlett-Packard Company, 1974.

(36) Knapp, Robert T., James W. Daily, and Frederick G. Hammitt. Cavitation. New York: McGraw-Hill, 1970.

(37) Varga, J. J., and Gy. Sebestyèn. Determination of Hydrodynamic Cavitation Intensity by Noise Measurement. Tokyo: The Second International Japanese Society of Mechanical Engineers Symposium Fluid Machinery and Fluidics, Sept., 1972, 285-292.

(38) Schweitzer, P. H., and V. G. Szebehely. "Gas Evolution in Liquids and Cavitation." Journal of Applied Physics, 21 (December, 1950), 1218-1224.

(39) Bose, R. E. "The Effect of Cavitation on Particulate Contamination Generation." (Unpublished Doctoral Thesis, Oklahoma State University, 1966.)

(40) Thiruvengadam, A. "Prediction of Cavitation Damage." (Unpublished Ph.D. Thesis, Indian Institute of Science, Bangalor, 1961.)

(41) McCloy, Donaldson. Cavitation and Aeration: The Effect on Valves and Systems. Milwaukee, Wisc.: Cavitation Seminar, Milwaukee School of Engineering., May, 1967.

(42) Fitch, E. C., J. D. Parker, C. R. Gerlach, H. C. Hewitt, G. Maples, E. Mitwally, and R. Stuntz. Study of Fluid Transients in Closed Conduits. Annual Report No. 1, Contract NAS 8 11302, prepared for George C. Marshall Space Flight Center. Stillwater, Oklahoma: School of Mechanical Engineering Fluid Power and Controls Laboratory, Oklahoma State University, July, 1965.

(43) Guralnik, David B. (Ed.-in-Chief). Webster's New World Dictionary of the American Language. 2nd College Edition. New York: The World Publishing Company, 1970.

(44) Lichtarowicz, A. (Professor and Sr. Lecturer, The University of Nottingham, Deparment of Mechanical Engineering, U. K.) Personal visit and lecture at the Fluid Power Research Center, Oklahoma State University, Stillwater, Okla., August, 1975.

(45) Magorien, Vincent G. "Effects of Air on Hydraulic Systems." Hydraulics and Pneumatics, 6 (October, 1967), 128-131.

(46) N. E. L. Report. National Engineering Report, Number 75. Great Britian: National Engineering Laboratory, January, 1963.

(47) Hess, Fred C. Chemistry Made Simple. New York: Doubleday and Company, Inc., 1955.

(48) Magorien, V. G. "Techniques for Measuring and Removing Air From Hydraulic Control Systems." Proceedings of the National Conference on Fluid Power, 17 (1966), 203-210.

(49) Brenkert, Karl Jr. Elementary Theoretical Fluid Mechanics. New York: John Wiley and Sons, Inc., 1964.

(50) Tyrone Hydraulics Catalog. Corinth, Mississippi: Tyrone Hydraulics, 1975.

(51) Cessna Fluid Power Products Catalog. Hutchinson, Kansas: Fluid Power Division, Cessna Aircraft Company, 1975.

(52) Doeblin, Ernest O. Measurement Systems: Application and Design. New York: McGraw-Hill Book Company, 1966.

(53) Editors, Fluid Power Handbook and Directory. "Hydraulics and Pneumatics." Cleveland: Industrial Publishing Company, 1968-1969.

(54) Baker, Stephen F. The Elements of Logic. New York: McGraw-Hill Book Company, 1965.

(55) Poritsky, H. "The Collapse or Growth of a Spherical Bubble or Cavity in a Viscous Fluid." Proceedings of the First U. S. National Congress on Applied Mechanics (ASME), 00813-821, 1952.

(56) Plesset, M. A. "The Dynamics of Cavitation Bubbles." Trans. ASME Journal of Applied Mechanics, 16 (1949), 228-231.

(57) Raven, Francis H. Automatic Control Engineering. New York: McGraw-Hill Book Company, 1968.

(58) Hayward, A. T. J. Aeration in Hydraulic System: Its Assessment and Control. Conference on Oil Hydraulic Power Transmission and Control. London: Institute of Mechanical Engineers, November, 1961.

(59) Hayward, A. T. J. Air Bubbles in Oil- Their Effect on Viscosity and Compressibility. National Conference on Industrial Hydraulics, 17th Annual Meeting, 1961, 124-132.

(60) Varga, J., and G. Sevestyén. "Experimental Investigation of Cavitation Noise." Extrait De. La Houille Blanche, Numero 8 (1966).

(61) Thoma, D. "Die Experimentelle Forshung im Wasserkraftfach." Zeitschrift des Vereines deutscher Ingenieure, 69, 11 (1925), 329.

(62) Thoma, D. "Die Kavitation der Vasserturbinen." In Wasserkraftjahrbuch. Suggart: Groteer, 1924, 409-420.

(63) Harvey, E. N., D. K. Barnes, W. D. McElroy, A. H. Whiteley, D. C. Pease, and K. W. Cooper. "Bubble Formation in Animals. I, Physical Factors." Journal Cellular and Comp. Physiol., 24, 1 (August, 1944), 1-22.

(64) Fox, F. E., and K. F. Herzfeld. "Gas Bubbles With Organic Skin as Cavitation Nuclei." Journal Acoustical Society America, 26 (1954), 984-989.

(65) Amyx, James W., Daniel M. Bass, Jr., and Robert L. Whiting. Petroleum Reservoir Engineering. New York: McGraw-Hill Book Company, Inc., 1960.

(66) Calibration of Liquid Automatic Particle Counters. Recommended Procedures for Evaluating Fluid Power Components and Systems. Stillwater, Oklahoma: Fluid Power Research Center, Oklahoma State University, 1972, 93-99.

(67) Bensch, L. E., and W. T. Bonner. Field System Contaminants- Where, What, How Much. Paper No. P73-CC-1. Stillwater, Oklahoma: Seventh Annual Fluid Power Research Conference, Fluid Power Research Center, 1973, 187-193.

(68) Method for Evaluating the Filling Characteristics of a Fixed Displacement, Fluid Power Pump. Recommended Procedures for Evaluating Fluid Power Components and Systems. Stillwater, Oklahoma: Fluid Power Research Center, Oklahoma State University, 1972, 55-58.

(69) Becker, Ronald J. "How to Quiet Hydraulic Systems and Components." Hydraulics and Pneumatics, 22 (April, 1971), 122-132.

(70) Tessmann, Richard K. The Effect of Aerated Fluid on Hydraulic Pumps. Paper 72-CC-15. Stillwater, Oklahoma: Sixth Annual Fluid Power Research Conference, Fluid Power Research Center, Oklahoma State University, October, 1972, 341-365.

(71) Peterson, Arnold P. G., and Ervin E. Gross, Jr. Handbook of Noise Measurement. 7th Edition. Concord, Mass.: General Radio, 1972

(72) Maroney, G. E., and L. R. Elliott. "An Acoustical Performance Appraisal Technique for Fluid Power Pumps." Society of Automotive Engineers Transactions (1974), 1658-1663.

(73) Beranek, Leo L. (Ed.) Noise and Vibration Control. New York: McGraw-Hill Book Company, 1971.

(74) Maroney, G. E., and S. E. Wehr. Fluidborne Noise Attenuator Performance Evaluation. Society of Automotive Engineers Paper 750831, presented at the 1975 SAE Off-Highway Vehicle Meeting, at Milwaukee, Wisconsin. Warrendale, Pennsylvania: Society of Automotive Engineers, 1975.

(75) Willenbrock, F. K. "Noise Regulation- The Role of Management." Noise-News, 1, 6 (November-December, 1972), 141.

(76) Roberts, G. A. Measurement Uncertainty - A Roadblock in Standardization. Paper No. 74-8, Eighth Annual Fluid Power Research Conference. Stillwater, Oklahoma: Fluid Power Research Center, Oklahoma State University, 1974, 8-11.

(77) Instruction Manual Stepped 1/3 Octave-Band-Analyzer Plug-In. Concord, Massachusetts: General Radio, 1972.

(78) Decker, R. L. Improving Engineering Productivity With Factorial Experiments. Paper No. P73-RQ-3, Seventh Annual Fluid Power Research Conference. Stillwater, Oklahoma: Fluid Power Research Center, Oklahoma State University, 1973.

(79) Snedecor, G. W., and W. G. Cochran. Statistical Methods. 6th Edition. Ames, Iowa: The Iowa State University Press, 1968.

(80) Dixon, W. J., and F. J. Massey, Jr. Introduction to Statistical Analysis. New York: McGraw-Hill Book Company, 1957.

(81) Proposed NFPA Recommended Standard Method of Establishing the Flow Degradation of Hydraulic Fluid Power Pumps When Exposed to Particulate Contaminant. Project T3.9.18-1975. Thiensville, Wisconsin: National Fluid Power Association, Inc., 1975.

(82) Elliott, L. R. "Dynamic Determination of the Air Content in High Pressure Fluid Systems Through Sonic Velocity Measurement." (Unpublished M.S. Thesis, Oklahoma State University, 1974.)

(83) Instruction Manual Wave Analyzer Plug-In. Concord, Massachusetts: General Radio, 1973.

(84) Tessmann, R. K., and J. M. Howsden. A Practical Device for Measuring Aeration Levels in Operating Hydraulic Systems. Paper No. P75-15, Fluid Power Research Conference. Stillwater, Oklahoma: Fluid Power Research Center, Oklahoma State University, 1975.

(85) Engineering Data Aire-Ometer Model AF-4000 and Engineering Data Aire-Ometer Model AD-4001. Burbank, California: Seaton-Wilson Manufacturing Company, 1967.

(86) USA Standard Specification for Octave, Half-Octave, and Third-Octave Band Filter Sets. USAS S1.11-1966. New York: American National Standards Institute, 1966.

(87) Miller, Irwin, and J. E. Freund. Probability and Statistics for Engineers. Englewood Cliffs, New Jersey: Prentice-Hall, 1965.

(88) Baniak, E. A., Research and Technical Department, Texaco, Inc., Beacon, New York. Personal Communication, April 2, 1974.

(89) Handbook of Chemistry and Physics. 47th Ed. Cleveland, Ohio: The Chemical Rubber Co., 1966-1967.

(90) Moroney, M. J. Facts From Figures. 2nd Ed. with minor revisions. London: Penguin Books, 1951. Reprinted 1974.

APPENDIX A

DEFINITIONS

"A" Weighting: A technique for converting noise levels at various frequencies to levels that are relative to the manner in which the human ear "hears" sound. See Reference (71).

All-Pass: An all-pass network is a network designed to introduce phase shift or delay without introducing appreciable attenuation at any frequency (14).

Anechoic: Free from echoes (an anechoic room is one whose boundaries absorb effectively all of the noise incident thereon) (14) (43).

Cavitation: Cavitation is the dynamic process of gas cavity growth and collapse in liquid.

Complex Periodic Data: Those types of periodic data which can be defined mathematically by a time-varying function whose wave-form exactly repeats itself at regular intervals such that $x(t) = x(t \pm n\ T_p) n = 1,2,3, \ldots$ where $T_p = 1/f_1$. (15).

Decibel: The decibel is one-tenth of a bel. Thus, the decibel is a unit of level when the base of the logarithm is the tenth root of ten, and the quantities concerned are proportioned to power (14).

Filter: Wave filter - A wave filter is a transducer for separating waves on the basis of their frequency. It introduces relatively small insertion loss to waves in one or more frequency bands and relatively large insertion loss to waves of other frequencies (14).

Hertz: The international unit of frequency, equal to one cycle per second (43).

Impedance, Acoustic: The ratio of the pressure to the associated volume velocity (noise radiation) (18).

Impedance, Radiation: The ratio of the force to velocity (coupling between acoustic waves and source or load) (18).

Impedance, Specific Acoustic: The ratio of acoustic pressure in a medium to the associated particle velocity (wave transmission) (18).

Intensity, Acoustic: Acoustic intensity, I, of a noise wave is the average rate of flow of energy through a unit area normal to the direction of wave propagation (18).

Intensity, Level: Intensity level, IL, of a noise of intensity I is: $IL = \log_{10} (I/I_{ref})$, where IL is in decibels and I_{ref} is a reference intensity (14).

Noise: Noise is an erratic, intermittent, or statistically random oscillation (14).

1/3 Octave: Commonly used to define the characteristics of an analyzer. The nominal mean frequencies for third-octave bands is $f_m = 10^{3n/30}$. The nominal lower band-edge frequency is $f_1 = 2^{-1/6} f_m$. The nominal upper

band-edge frequency is $f_2 = 2^{1/6} f_m$. The bandwidth is $f_2 - f_1 = 0.2316 f_m$. The transmission loss of a 1/3 octave-band filter is usually greater than 30 dB for values of f/f_m of 0.5 and 2.0, where f is a frequency (14) (86).

Periodic: Occurring, appearing, or recurring at regular intervals (43).

Power Level: In decibels, is 10 times the logarithm to the base 10 of the ratio of a given power to a reference power. (For this study, the reference power is 10^{-12} watts.) (14).

Pressure Level: The pressure level, in decibels, is 20 times the logarithm to the base 10 of the ratio of the measured pressure to the reference pressure. (For this study the reference pressure is 20 N/m^2) (Unless otherwise explicitly stated, it is to be understood that the noise pressure is the effective (rms) pressure.) (14).

Rated Flow: The expected flow from a high pressure pump operating at a specified speed under ideal conditions with a low outlet pressure.

Signature: An identifying characteristic (43).

Signature Analysis: The examination of the identifying characteristic parameters of a system. Used to detect pathological cases and predict incipient failure. In the area of acoustics the analysis is conducted on noise spectra (6) (23).

Sinusoidal Periodic Data: Those types of periodic data which can be defined mathematically by a time-varying function of the form $x(t) = X \sin(2\pi f_1 t + \theta)$, where X = amplitude; f_1 = cyclical frequency in cycles per unit time; θ = initial phase angle with respect to the time origin in radians; x(t) = instantaneous value at time t (15).

Solute: The substance dissolved in a solution (47).

Solution: A mixture of two components, a solvent and a solute. The solute is dispersed into molecules or ions, and the distribution of the solute is perfectly homogeneous throughout the solution (47).

Solvent: The dissolving medium in a solution (47).

Sound: Sound is an oscillation in pressure, stress, particle displacement, particle velocity, etc., in a medium with internal forces. Also, sound is an auditory sensation evoked by the oscillation described above.

Spectrum: The spectrum of a function of time is a description of its resolution into components, each of different frequency and (usually) different amplitude and phase (14).

Time Constant: The time required for an exponential system response to reach 63.2 percent of its total change in response to a step input (57).

Vapor: Gaseous form of a substance (43).

Vapor Pressure: The equilibrium pressure, at a specified

temperature, of the liquid's vapor which is in contact with an existing free surface.

APPENDIX B

INSTRUMENTATION

This appendix lists the major items of instrumentation used for the experimental phase of this study, discusses why different bandwidth filters might give different noise levels, and outlines the record-playback procedures for the narrow-band data acquisition technique.

Table XII lists the major items of instrumentation used for this study. Some of the instrumentation is shown in Figure 57.

The intensity measured by a filter of width Δf when exposed to a spectrum that has the same intensity in every 1 Hz band, I_1, is (19):

$$I_{total} = I_1 \Delta f$$

Thus a 10 Hz filter and a 1/3 Octave band filter will not generally measure the same noise level when their input is a flat spectrum. However, if the two filters are exposed to a pure-tone signal whose frequency is fairly close to the center frequency of the 1/3 Octave-Band, the two filters could be expected to yield the same measurement.

During data recording for subsequent narrow-band analysis approximately 2.0 m of data was recorded. 1.1 to 1.2 m

TABLE XII

MAJOR ITEMS OF INSTRUMENTATION USED DURING EXPERIMENTAL STUDY

Item	Part Number	Serial Number	Manufacturer
One-Half Inch Flat-Random Incidence Response Microphone	1962-9601	612 & 152	General Radio
Wave Analyzer	1523-P4	110	General Radio
Level Recorder	1523	124	General Radio
Preamplifier Plug-in	1523-P1	107	General Radio
1/3 Octave-Band Analyzer	1523-P3	101	General Radio
Potentiometer, 50 dB	1523-9622	---	General Radio
Microphone Preamplifier	1560-P42	365	General Radio
Vibration Pick-up System	1560-P13	AY 32 & 3807	General Radio
Acoustic Calibrator	1562-A	3974	General Radio
Sound Level Meter & Octave-Band Analyzer	1933	286	General Radio
Vibration Calibrator	1557-A	1742	General Radio
Calibrated Acoustical Airborne Noise Source	A8501-0322	OSU-1	Ilg & Riverbank Laboratories
Pressure Transducer	118A02	646	PCB Piezotronics Inc.
Pressure Amplifier	402A	1120	PCB Piezotronics Inc.
ICP Power Supply	482A	379	PCB Piezotronics Inc.
Tape Deck	1230	119231	TEAC

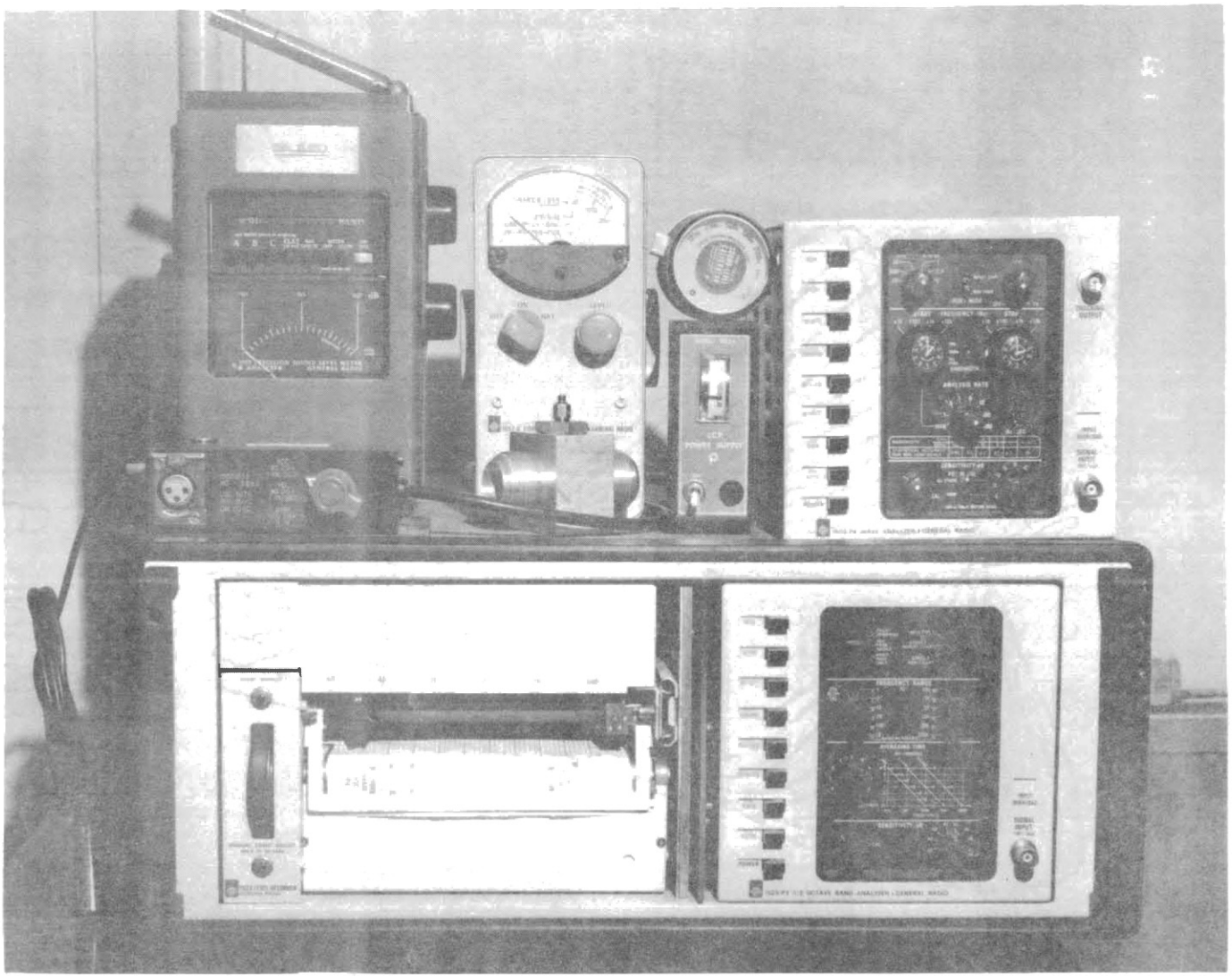

Figure 57. Selected Instrumentation Used for Data Acquisition Showing Level Recorder, 1/3 Octave-Band, and Narrow-Band Plug in Modules

of the data tape was spliced and "played-back" with a "loop" adapter on the tape recorder. The signal from the "loop" was the input for the narrow-band analyzer. The recording and playback procedures are summarized below:

Recording Procedure:

1. Select high-speed (7.5 ips), high bias, left and right record made switches "on".
2. Install acoustical calibrator on microphone, 114.0 dB, 1000 Hz input to right channel, line.
3. Connect voice microphone to left channel.
4. Select "record" mode with drive in "pause". Record light should be illuminated.
5. Set VU-Meter level (for data input) to "0" with calibrator input signal.
6. Record 2.0 m of calibration signal. Simultaneously record calibration I.D. with "voice" on left channel.
7. Leave recorder in "record" mode; remove acoustical calibrator.
8. Operate noise source and record data. Voice identifications should be recorded on the "left" channel. Record 2.0 m of data at each condition of interest.

Playback Procedure:

1. Install calibration tape on recorder and loop adapter, select high-speed mode.

2. Play calibration tape and set VU-Meter level at "0".
3. Calibrate noise level recorder for 114.0 dB, 1000 Hz.
4. Install noise source data tape and plot noise levels on level recorder. Note voice identifications on level plot.

APPENDIX C

TEST SYSTEMS

A schematic of the FPRC Acoustics Laboratory Pump Cavitation Sensitivity Test System is shown in Figure 58. The volume of the air injection chamber is 2.07 liters and the total system volume is approximately 30 liters. The inlet pressure correction because of the location of the inlet pressure gauge is +5.79 kPa. All of the inlet pressure data reported in this study is corrected.

Figure 59 illustrates the drive system for the FPRC Acoustics Laboratory Test System. The air injection chamber, reservoirs, and air injection controls for the FPRC Acoustics Test System are shown in Figure 60. Figure 61 illustrates the fluid conditioning and fluid level control panel that is part of the FPRC Acoustics Laboratory Hydraulic Test System.

The FPRC Pump Contaminant Sensitivity Test Circuit is shown in Figure 62.

Figure 63 illustrates a typical hydraulic pump installed in the FPRC Acoustics Laboratory Reverberant Facility. The figure illustrates how a microphone might be located in the pump's acoustical near-field for noise level measurements. A typical plastic "sight" tube is shown on the inlet of the pump.

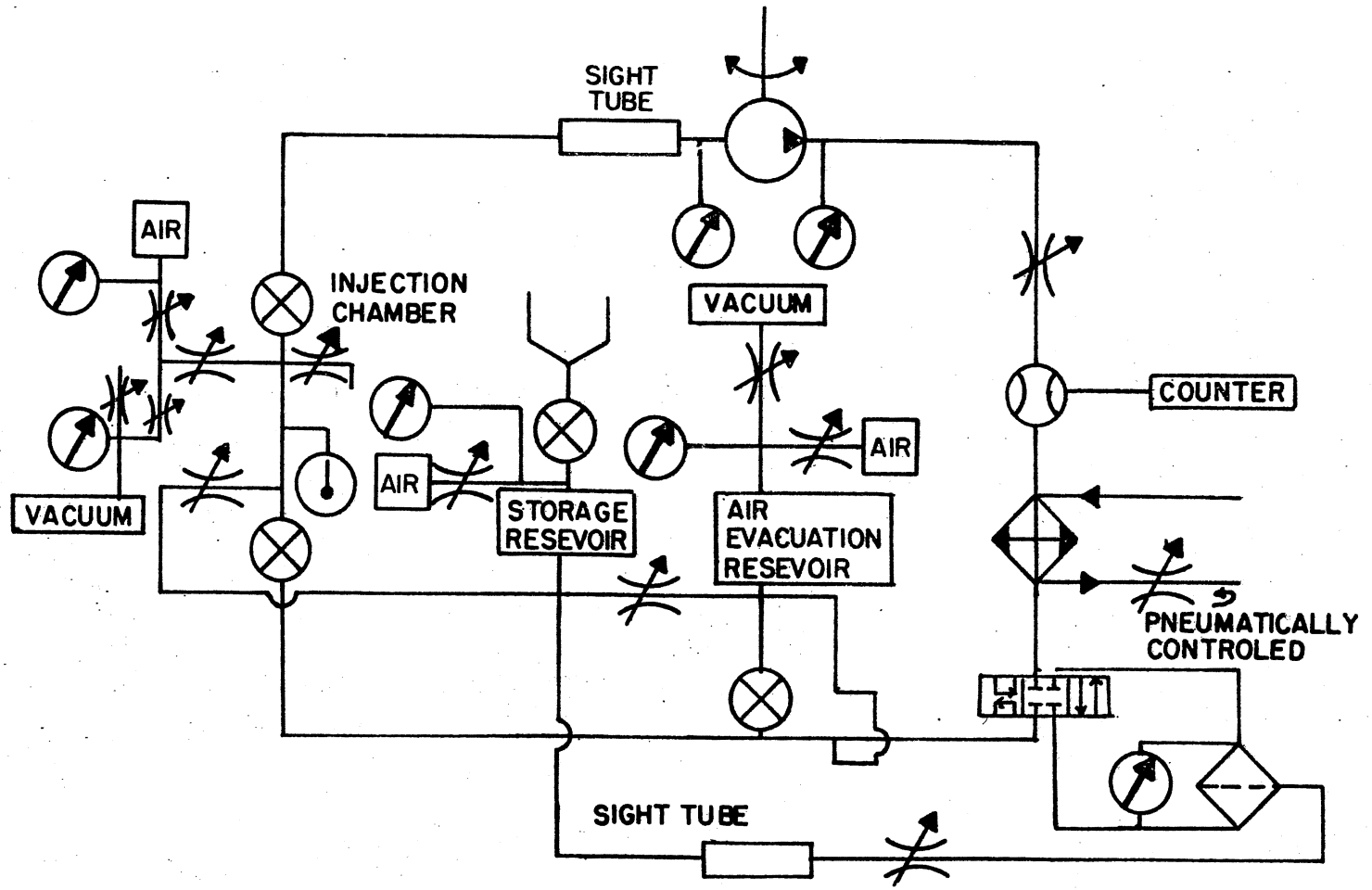

Figure 58. Fluid Power Research Center Acoustics Laboratory Pump Cavitation Sensitivity Test System Schematic

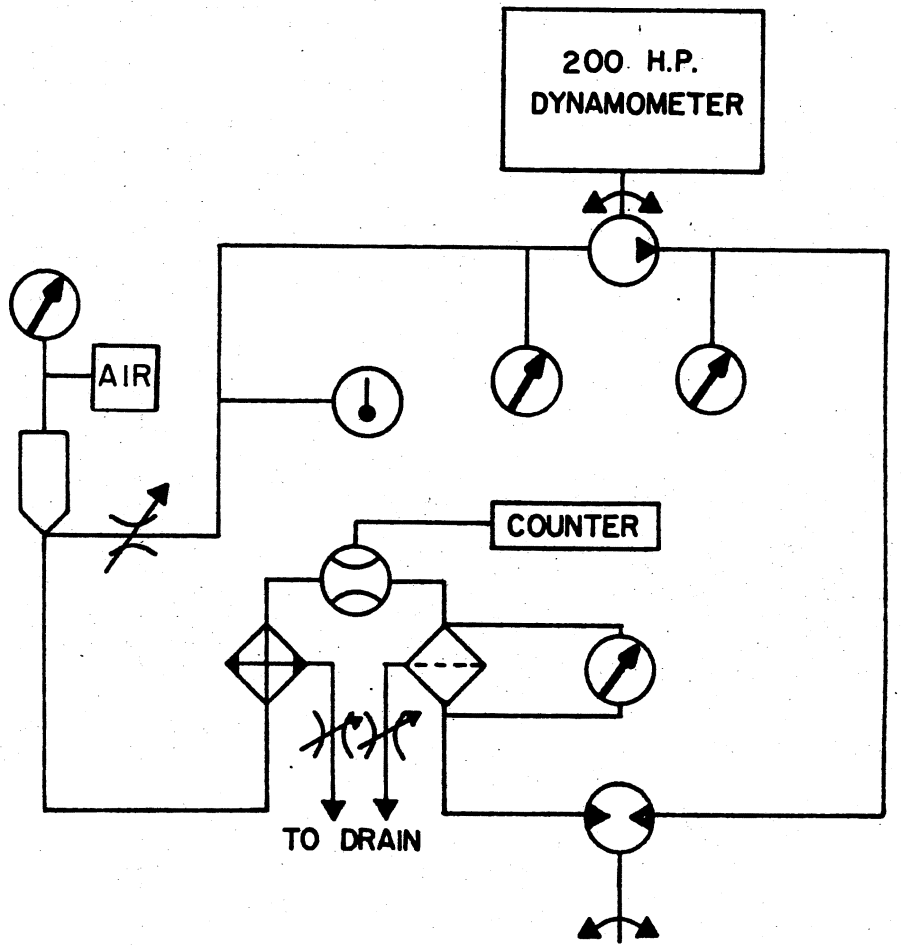

Figure 59. Schematic of Prime System for FPRC Acoustics Laboratory Hydraulic Test System

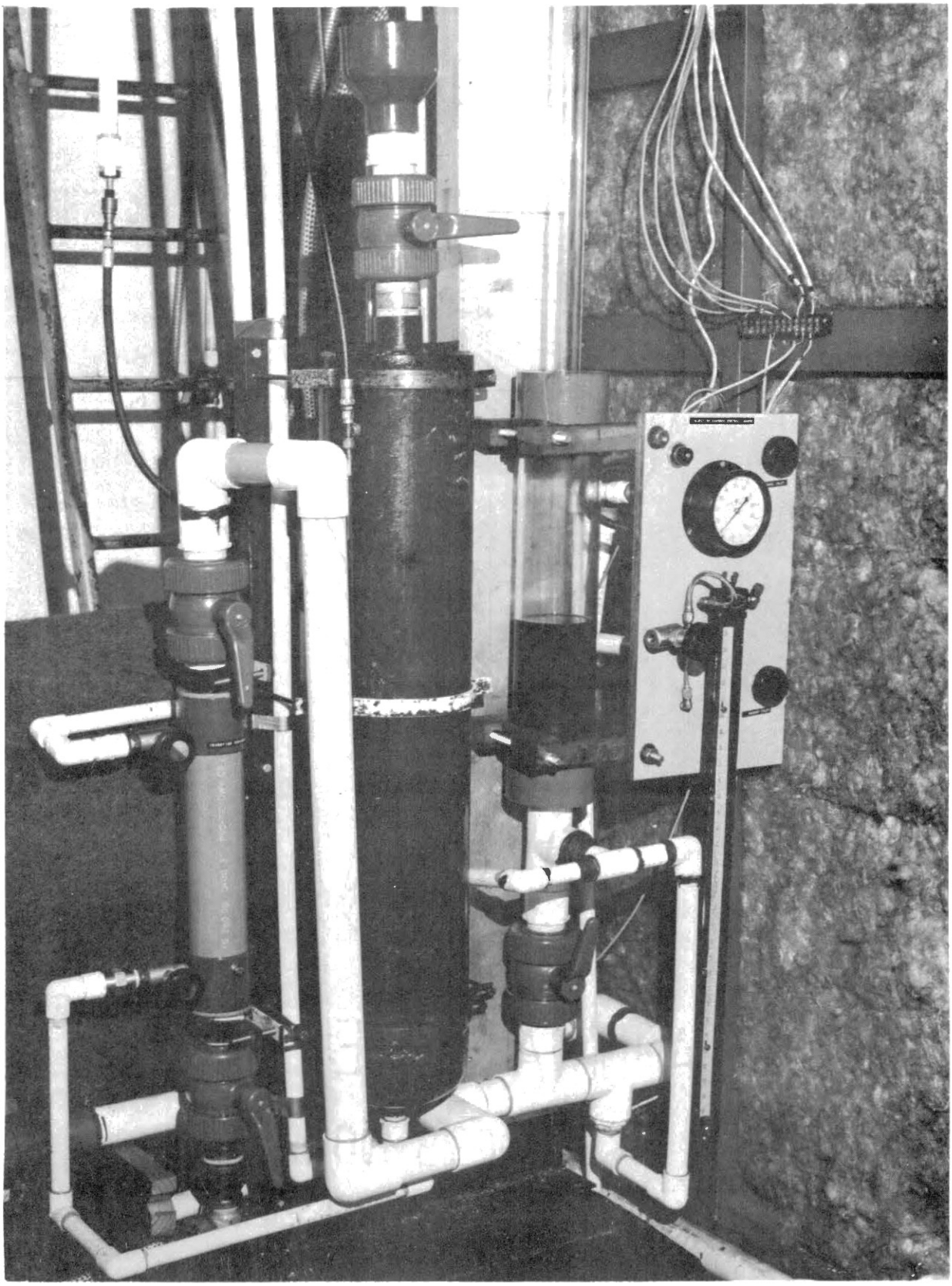

Figure 60. FPRC Acoustics Laboratory Hydraulic Test System Reservoirs and Air Injection Controls

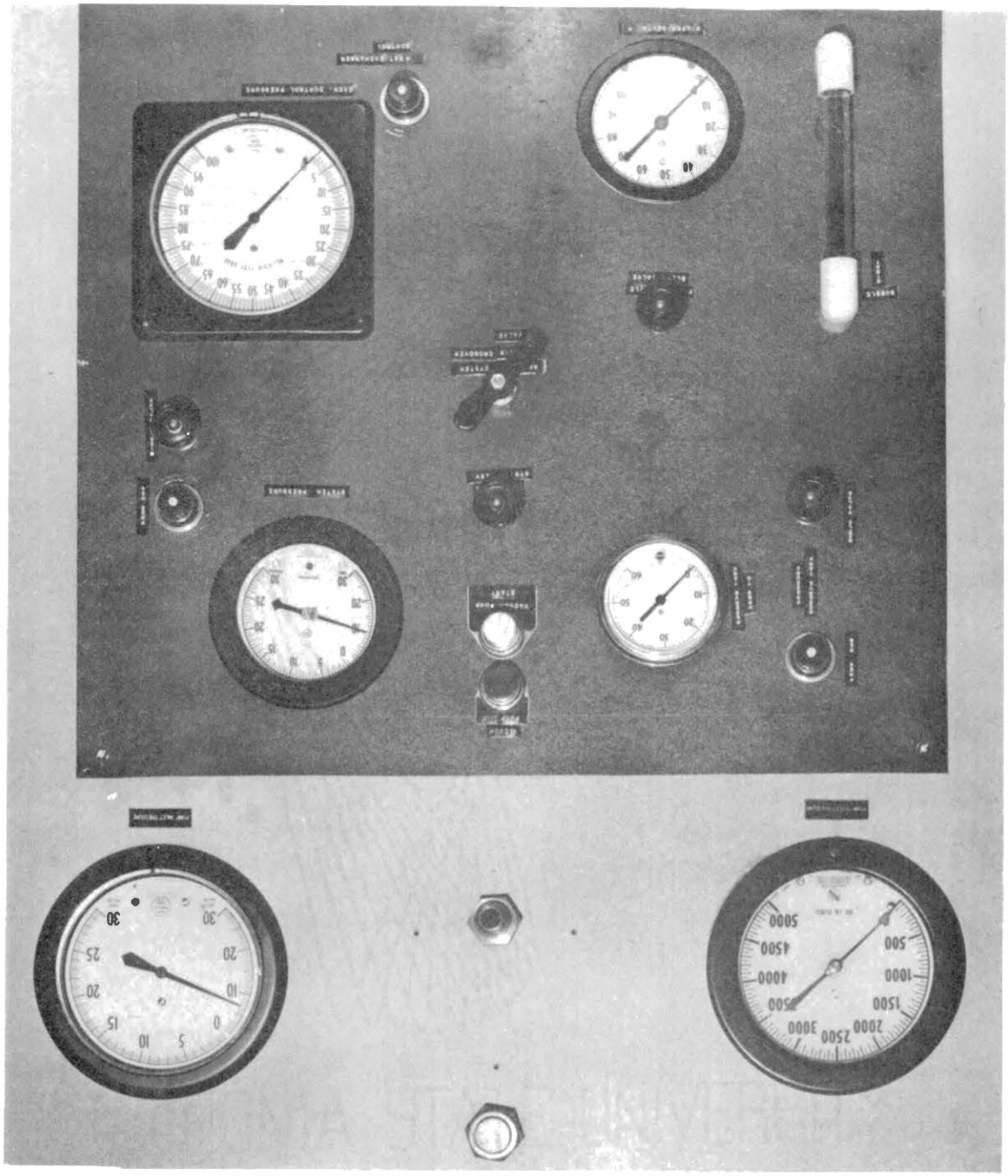

Figure 61. Control Panel for Fluid Conditioning and Fluid Level Control of FPRC Acoustics Laboratory Hydraulic Test System

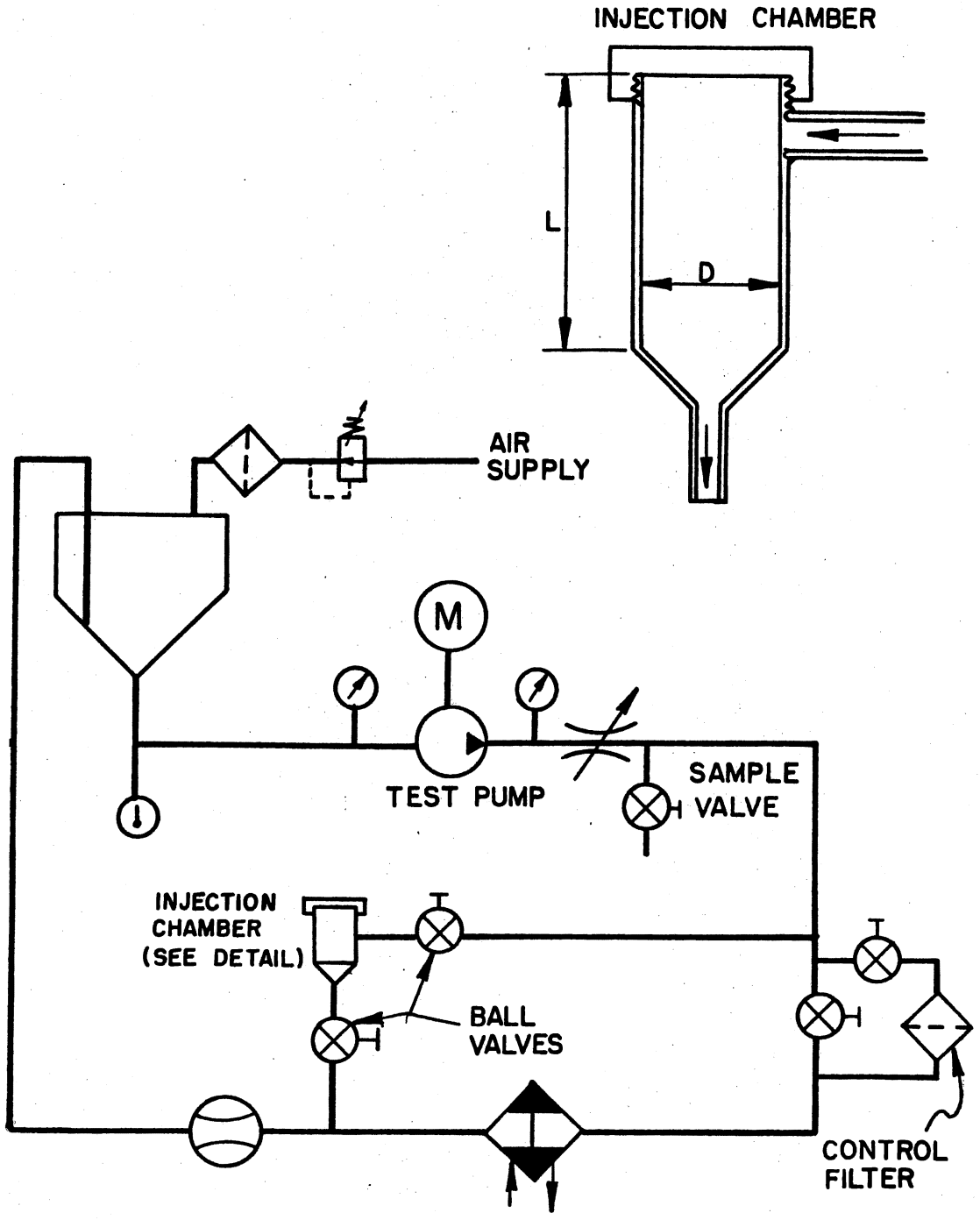

Figure 62. Typical Pump Contaminant Sensitivity Test Circuit (81)

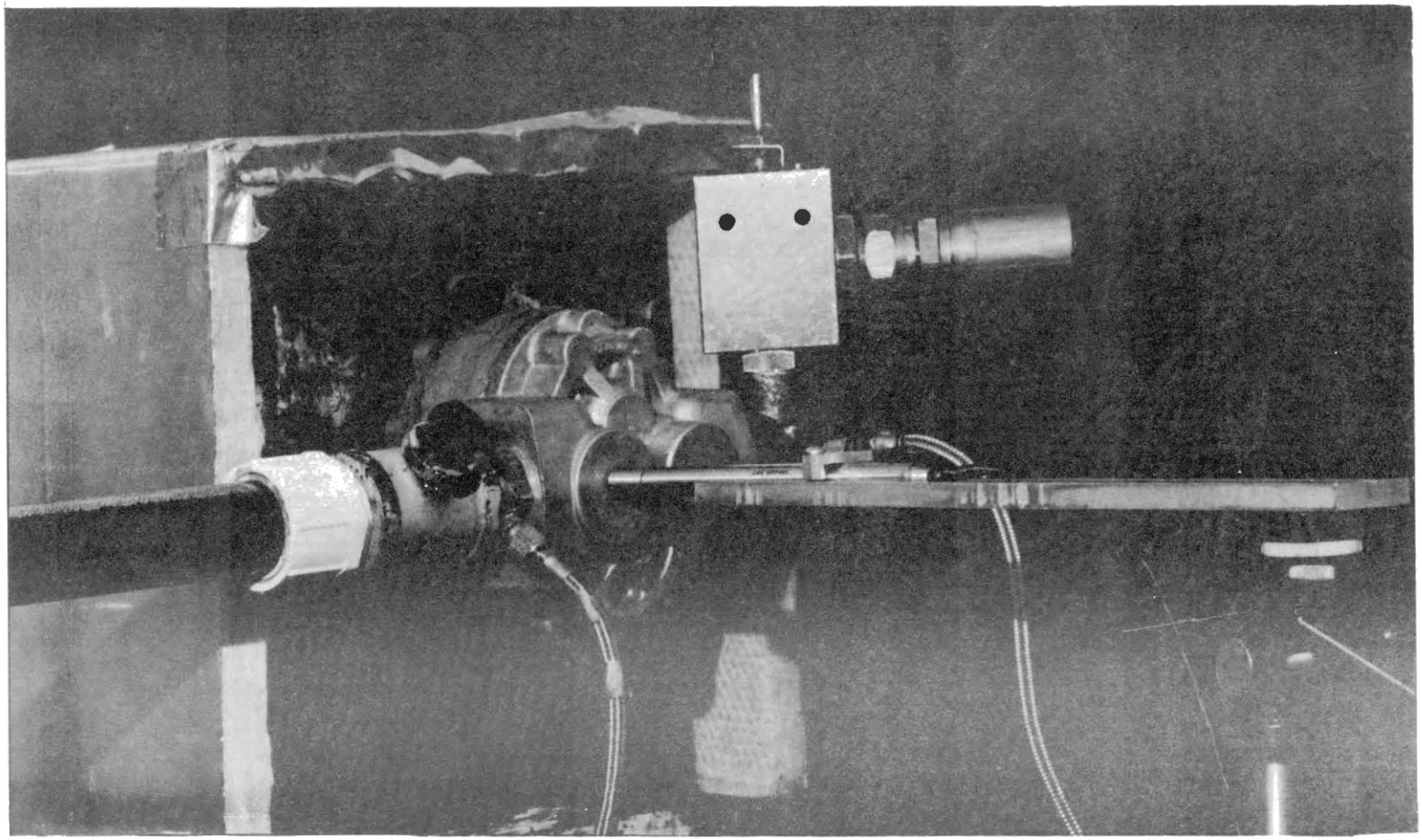

Figure 63. Typical Hydraulic Pump Installation With Inlet Sight Tube and Outlet Load Valve. (Illustration shows how a microphone might be located in the pump's acoustic near-field.)

APPENDIX D

SELECTED EXPERIMENTAL DATA

Figures 64 and 65 illustrate typical narrow-band noise level data. 1/3 Octave-Band data from near-field ABN and SBN tests are shown in Figures 66 through 70. The noise level data includes measurements of "normal" pump noise, pump noise while cavitation was occurring, pump noise when a high contamination level existed in the system fluid, and pump noise during the factorial experiment. Figures 71 and 72 illustrate the general appearance of the inlet fluid for Unit 4327 during selected conditions of speed and A*.

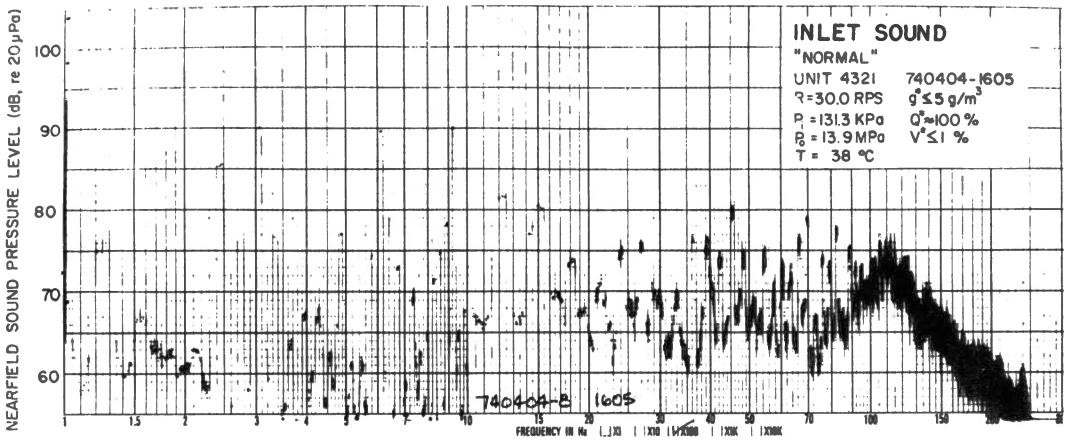

(a) "Normal" Near-Field Inlet Noise Level, Unit 4321

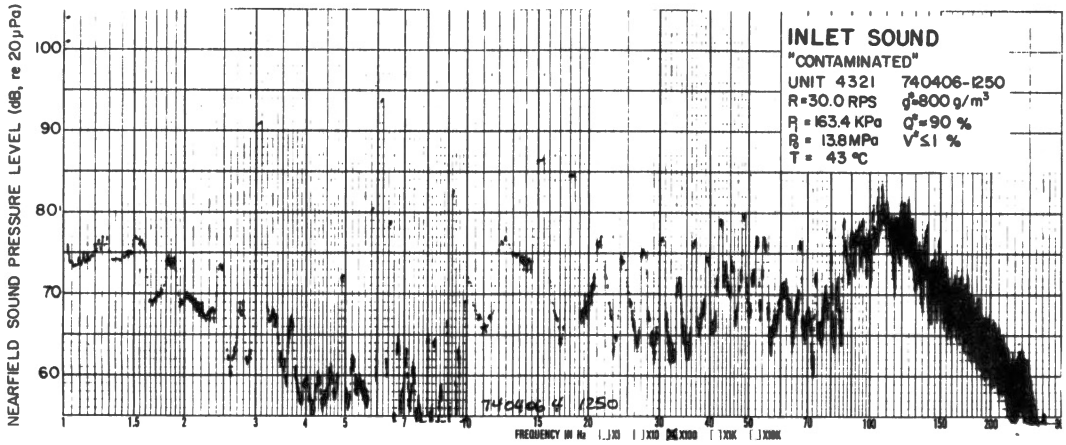

(b) "Contaminated" Near-Field Inlet Noise Level, Unit 4321

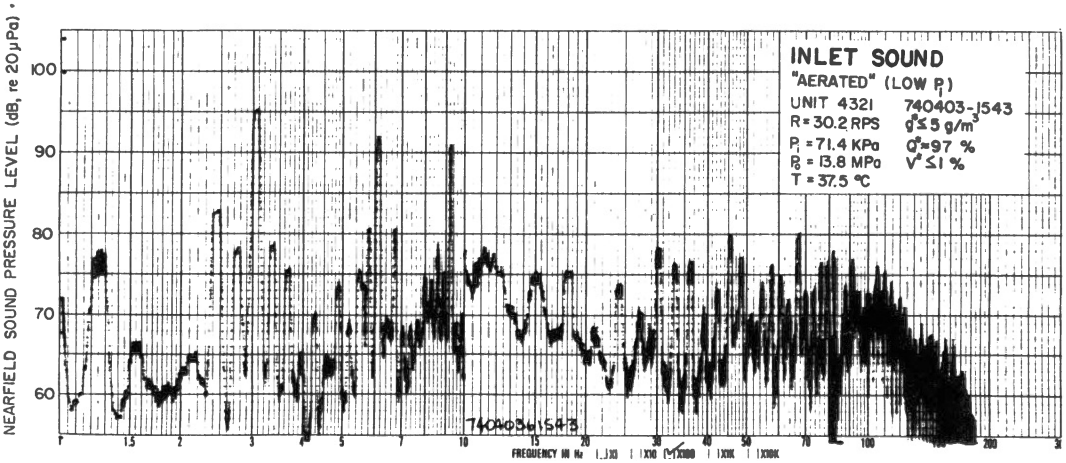

(c) "Aerated" Near-Field Inlet Noise Level, Unit 4321

Figure 64. Narrow-Band Noise Levels, Unit 4321

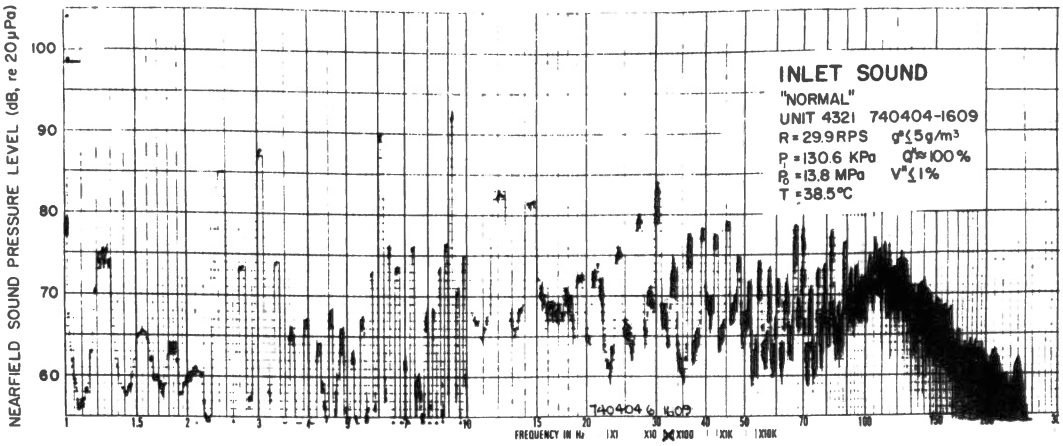

(a) "Normal" Near-Field Noise Level, Unit 4321

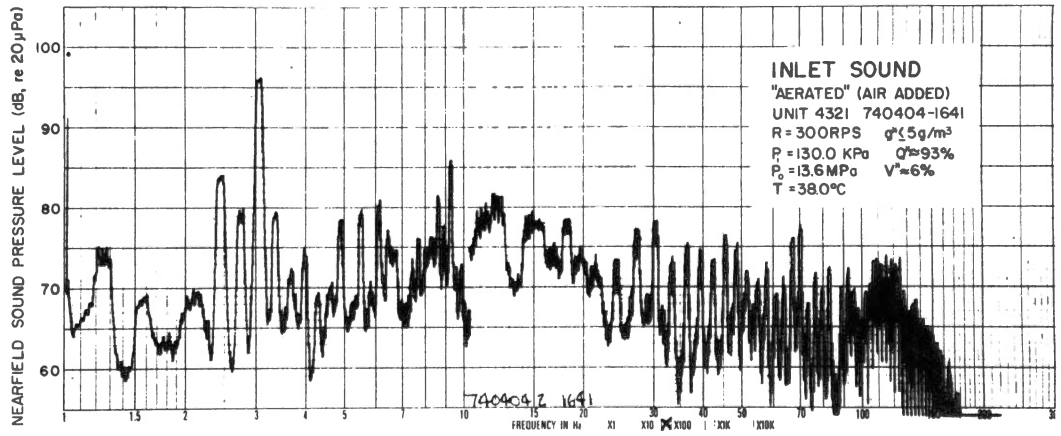

(b) "Aerated" Near-Field Noise Level, Air Added, Unit 4321

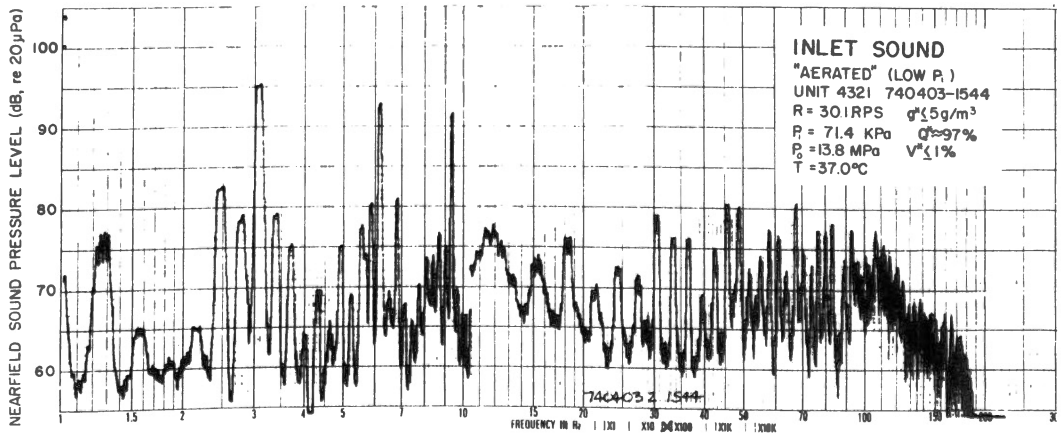

(c) "Aerated" Near Field Noise Level, Low Inlet Pressure, Unit 4321

Figure 65. Narrow-Band Noise Levels, Unit 4321

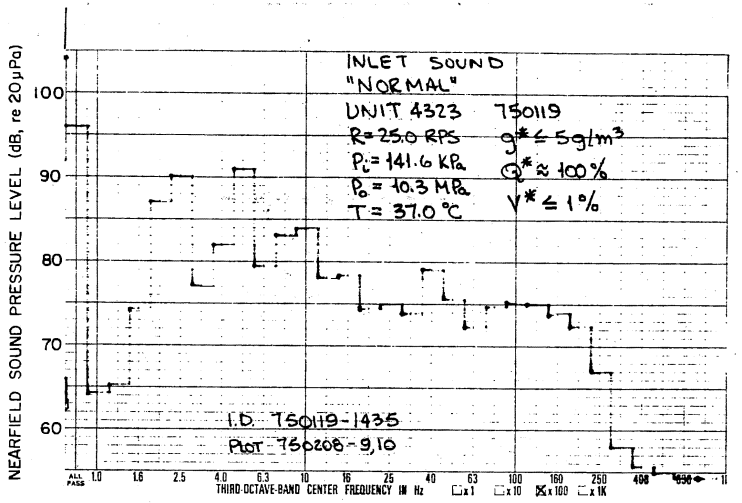

(a) "Normal"

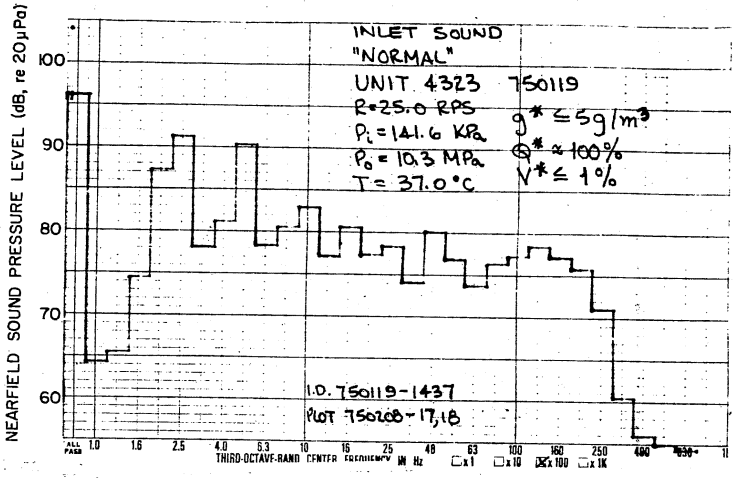

(b) "Normal"

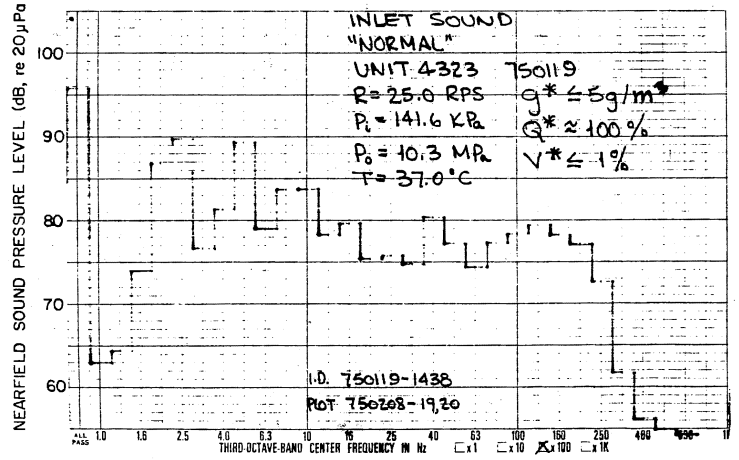

(c) "Normal"

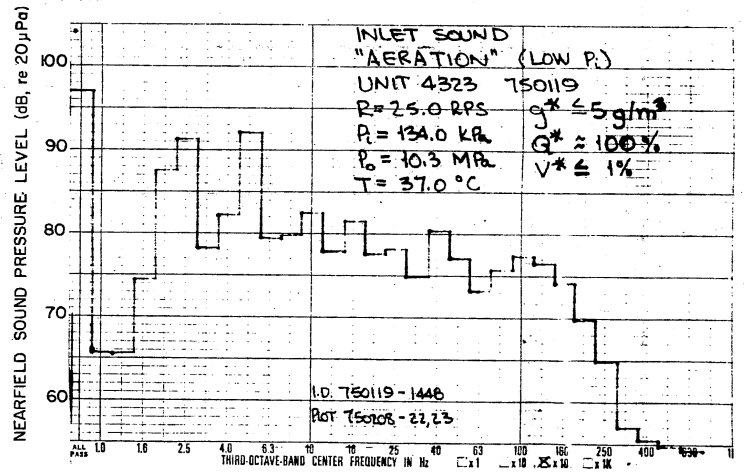

(d) "Aerated"

Figure 66. Third-Octave Noise Levels, Unit 4323

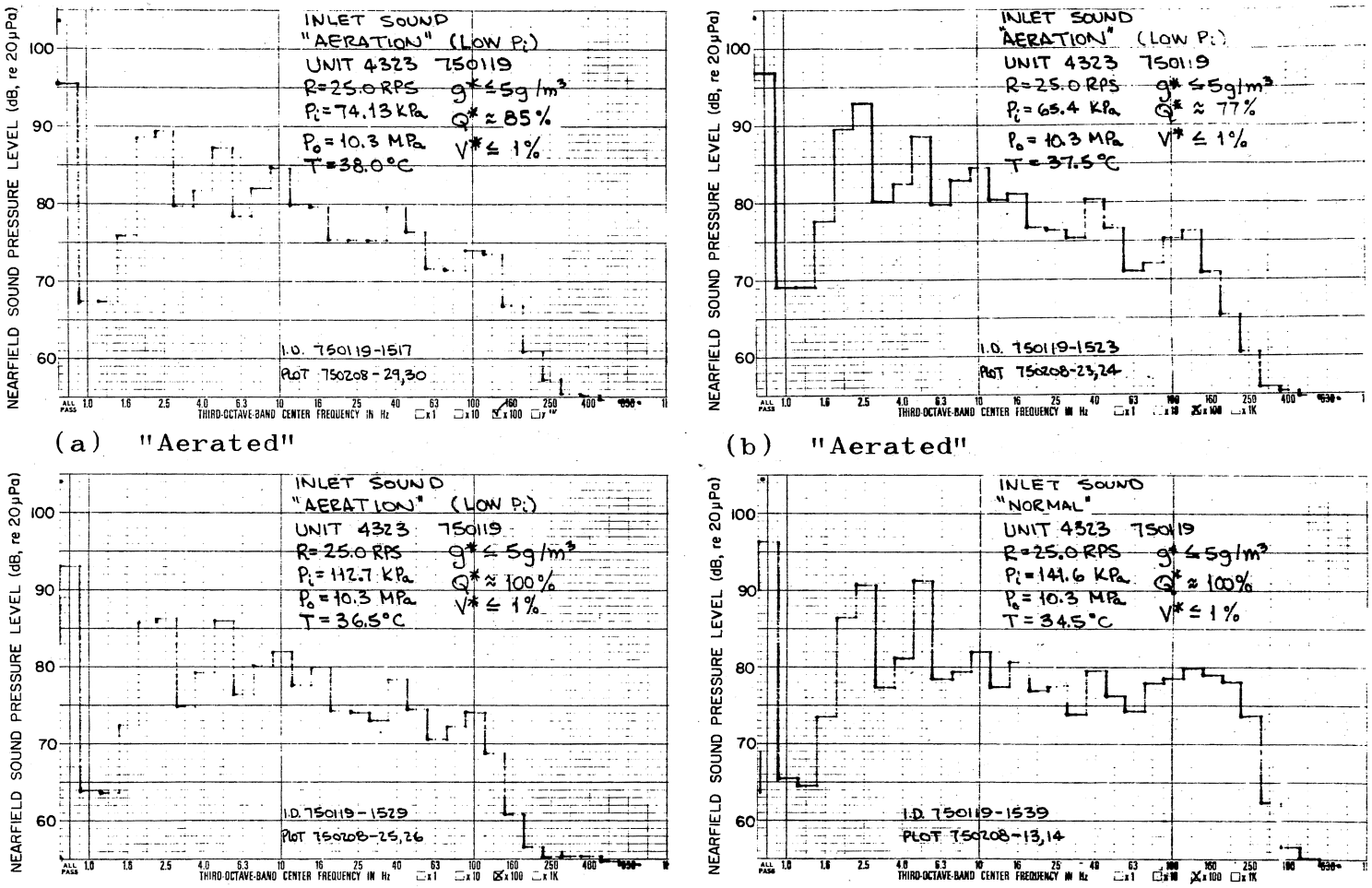

Figure 67. Third-Octave Noise Levels, Unit 4323

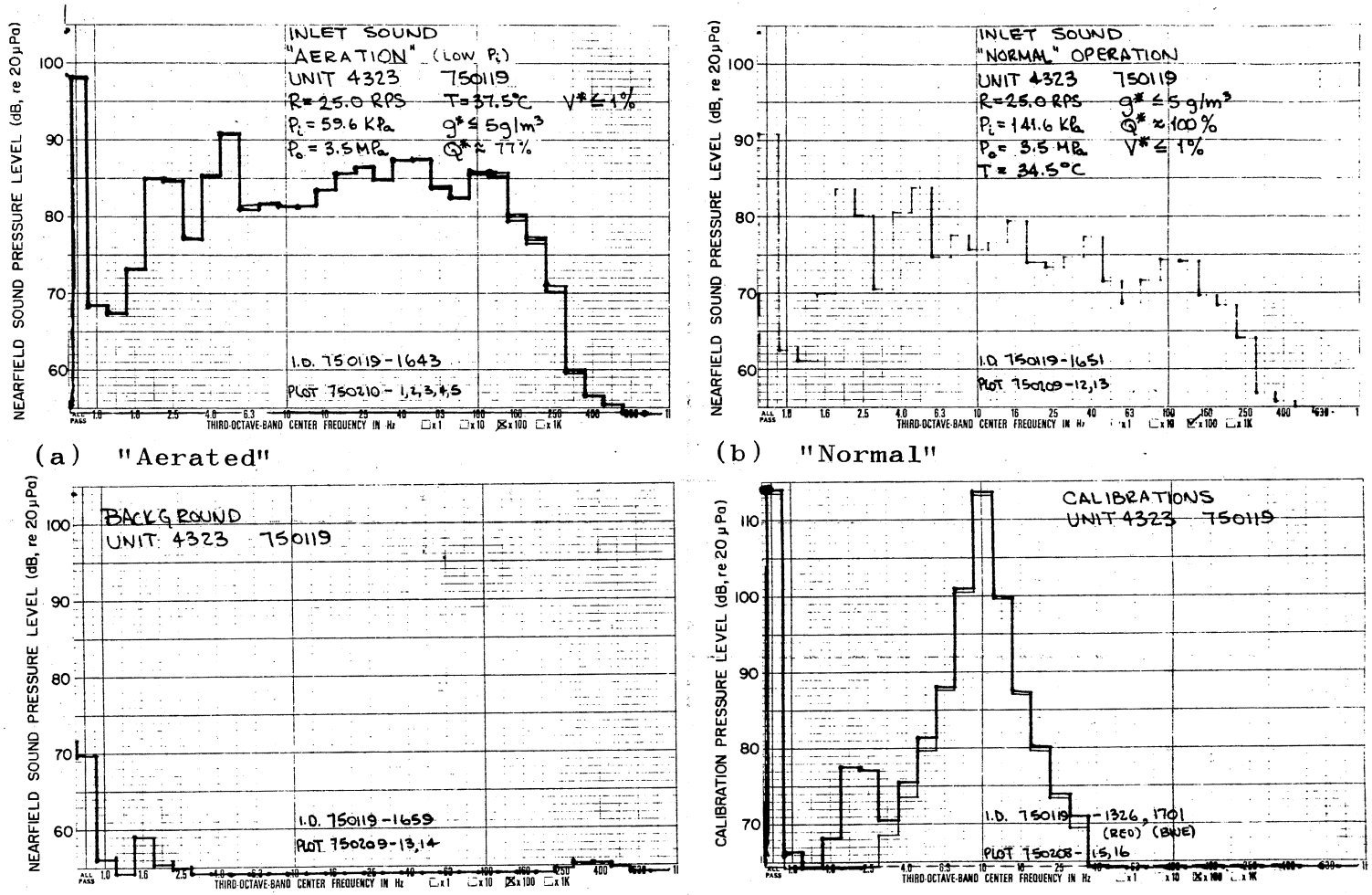

Figure 68. Noise Levels, Background Levels, and Calibrations Associated With Unit 4323

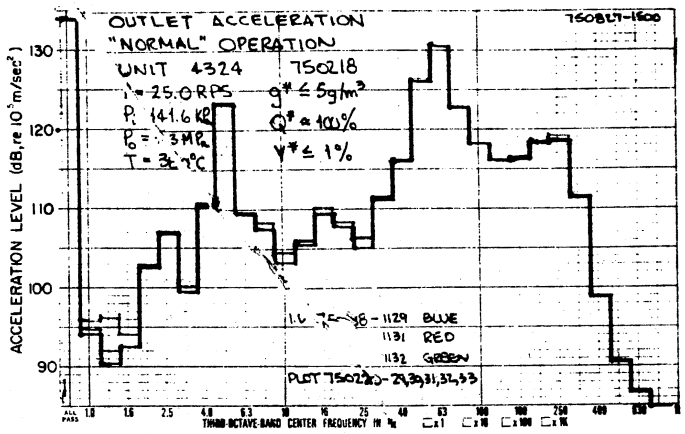

(a) Acceleration

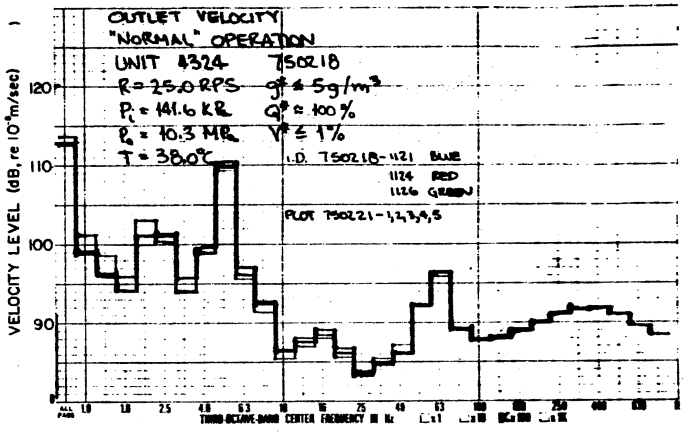

(b) Velocity

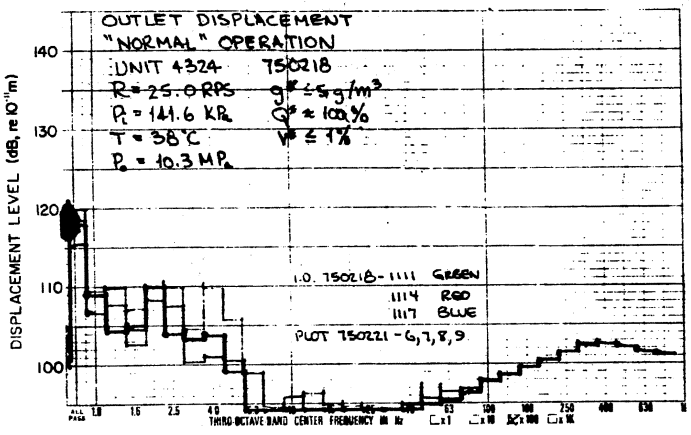

(c) Displacement

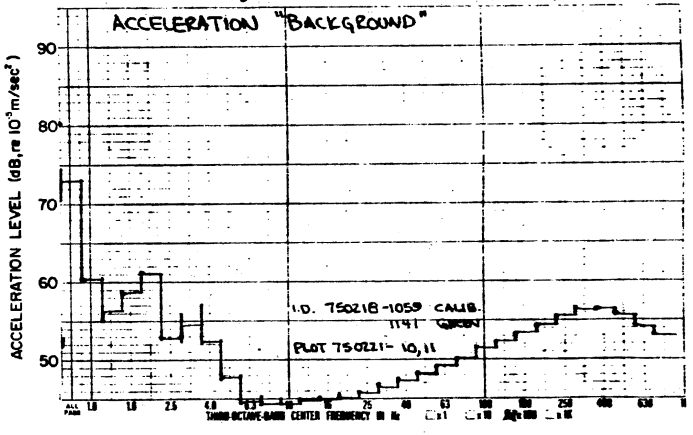

(d) Acceleration Background

Figure 69. Structureborne Noise Levels and Background for Unit 4324

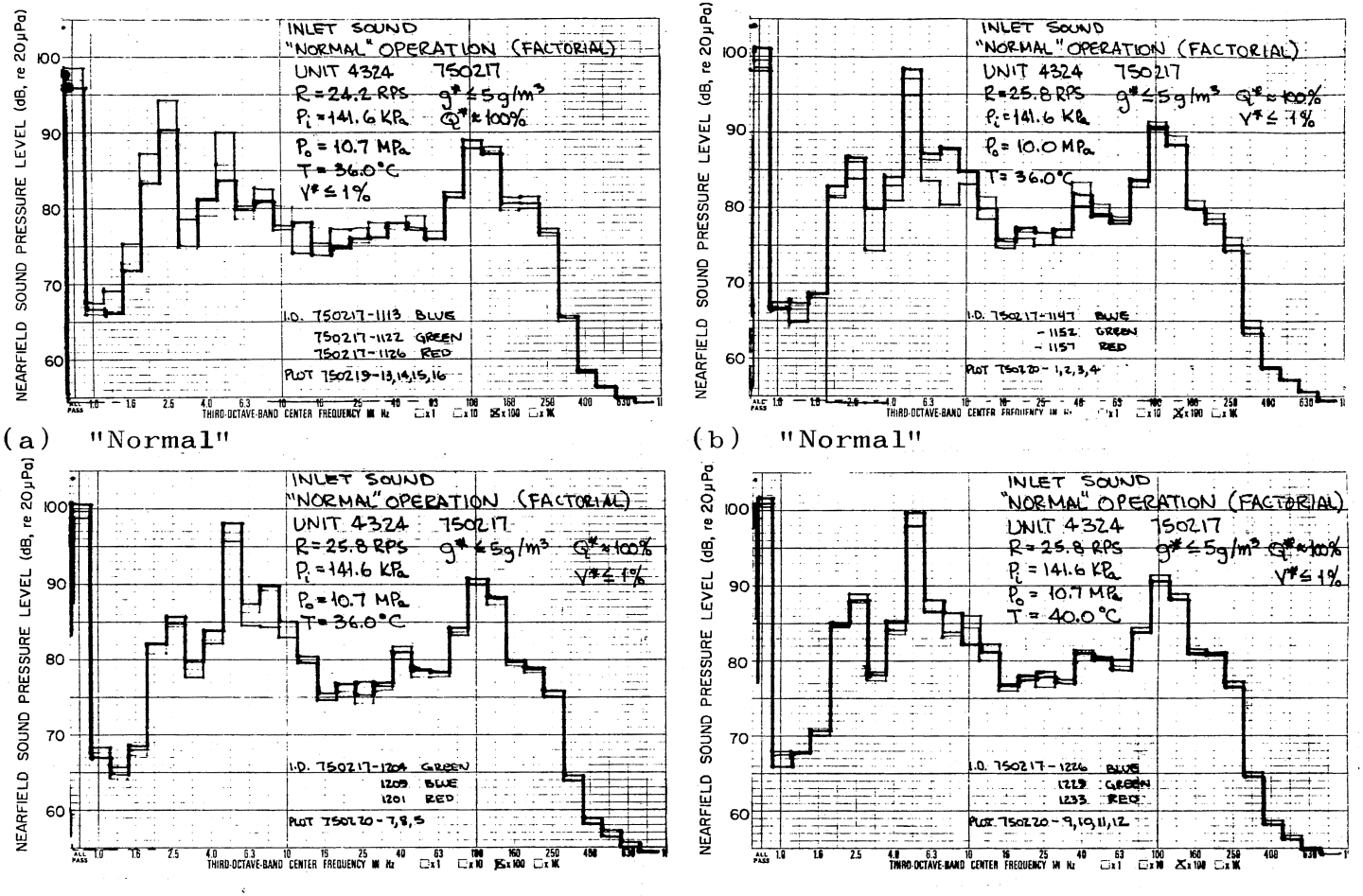

Figure 70. Factorial Test Third-Octave Plots for Unit 4324

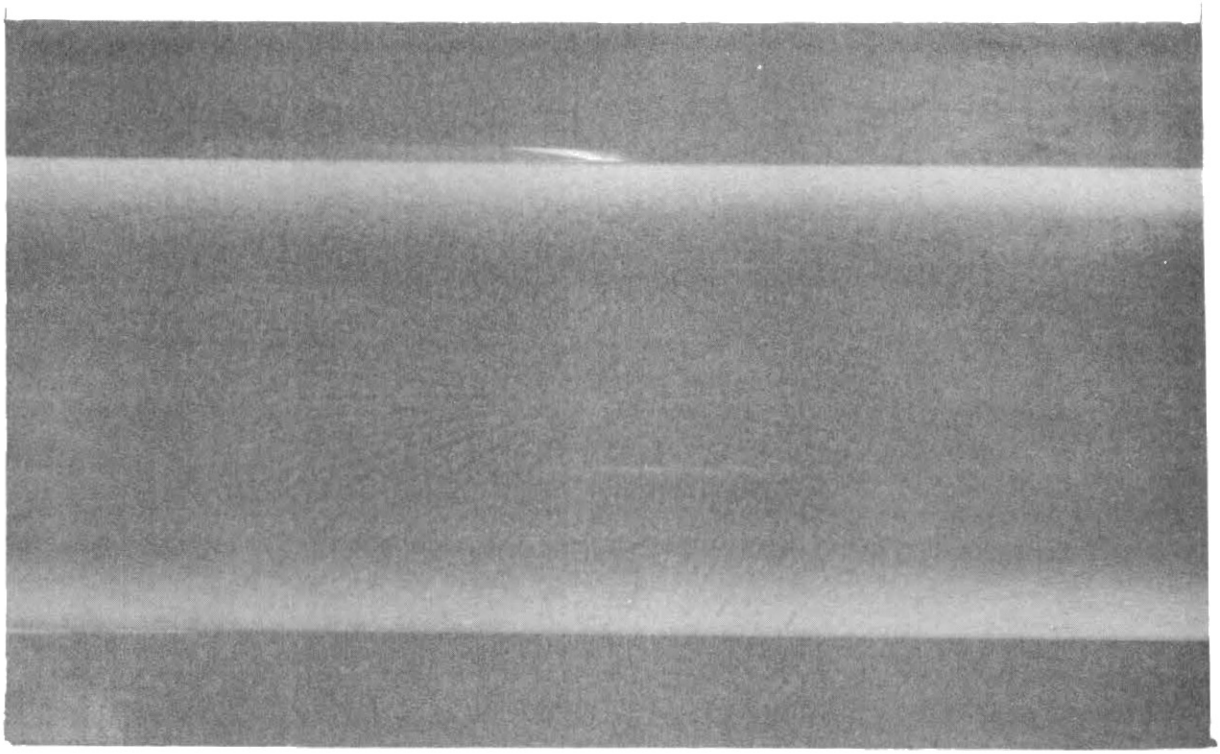

(a) Inlet Pressure, 90 kPa

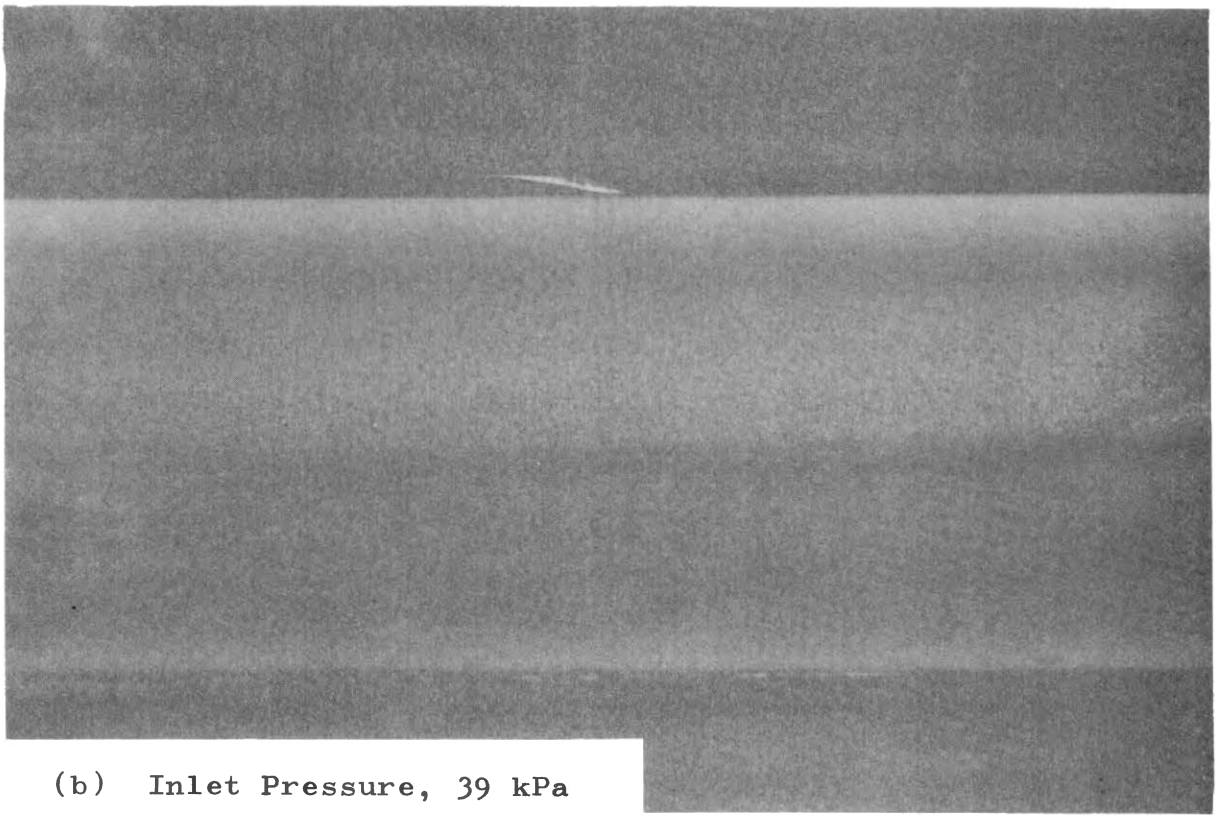

(b) Inlet Pressure, 39 kPa

Figure 71. Low Inlet Velocity Inlet Sight Tube Photos, 22°C, 10 RPS, Unit 4327, A* = 6.5%

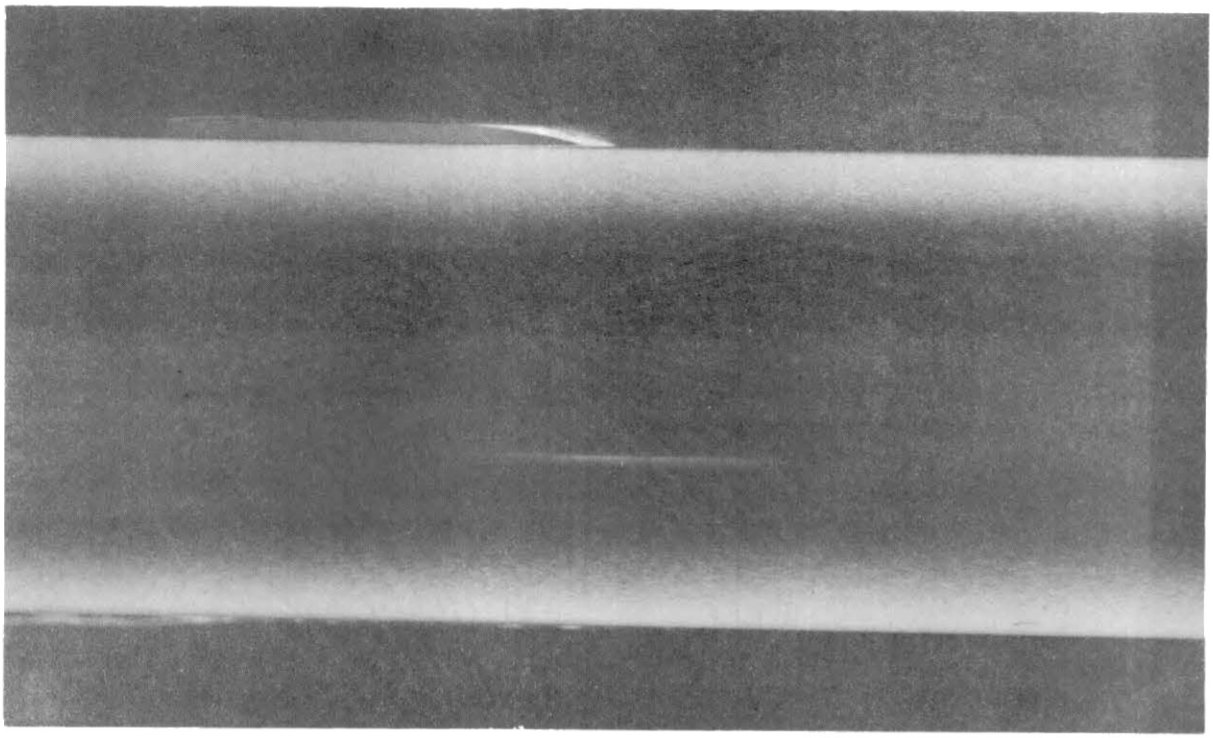

(a) Inlet Pressure, 90 kPa

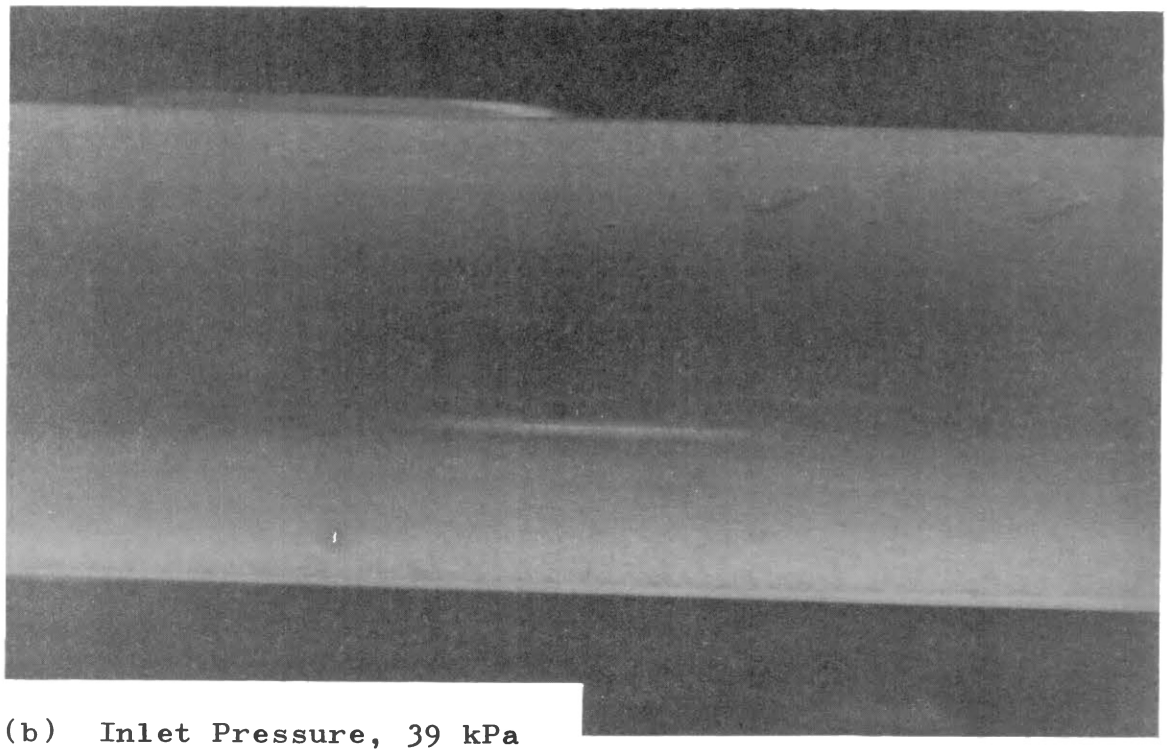

(b) Inlet Pressure, 39 kPa

Figure 72. High Inlet Velocity, Inlet Sight Tube Photos, 22°C, 20 RPS, Unit 4327, A* = 6.5%

APPENDIX E

LINEAR REGRESSION

In statistics the term regression is used to describe the relationship between a variable Y and a variable X (79). Sometimes the variable Y is called the dependent variable and the variable X is called the independent variable. In general it is not appropriate to use the terms dependent and independent in reference to X and Y, since dependency is often assumed to exist, not known to exist. When dependency is established then the relationship is frequently called a function, Y is a function of X. Many of the regression analyses conducted during this study are not, in the strictest sense, linear regressions, but the data was manipulated to form a linear relationship that could be examined using least square methods with a linear equation (34), (35).

Three assumptions are made about the relation between Y and X in standard linear regression (79):

1. Y is drawn at random from a normal distribution at each value of X. More than on Y may be drawn.
2. For each X the population Y has a mean μ that is on the straight line $\mu = \alpha + \beta x$, where α and β are parameters.

3. Each population of Y has a constant standard deviation, about its mean $\mu = \alpha + \beta x$, often denoted by $\sigma_{y.x}$.

The sample correlation coefficient, r, is a "measure of the degree of closeness of the linear relationship between two variables" (79, p. 173). The coefficient of determination, r^2, is the "portion of the variance of Y that can be attributed to its linear regression on X, while $(1 - r^2)$ is the proportion free from X" (79, p. 176).

Snedecor and Cochran also note that (79, p. 177):

> . . . a verdict of statistical significance shows merely that there is a linear relation with non-zero slope. Remember also that convincing evidence of an association, even though close, does not prove that X is the cause of Y. Evidence of causality must come from other sources.

The coefficient of determination does not directly provide the degree of confidence associated with rejecting the hypothesis that a slope b does not exist. The significance of the calculated slope, b, can be obtained using the "t" statistic (79), (90). Given the coefficient of determination and the total number of samples the "t" statistic for the calculations in this study can be determined using (90, p. 311):

$$t = \frac{r\sqrt{n-2}}{\sqrt{1-r^2}} \qquad \text{(E.1)}$$

where:

n = total number of data points

n-2 = degrees of freedom (d.f.)

A set of "t" statistic tables can be used to determine the level of significance of the observed value of the correlation coefficient. The entire procedure of determining the significance of, b, can be simplified by: (1) defining a significance of correlation parameter, in percent, which is one minus the probability of a larger value of t; and (2) plotting the parameter as a function of r and d.f. Figure 73 is a plot of the suggested parameter, "Significance of Correlation", versus r for several degree of freedom values.

A calculator such as the HP-55 (35) provides the slope, b, of the regression equation and the sample standard deviations for x and y, r can readily be obtained with (79, p. 177):

$$r = b \frac{S_x}{S_y} \qquad \text{(E.2)}$$

Given b, S_x, S_y, and the d.f., Equation (E.2) and Figure 74 provide the significance of the correlation for a regression analysis, or the confidence that the calculated slope, b, is a good estimate of β.

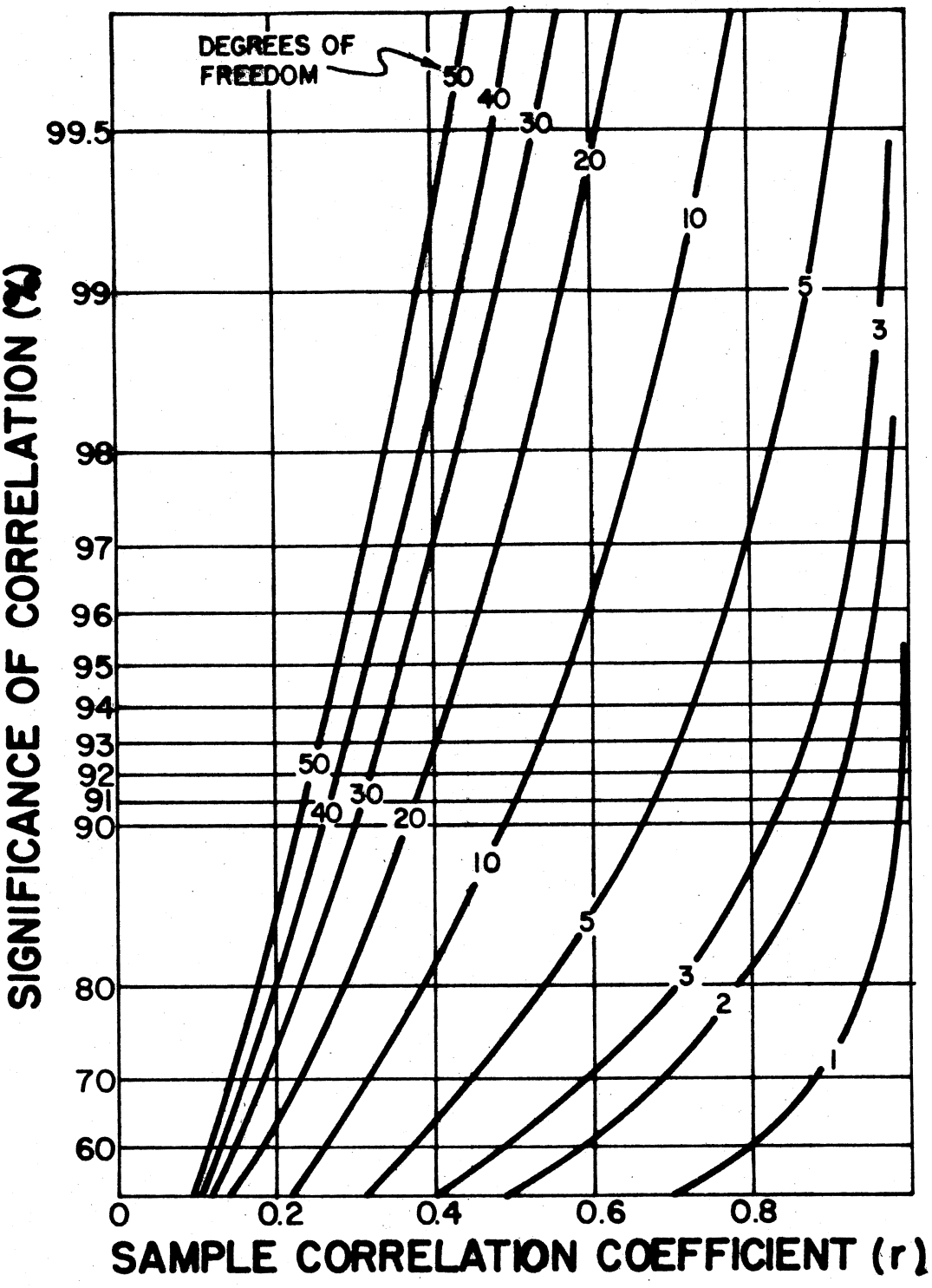

Figure 73. Significance of Correlation as a Function of Sample Correlation Coefficient and Degrees of Freedom. (Assumes sample is normally distributed.)

APPENDIX F

FACTORIAL EXPERIMENTS

The multi-factor (factorial) experiment for this study was conducted and analyzed in accordance with guidance in references (78), (79), (80), and (87). The object of the factorial experiment is to determine (hopefully) if some treatment (factor) has a significant effect on the outcome of an experiment. A null hypothesis is formulated stating that the treatment has no effect and the object is to determine if the data indicates that the hypothesis can be rejected with some pre-selected confidence. The analysis assumes that the data is normally distributed, the populations have equal variances, and the sampling is random in nature (80). Another approach to discussing the factorial experiment is to state that the analysis will test the hypothesis that all of the samples are from the same distribution; that is, the mean of all samples is the same.

Dixon and Massey (80, p. 177) state the following regarding the analysis-of-variance associated with the factorial experiment:

> The procedure outlined for testing hypotheses includes the agreement to say, 'We reject the hypothesis' if a significant result is obtained. In testing for interaction it can be noted that some possible factors causing a significant result are:

1. There is no interaction, but we have obtained a value which we have declared significant. This will occur with a chance equal to the level of significance when there is no interaction in the populations.

2. The two variables are interacting, and we have correctly recognized this fact.

3. An uncontrolled and unmeasured variable may be of sufficient importance to appear as an interaction effect.

4. The items in the subgroups are not randomly drawn.

Snedecor and Cochran (79, p. 346) state that the "presence of an interaction denotes that the effects are not additive."

For the three factor experiment conducted for this study the summations needed for the analysis of variance (AOV) totals are illustrated in Tables XIII and XIV.

TABLE XIII

SUMMARY OF SUMMATIONS NEEDED FOR OBTAINING ANALYSIS OF VARIANCE TOTALS ASSOCIATED WITH VARIABLES 1 AND 3 IN A THREE FACTORIAL EXPERIMENT

V_1	V_2	V_3: V_{31}	V_3: V_{32}	Cell Sums	Row Sums	V_1 Sums
V_{11}	V_{21}	O_{111} ⋮ O_{11n}	O_{121} ⋮ O_{12n}	$\sum_{k=1}^{n} O_{11k}$	$\sum O_{12k}$	$\sum_{i=1}^{2} O_{ixx}$
	V_{22}	O_{211} ⋮ O_{21n}	O_{221} ⋮ O_{22n}	$\sum O_{21k}$	$\sum O_{22k}$	$\sum O_{2xx}$
V_{12}	V_{21}	O_{311} ⋮ O_{31n}	O_{321} ⋮ O_{32n}	$\sum O_{31k}$	$\sum O_{32k}$	$\sum_{i=3}^{4} O_{ixx}$
	V_{22}	O_{411} ⋮ O_{41n}	O_{421} ⋮ O_{42n}	$\sum O_{41k}$	$\sum O_{42k}$	$\sum O_{4xx}$
V_3 Sums	Col. Sums	$\sum_{i=1}^{4} O_{i1x}$	$\sum_{i=1}^{4} O_{i2x}$			G

$$G = \sum_{i=1}^{4} \sum_{j=1}^{2} \sum_{k=1}^{n} O_{ijk} \qquad C = \frac{G^2}{i \cdot j \cdot k}$$

TABLE XIV

SUMMARY OF SUMMATIONS REQUIRED FOR ANALYSIS OF VARIANCE FOR THREE VARIABLE FACTORIAL EXPERIMENT

V_1	V_2	V_3: V_{31}	V_3: V_{32}	Cell Sums		Row Sums	V_1 Sums
V_{11}	V_{21}	Cell 1	Cell 2	$\Sigma 1$	$\Sigma 2$	$\Sigma 1 + \Sigma 2$	$\Sigma 1 + \Sigma 2$
	V_{22}	Cell 3	Cell 4	$\Sigma 3$	$\Sigma 4$	$\Sigma 3 + \Sigma 4$	$\Sigma 3 + \Sigma 4$
V_{12}	V_{21}	Cell 5	Cell 6	$\Sigma 5$	$\Sigma 6$	$\Sigma 5 + \Sigma 6$	$\Sigma 5 + \Sigma 6$
	V_{22}	Cell 7	Cell 8	$\Sigma 7$	$\Sigma 8$	$\Sigma 7 + \Sigma 8$	$\Sigma 7 + \Sigma 8$
V_2 Sums	$\Sigma 1,2,5,6$	$\Sigma 1 + \Sigma 5$	$\Sigma 2 + \Sigma 6$	$\Sigma 1,3$	$\Sigma 2,4$	$V_{1,2}$ Sums	Total Sum of Cells
	$\Sigma 3,4,7,8$	$\Sigma 3 + \Sigma 7$	$\Sigma 4 + \Sigma 8$	$\Sigma 5,7$	$\Sigma 6,8$		
		$V_{2,3}$ Sums					
V_3 Sums	Col. Sums	$\Sigma 1,3,5,7$	$\Sigma 2,4,6,8$	$V_{1,3}$ Sums			G $\Sigma 1,\ldots,8$

$C = \frac{G^2}{n}$, n = total number observations

The equation for the individual observations is (78):

$$Y_{ijk} = \mu + T_i + \beta_j + e_{ijk} \qquad (F.1)$$

where:

Y_{ijk} = observation

μ = average

T_i = effect of treatment

β_j = environmental effects

e_{ijk} = experimental error

Thus, i, is associated with the treatment; j, is associated with the block or cell; and k, is associated with the replication in a block (78). Three replications were taken for each block during the experiment discussed in this study.

The data and summaries for individual frequency band noise levels are shown in Tables XV through XXIV. The summary for the analysis of variance is shown in Table VIII. Although a 95% confidence level was selected for the study, the rejections listed in Table VIII are also valid at the 99% confidence level. The data was tested using the "F" statistic and values for the "F" statistic were taken from tables in reference (79).

TABLE XV

TEST DATA (dB) AND SUMMATIONS FOR ANALYSIS OF VARIANCE OF ALL-PASS SOUND PRESSURE, UNIT 4324, 750217

UNIT 4324		Temperature (°C)		ALL-PASS (dB)			
Speed (RPS)	Press. (MPa)	36	40	Cell Sums		Row Sums	Speed Sums
24.2	10.0	97.2 97.3 98.4	96.7 96.8 97.0	292.9	290.5	583.4	1162.9
	10.7	95.9 96.9 98.5	95.6 96.2 96.4	291.3	288.2	579.5	
25.8	10.0	98.3 99.5 101.2	101.1 101.5 101.7	299.0	304.3	603.3	1205.5
	10.7	98.8 99.7 100.6	100.5 100.9 101.7	299.1	303.1	602.2	
Press. Sums	1186.7	591.9	594.8	584.2	578.7	Speed-Press. Sums	
		Press-Temp Σ					
	1181.7	590.4	591.3	598.1	607.4		
Temp. Sums	Col. Sums	1182.3	1186.1	Speed-Temperature Sums			G 2368.4

$$C = \frac{G^2}{n} = 233721.6$$

TABLE XVI

SUMMARY OF ANALYSIS OF VARIANCE FOR ALL-PASS (dB)
SOUND PRESSURE, UNIT 4324, 750217

Variation Source	Initial Results: Degrees Freedom	Sum of Squares	Mean Square	F Calc.	F-Table (1-15-95)	Reject Null
Temperature	1	0.61	0.61	0.85	4.54	No
Speed	1	75.62	75.62	105.21	4.54	Yes
Pressure	1	1.05	1.05	1.46	4.54	No
Temp.-Speed	1	9.12	9.12	12.69	4.54	Yes
Temp.-Press.	1	0.16	0.16	0.22	4.54	No
Speed-Press.	1	0.32	0.32	0.45	4.54	No
Temp.-Speed-Press.	1	0.02	0.02	0.03	4.54	No
Residual	16	11.5	0.72	/	/	/
TOTAL	23	98.4				

	Pooled Results: Degrees Freedom	Sum of Squares	Mean Square	F Calc.	F-Table (1-20-95)	Reject Null
Temperature	0	0	0	0	4.35	No
Speed	1	75.62	75.62	119.94	4.35	Yes
Pressure	1	1.05	1.05	1.67	4.35	No
Temp.-Speed	1	9.12	9.12	14.46	4.35	Yes
Temp.-Pressure	0	0	0	0	4.35	No
Speed-Pressure	0	0	0	0	4.35	No
Temp.-Speed-Press.	0	0	0	0	4.35	No
Residual	20	12.61	0.63	/	/	/
TOTAL	23	98.4				

TABLE XVII

TEST DATA (dB) AND SUMMATIONS FOR ANALYSIS OF VARIANCE OF 250 HZ SOUND PRESSURE, UNIT 4324, 750217

UNIT 4324		Temperature (°C)		250 HZ (dB)			
Speed (RPS)	Press. (MPa)	36	40	Cell Sums		Row Sums	Speed Sums
24.2	10.0	90.9 91.0 94.9	89.3 89.4 89.8	276.8	268.5	545.3	1084.2
	10.7	90.3 90.3 94.3	87.8 87.9 88.3	274.9	264.0	538.9	
25.8	10.0	83.9 86.2 86.6	87.8 88.0 88.3	256.7	264.1	520.8	1040.4
	10.7	84.3 84.7 85.7	87.8 88.2 88.9	254.7	264.9	519.6	
Press. Sums	1066.1	533.5	532.6	551.7	532.5	Speed-Press. Sums	
		Press-Temp Σ					
	1058.5	529.6	528.9	511.4	529.0		
Temp. Sums	Col. Sums	1063.1	1061.5	Speed-Temperature Sums			G 2124.6

$$C = \frac{G^2}{n} = 188080.22$$

TABLE XVIII

SUMMARY OF ANALYSIS OF VARIANCE FOR 250 HZ (dB)
SOUND PRESSURE, UNIT 4324, 750217

Variation Source	Initial Results: Degrees Freedom	Sum of Squares	Mean Square	F Calc.	F-Table (1-15-95)	Reject Null
Temperature	1	0.10	0.10	0.06	4.54	No
Speed	1	79.93	79.93	46.75	4.54	Yes
Pressure	1	2.40	2.40	1.41	4.54	No
Temp.-Speed	1	56.43	56.43	32.99	4.54	Yes
Temp.-Press.	1	0.0	0.0	0.0	4.54	No
Speed-Press.	1	1.13	1.13	0.65	4.54	No
Temp.-Speed-Press.	1	1.22	1.22	0.71	4.54	No
Residual	16	27.40	1.71	/	/	/
TOTAL	23	168.61				

	Pooled Results: Degrees Freedom	Sum of Squares	Mean Square	F Calc.	F-Table (1-20.95)	Reject Null
Temperature	0	0	0	0	4.35	No
Speed	1	79.93	79.93	53.58	4.35	Yes
Pressure	1	2.40	2.40	1.62	4.35	No
Temp.-Speed	1	56.43	56.43	37.82	4.35	Yes
Temp.-Press.	0	0.0	0	0	4.35	No
Speed-Press.	0	0	0	0	4.35	No
Temp.-Speed-Press.	0	0	0	0	4.35	No
Residual	20	29.85	1.49	/	/	/
TOTAL	23	168.61				

TABLE XIX

TEST DATA (dB) AND SUMMATIONS FOR ANALYSIS OF VARIANCE OF 500 HZ SOUND PRESSURE, UNIT 4324, 750217

UNIT 4324		Temperature (°C)		500 HZ (dB)			
Speed (RPS)	Press. (MPa)	36	40	Cell Sums		Row Sums	Speed Sums
24.2	10.0	87.2 88.1 89.3	83.8 85.3 86.6	264.6	255.7	520.3	1035.8
	10.7	83.7 85.7 90.0	84.7 84.8 86.6	259.4	256.11	515.5	
25.8	10.0	94.9 97.2 98.3	98.8 99.5 99.7	290.4	298.0	588.4	1174.6
	10.7	95.7 96.8 98.1	97.9 98.0 99.7	290.6	295.6	586.2	
Press. Sums	1108.7	555.0	533.7	524.0	511.8	Speed-Press. Sums	
	Press-Temp Σ						
	1101.7	550.0	551.7	581.0	593.6		
Temp. Sums	Col. Sums	1105.0	1105.4	Speed-Temperature Sums			G 2210.4

$$C = \frac{G^2}{n} = 203577.84$$

TABLE XX

SUMMARY OF ANALYSIS OF VARIANCE FOR
500 HZ (dB) SOUND PRESSURE,
UNIT 4324, 750217

Variation Source	Initial Results: Degrees Freedom	Sum of Squares	Mean Square	F Calc.	F-Table (1-15-95)	Reject Null
Temperature	1	0.01	0.01	0.0	4.54	No
Speed	1	802.73	802.73	330.34	4.54	Yes
Pressure	1	2.04	2.04	0.8	4.54	No
Temp.-Speed	1	23.58	23.58	9.7	4.54	Yes
Temp.-Press.	1	0.37	0.37	.01	4.54	No
Speed-Press.	1	0.28	0.28	.01	4.54	No
Temp.-Speed-Press.	1	6.56	6.56	2.70	4.54	No
Residual	16	38.85	2.43	/	/	/
TOTAL	23	874.42				

	Pooled Results: Degrees Freedom	Sum of Squares	Mean Square	F Calc.	F-Table (1-20-95)	Reject Null
Temperature	0	0	0	0	4.35	No
Speed	1	802.73	802.73	385.93	4.35	Yes
Pressure	0	0	0	0	4.35	No
Temp.-Speed	1	23.58	23.58	11.62	4.35	Yes
Temp.-Pressure	0	0	0	0	4.35	No
Speed-Pressure	0	0	0	0	4.35	No
Temp.-Speed-Press.	1	6.56	6.56	3.23	4.35	No
Residual	20	41.55	2.08	/	/	/
TOTAL	23	874.42				

TABLE XXI

TEST DATA (dB) AND SUMMATIONS FOR ANALYSIS OF VARIANCE OF 10K HZ SOUND PRESSURE, UNIT 4324, 750217

UNIT 4324		Temperature (°C)		10 K HZ (dB)			
Speed (RPS)	Press. (MPa)	36	40	Cell Sums		Row Sums	Speed Sums
24.2	10.0	88.7 89.3 89.3	89.9 90.3 90.2	267.3	270.4	537.7	1070.7
	10.7	87.9 88.9 89.0	88.8 89.2 89.2	265.8	267.2	533.0	
25.8	10.0	90.3 90.7 91.3	90.6 90.7 90.8	272.3	272.1	544.4	1087.6
	10.7	89.9 90.1 90.7	90.5 90.6 91.4	270.7	272.5	543.2	
Press. Sums	1082.1	539.6	542.5	533.1	537.6	Speed-Press. Sums	
		Press-Temp Σ					
	1076.2	536.5	539.7	543.0	544.6		
Temp. Sums	Col. Sums	1076.1	1082.2	Speed-Temperature Sums			G 2158.3

$$C = \frac{G^2}{n} = 194094.12$$

TABLE XXII

SUMMARY OF ANALYSIS OF VARIANCE FOR 10K HZ (dB)
SOUND PRESSURE, UNIT 4324, 750217

Variation Source	Initial Results: Degrees Freedom	Sum of Squares	Mean Square	F Calc.	F-Table (1-15-95)	Reject Null
Temperature	1	1.55	1.55	9.8	4.54	Yes
Speed	1	11.9	11.9	75.1	4.54	Yes
Pressure	1	1.45	1.45	9.16	4.54	Yes
Temp.-Speed	1	0.35	0.35	2.2	4.54	No
Temp.-Press.	1	0.005	0.005	.03	4.54	No
Speed-Press.	1	0.511	0.511	3.23	4.54	No
Temp.-Speed-Press.	1	0.57	0.57	3.6	4.54	No
Residual	16	2.534	0.158	≠	≠	≠
TOTAL	23	18.87				

	Pooled: Degrees Freedom	Sum of Squares	Mean Square	F Calc.	F-Table (1-17-95)	Reject Null
Temperature	1	1.55	1.55	10.38	4.54	Yes
Speed	1	11.9	11.9	79.7	4.54	Yes
Pressure	1	1.45	1.45	9.71	4.54	Yes
Temp.-Speed	1	0.35	0.35	2.34	4.54	No
Temp.-Pressure	0	0	0	0	4.54	No
Speed-Pressure	1	0.511	0.511	3.421	4.54	No
Temp.-Speed-Press.	1	0.57	0.57	3.82	4.54	No
Residual	17	2.539	0.149	≠	≠	≠
TOTAL	23	18.87				

TABLE XXIII

TEST DATA (dB) AND SUMMATIONS FOR ANALYSIS OF VARIANCE OF 20K HZ SOUND PRESSURE, UNIT 4324, 750217

UNIT 4324		Temperature (°C)		20K HZ (dB)			
Speed (RPS)	Press. (MPa)	36	40	Cell Sums		Row Sums	Speed Sums
24.2	10.0	80.5 81.3 82 3	81.0 82.0 83.3	244.1	246.3	490.4	976.9
	10.7	79.9 80.6 81.5	80.3 81.9 82.3	242.0	244.5	486.5	
25.8	10.0	77.9 78.5 79.3	79.9 80.3 80.5	235.7	240.7	476.4	955.1
	10.7	78.3 78.7 78.9	80.7 81.0 81.1	235.9	242.8	478.7	
Press. Sums	966.8	479.8	487.0	486.1	490.8		
		Press-Temp Σ					
	965.2	477.9	487.3	471.6	483.5		
Temp. Sums	Col. Sums	957.7	974.3	Speed-Temperature Sums			G 1932.0

$$C = \frac{G^2}{n} = 155526.00$$

TABLE XXIV

SUMMARY OF ANALYSIS OF VARIANCE FOR 20K HZ (dB)
SOUND PRESSURE, UNIT 4324, 750217

Variation Source	Initial Results Degrees Freedom	Sum of Squares	Mean Square	F Calc.	F-Table (1-15-95)	Reject Null
Temperature	1	11.48	11.48	19.84	4.54	Yes
Speed	1	19.80	19.80	34.21	4.54	Yes
Pressure	1	0.11	0.11	0.19	4.54	No
Temp.-Speed	1	2.16	2.16	3.73	4.54	No
Temp.-Press.	1	0.2	0.2	0.35	4.54	No
Speed-Press.	1	1.6	1.6	2.76	4.54	No
Temp.-Speed-Press.	1	0.11	0.11	0.19	4.54	No
Residual	16	9.26	0.58	/	/	/
TOTAL	23	44.72				

	Pooled Results Degrees Freedom	Sum of Squares	Mean Square	F Calc.	F-Table (1-20-95)	Reject Null
Temperature	1	11.48	11.48	22.51	4.35	Yes
Speed	1	19.80	19.80	38.82	4.35	Yes
Pressure	0	0	0	0	4.35	No
Temp.-Speed	1	2.16	2.16	4.24	4.35	No
Temp.-Pressure	0	0	0	0	4.35	No
Speed-Pressure	1	1.6	1.6	3.14	4.35	No
Temp.-Speed-Press.	0	0	0	0	4.35	No
Residual	19	9.68	0.51	/	/	/
TOTAL	23	44.72				

APPENDIX G

FLUID PROPERTIES

This appendix contains important fluid properties that were referenced in the discussions and used during the experimental studies. Tables XXV and XXVI contain typical properties of hydraulic oils and vapor pressures for water, respectively. Figure 74 gives the viscosity of the test liquid, MIL-L-2104. Figure 75 provides information about the air/liquid solution volume ratio of hydraulic oil as a function of viscosity.

TABLE XXV

TYPICAL PHYSICAL DATA ON HYDRAULIC FLUIDS (88)

Type Product	MIL-5606 C	Solvent Neutral* Oils		Heavy Duty Industrial Hydraulic Oil
Vapor Press, mm Hg				
at 100 F	0.17	-	-	<0.001
160 F	1.5	-	-	-
200 F	6.4	0.001	0.002	0.001
300 F	59	0.08	0.07	0.05
400 F	-	1.5	1.1	1.0
500 F	-	16	9.0	11.0
Gravity, °API	33.0	30.4	29.3	28.9
Flash, COC, °F	205	420	450	445
Viscosity, SUS at 100 F	75.2	152	340	315
SUS at 210 F	43.5	42.3	54.5	54
cSt at 100 F	14.43	32.4	73.4	68
cSt at 210 F	5.26	4.89	8.60	8.45

*Letter (88) indicated that the viscosity of 10W Motor Oil (MIL-L-2104) would be slightly higher than the lighter of the solvent neutral oils. Estimated 10W oil as 185 SUS at 100°F.

TABLE XXVI

VAPOR PRESSURE OF WATER AT VARIOUS TEMPERATURES (89)

Temperature		Vapor Pressure	
°F	°C	mmHg	kPa
70	21.1	18.7	2.5
100	37.8	49.2	6.6
150	65.6	192.6	25.6
200	93.3	595.0	79.2

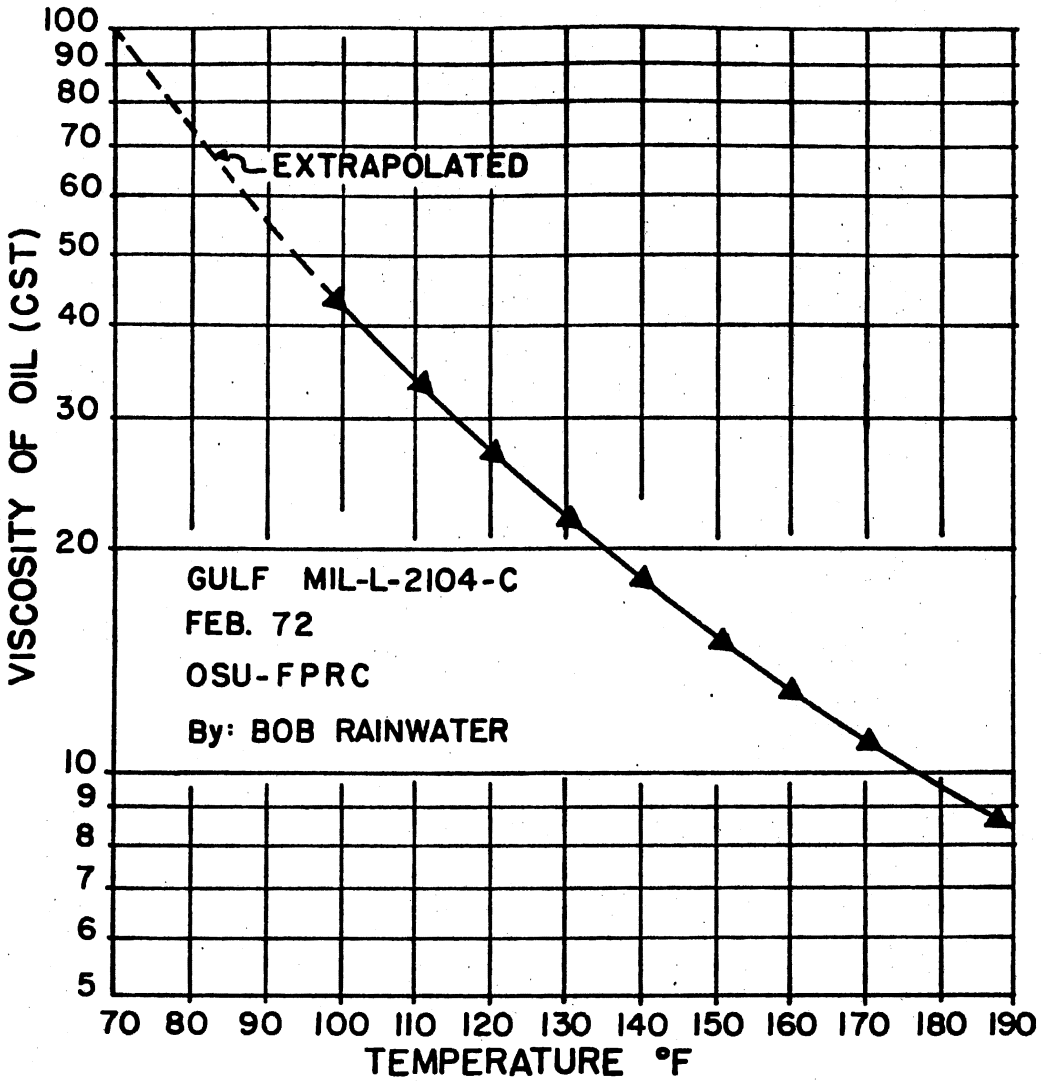

Figure 74. Viscosity (centistokes) of Mil-L-2104-C as a Function of the Temperature (°F)

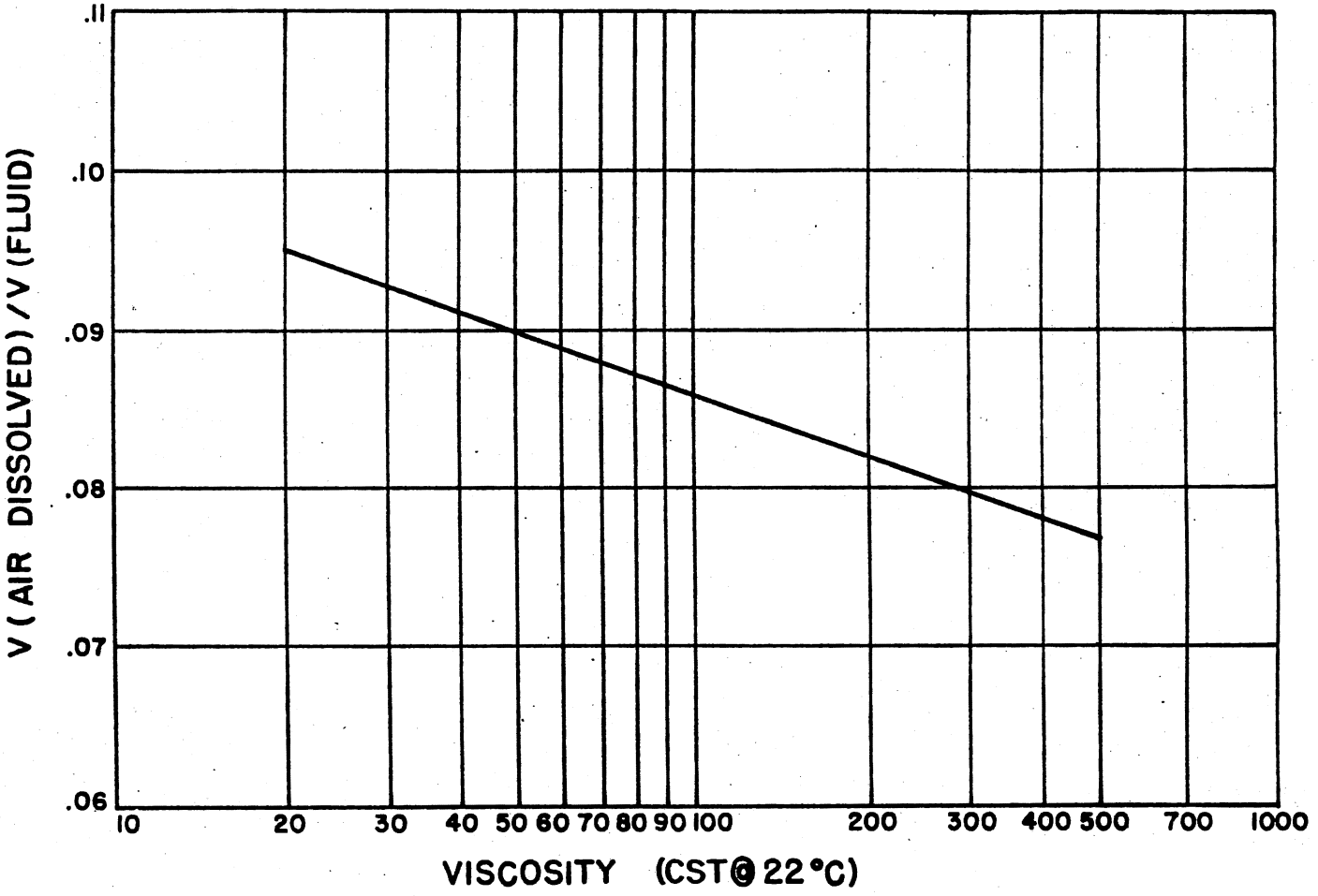

Figure 75. Empirically Derived Relationship Between the Viscosity of Oil and the Volume of Air That Will Enter Into Solution (46)

VITA

George Earl Maroney

Candidate for the Degree of

Doctor of Philosophy

Thesis: ACOUSTICAL SIGNATURE ANALYSIS OF HIGH PRESSURE FLUID PUMPING PHENOMENA

Major Field: Mechanical Engineering

Biographical:

Personal Data: Born in Topeka, Kansas, December 21, 1937, the son of Marjory Duncan (Hagen) Maroney and Richard Wendell Maroney. Married in Wichita, Kansas, August 30, 1964 to Vivian DeAnn Hopkins. Beget Angela Christine Maroney, February 3, 1968, and Shane Earl Maroney, November 19, 1970.

Education: Graduated from Hutchinson High School, Hutchinson, Kansas, in May, 1955; received the Associate in Arts Degree from Hutchinson Junior College, Hutchinson, Kansas in 1959, with a major in Arts and Science; received the Bachelor of Science degree from Oklahoma State University in 1967, with a major in Mechanical Engineering; received the Master of Science degree from Oklahoma State University in 1969, with a major in Mechanical Engineering; completed requirements for the Doctor of Philosophy degree at Oklahoma State University in May, 1976.

Professional Experience: Engineering Draftsman, Fluid Power Division, Cessna Aircraft, 1958-1962; Designer, Fluid Power Division, Cessna Center, 1964-1968; Design Engineer, Fluid Power Division, Cessna Aircraft, Summers 1965-1966; Research Engineer, Barnes Drill Company, Summer 1967; Project Engineer, Fluid Power Research Center, 1968-1969; Research Associate, Fluid Power Research Center, 1969-1971; Research Engineer, Fluid Power Research Center, 1971-Present; Industrial Consultant 1967-Present.

Professional Affiliations: American Society of Mechanical Engineers, American Society for Engineering Education, Society of Automotive Engineers, Fluid Power Society, Acoustical Society of America, Institute of Noise Control Engineering, National Fluid Power Association.

Publications: Forty papers and twenty-four technical reports in the areas of Hydraulic Component Design, Automatic Controls, Contamination Control, Fluid Logic, Noise Control, and Material Failure.